B Cells Selection In The Germinal Centre

Khaled Rashed Alzhrani

A thesis submitted to the University of Birmingham for the degree of

DOCTOR OF PHILOSOPHY

Institute of Immunology and Immunotherapy

College of Medical and Dental Science

University of Birmingham

February 2024

Abstract

Vaccination triggers the long-term production of high-affinity antibodies. Germinal centers (GCs) are sites within lymphoid tissues where B cells undergo clonal expansion and affinity maturation during T cell-dependent antibody responses. However, the regulation of affinity-matured B cell selection within GCs remains poorly understood. In this study, we examined the roles of antibody secretion and feedback in GC regulation using various mouse models: those incapable of secreting IgM or undergoing class-switching (IgMi), those unable to undergo affinity maturation or class-switching (AIDKO), and those restricted to producing and secreting IgG1 antibodies (IgG1M). Following immunisation with a T cell-dependent (TD) antigen, IgMi and AIDKO mice exhibited an increased percentage of GC B cells. In contrast, the percentage of GC B cells in IgG1M mice was reduced compared to wild-type mice. Introducing antibody feedback by injecting antigen-specific IgM into IgMi or AIDKO mice slightly reduced the proportion of GC B cells. It was shown that more stringent antibody feedback strongly inhibits B-Tfh cell interactions.

The Nr4a3-Tocky reporter system is unstable fluorescent protein that changes fluorescence from blue to red and can record the timing of TCR signalling. It was utilized to track interactions between GC B cells and Tfh cells in mice with altered B cell receptors (IgMg1 and IgG1M mice) or absence of affinity maturation (AIDKO mice). IgMg1 enhances interaction with and activation of Tfh cells, also reflected by higher Tfh frequencies. Additionally, testing expression of Nr4a3-blue and red forms of the reporter reveals an increase in newly activated Tfh cells in IgMg1 and IgG1M versus wildtype mice after immunisation. There was no change in Nr4a3-reporter expression in Tfh cells of AID-deficient mice, indicating unaffected Tfh cell activation in AID-deficient GCs.

This work gives insight, by using mouse models with altered antibody feedback, into how IgM and IgG1 antibody secretion shapes GC developments and how altering BCR isotypes and signalling regulates Tfh cell activity through antigen presentation within the GC.

ACKNOWLEDGEMENTS

First, I would like to acknowledge my supervisor, Professor Kai-Michael Toellner, to whom I am extremely grateful for the opportunity to work on this project in his lab. I thank him for his invaluable guidance, support, explaining scientific concepts, and encouragement throughout my PhD study. It has been an honour and privilege to work under his guidance over these past few years.

I am also deeply grateful to Dr Yang Zhang. Thank you for your continued support and efforts advising me on this thesis project. I appreciate you training me in experimental techniques, troubleshooting problems, and helping with mouse experiments. Your assistance was invaluable.

I would also like to thank: Dr Margaret Goodall for her help in producing and purifying monoclonal antibodies. Dr David Bending for providing the Nr4a3-Tocky and Nur77- Tempo mice and for much appreciated advice and discussions. My thanks also go to the BMSU staff and flow cytometry staff for their support.

To past and present members of the Toellner lab, especially Dr Ashley Hudson for helping me as a thesis advisor, as well as Amani, Fernanda, and Mohammed for their support and assistance in the lab - I am very grateful. I would also like to thank my 4th floor colleagues and PhD students for their kindness and help over the past few years.

I am especially grateful to my parents for their patience, unwavering love and constant presence, support, advice, thoughts and prayers which have kept me motivated throughout these years. Huge thanks also to my brother Abdulaziz, and sisters Wafa, Norah, Manal, Asma, and Shahad for offering their support whenever I needed it.

I owe the greatest debt to my wife Sahar, who has stood by me over the last 12 years. It is fair to say that without her I would not be where I am today. To my son Alwaleed and daughter Ghina, thank you for your unconditional love and understanding during this PhD journey. I deeply regret that my frequent absence from your lives while working in the lab or writing this thesis was difficult. I plan to give you all the time and a better life that you deserve from this point forward. That you are proud of me means everything.

I extend my thanks to my best friends, Maher Alwethaynani, Abdullah Alawam, and Mohammad Alqhatani, for their encouragement and the lovely times we shared together. I truly enjoyed all our moments spent together.

Lastly, I would also like to acknowledge and appreciate Jouf University and the Saudi Cultural Bureau for awarding me the scholarship that enabled me to undertake and complete this PhD program.

List of Abbreviations

AID	Activation-induced cytosine deaminase
Alum	Aluminium potassium sulphate
AP	Alkaline phosphatase
APC	Antigen presenting cell
APRIL	A proliferation-inducing ligand
Bcl6	B-cell Lymphoma 6
BCR	B cell receptor
Blimp-1	B lymphocyte-induced maturation protein-1
BLNK	B cell linker
BSA	Bovine serum albumin
CCR7	C-C chemokine receptor 7
CCL19	C-C chemokine ligand 19
CCL21	C-C chemokine ligand 21
CD	Cluster of differentiation
CDR	Complementarity-determining region
CGG	Chicken gamma globulin
CSR	Class-switch recombination
CXCR4	C-X-C chemokine receptor 4
CXCR5	C-X-C chemokine receptor 5
CXCL12	C-X-C chemokine ligand 12
CXCL13	C-X-C chemokine ligand 13
DrLN	Draining lymph node
D-PBS	Dulbecco's phosphate buffered saline
DC	Dendritic cell
DNA	Deoxyribonucleic acid
DSB	Double strand DNA breaks
DZ	Dark zone
EBI2	Epstein-Barr virus-induced G-protein coupled receptor 2
ELISA	Enzyme linked immunosorbent assay

ERK	Extracellular signal-regulated
FACS	Fluorescence activated cell sorting
FBS	Foetal bovine serum
FcR	Fc receptor
FDC	Follicular dendritic cell
FITC	Fluorescein isothiocyanate
FO	Follicular
Foxp3	Forkhead box Protein
FRC	Fibroblastic reticular cell
GC	Germinal centre
GFP	Green fluorescent protein
HEV	High endothelial venule
ICOS	Inducible T-cell costimulatory
i.p.	Intraperitoneal
Ig	Immunoglobulin
IL	Interleukin
IRF4	Interferon regulatory factor 4
ITAM	Immunoreceptor tyrosine-based activation motif
i.v	Intravenous
J	Joining
KLH	Keyhole Limpet Hemocyanin
KO	Knock out
LN	Lymph node
LPS	Lipopolysaccharide
LZ	Light zone
MAdCAM-1	Mucosal adressin cell adhesion molecule 1
MAPK	Mitogen-activated protein kinase
MHC	Major histocompatibility complex
MRC	Marginal reticular cell
MZ	Marginal zone
NFAT	Nuclear factor of activated T cells

NF-κB	Nuclear factor kappa-light-chain-enhancer of activated B cells
NK	Natural killer
NOD	Non-obese diabetic
NP	4-hydroxy-3-nitrophenyl-acetyl
Nr4a1	Nuclear receptor 4a1
Nr4a3	Nuclear receptor 4a3
OVA	Ovalbumin
PAMP	Pathogen-associated molecular patterns
PB	Plasmablast
PC	Plasma cell
PD-1	Programmed cell death protein 1
PRR	Pattern recognition receptor
QM	Quasimonoclonal
RAG	Recombination activating gene
RNA	Ribonucleic acid
s.c	Subcutaneous
S1PR2	Sphingosine-1-phosphate receptor 2
SHM	Somatic hypermutation
SLOs	Secondary lymphoid organs
TCR	T cell receptor
TD	T cell-dependent
Tfh	T follicular helper cell
TI	T cell-independent
TI-I	T cell-independent type I
TI-II	T cell-independent type II
TLR	Toll-like receptor
V	Variable
WT	wildtype

Table of Contents

List of figures

List of tables

Chapter 1. Introduction

1.1. The immune system

The immune system is a complex and intricate defence network within the human body that serves to protect against a wide range of harmful agents, including pathogens (such as bacteria, viruses, and fungi), as well as aberrant or potentially harmful cells like cancer cells. Furthermore, it is of vital importance for the immune system to exhibit tolerance toward our body's own tissues, effectively warding off the potential development of autoimmune diseases. This system is broadly categorized into innate and adaptive immunity. An effective immune response relies on innate and adaptive cell communication.

1.2. Innate immunity

Innate immunity is the rapid and non-specific initial defence against pathogens. It includes physical barriers (skin and mucous membranes), which help prevent pathogens from entering the body. Additionally, cell types such as natural killer cells, neutrophils, macrophages, and dendritic cells (DC) have specialised receptors called pattern recognition receptors (PRRs) comprise of structurally different proteins, including Toll-like receptors (TLR), NOD-like receptors (NLRs), RIG-I-like receptors (RLRs) and C-type lectin-like receptors (CLRs) , which can recognise specific molecular structures or motifs called pathogen-associated molecular patterns (PAMPs) that are commonly found on the surface of various pathogens, such as bacteria, viruses, and fungi. When immune cells encounter PAMPs, they trigger a series of signalling events that lead to the activation of the innate immune response. This includes the recruitment of immune cells to the site of infection, the release of inflammatory molecules, and the initiation of the process of phagocytosis, where immune cells engulf and destroy the pathogens (Janeway and Medzhitov, 2002).

1.3. Adaptive immunity

In contrast to the rapid response by innate immunity cells, adaptive immune responses typically take a few days to fully develop and become functional effectors cells. B and T cells serve as the primary effectors in the adaptive immune response. They originate in distinct locations: B cells develop in the bone marrow, while T cells mature in the thymus. The receptors on B and T cells, known as B cell receptors (BCRs) and T cell receptors (TCRs) respectively, arising from a complex mechanism of genetic rearrangement. This involves variable (V), diversity (D), and joining (J) gene segments rearranging semi-randomly to complete α and β chains that constitute TCRs in T cells, and V, D, and J gene segments that code for the assembly of heavy and light chains that form antibodies and BCRs. This happens during lymphocyte development in thymus for T cells and bone marrow for B cells. Random gene rearrangements, and insertions of nucleotide additions as well as mutations introduced by the actions of rag enzymes and terminal deoxynucleotidyl transferase during the recombination process generate a vast repertoire of TCRs and BCRs that can target a wide range of antigens (Chaplin, 2010).

The significant differences between B cells and T cells are based on their antigen recognition mechanisms. B cells, via their BCR, can recognise native antigens, internalise them by endocytosis and break them down into smaller peptide fragments to be loaded onto major histocompatibility complexes (MHC) molecules II for antigen presentation. T cells recognise processed peptides that are displayed on MHCs through interactions with professional antigen-presenting cells (APCs). These APCs mainly include on one hand DCs initiating T cell responses, and on the other hand B cells, monocytes, and macrophages that receive stimulation or regulation from T cells.

T cells can be categorised into two conventional T cells subsets, distinguished by their expression of CD8 and CD4 cell surface markers. CD8+ T cells engage with peptides displayed on MHC class I molecules, and upon activation, differentiate into cytotoxic T cells capable of promptly eliminating infected cells. Conversely, CD4+ T cells engage peptides presented on MHC class II molecules. Once activated, they play a role in boosting monocytes/macrophage activity and supporting antibody generation by B cells, thereby contributing to humoral immunity. T helper (Th) cells are another name for this subset of CD4+ T cells (Chaplin, 2010). Th cells develop diverse characteristics depending on the type of immune response needed and are then further divided into subsets based on their specific functions. B cells exhibit the remarkable ability to undergo differentiation into plasma cells with a distinct specialisation in the secretion of antibodies. The development of long-lived memory effector T/B cells is also crucial in the context of adaptive immunity. These specific cells facilitate a more rapid and effective response to the same pathogen in the future.

Invariant Natural Killer T (iNKT) cells are also a subset of T cells which display properties of both T cells and NK cells and express markers of NK cells and are different from conventional αβ T cells despite bearing an αβ TCR and they able to recognise lipids and glycolipids presented by the monomorphic MHC-like molecule CD1d (Brennan et al., 2013). iNKT cells can rapidly produce large amounts of cytokines upon activation, for example, Th1-type cytokines (e.g., IFN-γ) and Th2-type cytokines (e.g., IL-4 and IL21), this makes them an important bridge between the innate and adaptive immune systems which enables them to respond quickly to infections. BCR-mediated engagement of CD1d-restricted antigens and CD1d expression on B cells are necessary for iNKT cell cognate help (Barral et al., 2008, Lang et al., 2008). Also, activated iNKT cells must engage through CD80/86 and CD40 on B cells via CD28 and CD40L.

Cytokines generated by iNKT cells, also influence B cell response and produce high levels of IgM in response to cognate iNKT cell help. This triggers a primary response and the production of plasmablasts and short-lived plasma cells (King et al., 2011).

1.4. Secondary lymphoid organs

Secondary lymphoid organs (SLOs), such as the spleen, lymph nodes (LN), or mucosa associated lymphoid tissues, are crucial for facilitating the interaction between lymphocytes, lymphocytes and antigen-presenting cells, and with other non-lymphoid cells. These interactions are essential for lymphocyte development, the initiation of adaptive immune responses, and the maintaince of immune responses. The effectiveness of SLOs in allowing lymphocyte activation is dependent on the migration of cells and their ability to scan and eliminate antigens that enter the body via several body cavities.

SLO, such as lymph nodes, contain various stromal (non-hematopoietic, CD45-) cell types that provide structure and organise immune cells. These include blood endothelial cells (BECs) lining blood vessels (CD31+gp38-), lymphatic endothelial cells (LECs) lining lymphatic vessels (CD31+gp38+), fibroblastic reticular cells (FRCs) forming conduits (CD31-gp38+), and other stromal cells (CD31-gp38-) (Rodda et al., 2018). These stromal cells structure the architecture to organise lymphocytes in the LN and facilitate immune responses.

Recently, multiple subsets of FRCs have been identified in lymph nodes based on their surface markers, functions and localization. All FRC produce CCL19 and CCL21, important to direct immune cells homing into LN (Luther et al., 2000). T zone reticular cells (TRC) also produce IL7 and contribute to the naïve T cell homeostasis and survival, organization and proper functioning of the T-cell zone, where T cells interact with antigen-presenting cells and initiate adaptive immune responses (Knop et al., 2020). Marginal reticular cells (MRCs) adjacent to

subscapular sinus (MadCAM+), producing CXCL13, are essential for homing of CXCR5+ B cells and their migration into the follicles (Katakai et al., 2008, Katakai, 2012). Furthermore, MRCs upregulate RANKL, which promotes the maintenance of the structure of LNs (Katakai et al., 2008, Rodda et al., 2018)

Follicular Dendritic cells (FDC, CD21/35+) in the centre of the B cell follicle, producing CXCL13 and essential survival factors such as IL6, are dynamic for maintaining the structure of B cell follicles, where B cells proliferate and differentiate after response to antigens with the support of follicular helper T cells. FDCs also present antigen to B cells and in this way play a crucial role during the GC B cell selection (Barnett et al., 2014, Jarjour et al., 2014, Zhang et al., 2018).

The structure of SLOs (lymphnodes and spleen) are discussed in more detail below. Lymph nodes are surrounded by the subcapsular sinus where afferent lymph vessels enter. From here intranodal lymphatics enter and penetrate the lymph node. Naïve T and B cells use CCR7 to detect CCL19 and CCL21 that are produced by the FRCs and transcytosed through the HEV in the endothelium lumen, guiding them into lymph nodes and other lymphoid tissues. Additionally, B cells express CXCR5 that promotes LN entry by binding to CXCL13 expressed by FDCs. Also, CCL21-CCR7 signalling helps DCs mature into potent antigen-presenting cells, guiding their migration from sites of antigen exposure to local lymph nodes via afferent lymphatic vessels(Comerford et al., 2013).

The lymph node parenchyma encompasses three main sections: the cortex, the paracortex, and the medulla (Figure 1.1). The cortex, the outmost layer, contains B cells, macrophages, and follicular stromal cells organised into primary follicles. The cortex is the region where B cell follicles are located, and it assists as the site for germinal centre development after

antigen stimulation. Next to the cortex, the paracortex forms the second outer layer, housing T cells, dendritic cells, macrophages, and FRCs. FRCs function as a channel network surrounded by collagen and fibers inside a basement membrane, which form conduit tubular system that transport fluid from sinus to HEV that enables DC to access along the conduit membrane gaps to acquire small antigens and penetrated into the paracortex and cortical structures of the LN and promote longer interactions between the T cells and dendritic cells within this compartment (Roozendaal et al., 2008). Here, high endothelial venules (HEV), which are part of the LN's blood vessel network, allow T and B lymphocytes to reach the organ from the blood. The innermost layer of the lymph node is known as the medulla, composed of lymphatic tissue referred to as medullary cords, which contains mainly plasma cells, macrophages, and medullary reticular cells. These cords are interspersed with medullary sinuses which lymph vessels that drain lymph towards the efferent lymph vessel. The lymph node's lymphatic vessels are bordered by lymphatic endothelial cells (Burrell et al., 2011).

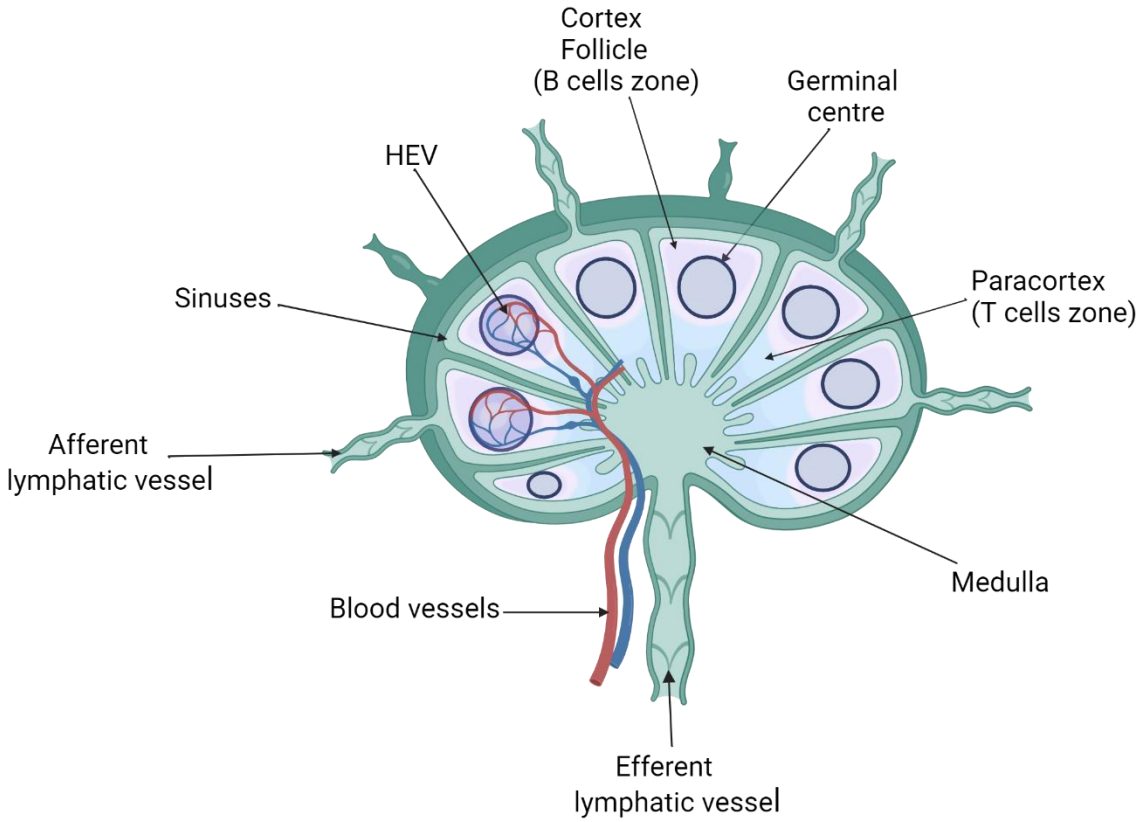

Figure 1.1 The structure of lymph nodes.
The lymph node's structure is designed to enable for the efficient filtering and processing of lymph, which contains immune cells, antigens, and other substances. They are divided into different distinct regions. The subcapsular sinus: is the area beneath the capsule where lymph enters the node from afferent lymphatic vessels. This is the first site at which antigens and pathogens come into interactions with immune cells e.g. macrophages. Cortex: The lymph node's outer area, which contains a high density of lymphocytes, particularly B and T cells. Follicles: Concentrated regions of B cells within the cortex. Paracortex: The region between the lymphoid follicles, mainly containing T cells and dendritic cells. HEVs: Specialized blood vessels that allow lymphocytes to enter the lymph node. Medulla: The central region of the lymph node, containing medullary cords and medullary sinuses. Created and adapted from biorender template Dr Akiko Iwasaki.

The murine spleen, like other mammalian spleens, plays a significant role as a secondary lymphoid organ in immunological responses and to filter blood. It has two majors functionally and morphologically different compartments: the red pulp and the white pulp (Janeway CA 2005). The red pulp is utilised for blood filtration and processing. It is comprised up of a network of splenic sinuses and cords. The red pulp is responsible for eliminating old or damaged red blood cells, storing platelets, and collecting pathogens in the blood. Macrophages in the red pulp are important for filtering and phagocytosing debris from cells and pathogens.

The white pulp is divided into three distinct parts: periarteriolar lymphoid sheaths (PALS) also called T cell zone, the follicles, and the marginal zone. Within the white pulp, lymphocytes (including B cells and T cells) and other hematopoietic cells are found alongside plasma cells and plasmablasts, which migrate from the follicles and outer PALS after undergoing antigen-specific differentiation (Mebius and Kraal, 2005) (Figure 1.2). It is a major site of lymphocyte traffic and the development of plasma cells (Cesta, 2006). The follicles in the mouse spleen are continuous with the PALS and are typically seen at the bifurcation sites of the central arterioles (Ward, 1999, Cesta, 2006). As in the lymph nodes, B-cells dominate the splenic follicles, with follicular dendritic cells (FDCs) and CD4+ T-cells present in smaller numbers. CD8+ T-cells, on the other hand, are usually lacking within the follicles. The follicular centre is surrounded by a mantle zone which is outer ring of small frequent of B lymphocytes surrounding a germinal center (Cesta, 2006). Furthermore, germinal centres (GCs) can develop within the follicles in response to antigenic stimulation. GCs contain activated B cells, FDCs, CD4+ T cells, apoptotic B-cells and tingible-body macrophages. The last part of the white pulp is marginal zone (MZ) which is a specialised region surrounding the PALS and follicles, is separated from the follicles by the marginal sinus and forms the outermost part of the white

pulp touching the red pulp. It is frequently regarded as a separate compartment rather than as a component of the white pulp. The marginal zone acts as a screening region for antigens and pathogens in the systemic circulation and is important in antigen processing. The zone features different cell populations that distinguish it from the PALS and follicles, including marginal zone metallophilic macrophages, which form the inner ring of MZ adjacent to the follicle and T zone and the marginal sinus (den Haan et al., 2012). The marginal sinus is continuous with vessels that feed the capillary beds of the white pulp. Marginal zone macrophages expressing Toll-like receptors (TLRs) and macrophage receptor with collagenous structure (MARCO), form an outer ring of macrophages, and assist in the clearance of bacteria and viruses (Mebius et al., 2004, Kraal et al., 2000, Elomaa et al., 1995). Furthermore, marginal zone B-cells are a unique subset, non-circulating B-cells with an IgM^{high}/IgD^{low} characteristic, distinguishing them from circulating B-cells IgM+/IgD+ follicular B-cells (Martin and Kearney, 2002). Because of its distinct characteristics and functions, the marginal zone plays an important role in the spleen's immunological response.

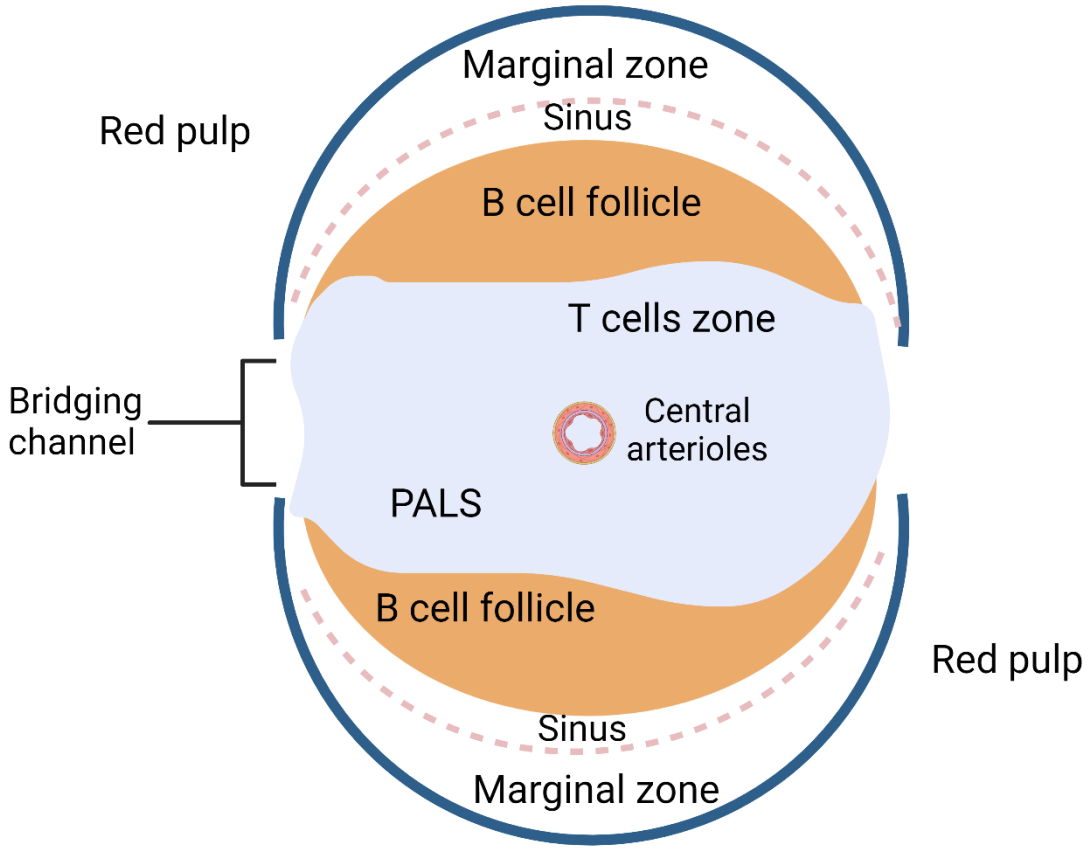

Figure 1.2 The morphology of the spleen's white pulp

The mouse white pulp's morphology is divided into different areas, including periarteriolar lymphoid sheaths (PALS), B cell follicles. PALS are regions of T cell dominance found around the central arterioles. They consist mainly of T cells. B cell follicles, which are regions where B cells are organised around central arterioles. These B cell-rich areas provide the initial locations for B cell responses and the development of germinal centre in response to antigenic stimulation. Modified and cited from (Golub et al., 2018).Created by Biorender.

1.5. B cell development

1.5.1. B cell development in the bone marrow

B cells arise from hematopoietic stem cells (HSCs) and develop in both the fetal liver and bone marrow of mammals (Hardy and Hayakawa, 2001b). HSCs initiate the process, which progresses to multipotent progenitor (MPP) cells and eventually to common lymphoid progenitor (CLP) cells (Figure 1.3). CLP cells then go through several more phases of maturation before becoming fully functional mature B cells. The Pro-B cell is the earliest lineage occurring after the CLP cells. During this stage, pro-B cells express RAG (Recombination-activating genes) enzymes, which initiate the process of VDJ recombination(Oettinger et al., 1990, Shinkai et al., 1992). This involves the rearrangement of gene segments encoding the VDJ regions of the immunoglobulin heavy chain. After the successful rearrangement V(D)J segments of the heavy chain, the functional heavy chain combines with surrogate light chain components (λ5 and VpreB) to form a pre-B cell receptor (pre-BCR) (Hardy and Hayakawa, 2001b, Karasuyama et al., 1993). The pre-BCR also associates with the signalling molecule Igα/Igβ (CD79a/CD79b) (Karasuyama et al., 1996) signals the presence of a functional Ig heavy chain and delivers essential survival and proliferation signals to the pre-B cell. Following the formation of the pre-BCR, the pre-B cell begins to rearrange and produce light chains. The light chain replaces the surrogate light chain, and the B cell now forms a functional B cell receptor – the surface IgM molecule (Hardy and Hayakawa, 2001b).

Bone marrow stromal cells also are important for B cells development by producing factors like interleukin-7 (IL-7) and the chemokine CXCL12. IL-7 supports the survival and proliferation of pro-B and pre-B cells, while CXCL12, via its receptor CXCR4 on B cell progenitors, helps localize developing B cells to the bone marrow (Zehentmeier and Pereira, 2019).

The BCR functions as a checkpoint during B cell development. Immature IgM B cells with non-functional or self-reactive BCRs are eliminated through negative selection and clonal deletion (Pelanda and Torres, 2012). Immature B cells that successfully pass the negative selection continue to differentiate and acquire cell surface markers such as IgD, CD21 and CD23 (Su and Rawlings, 2002, Tarlinton, 2008). B cells continue their final maturation in the spleen as transitional B cells, which is a short phase when they are still prone to negative selection to prevent the emergence of autoreactive cells. The differentiation of marginal zone (MZ) B cells relies on NFκB signaling and is facilitated by signals from the B cell receptor (BCR), Notch2, and the B cell activating factor receptor (BAFF-R). A deficiency in APRIL or BAFF-R results in a significant decrease in MZ B cell (Rauch et al., 2009). B cells then migrate into the peripheral lymphoid tissues, such as lymph nodes, and mucosal-associated lymphoid tissues and spleen, where they are ready to encounter antigen and become activated.

1.5.2. B cell development and subsets in spleen: phenotype and function

Mature naïve B cells have been classified into three subsets, B-1 B cells, follicular B cells (FO), and marginal zone (MZ) B cells and this classification is based on their developmental stage, expression of surface markers, and functional properties (Yam-Puc et al., 2018).

1.5.2.1. B-1 B cells

B-1 B cells are a subpopulation of B cells that are found predominantly in the peritoneal and pleural cavities, but also can be detected in spleen and lymph nodes (Hardy and Hayakawa, 1994). B1 B cells can be recognized by their surface markers ($B220^{lo}$ IgM^{hi} $CD23^{-}$ $CD43^{+}$ IgD^{lo}) and further can be subdivided to B1a cells, which express surface marker CD5, and B1b with low expression of CD5 (Hardy and Hayakawa, 2001a, Baumgarth, 2011). Splenic B-1 B cells do not express CD11b, while peritoneal B-1 B cells do.

B-1 B cell repertoires in body cavities and the spleen reflect their developmental pathways. The absence of non-template-derived nucleotide (N-region) insertions at the VDJ joining ends in B-1 cells is consistent with the fetal lack of terminal deoxynucleotidyl transferase (TdT) expression(Feeney, 1990). B-1 B cell immunoglobulin genes have less N insertions, and do not typically have somatic mutations (Berland and Wortis, 2002). The repertoire of B-1 B cells is limited and oriented toward reactivity with common bacterial and self-antigens.

B-1 B cells are involved in responses to Thymus independent type 2 antigens (TI-2 antigens), which are molecules with repetitive epitopes that can stimulate B cells without T cell help. The study by Schager et al. (2018) on STmGMMA (Salmonella Typhimurium Generalized Modular Glycoengineering Modified Antigen) shows that it induces T-cell-independent switching to all IgG isotypes except IgG1. In T-cell-deficient mice, STmGMMA prompted the production of IgM and IgG antibodies by 7 days, increased the proportion of B1b cells, and induced antigen-specific IgG to porins but not to LPS. All IgG isotypes except IgG1 were produced, indicating that T cells are crucial for switching to IgG1. Thus, STmGMMA elicits a strong T-cell-independent response, involving B1b cells, while T cells are necessary for IgG1 production.

In response to TI-2 antigens, B1 B cells predominantly produce isotypes of antibodies, like IgM, IgA and all IgG except IgG1, known as natural antibodies. They have a relatively low affinity because they lack somatic mutations that are the primary hallmark of affinity maturation in GCs, and wide-ranging specificity, which allows them to recognize a wide range of antigens. While B-2 B cells, also called follicular B cells, develop high affinity and are specific for exogenous non-self-antigens (Lalor and Morahan, 1990).

Studies have shown that B-1 cells not only produce natural antibodies but also enhance IgM production in response to various pathogens, including Borrelia hermsii, Salmonella typhi, Streptococcus pneumoniae, and influenza (Colombo and Alugupalli, 2008, Cunningham et al., 2014, Haas et al., 2005, Baumgarth et al., 1999). For example, a study on influenza showed that while local IgM levels increase during infections, natural serum IgM levels remain unchanged, and around 90% of IgM-secreting B-1 cell produce antibodies that are not specific to the influenza virus, implying antigen-nonspecific activation. BCR signalling likely doesn't regulate this response, as B-1b cells do not participate to the acute anti-viral response, and increased antibody production is limited to the respiratory tract(Choi and Baumgarth, 2008). Suggesting that different B-1 cell subsets regulate systemic versus infection-induced antibody responses.

1.5.2.2. Follicular B cells (FO)

FO B cells express high levels of IgD and CD23, but low levels of IgM and CD21, and do not express CD5 in mice. Immature B cells migrate to the spleen to continue their maturation into either FO B cells or MZ B cells based on BCR signalling (Yam-Puc et al., 2018). B cells leave the bone marrow and enter the bloodstream, where they circulate throughout the body. Expression of the chemokine receptor CXCR5 guides their migration to B cell follicles once they have entered the spleen, Peyer's patches or lymph nodes. CXCR5 binds CXCL13, which is abundant in the follicular areas (Forster et al., 1996). Due to their location within the lymphoid follicles adjacent to the T cell zones, FO B cells have been particularly well-suited to participating in T-dependent immune responses (Pillai and Cariappa, 2009a). Following antigen-binding, activated FO B cells migrate to the outer T zone to interact with activated T helper cells. In the outer T zone, activated B cells present antigen peptides derived from captured antigens via MHCII to antigen-specific activated $CD4^+$ T help cells. B cells have high

expression of CD40, a co-stimulatory receptor that is required for B cells activation. Interaction with antigen-specific activated T helper cells leads to their rapid expression of CD40L (Casamayor-Palleja et al., 1995). Activated B blasts undergo proliferation. Some move to extrafollicular foci, where they form early extrafollicular plasmablasts, enabling an early extrafollicular humoral response that produces low-affinity antibodies. They may have undergone class switch recombination (CSR) but not somatic hypermutation (SHM) and differentiate into short-lived plasma cells (MacLennan et al., 2003). Other activated FO B cells return to the B cell follicle to proliferate and become GC founder cells. Activated CD4 T cells produce cytokines such as interleukin-4 (IL-4), interleukin-5 (IL-5), and INF-γ based on the types of antigen (Toellner et al., 1996) These cytokines and CD40-CD40L signalling provide critical signals that promote CSR and differentiation of the activated FO B cells and result in the production of different antibody isotypes with distinct effector function. In the GC, CD4 follicular helper T cells also produce interleukin-21 (IL-21) (Zotos et al., 2010, Zhang et al., 2018, Petersone et al., 2023). This thesis will focus on the differentiation of FO B cells.

1.5.2.3. Marginal zone B cells (MZ B cells)

MZ B cells are located in an area of the spleen with high blood flow that lies between the spleen's white pulp and red pulp. The cell-surface phenotype of MZ B cells typically includes the expression of $IgM^{hi}CD21^{hi}CD23^{lo}IgD^{lo}CD1d^{+}$. In mice they do not express CD5 or CD11b (Martin and Kearney, 2002). Like B1 B cells, MZ B cells exhibit innate-like features and can respond rapidly to blood-borne antigens without the need for prior exposure or activation by T cells, which then results in the generation of short-lived plasma cells. MZ B cells also play a significant role in T-dependent B cell responses by facilitating the transport of antigen-antibody complexes towards follicular dendritic cells (FDCs) in B cell follicles via complement

receptor CR1/2 (Gray et al., 1984). This process is vital for the initiation of robust antibody responses and the generation of immunological memory.

MZ B cells demonstrate constitutive shuttling between the MZ and the follicles of the spleen. This process is regulated trough CXCR5, and sphingosine 1-phosphate receptors (S1PR1/S1PR3). The migration of MZ B cells to the follicles is predominantly influenced by the upregulation of CXCR5, a chemokine receptor that facilitates migration towards CXCL13 generated by Follicular Dendritic Cells (FDCs) and follicular stromal cells within the follicles. Whereas their return to the marginal zone is dependent on the activity of the S1P1 receptors (Cinamon et al., 2008, Arnon et al., 2013).

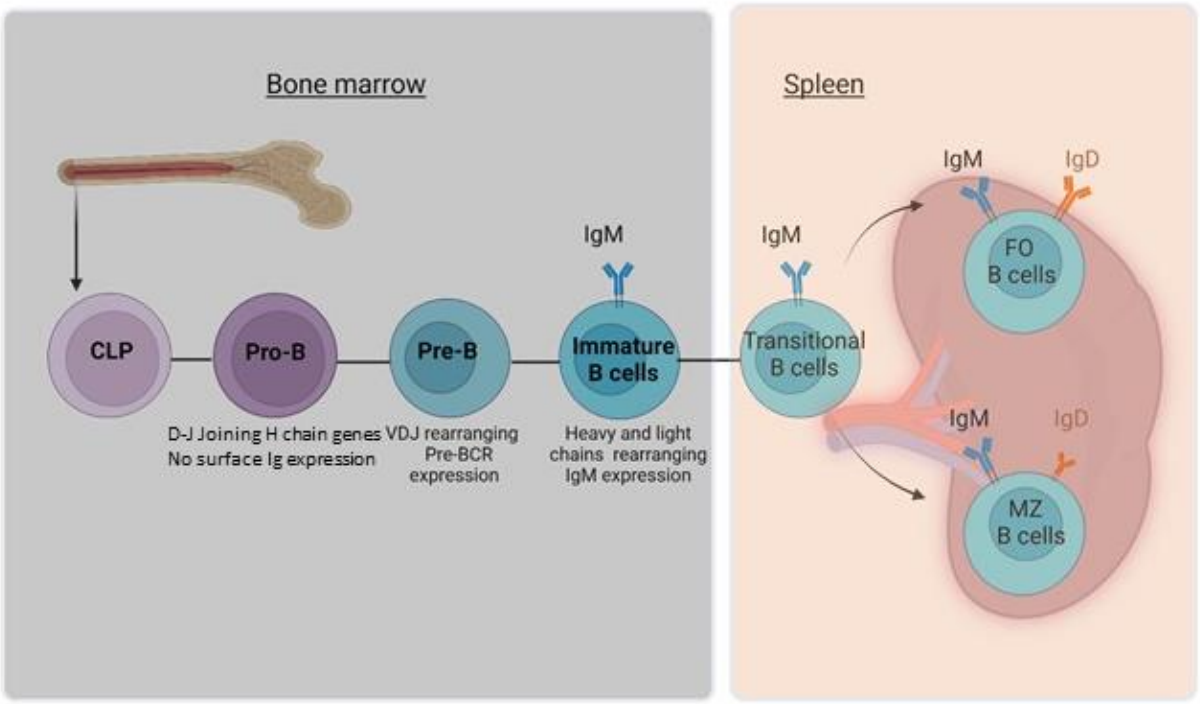

Figure 1.3 B cells development in bone marrow and spleen.
A simplified overview of B cell development. B cell development begins in the bone marrow, where common lymphoid progenitor (CLP) differentiate into pro-B cells. Pre-B cells start the VDJ Igs heavy chain rearrangement process. Pre-B cells undergoing successful rearrangement express the pre-BCR. They then start rearranging light chain, and differentiate into immature B cells which are the first cells that express a complete BCR. Immature B cells leave the bone marrow and enter the spleen as transitional B cells. At this stage (auto-)antigen encounter will lead to BCR editing or negative selection. After a few days they differentiate into mature B cells that after encounter of antigens become activated, leading to clonal expansion and differentiation. Mature B cells express both membrane-bound IgM and IgD isotypes. Created by Biorender.

1.6. B cells activation and differentiation

Antibodies play an essential role in the protection from infectious pathogens and subsequent re-exposure. Memory B cells and long-lived plasma cells, both of which are produced in response to primary antigen exposure, are responsible for the production of antibodies that are capable of providing long-term protection. The activation of a B-cell response to an antigen can proceed via two distinct mechanisms, namely, thymus-independent and thymus-dependent pathways.

1.6.1. Thymus independent antigen (T-I) antigen

T-I antigen responses trigger an immunological response from B cells without the involvement of CD4+ helper T cells. T-I antigens are classified into two types: type 1 (TI-1) and type 2 (TI-2). Type 1 antigens (TI-1) are also known as B cell mitogens, which directly engage with Toll-like receptors (TLRs) on B cell surface, for example TLR4 binding lipopolysaccharide (LPS), associated with the outer cell membrane layer of Gram-negative bacteria. This interaction occurs with any B cell, regardless of its BCR specificity, and exhibits less evidence of memory. High doses of TI-1 antigens can lead to polyclonal B cell activation that lead to non-antigen-specific polyclonal antibody production (Murphy et al., 2008). TI-I antigens present at low dose can amplify antigen-specific activation through the BCR.

Type 2 antigens (TI-2) are typically large polysaccharides with multiple repeating antigenic epitopes, such as s flagella or bacterial cell wall polysaccharides. These antigens normally evoke antibody response in human after the age of 2. They can simultaneously bind to multiple B-cell receptors (BCRs) on a single B cell. This extensive surface Ig cross-linking provides a sufficiently strong signal to activate the B cell, and induce an antibody response from antigen-specific B-cells even without help from T cells. It directly promotes B cells to become short-lived plasma cells in the extrafollicular regions. While TI-2 antigens do not induce a strong memory response, and although the persistence of memory B cells has been noted, studies have explored the characteristics of various memory B cell subsets. Study on peritoneal cavity-resident memory B1a cells and memory B1b cells has shown that memory B1a cells migrate to the spleen and differentiate into plasma cells upon re-challenge. Additionally, studies of antibody responses to *Borrelia hermsii* and *Streptococcus pneumoniae* infections have revealed that memory B1b cells persist in the peritoneal cavity, similar to memory B1a cells(Alugupalli et al., 2004, Haas et al., 2005). Additional study demonstrated

that antigen-specific memory B1b cells, traced and analysed using NP-Ficoll, retain the phenotypic characters of their naïve B1b counterparts, including longevity and sensitivity to antigen stimulation (Obukhanych and Nussenzweig, 2006). Some studies have shown that TI-2 antigens can trigger antigen-specific B cells to mount a strong GC response. However, these GC B cells have shorter lifespans compared to T cell-dependent responses, as there is no T cell help provided. Despite their shorter durations, the GC B cells induced by TI-2 antigens have many molecular features similar to those seen in GC B cells from T cell-dependent responses (de Vinuesa et al., 2000, Lentz and Manser, 2001). Somatic hypermutation is low, probably due to absence of B cell recycling in the absence of T helper signals from Tfh cells (Toellner et al., 2002).

1.6.2. Thymus dependent antigen (T-D) antigen

Most antibody responses to proteins and glycoproteins require help from T cells for B cell effective activation. This is due to that the vast majority of protein antigens are T cell-dependent antigens, indicating that they require the presence of helper T cells in order to elicit a functional antibody response. T-D immune responses are triggered when B cells and T cells with specificity for the same antigen engage in cognate interactions that take place at the boundary between B cell follicles and T cell zones within secondary lymphoid organs (Garside et al., 1998). B cell activation is initiated by important signals. First, B cells recognise antigens through their unique B cell receptors (BCRs). Following recognition of the antigen, B cells can serve as antigen-presenting cells (APCs) by expressing processed peptides on major histocompatibility complex (MHC) class ll molecules on their surface. Once the antigen binds to the BCR, the antigen is degraded in the cytosol and transported into late endosomes, where it encounters MHC class II molecules derived from the endoplasmic reticulum (Blum et al.,

2013). The peptide fragments that can be loaded onto MHC class II molecules are presented to activated CD4 T lymphocytes. Helper T cell recognition leads to delivery of activation signals for the antigen-presenting B cell. Helper T lymphocytes with a TCR specific for the given MHC class II-loaded epitopes express co-stimulatory signals such as CD40L and OX40 and secrete such as cytokines IL-4 and IL-21 (Toellner et al., 1998, Zotos et al., 2010, Petersone et al., 2023). These molecules produced by the T helper cells can support activated B cell differentiation and class switch recombination (Toellner, 2014).

The result of these interactions of activated B cells with T cells is the differentiation of short-lived extra-follicular plasmablasts secreting low-affinity antibodies, and early recirculating IgM^+ memory B cells (MacLennan et al., 2003). Some activated B cells enter the follicle to form germinal centres, resulting in the development of memory B cells and long-lived PCs with high affinity (Weisel et al., 2016).

1.6.3. Hapten 4-hydroxy-3-nitrophenyl-acetyl

Haptens refer to small chemical structures which serve as efficient B cell antigens. Accordingly, these entities are used for investigating antigens and their interaction with antibodies. In order to recruit efficient T cell help, chemical haptens need to be coupled to carrier proteins like chicken gamma globulin (CGG) that can be processed into peptide antigens that the B cell can present via MHCII to T helper cells. 4-hydroxy-3-nitrophenol (NP) has proven to be a good immunogen which can be bound to several different carriers and has long been used for eliciting immune response in mice. This hapten has been used by researchers since it can induce a canonical response typically involving V186.2 IgH chain and Igλ light chain (Bothwell et al., 1981). Responses to hapten conjugated with carrier proteins to form NP-CGG have been well studied with affinity maturation and key mutations conferring higher affinity are known (Bothwell et al., 1981, Maizels et al., 1988). Haptens can

also be coupled to T independent carriers, e.g. the polysaccharide Ficoll and used in the study of TI B cell responses (de Vinuesa et al., 2000, Toellner et al., 2002)

1.7. The germinal centre

1.7.1. Germinal centre response

The germinal centre response, a hallmark of T-D responses, is a specialised microenvironment found within secondary lymphoid tissues, where B cells undergo intense proliferation, somatic hypermutation, and affinity maturation leading to the production of high-affinity antibodies, plasma cells, and memory B cells (Figure 1.4).

The germinal centre (GC) response is triggered when B cells encounter antigens and receive help from T follicular helper (Tfh) cells in secondary lymphoid tissues. When an infection occurs, B cells quickly detect pathogens and trigger a humoral response. How B cells encounter antigens depends on the antigen's size. Small soluble antigens can diffuse directly into lymphatic tissue, where B cells recognize them. However, larger pathogens usually require presentation by subcapsular sinus macrophages, dendritic cells (DCs), and follicular dendritic cells (FDCs) (Carrasco and Batista, 2007, Allen and Cyster, 2008, Batista and Harwood, 2009). After B cells encounter antigen, they rapidly upregulate the expression of chemokine receptor CCR7, attracting them to their ligands CCL19 and CCL21, which are present in the T cell zone and guiding them towards the T:B border, where they interact with primed CD4+ T-helper cells (Okada et al., 2005). After B cells interact with CD4 T cells and undergoing cell division, activated B cells either contribute to the low affinity extrafollicular antibody response , or migrate back to the follicle mantle by upregulating Epstein-Barr virus-induced G protein coupled receptor 2 (EBI2) (Chan et al., 2009, Pereira et al., 2009). These B

cells differentiate into GC B cells. GC B cells express S1PR2, which helps to locate GC B cells in the central follicle (Green et al., 2011).

GCs divided into the dark zone (DZ) and the light zone (LZ) (Allen et al., 2007b). The DZ is mainly made up of centroblasts, a type of rapidly dividing B cell. The chemokine receptor CXCR4 is highly expressed on centroblasts, which aids their migration towards CXCL12, which is produced by DZ reticular cells (called CXC12-reticular cells)(Bannard et al., 2013), and thus positions them within the DZ (Allen et al., 2004). Centroblasts undergo random mutations in their antibody variable region genes by a process called somatic hypermutation (SHM), which is triggered by activation-induced deaminase (AID) (Muramatsu et al., 2000). During transcription, the immunoglobulin variable (V) region of the antibody-encoding genes is exposed as single-stranded DNA. AID targets these single-stranded DNA regions and catalyses the conversion of cytidine (C) to uracil (U) (Chaudhuri et al., 2003, Dickerson et al., 2003, Ramiro et al., 2003). This deamination process induces point mutations in the V region. The introduction of uracil into the DNA can be problematic if not repaired properly. It can lead to the formation of DNA double-strand breaks (DSBs), which poses a threat to genomic stability. However, B cells have developed error-prone repair mechanisms to cope with these DSBs and the repair process itself facilitates the generation of mutations (Di Noia and Neuberger, 2007, Peled et al., 2008). The lack of AID enzyme has profound consequences on the adaptive immune response including impaired somatic hypermutation, limited ability of immunoglobulin to switch to other antibody isotypes, and hypertrophic GCs with lymph node hyperplasia (Revy et al., 2000). One of the hallmark consequences of AID deficiency is the development of Hyper-IgM syndrome. This is characterised by elevated levels of immunoglobulin M (IgM) and significantly reduced or absent levels of other antibody isotypes. Additionally, AID deficiency is associated with an increased risk of autoimmune

disorders, such as systemic lupus erythematosus (SLE) and common variable immunodeficiency (CVID). AID deficiency could result in abnormal B-cell expansion and the generation of autoreactive B cells, which, in turn, promotes the formation of Tertiary Lymphoid Organs (TLOs) within inflammatory tissues, supporting organ-specific autoimmune effector CD4+ T cells to proliferate (Hase et al., 2008).

The centroblasts subsequently exit the cell cycle and become smaller centrocytes, which migrate to the light zone. Within the light zone, FDCs produce abundant CXCL13, which attracts GC B cells with higher expression of CXCR5 (Allen et al., 2004). Chemokines involved in the formation and function of GC B cells are summarised in (Table1.1). However, recent study showed that during a *Salmonella Typhimurium* infection, the FDC networks in secondary lymphoid organs are disrupted, altering their distribution and density. This disruption delays GC formation until FDCs recover around day 28 (Marcial-Juarez et al., 2023).

Different from the hypermutating centroblasts, centrocytes express the mutated BCR on their surface. Centrocytes test the specificity of their BCR by binding antigens presented on FDC. Antigens are not deposited free on FDC, but always complexed with antibody. Centrocytes have to engage in competitive interaction with the antibody-antigen immune complexes on FDC. Only centrocytes with higher-affinity B-cell receptors are able to outcompete antibodies present in the immune complexes. Successful competition will allow antigen uptake and presentation via MHCII. These centrocytes then competitively interact with follicular helper T cells, which provide more essential signals for centrocyte differentiation into plasma cells or memory B cells. While centrocytes unable to bind antigen or with low affinity BCRs may undergo apoptosis (cell death). Some low affinity centrocytes may become memory B cells (Suan et al., 2017a). B-cells with higher affinity BCRs undergo positive selection that signals

them to re-enter the dark zone for additional rounds of SHM. This iterative process allows B-cells to undergo affinity maturation, gradually increasing their ability to recognize and neutralize the antigen more effectively (Allen et al., 2007a, Victora et al., 2010).

A recent study in our lab (Zhang et al., 2013) suggests that antibody-mediated feedback is another process which contributes to GC B cell selection. During this process, early low affinity antibody or natural antibody masks antigens present as immune complexes on FDCs. GC B cells have to compete with these antibodies by expressing BCRs with higher affinity for the antigen. Only higher affinity BCR variants are able to outcompete the antibodies that are already covering the antigen. Therefore, only higher affinity B cell variants are able to access antigen, phagocytose this, and present antigenic peptide to Tfh cells, that then would provide survival and differentiation signals. This model is capable of explaining a persistently increasing affinity selection threshold during the GC response, as antibodies in immune complexes on FDCs are continuously substituted by variants of antibody generated by GC-derived plasma cells with produce antibodies that with affinities that increase over the course of the GC response.

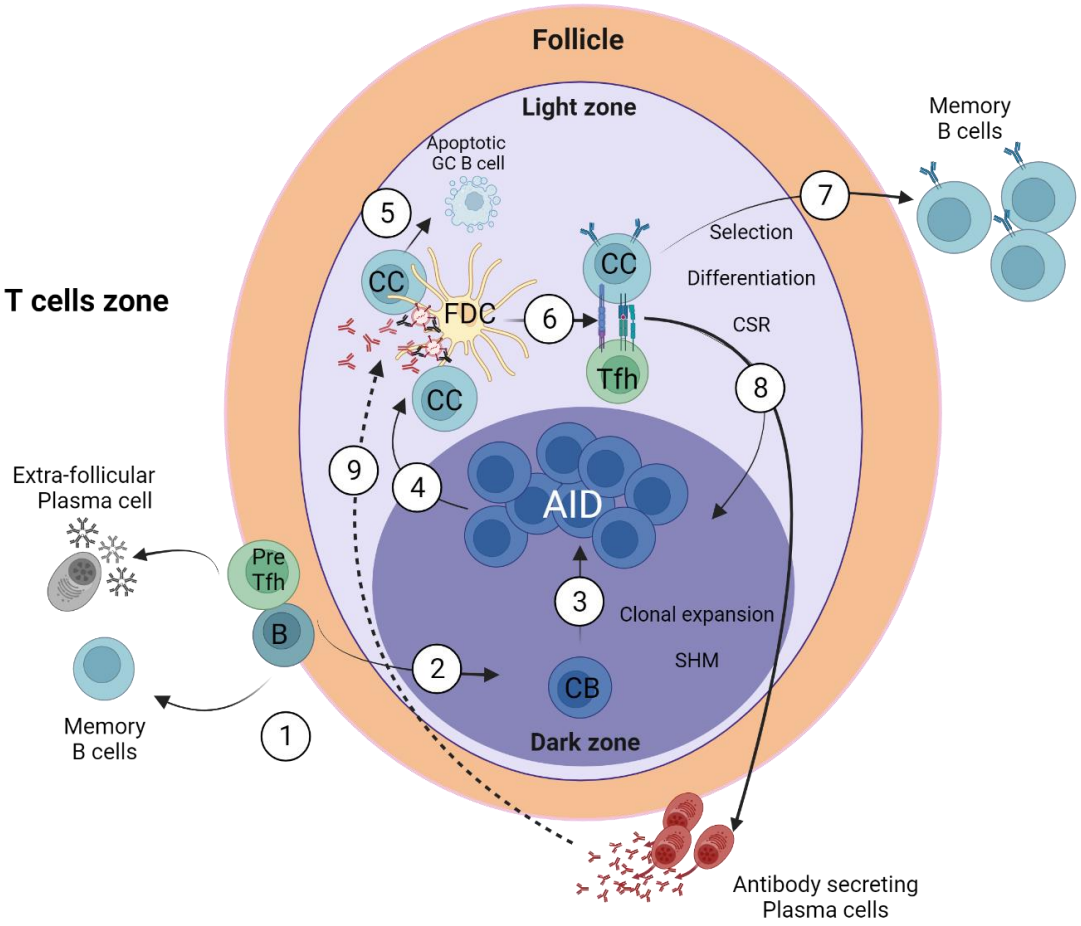

Figure 1.4 The structure of Germinal centre reaction.
(1) Activated B cells migrate to the T-B border in secondary lymphoid organs (SLOs) and receive help from cognate T cells. The B cells can then differentiate into extrafollicular plasma cells and a few memory B cells. (2) Alternatively, the activated B cells can undergo rapid proliferation and enter B cell follicles to start forming germinal centres (GCs). (3) Inside the GC dark zone, centroblasts undergo clonal expansion, and express activation-induced cytidine deaminase (AID) to initiate somatic hypermutation of their B cell receptors (BCRs). (4) B cell clones with successful mutations in their BCRs migrate to the GC light zone as centrocytes. Here they compete to test specificity of BCR by capturing antigens deposited on follicular dendritic cells (FDCs). (5) B cell clones that are not positively selected undergo apoptosis. (6) B cells with higher affinity BCRs can present more antigen to cognate follicular helper T cells (Tfh). (7) Positively selected B cell clones differentiate into memory B cells, (8) antibody-secreting plasma cells, or migrate back to the dark zone for further rounds of mutation and selection. (9) Antibody feedback: early extrafollicular antibody responses produce low-affinity antibodies (black), but these are replaced over time by high-affinity antibodies (red) generated from GC derived plasma cells. Adapted from (Zhang et al., 2016). Created by Biorender.

Table 1.1Chemokines involved in the formation and function of germinal centers within secondary lymphoid organs

Molecule	Source	Target Cells	Function
CXCL13 (BLC)	Follicular dendritic cells, stromal cells	B cells (CXCR5+), follicular helper T cells (Tfh, CXCR5+)	Attracts B cells and Tfh cells to follicles, promotes germinal center formation and maintenance
CXCL12 (SDF-1)	Stromal cells, endothelial cells	Centroblasts, centrocytes (CXCR4+)	Retains centroblasts and centrocytes within germinal centers
CCL19 (ELC)	Stromal cells, dendritic cells	Tfh cells (CCR7+)	Attracts Tfh cells to follicles, promotes Tfh-B cell interactions
CCL21 (SLC)	Stromal cells, endothelial cells	Tfh cells (CCR7+)	Attracts Tfh cells to follicles, promotes Tfh-B cell interactions
CXCL10 (IP-10)	Stromal cells, endothelial cells	CXCR3+ Tfh cells	Attracts CXCR3+ Tfh cells to germinal centers
CCL22 (MDC)	Follicular dendritic cells	CCR4+ Tfh cells	Attracts CCR4+ Tfh cells to germinal centers
CD80 (B7-1)	Activated B cells, dendritic cells	CD28 on T cells	Co-stimulatory signal for T cell activation and Tfh differentiation
CD86 (B7-2)	Activated B cells, dendritic cells	CD28 on T cells	Co-stimulatory signal for T cell activation and Tfh differentiation
ICOSL (B7-H2)	Activated B cells, dendritic cells	ICOS on Tfh cells	Co-stimulatory signal for Tfh cell differentiation and function
PD-L1 (B7-H1)	Germinal center B cells, dendritic cells	PD-1 on Tfh cells	Regulates Tfh cell function and germinal center responses
CXCR4	Centroblasts	CXCL12	Retains centroblasts and centrocytes within germinal centers
CXCR5	B cells, Tfh cells	CXCL13	Guides migration of B cells and Tfh cells to follicles and germinal centers

1.7.2. Role of T follicular helper cells in GC B cells selection and affinity maturation

Tfh cells are a crucial subsets of CD4+ helper T cells responsible for establishing and sustaining the germinal centre response (Crotty, 2011). CD4 T cells are primed by dendritic cells (DCs) through two signals: TCR engagement through antigen peptide fragments on MHC-II molecules and CD28 receptor binding to CD80 or CD86 ligands (Grakoui et al., 1999, Sharpe and Freeman, 2002). DC activation prompts primed CD4 T cells to adopt a distinct transcriptional profile with expression of Bcl6, directing them towards the Tfh cell fate (Crotty, 2011).

During interactions with DCs, the interaction of inducible co-stimulator (ICOS) on T cells by ICOS ligand (ICOS-L) on DCs, combined with cytokines like IL-6, IL-12, and TGF-β, initiates the initial stages of pre-Tfh differentiation. In mice, IL-6 and IL-21 trigger the activation of signal transducer and activator of transcription (STAT) 3, while in humans, IL-12, IL-21, IL-23, and TGF-β activate both STAT3 and STAT4 (Bossaller et al., 2006, Ma et al., 2009, Simpson et al., 2010). These activated STAT molecules migrate to the nucleus, where they trigger the activation of the key Tfh transcription factor, B cell lymphoma (Bcl-6) (Nurieva et al., 2009, Ma et al., 2009, Linterman et al., 2010). Bcl-6 is essential for Tfh cell differentiation as it suppresses the expression of transcription factors associated with other CD4+ T cell subsets, such as T-bet, GATA 3, RORγt, and Foxp3 (Nurieva et al., 2009). Bcl-6 could be repressed and inhibited by the transcription factor B-lymphocyte-induced maturation protein-1 (Blimp1) (Johnston et al., 2009), making it a critical factor in determining the effector cell fate of primed T cells.

Through interactions with activated B cells, pre-Tfh cells become fully GC Tfh cells. Moreover, Bcl6-driven Tfh programming changes the homing receptor profile of Tfh cells, enhancing

CXCR5 for migration towards CXCL13 and upregulating early EBI2 expression (Pereira et al., 2009, Cinamon et al., 2008, Allen et al., 2007a), directing pre-Tfh cells to the follicle. Essential cognate interactions at the T-B border promote both GC formation and Tfh cell development. Maintenance of these interactions relies on SLAM family members CD84 and Ly108, signalled by the intracellular adapter SAP (Crotty et al., 2003). Pre-Tfh and B cells exchange signals through CD40L/CD40 and ICOS/ICOSL, sustaining Bcl-6 expression. Fully committed Tfh cells enter the GC, crucially influencing GC B cell selection and survival (Elgueta et al., 2009, Linterman et al., 2014, Gigoux et al., 2009).

After centroblasts undergo SHM, centroblasts transition from the DZ to the LZ and scan the FDC network for antigens. GC B cells engage in affinity-based selection through interactions with Tfh cells (Allen et al., 2007). Upon binding antigens with their newly mutated BCRs, centrocytes process these antigens and present them via MHC-Class II to Tfh cells in the LZ (Batista and Neuberger, 2000). Centrocytes with higher affinity BCRs present more peptide:MHC to Tfh cells, gaining survival signals that outcompete lower affinity cells for T cell help (Meyer-Hermann et al., 2006, Allen et al., 2007b, Victora et al., 2010, Shulman et al., 2013). This selection enriches the population with high-affinity B cell clones. In the LZ, Tfh cells can provide essential signals via CD40/CD40L, ICOS/ICOSL ligation, and produced cytokine such as IL-21 and IL-4 (Linterman et al., 2010, Zotos et al., 2010). Because of central T cell tolerance, self-reactive BCRs should lead to presentation of antigens for which no cognate Tfh cells can be engaged. Absence of Tfh help would lead to apoptosis (Victora et al., 2010). Positively selected B cells re-enter the DZ for more SHM and proliferation, enhancing affinity maturation. These cells differentiate into long-lived antibody-secreting plasma cells or memory B cells (Allen et al., 2007b, Victora et al., 2010, Zhang et al., 2018).

1.7.3. Class switch recombination

Class switch recombination (CSR) has often been thought to take place within germinal centre B cells, because of the correlation of the GC reaction with the emergence of class switched cells. However, extensive research over the last 30 years showed that activated B cells start to switch before GC are formed (Toellner et al., 1996, Toellner et al., 1998). Class switch recombination (CSR) has often been thought to take place within germinal centre B cells, because of the correlation of the GC reaction with the emergence of class switched cells. However, extensive research over the last 30 years showed that activated B cells start to switch before GC are formed (Toellner et al., 1996, Toellner et al., 1998). This study examined the association between immunoglobulin class switch recombination and the production of germline IgCH messenger RNA (mRNA) transcripts. Specifically, they examined the levels of γ1 transcripts in mouse spleen sections during primary and secondary antibody responses to chicken gamma globulin (CGG). In the primary response to CGG, γ1 switch transcripts appeared 4 days after immunization. In contrast, after secondary challenge with CGG, a 7-fold increase in transcripts occurred within the first day, doubling by day 3 to reach a level 6 times the peak of the primary response. The rapid early rise in switch transcripts during the secondary response, occurring before antigen-specific B cells had completed their first cell cycle, suggests that switching is closely associated with the cognate interaction of these cells with primed T cells in the outer T zone. The lower transcript levels seen later, as the antigen-specific B cells proliferate in extrafollicular foci or GC, indicate that switching also occurs in these other sites but to a low level (Toellner et al., 1996, Roco et al., 2019). The purpose of CSR is to alter the effector function of immunoglobulin (Ig) while maintaining the same antigen specificity. The AID enzyme is not the only factor required for both CSR and SHM (Muramatsu et al., 2000).

CSR is a DNA deletional-recombination reaction that involves specific genetic regions known as switch (S) regions upstream of constant (CH) gene segments. The process proceeds through the generation of double-strand breaks (DSBs) in the switch regions, which are followed by non-homologous end joining (NHEJ) between donor and acceptor S regions. The S regions are specific DNA sequences located upstream of each CH gene containing recognition sites for AID, which initiates the DNA breaks. Upon generating two breaks—one at the Sμ region and another at the targeted switch region (Sγ, Sα, or Sε)—the excised DNA sections are connected at their ends, forming an extrachromosomal switch circle (Figure 1.5 A). This action leads to the permanent excision of one or more C-regions located between the VDJ region and the target isotype. The remaining two chromosome segments are fused by proteins associated with the DNA damage response mechanism (Manis et al., 2002, Honjo et al., 2002). As a result, the variable region is brought nearer to the targeted constant region. This VDJ arrangement ensures that the B cell and its offspring exclusively produce the antigen- specific antibodies, enhancing the immune response's specificity and efficacy.

Mature naïve B cells express IgM and IgD, which originate from the two most upstream segments of the immunoglobulin heavy chain locus. Exposure to antigens activates B cells through BCR stimulation followed by further signals from T helper cells. These signals involve interactions like CD40 and engagement of cytokine receptors. Cytokines can direct B cells to switch to specific antibody classes. Different cytokines guide B cells toward switching to IgG, IgA, or IgE classes and subclasses. For example, IL-4 in mice promotes switching to IgG1 and IgE, whereas INF-γ induces switching to IgG2a, while IL-5 induces switching to IgA (Hodgkin et al., 1996, Rush et al., 2005, Toellner et al., 1996, Coffman et al., 1993).

1.7.4. Antibodies

A fundamental component of the adaptive immune response is humoral immunity, which is orchestrated through immunoglobulins (Igs) or antibodies. Antibodies consist of two identical heavy (H) chains and two identical light (L) chains. The light chain can be kappa (κ) or lambda (λ) class (Figure 1.5 B). The light chain structural properties allow for more variability within the antigen-binding domain, boosting the antibody's ability to engage with various types of antigens.

The numbers of V, D, and J gene segments vary between species. The H-chain gene segments are found on chromosome 12 in mice and on chromosome 14 in humans. The gene segments for the κ L-chain and λ L-chain are situated on chromosomes 2 and 22, respectively (de Bono et al., 2004, Dunn-Walters et al., 2018). During B cell maturation, V(D)J recombination is a crucial DNA recombination event that forms a specific combination, ensuring that each individual B cell exclusively generates a particular combination of three gene segments (V, D, and J). The L-chain undergoes a similar process involving the selection of one V and one J gene segment. The L-chains are bound to the H-chains by many noncovalent and disulfide bonds.

Dependent on the antibody class, the C-region of H-chains interacts with different types of Fc receptors (FcR) expressed on various immune cells and complement proteins with varying affinity. There are five distinct subclasses of human and mouse antibodies (IgM, IgD, IgG, IgA, and IgE), which use different C-region genes (Figure 1.5 C). During B cell development, IgM is the first type of antibody expressed, and serves as the initial B cell receptor on the surface of naïve B cells. Being expressed by naïve B cells, IgM is the first class of antibodies produced in the early immune response during primary infection. IgM is secreted in a pentameric form with 10 antigenic binding sites. This increases the avidity for antigen, even though the individual antigen-binding sites may be low affinity. Upon binding to antigens, IgM is

particularly efficient through its interaction with C1q and activation of the classic pathway of the complement system (Nimmerjahn and Ravetch, 2005, Murphy et al., 2008). The role of IgD in humoral immune responses is still unclear. IgD is expressed on the surface of naive, immature B cells along with IgM, and less commonly secreted. Follicular B cells have high expression of both IgD and IgM, which serve as antigen receptors. Upregulation of IgD occurs during the transition of immature to mature B cells within the marginal zone of the secondary lymphoid organ (Pillai and Cariappa, 2009b). IgG, the most abundant antibody in serum, exists in different subclasses, each with distinct properties and functions. In humans, there are four main subclasses of IgG antibodies: IgG1, IgG2, IgG3, and IgG4 (Salfeld, 2007). Human IgG1 leads to a variety of events, including the ability to bind the C1q component of the complement cascade, depending on the receptor or protein bound, leading to activation of the classical complement pathway, and crosslink IgG1-antigen complexes on target cells with Fc gamma receptors (FcRs), which activates immune cells (e.g. macrophages) to induce antibody-dependent cell-mediated cytotoxicity (ADCC). IgG antibodies can trigger cytokine production in various human cell types. Among these, the production of proinflammatory cytokines such as TNF, IL-1β, and IL-23 by myeloid immune cells is strongly influenced by IgG1, and even more so by IgG2 (Hoepel et al., 2020). Like IgG1, all FcRs are recognised by human IgG3, which promotes potent antibody-dependent cellular cytotoxicity and immune-mediated cell death. Additionally, IgG3 has a high-affinity interaction with C1q that activates classical and alternative pathways of the complement cascade (Izadi et al., 2023). IgG4 is the least abundant subtype, comprising around 4% of total IgG in serum, with the lowest binding affinity for FcRs, which reduces its potential to trigger inflammatory responses, making it less efficient at ADCC. IgG4 is generated by class switching from more upstream IgG subtypes in response to repeated or chronic antigen exposure, which is often associated with immune

tolerance to allergens (Vidarsson et al., 2014). Mice have the four IgG subclasses IgG1, IgG2a, IgG2b, and IgG3. Mouse IgG1 binds weakly to the activating FcRI, FcRIII, and FcRIV receptors on monocytes, macrophages, neutrophils, and other phagocytic cells (Neuberger and Rajewsky, 1981). IgG1 in mice has a higher affinity for inhibitory FcRIIB than IgG2a and IgG2b, allowing it to exert more anti-inflammatory effects. Whereas IgG2a and IgG2b strongly bind activating FcRs (FcRI, FcRIII, and FcRIV), allowing them to trigger the classical complement pathway and clearing pathogens through opsonisation (Nimmerjahn and Ravetch, 2005). Additionally, production of IgG2a/b isotype antibodies has been reported in *Salmonella Typhimurium* (STm) infection, where it is induced by a strong Th1 response within 5 to 7 days after infection (Cunningham et al., 2007). Dimeric IgA is the predominant form secreted across mucosal membranes. Hence, IgA provides immune protection by neutralising pathogens and toxins before they can invade the body's mucosal surfaces, such as the gut and lung (Woof and Kerr, 2006). IgE is a key antibody for parasitic immunity, but also mediates hypersensitivity reactions in allergies by triggering mast cell and basophil activation (Abramson and Pecht, 2007). The strategic advantage of multiple antibody isotypes and subclasses is that they provide the immune system with a variety of antibodies with different effector functions suited for responses against different types of pathogens, whether bacterial, viral, fungal, or parasitic. This repertoire of antibodies with specific effector activities is critical for broad protection to different pathogens.

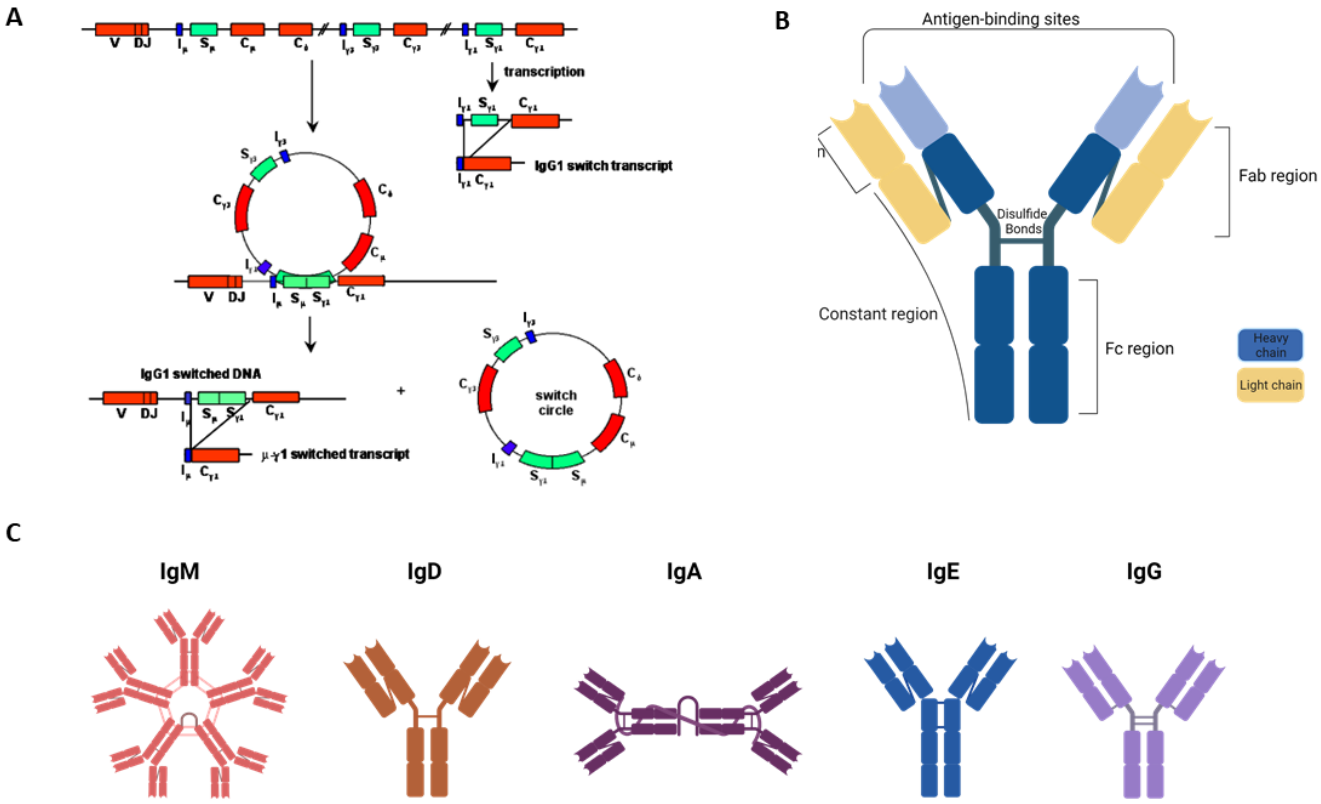

Figure 1.5 The mechanism of CSR and structures of antibodies classes.
(A) CSR showed by the switching to IgG1. Transcription from Iγ1 locus produces a germline switch transcript, which is spliced by looping out intervening DNA, resulting in a switch circle and a rearranged heavy chain transcript. (B) The basic structure of an antibody molecule comprises two identical heavy chains (shown in blue) and two identical light chains (shown in yellow). These chains are inter-connected by disulfide bonds. Each heavy and light chain is composed of constant and variable domains. The variability in the variable domains located in the Fab region enables the binding of antigens. The Fc region facilitates the interaction of immune complexes with other immune cells like phagocytes (e.g. macrophages, NK cells) and complements. (C) The five main classes of antibodies (immunoglobulins): IgM, IgD, IgA, IgE, and IgG. (A, Taken from Prof. K-M Toellner. B-C Created by Biorender)

1.7.5. Outputs of germinal centre

After undergoing affinity-based selection in the GC, GC B cells that have acquired higher-affinity BCRs can differentiate into either plasma cells (PC), which secret high affinity antibody(Nutt et al., 2015), or memory B cells (Bmem), which are capable of producing high-affinity antibodies up on re-encounter of antigen (Suan et al., 2017a) . PCs, defined by their specific regulatory patterns by downregulation of CD19, IgM, IgD, B220, and by upregulation of CD138, can be long-lived or short-lived depending on their origin. PCs from FOB cells are usually long-lived, while those from B1 cells, MZ B cells, or extrafollicular reactions have shorter lifespans (Sage et al., 2019, Nakagawa and Calado, 2021). Plasmablasts (PBs), are short-lived proliferating ASCs with reduced antibody secretion and retained CD19 expression (Vijay and Singh, 2021).

High affinity B cells that differentiate into PC or Bmem cells return to the DZ to undergo further of proliferation and SHM. This process results in PCs with even higher antigen affinity and prolonged longevity (Nakagawa and Calado, 2021). The strength of the BCR signalling is directly proportional to IRF4 expression, predisposing GC cells to differentiate into PBs/PCs (Ochiai et al., 2013). Enhanced T cell assistance and CD40 signalling lead to the production of IL21, promoting the differentiation of LZ B cells into PCs and facilitating migration into the DZ (Ding et al., 2013, Zhang et al., 2018). The most elevated IRF4 expression is observed in LZ plasma cells with relatively higher antigen affinities. IRF-4 promote GC fate, and its upregulation at high level facilitate PC differentiation by repressing Bcl-6 and inducing Blimp-1 expression (Nutt et al., 2015). PBs/PC with high IRF4 expression are observed at the GC-T zone border, where GC-T interface reticular cells (GTIRCs) produce A Proliferation-Inducing Ligand (APRIL) and IL6, and chemokine CXCL12, suggesting that PCs migrate out from DZ, and through DZ-T interface (Zhang et al., 2018).

Blimp-1 (B lymphocyte-induced maturation protein-1) is a master transcriptional regulator of plasma cell differentiation. It drives the transformation of activated B cells into antibody-secreting plasma cells (Angelin-Duclos et al., 2000, Minnich et al., 2016). Blimp-1 represses a variety of GC B cells genes. For instance, it represses BCL6, a master regulator of germinal centre B cells, and PAX5. This transcription factors maintain cells in the B cell lineage. c-Myc are associated with cell proliferation in DZ (Lin et al., 2002, Lin et al., 1997, Saito et al., 2007). c-Myc expression is restricted in a small number of LZ B cells, and is expressed during LZ B cell selection (Dominguez-Sola et al., 2012, Calado et al., 2012).

After B cells have been selected within the GC, a subset of B cells undergoes a fate decision towards the formation of memory B cells. These memory B cells can mount a rapid, high affinity response to antigen upon re-exposure in comparison to those produced by the naive B cells, leading to a more rapid and robust immune response compared to the primary response. Reactivated memory B cells undergo differentiation into antibody-secreting cells or GC B cells during the recall response. CD27 is a cell surface marker commonly used to identify memory B cells in humans (Tangye et al., 1998). Unlike human, the initial classification of memory B cell subpopulations in mice was based on Ig expression. Bmem cells that express IgG produce antibodies, whereas IgM-expressing B cells initiate GC reactions (Dogan et al., 2009). Regardless of the Ig isotype, CD80 and PD-L2 act as functional markers to identify high affinity memory B-cell subsets. While $CD80^{-}$ $PD\text{-}L2^{-}$ Bmem develop into GC B cells, those $CD80^{+}PD\text{-}L2^{+}$ Bmem are more likely to evolve into antibody-secreting cells during the recall response (Zuccarino-Catania et al., 2014). Bmem cells precursors are defined by high CCR6 expression. CCR6 has a critical role of in the detection of HEL-specific low-affinity BCRs on precursor cells within GC light zones (Suan et al., 2017a). According to a transgenic mouse model study called *S1pr2*^{CreERT2} BAC-transgenic, the development of Bmem cells is more likely

in light zones with lower-affinity BCRs (Shinnakasu et al., 2016). The transcriptional repressor BACH2, which has an inverse correlation with T cell strength, was expressed frequently by these memory B cells, thus, the B cell will receive minimal or no assistance from T cells when it encounters an antigen. This supports the idea that T cells may affect BACH2 expression, causing B cells to differentiate into memory B cells (Shinnakasu et al., 2016). When tracking the fate of antigen-specific B cells in C57BL/6 mice post-immunization, both IgM+ and isotype-switched immunoglobulins (swIg+) memory B cells are generated. However, during secondary response, IgM^+ memory B cells were more abundant and had greater longevity. SwIg+ memory B cells dominated in the response, generating plasma cells and new memory B cells but not contributing to GC B cell formation (Pape et al., 2011). Bmem cells can indeed be triggered by T cell-independent type II polysaccharide antigens. However, these GC-independent Bmem exhibit little SHM and isotype switching, and often secret IgM (Obukhanych and Nussenzweig, 2006).

1.7.6. Memory B Cell Recall Response

Memory B cells rapidly proliferate and produce high levels of antibodies when they re-encounter the pathogens they were previously exposed to, a process known as the memory recall response.

For the recall response to begin, antigens are presented to Bmem by FDCs. These antigens are bound either to complement receptors CD21/CD35 or to FcγRIIB through immune complexes(Qin et al., 2000, Barrington et al., 2002). MBCs then take up the antigens and present peptides on MHC class II molecules, which are recognized by memory T helper (Th) cells through their T-cell antigen receptors (TCR). The TCR signal, along with co-stimulation from ICOS, activates the Th cells. In turn, the activated Th cells stimulate Bmem through CD40L and certain cytokines, promoting MBC proliferation and differentiation(Shimoda et al.,

2006, Mahajan et al., 2007). Recent findings show that Bmem reside in a subcapsular niche with Tfh cells in lymph nodes. Upon recognizing antigens on subcapsular sinus macrophages, Bmem either proliferate and differentiate into plasma cells in the subcapsular proliferative foci or become GC B cells in the recall response(Moran et al., 2018).

Negative regulation of the Bmem recall response also plays an important role. The inhibitory receptor gp49B, which is selectively expressed on Bmem and MZ B cells, suppresses their differentiation into plasma cells and production of antibodies, including IgE. This helps prevent excessive or autoimmune-like responses(Fukao et al., 2014). Recognition of repetitive, T cell-independent type II antigens can also tolerise high-affinity, IgG+ Bmem, further protection against autoantibody production(Haniuda et al., 2011).

The cytokine IL-9 has also appeared as an important positive regulator of MBC responses. IL-9 receptor is selectively expressed on Bmem, and IL-9 signalling promotes the expansion and plasma cell differentiation of MBCs during the recall response(Takatsuka et al., 2018). In contrast, IL-21, a signature cytokine of T follicular helper cells, appears to be dispensable for MBC generation and recall(Rankin et al., 2011).

1.8. Thesis aims.

Antibody feedback is an efficient mechanism to select for the highest affinity B cells during an immune response. We hypothesize that when high/intermediate low affinity anti-NP IgM^a antibodies are injected, they can outcompete and limits the availability of antigenic epitopes to B cells during selection in germinal centres. In the current thesis, we test the effects of antibody on GCs by using mouse strains that either are unable to secrete IgM nor class switch (IgMi mice), not affinity mature nor class switch (AIDKO), or only generate and secrete IgG1 (IgG1M). By injecting high and intermediate/low affinity anti-IgM antibodies into these strains, we can evaluate how antibody feedback modulates germinal center B cell selection and differentiation when specific aspects of the antibody response like isotype switching or somatic hypermutation. And to identify B cell responses in altered B cell receptor (BCR) signalling mouse models (IgMg1 and IgG1M mice) as a means to model T-dependent antigen responses. These mice, along with WT controls, were crossed with Nr4a3-Tocky mice to evaluate the impact of modulated BCR signals on the development of T follicular helper (Tfh) cells.

The general aims of this thesis are:

1. Analysis and characterisation of GC and Tfh cells within different models of mice.
2. Test the roles of IgM in antibody feedback in the germinal centre response in wildtype (WT), AIDko and IgMi mice.
3. Test whether random mutation affects GC B cell fitness using WT B cells transferred into AID wt or ko mice.
4. Analysis of B cell responses and evaluation of Tfh cell stimulation at different time points and with varying times of boosting with soluble antigen before culling the mice.

This will model T cell-dependent antigen responses in IgMg1, IgG1M-Nr4a3-Tocky mice.

5. Analysis of B cell responses to T cell-dependent antigens and evaluation of Tfh cell after stimulation with soluble antigen in AID knockout Nr4a3-Tocky mice.
6. Preliminary analysis of Nur77-Tempo mice to test for any function of the Nr4a1 gene following B cell responses.

Chapter 2. Materials and Methods

2.1. Mouse strains

All mice used in experiments were housed and bred under specific pathogen-free conditions at the Biomedical Service Unit (BMSU), University of Birmingham. All animal experiments were approved by University of Birmingham Ethnics Committee AWERB (Animal Welfare Review Board) and were carried out according to Home Office UK regulations under project license PP8702596. AID knockout mice or AID heterozygous mice, referred to as AIDcre/wt in this thesis, were used as controls and have been previously described (Muramatsu et al., 2000). IgHγ1μ mice, referred to as IgG1M mice in this thesis, have been previously described by (Waisman et al., 2007). IgMi mice were bred on a C57BL/6 background and have also been previously described by (Waisman et al., 2007). For adoptive transfer experiments, QM (Cascalho et al., 1996b) mouse were crossed with Cγ1Cre and mTmG mice, heterozygous for an NP-specific and Cre-inducible eGFP reporter (IgHNP/Cγ1 x mTmG) (Casola et al., 2006, Muzumdar et al., 2007, Zhang et al., 2022). C57BL/6N mice were used as wild type (WT) controls (Bred in house). Nr4a3-Tocky mice and Nr4a1-Tempo mice were kindly provided by Dr David Bending at the University of Birmingham (Bending et al., 2018, Elliot et al., 2022). IgMg1 mouse was generated by Medimmune (Lingling Zhang 2019 Thesis). Nr4a3-Tocky mice were bred with AIDko, AIDcre/wt, IgMg1/g1, IgG1M/G1M, and WT mice to generate mice homozygous for the Nr4a3-Tocky allele. Nr4a1-Tempo mice were bred with IgMg1 mice or WT mice heterozygous for the IgM allele to generate mice heterozygous for the Nr4a1-Tempo allele.

All mice used were aged 8-18 weeks old. Experimental groups were sex and age matched as closely as allowed by availability of mice. At the end of experiments, mice were humanely culled by cervical dislocation. If serum required, mice were anesthetized and blood was

collected by cardiac puncture. Tissues collected for analysis included the spleen and popliteal lymph nodes.

2.2. Immunisation

For GC response to T-dependent antigen. Mice were immunised intraperitoneally (i.p) with 50µg with either NP_{24}-Keyhole limpet hemocyanin (KLH) (Biosearch, cat: N-5060-5) or NP_{18}-chicken gamma globulin (CGG) (made in house) or NP-Ovalbumin (NP-OVA) (Biosearch) were precipitated in alum plus $5x10^7$ heat inactivated *Bordetella pertussis* in total volume of 200 µL. Mixtures were prepared by adding one-part of antigen to one-part 9 % aluminium hydroxide (alum). The pH of the mixture was adjusted to 6.5 using NaOH. The mixture was then rotated for an hour in a dark at room temperature. Next, sterile pH 7.4 1x phosphate buffered saline (PBS) was used to wash the mixture twice. Re-suspension of the precipitated antigen was performed in PBS to a final volume of 200 µl/mouse.

For immune complex experiment, mice were immunised with 10µg NP_{18}-CGG mixed with 90µg low avidity anti-NP IgM^a (clone Fab82) via intravenously (i.v)(Zhang et al., 2013). The immune complex was prepared one hour before injection. Or at day 8 mice were injected i.v with 90 µg either soluble antibody anti-NP IgM^a (clone Fab82) developed from QM mouse or high avidity (clone 1.197) from B1-8hi mouse.

In ongoing GC response experiment, mice immunised i.p with 50 µg with NP_{18}-CGG precipitated in alum plus $5x10^7$ heat inactivated *Bordetella pertussis*, and then at day 10 mice were injected i.v with 90µg intermediate low avidity antibody (clone 2.315) developed from B1-8 mouse.

All the hybridoma cell line work and production of anti-NP antibodies were performed by Dr.Margaret Goodall in University of Birmingham.

In Nr4a3-Tocky and Nr4a1-Tempo mice were immunised subcutaneously on the plantar surface of one foot with 10µg of NP_{21}-KLH (Made in house) precipitated in alum in total volume of 20 µL. For re-challenged to boost TCR signalling, mice were injected with 10ug of soluble NP_{21}-KLH in sterile PBS in plantar surface of the same foot.

2.3. Preparation of NP-conjugation

1. Dissolve KLH powder (Merck Millipore 374805-250MG) or BSA powder (Sigma A7906-100G) in freshly prepared 0.2 M sodium bicarbonate (NaHCO3) (Sigma 55761-1KG) solution at a concentration of 2 mg/mL.
2. Dissolve 4-Hydroxy-3-nitrophenylacetic acid succinimidyl ester (NP-OSu)(Biosearch N-1010) in dimethyl sulfoxide (DMSO)(Sigma D4818-50ML).
3. Add the NP-OSu solution dropwise to the protein solution while stirring continuously.
4. Incubate the mixture for 2 hours at room temperature on a rotator, protected from light.
5. Set up a 10K molecular weight cut-off Slide-A-Lyzer dialysis cassette (Thermo Scientific).
6. Dialyze the protein solution against the following buffers at 4°C, protected from light:
    a. 3x buffer changes with NaHCO3
    b. 2x buffer changes with phosphate-buffered saline (PBS) (Gibco 18912-014) at pH 7.45
7. After dialysis, recover the protein solution, measure the protein concentration by the Pierce bicinchoninic acid (BCA) Protein Assay kit.
8. Measure the absorbance of the protein solution at 430 nm by a Nanodrop 1000 (Thermo Scientific).
9. Calculate the concentration of NP by the absorbance value and Beer's law.

$$\text{Concentration (M)} = \frac{\text{absorbance at 430 nm}}{\varepsilon \times L} = \frac{\text{absorbance at 430 nm}}{4230\ \text{M}^{-1}\ \text{cm}^{-1} \times 1\ \text{cm}}$$

10. Determine the conjugation ratio by calculating the ratio of the molar concentration of NP (from step 10) to the molar concentration of the protein (from step 8).

2.4. Checking antibody avidity by BiaCore system

The BiaCore system employs surface plasmon resonance (SPR) technology as a detection approach to quantify and monitor the real-time interaction between NP protein conjugates and anti-NP antibodies.

1. Immobilize NP15-BSA onto the sensor chip surface via amine coupling:
    a. Activate the carboxyl groups on the sensor chip using a mixture of EDC (0.4M 1-ethyl-3-(3-dimethylaminopropyl)-carbodiimide in water) and NHS (0.1M N-hydroxysuccinimide in water) to form reactive succinimide esters.
    b. Inject NP15-BSA ligand (prepared in acetate buffer, pH 4) over the surface at a flow rate of 5µl/min for 30 minutes at 25°C to allow the esters to react with primary amines, covalently linking the ligand.
    c. Inject ethanolamine (1M ethanolamine-HCL pH 8.5) to deactivate any remaining reactive groups.
2. Prepare antibody samples by diluting antibodies to various concentrations ranging from 15.625µM to 2mM in degassed PBS.
3. Set up the BiaCore system for SPR analysis:
    a. Maintain the temperature at 38°C throughout the experiments.
    b. Set the flow rate to 5µl/second.
4. Inject each antibody dilution over the NP15-BSA immobilized surface for 1800 seconds (30 minutes).

5. Measure the background response by injecting the analyte over a flow cell containing immobilized BSA.
6. Subtract the background response from the sensorgram obtained for the NP15-BSA surface.
7. Analyze the sensorgram data by BIAevaluation software (version 3.2RC1) to evaluate antibody affinity and binding kinetics.

2.5. Adoptive cell transferred

Single cell suspensions of splenocytes were prepared in RPMI-1640 media (Sigma) under sterile conditions. Red blood cells were lysed by incubating with ACK lysing buffer (Gibco) for 3 minutes on ice. The reaction was stopped by adding 3 ml of RPMI-1640 media. Cells were stained with NP conjugated to APC (made in-house) to detect NP-specific B cells by flow cytometry.

2x10^5 NP+B220+ splenocytes from QM Cγ1Cre mTmG mice (Zhang et al., 2022) were transferred intravenously i.v into AIDcre/cr or AIDcre/wt recipient mice one day prior to immunisation. Recipient mice were immunized with 20µg NP-KLH in alum precipitation on the plantar surface of one rear foot.

2.6. Flow cytometry

2.6.1. Single cells preparation and surface marker staining

Freshly isolated spleens or lymph nodes were used to prepare single cell suspensions in RPMI-1640 media (Sigma) supplemented with 1% penicillin/streptomycin (Invitrogen) and 10% fetal calf serum (GIBCO 21875-034). Spleens were gently mashed and strained through a 70 µm cell strainer (BD Biosciences). Lymph nodes were minced using 25-gauge needles (Terumo) and filtered through 70 µm cell strainers. Cells were centrifuged at 1400 rpm for 3 minutes at

4°C and resuspended in FACS buffer (1% fetal calf serum and 5mM EDTA in sterile PBS). All steps were performed on ice (4°C) to prevent cell activation.

For cell surface staining, approximately 1 x 10^6 cells per stain were aliquoted into 250 µl 96-well V-bottom plates in 100 µl FACS buffer. Cells were incubated with Fc block (anti-CD16/32, Thermo Fisher Scientific) to block non-special binding for 20 minutes before adding fluorescently-labelled antibody cocktails. Surface marker antibodies were added and incubated for 20 minutes in the dark in fridge. For biotinylated antibodies, a second 20-minute incubation with streptavidin conjugate was performed. Fixable near-IR live/dead stain (Thermo Fisher Scientific L10119) was added and incubated for 20 minutes. Cells were washed twice with 200 µl FACS buffer in between incubations and centrifuged at 1400 rpm for 3 minutes at 4°C.

For Tfh cell staining, cells were incubated with purified anti-rat CXCR5 (BD Biosciences, Clone 2G8, Cat 551961) for 60 minutes in fridge, followed by donkey anti-rat AF647 secondary antibody for 30 minutes. Cells were then incubated with 10% normal rat serum (Sigma R9759-5ML) for 20 minutes to block non-specific binding, and finally stained with fluorescence-conjugated antibody cocktails for 20 minutes as described above.

Cells were acquired using a BD LSR Fortessa X20 flow cytometer (BD Biosciences) and analysed with FACSDiva software. FlowJo software (BD Biosciences, version 10.8.1) was used for data analysis.

2.6.2. Antibodies used for cell surface marker

Table 2.1 Flow cytometry surface marker antibodies

Marker	Conjugate	Clone	Supplier	Catalogue No.	Stock Conc.	Dilution
B220	BUV395	RA3-6B2	BD Biosciences	563793	0.2 mg/ml	1/800
CD3	BUV395	17A2	BD Biosciences	740268	0.2 mg/ml	1/400
CD3	FITC	145-2C11	eBioscience	11-0031-82	0.2 mg/ml	1/200
CD4	BV421	GK1.5	Biolegend	100438	0.2 mg/ml	1/400
CD4	FITC	GK1.5	eBioscience	11-0041-85	0.2 mg/ml	1/200
CD11b	BV510	M1/70	Biolegend	101245	0.2 mg/ml	1/400
CD19	BUV737	1D3	BD Biosciences	612781	0.2 mg/ml	1/800
CD38	BUV737	90	BD Bioscience	741748	0.2 mg/ml	1/1000
CD44	PerCPCy5.5	IM7	eBioscience	45-0041-82	0.2 mg/ml	1/300
CD44	Alexa700	IM7	Invitrogen	36-0441-82	0.2 mg/ml	1/300
CD62L	BV510	MEL-14	Biolegend	104441	0.2 mg/ml	1/300
CD86	BV421	GL1	BD Bioscience	564198	0.2 mg/ml	1/200
CD86	PE-Cy5.5	GL1	Biolegend	12-0862-82	0.2 mg/ml	1/200
CD86	Alexa700	GL1	Biolegend	105024	0.2mg/ml	1/200
CD95 (Fas)	BV605	Jo2	BD Biosciences	740367	0.2 mg/ml	1/300

CD95 (Fas)	PE-Cy7	Jo2	BD Biosciences	557653	0.2 mg/ml	1/300
CD138	BV711	281-2	Biolegend	142519	0.2 mg/ml	1/300
CD138	BV711	281-2	BD Biosciences	563193	0.2 mg/ml	1/300
CXCR4	Biotin	2B11	eBioscience	13-9991-82	0.2 mg/ml	1/200
CXCR5	purified	2G8	BD Biosciences	551961	0.5 mg/ml	1/125
IgG1	APC	X56	BD Biosciences	550874	0.2 mg/ml	1/500
IgG1	PerCPCy5.5	RMG1 1	eBioscience	406612	0.2 mg/ml	1/500
IgM	PE-Cy5	II/41	eBioscience	15-5790	0.2 mg/ml	1/600
IgM	PE-Cy7	RMM-1	BD Biosciences	406514	0.2 mg/ml	1/200
IgM	FITC	Polyclonal	Southern Biotech	1021-02	0.2 mg/ml	1/100
NP	APC	NA	NA	In house	0.63 mg/ml	1/600
NP	PE	NA	NA	In house	0.32 mg/ml	1/600
PD1	PE	J43	eBioscience	12-9985-82	0.2 mg/ml	1/200
PD1	PE-Cy7	29F.1A12	Biolegend	135215	0.2 mg/ml	1/200
Streptavidin	BV510	NA	Biolegend	405233	0.2 mg/ml	1/500

2.6.3. Buffers and media

Table 2.2.2 Details of buffers and media used in flowcytometry

Buffer	Components	Concentration	Supplier	Catalogue No.
Flow cytometry Buffer (FACS Buffer)	1xPBS FBS EDTA	 2% (v/v) 2mM	Sigma Sigma Sigma	D8537-500ML F9665-500ML E7889-100ML
R10 medium	RPMI 1640 (with L-glutamine) FBS Pen/Strep HEPES buffer	 10% (v/v) 100 U/mL (1X) 20 mM	Gibco Sigma Gibco Sigma	21875-034 F9665-500ML 15140-122 H0887-100ML
ACK Lysis buffer	(Ammonium chloride) (Potassium bicarbonate) (Disodium EDTA)	0.15 M 0.01 M 0.0001 M	Gibco	11509876

2.7. Determining levels of serum antibody

2.7.1. Serum collection and preparation

The mice were anaesthetized using O2 and Isoflurane before blood was collected by cardiac puncture. The blood samples were then incubated for 1 hour at 37°C in an incubator. Subsequently, they were subjected to centrifugation at a speed of 21,100 x g for 5 minutes. The supernatant was then collected and stored in a freezer at a temperature of -20°C until further required.

2.7.2. Enzyme-linked immunosorbent assay (ELISA)

For the detecting of NP-specific antibodies at a range of affinities, 5 µg/ml of NP_{15}-BSA was used to coat flat-bottomed Nunc immunosorb 96-well plates (Thermo Fisher 442404). Similarly, detection of NP-specific antibodies of high affinity was accomplished by coating the 96 well plates with 100 µl of NP_2-BSA (made in house). Solutions of both were made in coating buffer at concentrations of 5 µg / ml as detailed in (Table 2.2). The plates were washed three times in buffer followed by the addition of blocking buffer (200 µl). Plates were then incubated at 37°C for 60 min. The plates were washed in buffer. Serum was added at starting dilutions of 1/100 and then diluted in tripling dilutions using dilution buffer (Table2.2). The plates were once again incubated at 37°C for 60 min prior to washing three times using wash buffer. Next, 100 µL of the alkaline phosphatase (AP) conjugated antibody goat anti-mouse IgG1 AP (Southern Biotech) was added (diluted at 1/1000 in dilution buffer) and left at 37°C for 60 minutes and followed with three washes prior to adding substrate solution (100 µl). These were left to develop in an incubator at 37°C followed by absorbance measurement at 405 nm over a period of 20 to 30 minutes by using Spectramax ABS PLUS (Molecular Devices). The positive and negative control sera were used to plot standard calibration curves.

Table 2.3 List of Buffers used for ELISA and formula

Reagents	Formula and supplier
Coating Buffer	0.015 M Na2CO3, 0.035 M NaHCO3 at pH 9.6
Washing Buffer	1x PBS , 0.05 % Tween20 (Sigma)
Blocking Buffer	1xPBS + 1 % BSA (Sigma)
Dilution Buffer	1x PBS , 1 % BSA , 0.05 % Tween20 (Sigma)
Substrate	p-Nitrophenyl phosphate (NpNN-N2770 Sigma)

2.8. Statistical analysis

Statistical analyses were conducted using FlowJo v10 to analyse flowcytometry data and Graphpad Prism software (version 9.4.0) to generate data in graphs style. Data are stated as mean values ± standard error. The specific statistical test applied depended on the number of groups being compared and whether the data consisted of matched samples or categorical distributions as described in the figure's legends. For comparing two groups, a two-tailed T-test was used. When comparing two or more classes being assessed within each group across multiple groups, a two-way ANOVA with Tukey's test or a mixed-effects analysis with Šídák's test for matched data was applied. The statistical tests were performed on the log-transformed numbers if data were presented on a logarithmic scale.

Chapter 3. Characterisation of germinal centre and Tfh population and the effect of antibody in different model of mice

3.1. Introduction

The immune response to T-dependent antigens involves a gradual improvement in the affinity of antigen-specific antibodies. This process is facilitated by somatic hypermutation and the selection of B cells undergoing proliferation and differentiation within germinal centres (GCs). B blasts within GCs undergo rapid proliferation and mutations within their immunoglobulin genes, which results in the production of B cell receptors with a diverse spectrum of affinity towards the antigen (MacLennan, 1994, Victora and Nussenzweig, 2012). B lymphocytes with the greatest affinity for a specific antigen are chosen for differentiation into plasma cells, which can have prolonged lifespans. GC-derived memory B cells are less stringently selected for affinity (Suan et al., 2017b).

Predominantly expressed on the surface of specific mature B cell subsets, such as marginal zone and follicular B cells, is the complement receptor CR1/2. The CR2 receptor functions as a receptor that does not directly engage with antigens, but rather interacts with immune complexes (ICs) classically comprised of antigen–antibody, and then facilitates their transportation to follicular dendritic cells (FDCs) (Corley et al., 2005, Cinamon et al., 2008). During the germinal centre reaction, B cells that possess specificity for the antigen engage in interactions with antigens that are presented in ICs present on FDCs. This interaction leads to the induction of affinity maturation in B cell receptors by somatic hypermutation, hence enhancing their ability to bind to antigens (MacLennan, 1994). Antibody feedback regulates GC B cell selection through competition of antibodies depositing on immune complexes on FDC with mutated GC B cells. GC dynamics and affinity maturation have been reported to be

impacted after passively administering soluble antibodies by masking the antigen presented by FDCs and limiting GC B cells accessibility to antigen by competing with BCR for binding to target epitope, inhibiting B cell selection in an affinity-dependent manner of the antibodies as a result of terminating the GC reaction (Zhang et al., 2013). During initiation of GCs start antibodies present are produced by low affinity non-mutated plasmablasts of the early extrafollicular response. Antibody feedback may also enable communication and regulation between different GCs, and over time antibodies may shut down other GCs that contain lower affinity B cells (Zhang et al., 2013). Tfh cells can migrate between GCs, and in vivo experiments show they can invade established GCs and activated B cells can recycle existing ones (Shulman et al., 2013).

Positive selection of mutated GC B cells is dependent on uptake of antigen from FDC and presentation to T follicular helper (Tfh) cells. We published that the antibody covering antigen on FDCs provides a selection threshold that restricts GC B cells' access to antigen. Only B cells with BCR affinity higher than the prevalent antibodies access and present antigen to Tfh cells. As antibodies on FDC are in equilibrium with antibodies outside the GC, antibody feedback will generate a rising selection threshold for GC B cells that directs directional evolution towards higher affinity B cells (Zhang et al., 2013). Additional mechanisms affecting GC B cell fitness are random hypermutation as well as negative signals from class switched antibody through Fcγ receptor.

3.2. Chapter aims

This chapter aims to analyse the GC and Tfh cell populations in genetically altered strains of mice with changes in the class of BCR expressed or class of antibody that may generate antibody feedback being secreted. This may inform about the role of BCR signalling for GC B cell selection and the role of antibody class for antibody feedback.

The detailed aims of this chapter are:

1- Analysis and characterisation of GC and Tfh cells within different genetically altered strains of mice:

A) IgMi mice, which have no capacity for antibody secretion and no Ig class switching.

B) AIDko mice, which lack functional activation-induced cytidine deaminase (AID) in B cells resulting in absence of Ig hypermutation or Ig class switching.

C) IgHγ1μ mice, which express only IgG1 as B cells receptors and only secret IgG1 antibody (hereafter described as IgG1M mice)

2- Test the role of antigen-specific IgM for antibody feedback in the germinal centre response in wildtype (WT), AIDko and IgMi mice

3- Test whether Ig hypermutation affects GC B cell competitive fitness using adoptive transfer of WT B cells into AID wt or ko mice.

3.3. Results

3.3.1. IgMi mice show increased GC size and more Tfh cells compared with WT mice

The IgMi mouse exclusively expresses IgM as a B cell receptor on the surface of the B cells. It has been genetically modified to express only surface IgM and cannot secrete any antibodies. Specifically, the constant regions of the Ig heavy chain (IgH) are removed, except Ighm and and Ighg1. However, the Ighg1 locus is flanked by loxP sites and present in reverse orientation. Therefore, IgG1 can only be expressed if Cre recombinase is present. This mouse has been reported to have a normal development of B cells (Waisman et al., 2007). The main differences between IgMi and wild type are illustrated in (Figure 3.1 A).

The IgMi mouse differs from the WT mouse in the absence of antibody secretion. This should have implications for the regulation of antibody response and antibody feedback. To investigate whether the absence of antibodies has an effect on the size of GC and Tfh populations, WT and IgMi mice were immunised with an immune complex composed of 10 µg of NP_{18}-CGG plus 90 µg low-affinity anti-NP IgM^a (clone Fab82), injection of IC may only the way to help the antigen to deposit on FDC in IgMi strain, and spleen tissues were collected at two different time point: day 10, when there is high B cell proliferation and active affinity maturation, and day 21, representing the later stage of the GC response. By this time, Bmem and LLPC are being generated (Figure 3.1 B). Immunisation with low affinity immune complex will allow immune complex deposition on the FDC network, which is essential for induction of GCs. Low affinity antibody is used for this to simulate the conditions of the natural onset of an immune response, without competition from higher affinity antibody.

Immune complex was prepared with ratio of hapten to antibody antigen-binding site of 1:1, and mixed well 1 hour before i.v. injection (Zhang et al., 2013). Splenic GC B cells were identified and analysed by flow cytometry (Figure 3.2 A). GC were identified as $B220^{+}CD138^{-}$ $CD38^{-}$ Fas^{high}, further gating identified IgM^{+} non-switched and IgG1 switched GC B cells, DZ ($CXCR4^{+}CD86^{low}$) and LZ ($CD86^{+}CXCR4^{low}$) B cells, and NP-specific B cells. The FACS data confirmed that IgMi mice only express IgM and cannot class switch to IgG1 (Figure 3.3 A). Interestingly IgMi mice had significantly increased GC sizes at 10 d and 21 d after immune complex injection compared to the WT group and increased numbers of NP-specific GC B cells (Figure 3.4). Within WT mice GC sizes and NP-specific GC B cell numbers were significantly reduced over time, but no reduction was detected in IgMi mice (Figure 3.4 A, and B). We then assessed GC DZ and LZ B cells by following CXCR4 and CD86 expression (Figure 3.5 A). The ratio of DZ to LZ GC B cells can provide insight into the selective pressures determining B cell evolution within the GC. Compared to WT, IgMi mice had significantly more DZ B cells at day10 and day21 (Figure 3.5), and there was a small reduction (not statistically significant) in GC LZ B cells. The DZ/LZ ratio was significantly higher in IgMi mice at day 10 and trended higher at day 21 compared with WT mice (Figures 3.5 A and B).

Our previous study (Zhang et al., 2013) suggests that higher affinity antibodies secreted by GC-derived plasma cells enter the GC to replace the low affinity antibody in immune complexes on FDC and then negatively regulate GC selection by limiting the access of LZ B cells to antigens (Zhang et al., 2013) , therefore only high affinity GC B cells will be selected and then get help from Tfh cells for further proliferation in DZ or differentiation into plasma cells. The increased GC sizes in IgMi mice may indicate the absence of antibody feedback because of the absence of soluble antibodies. GC B cells may get easier selected in the LZ and

then move into DZ do more proliferation and mutation. Hence, a larger proportion of GC B cells is in DZ stage.

Tfh cells within the GC provide critical help for B cells, induce the formation of GC, select B cells expressing high-affinity B cell receptors, and maintain the GC reaction. At the same time, Tfh cells require interaction with GC B cells for the stability of GC and their survival (Baumjohann et al., 2013). We therefore tested the effect of absence of antibody feedback and IgG expression on Tfh cells in IgMi mice. As shown in Figure 3.6, Tfh cells were gated as $CD3^{+}CD4^{+}CD62L^{-}CD44^{+}$ $CXCR5^{hi}$ $PD1^{hi}$. In parallel with the increased GC size in IgMi mice after giving IC, IgMi mice had significantly more Tfh cells than WT mice at day 10 and trended higher at day 21. This shows that Tfh cell and GC B cells are highly interrelated, and selected GC B cells require larger numbers of Tfh cells for the survival. Further investigation is needed to confirm the selection of GC B cells. Techniques like immunofluorescence staining can help to visualize Tfh cells and GC B cells within the germinal center. Additionally, the dependency on cytokines like IL-21 can be examined. Gene expression profiling can reveal the pathways and survival signals that are upregulated in GC B cells that receive help from Tfh cells, such as the Bcl6 gene.

Overall, as IgMi mice do not have secrete IgM or any antibodies, there is no increase in antibody feedback after immunisation with low affinity immune complexes. The absence of an increase in B cell selection threshold seems to results in significantly bigger GCs proportion as percentage of total lymphocyte, because B cells can access antigens unrestricted by higher affinity antibodies and the GC reaction is not restricted. In WT mice, GCs were reduced which could be explained by higher affinity soluble antibodies produced from GC derived plasma cells entering the GC and masking the antigens on FDCs. This would limit availability of antigen

to low affinity GC B cells, leading to the selection of only high affinity GC B cells. Better access to antigen in IgMi mice would also lead to better antigen-presentation to Tfh cells, leading to larger numbers of Tfh cells present.

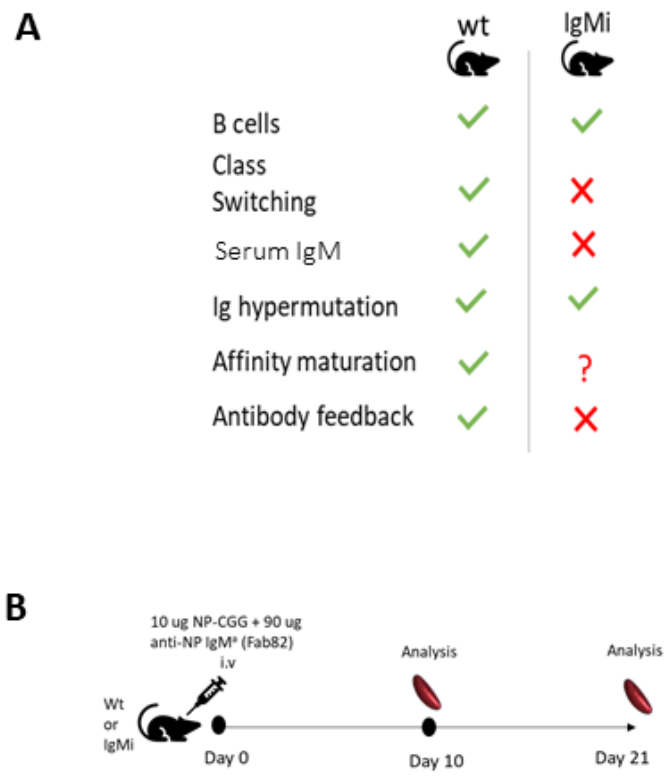

Figure 3.1 Summary of differences between WT and IgMi mice.
(A) IgMi mice express only surface IgM and do not secrete antibody. Therefore, there is no antibody feedback through affinity matured antibody, and no negative feedback through IgG. (B) Immunisation of WT and IgMi mice with low affinity anti-NP IgM^{a} plus NP-CGG to form immune complex (Antigen-antibody), spleen tissues were collected at day10 and 21.

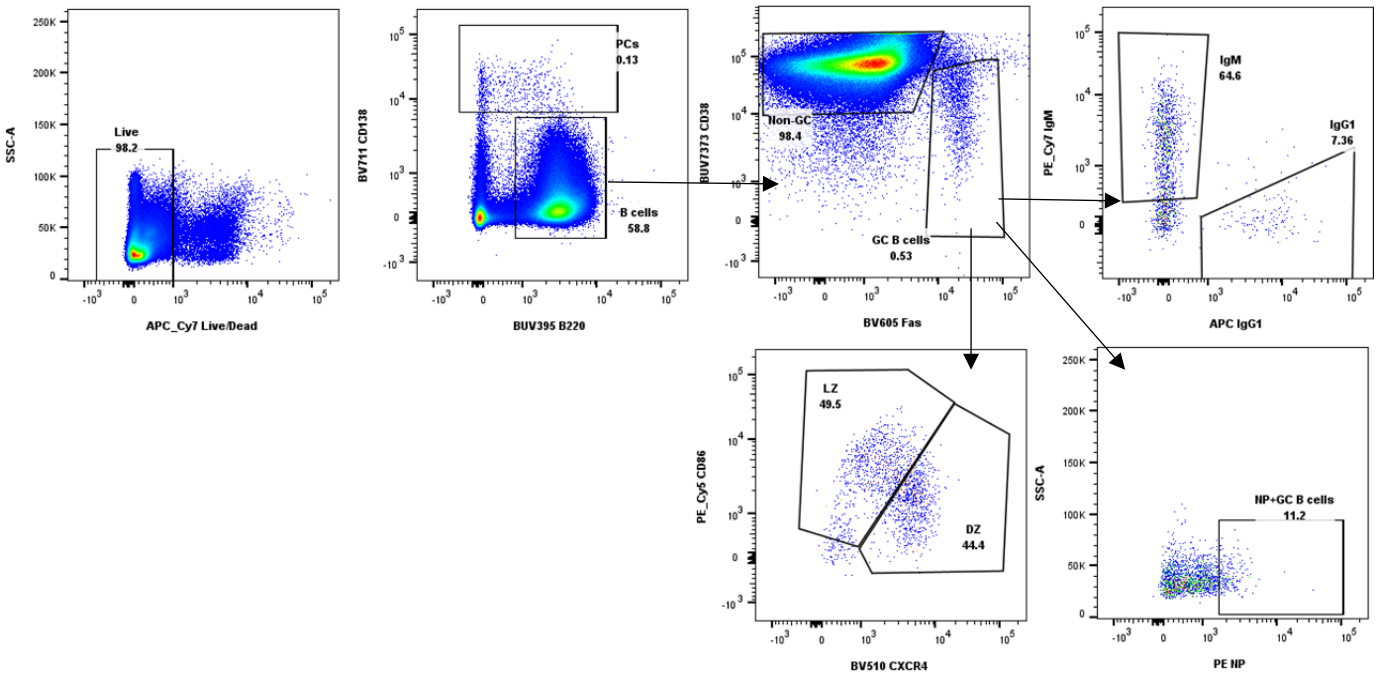

Figure 3.2 Flow cytometry plot and GC gating strategy

B cells and plasma cells gated from live cells. From B220^{+}CD138^{-} B cells, GC B cells were gated as CD38 ^{low} and Fas ^{high}. IgM, IgG1, Dark zone (DZ) as CXC4^{+}CD86^{low}, light zone (LZ) as CD86^{+}CXCR4^{low} and NP specific GC B cells were all gated from GC.

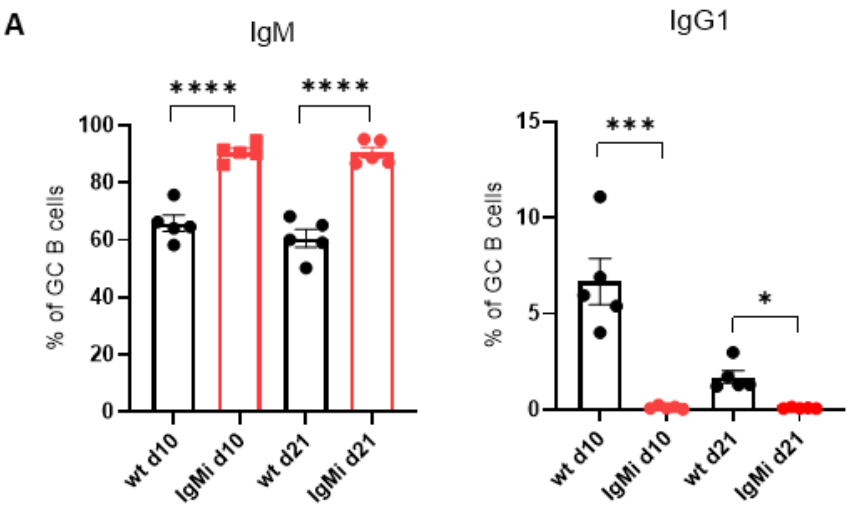

Figure 3.3 Absence of class switching in IgMi mice

WT and IgMi mice were immunised with an immune complex composed of 10 µg of NP_{18}-CGG plus 90 µg low-affinity anti-NP IgM^a (clone Fab82), and spleen tissues were collected at two different time point at days 10 and 21. (A) Frequency of IgM and IgG1 as a percentage of GC B cells. Data statistical tests were performed as mean ± SEM by a two-tailed unpaired T-test. (*p < 0.05, ***P ≤ 0.001, ****P ≤ 0.0001). Data from one experiment. Each symbol represents an individual mouse.

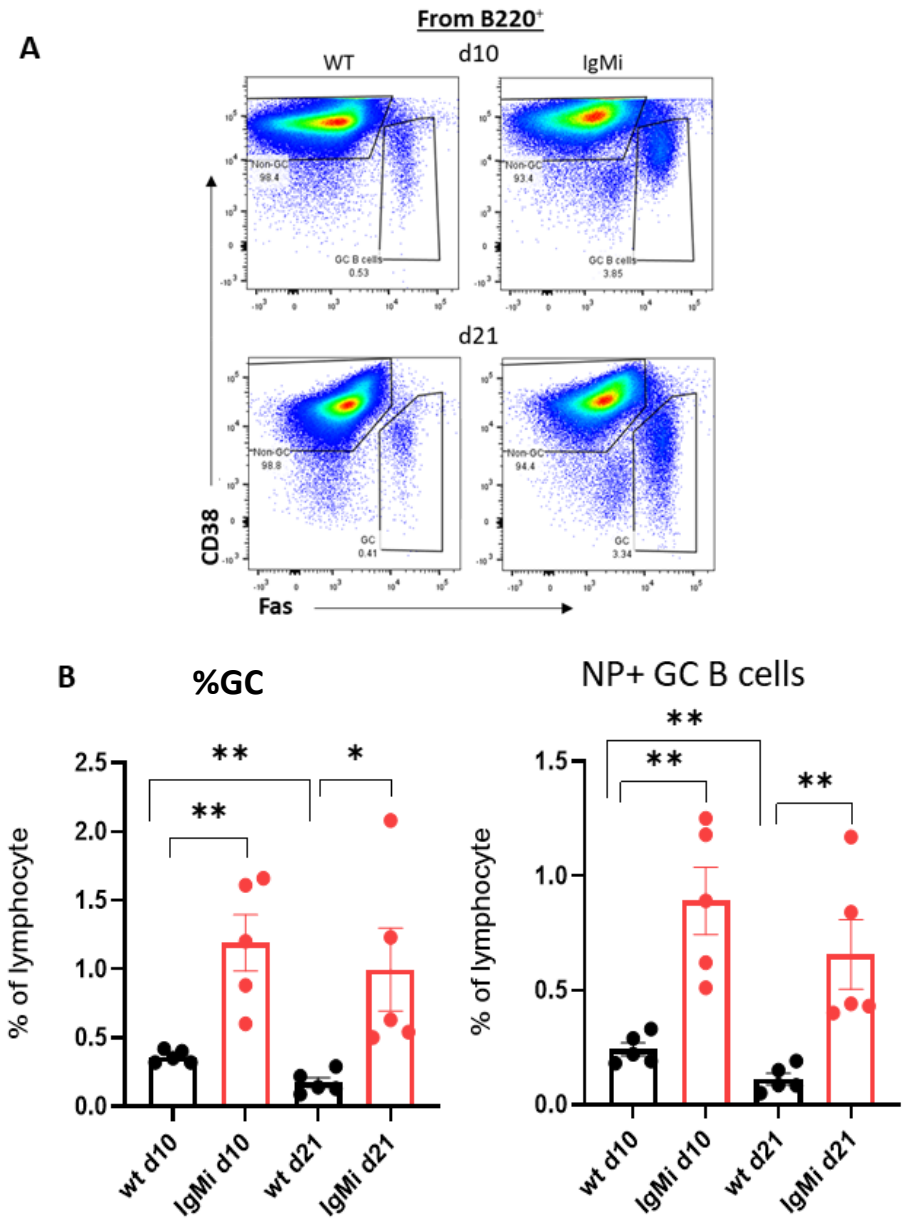

Figure 3.4 The percentage of GC B cells are increased in IgMi mice

WT and IgMi mice were immunised with an immune complex composed of 10 µg of NP_{18}-CGG plus 90 µg low-affinity anti-NP IgM^a (clone Fab82), and spleen tissues were collected at two different time point at days 10 and 21. (A) Flow cytometry plot of GC B cells identified as $CD38^{low}$ Fas^{high}, upper plots representative of WT and IgMi mice at day 10 and lower plots at day 21 after the injection of IC. (B) GC Size, showed as frequency of GC and NP- specific GC B cells within total lymphocyte. Statistical tests were performed as mean ± SEM by a two-tailed unpaired T-test. (*$p < 0.05$, **$P \leq 0.01$). Data from one experiment. Each symbol represents an individual mouse.

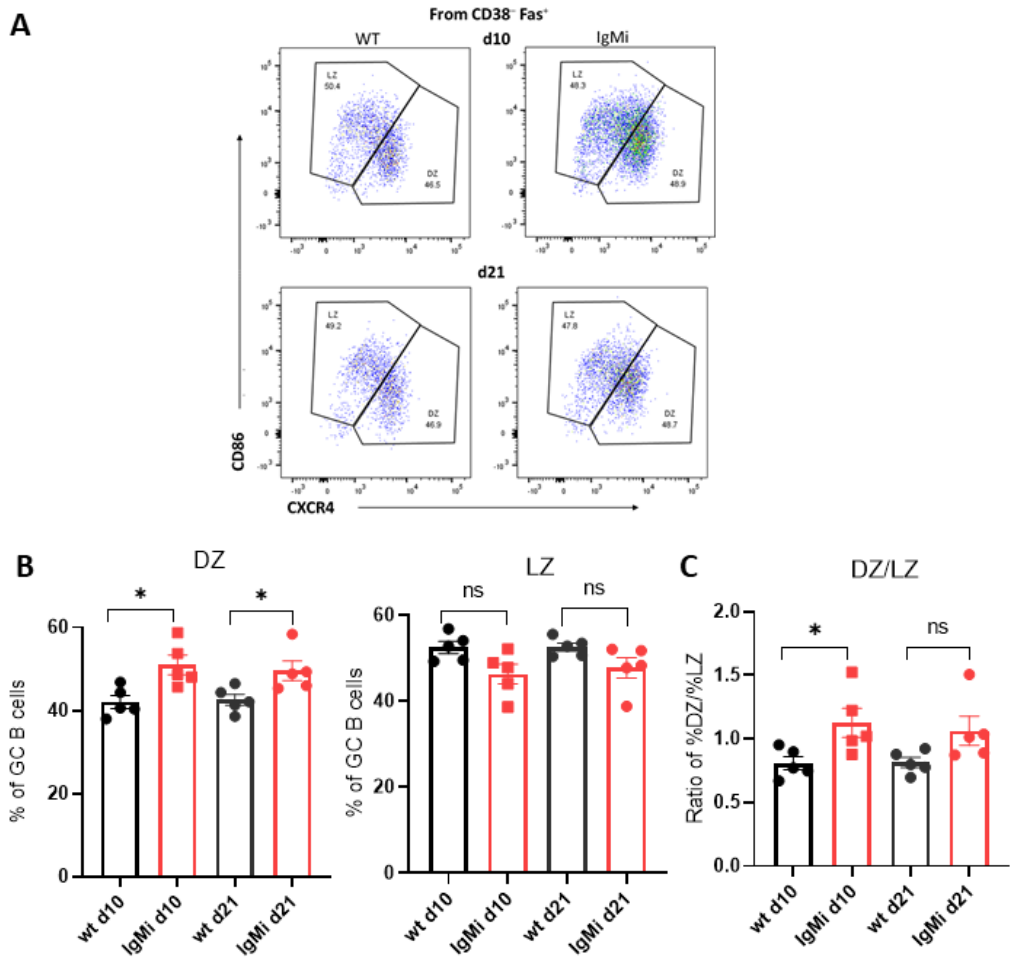

Figure 3.5 Increased DZ/LZ ratio in absence of soluble antibody

WT and IgMi mice were immunised with an immune complex composed of 10 µg of NP_{18}-CGG plus 90 µg low-affinity anti-NP IgM^a (clone Fab82), and spleen tissues were collected at two different time point at days 10 and 21. (A)Flow cytometry plot of CXCR4 and CD86 expression, identifying DZ and LZ compartments, with upper plots from representative WT and IgMi mice at day 10 and lower plots at day 21. (B) Frequency of DZ and LZ population as percentage of the GC. (C) Ratio of DZ and LZ GC B cells. Bars show mean ± SEM. Statistical testing was using a two-tailed unpaired T-test. (*$p < 0.05$, ns; not significant). Data from one experiment. Each symbol represents an individual mouse.

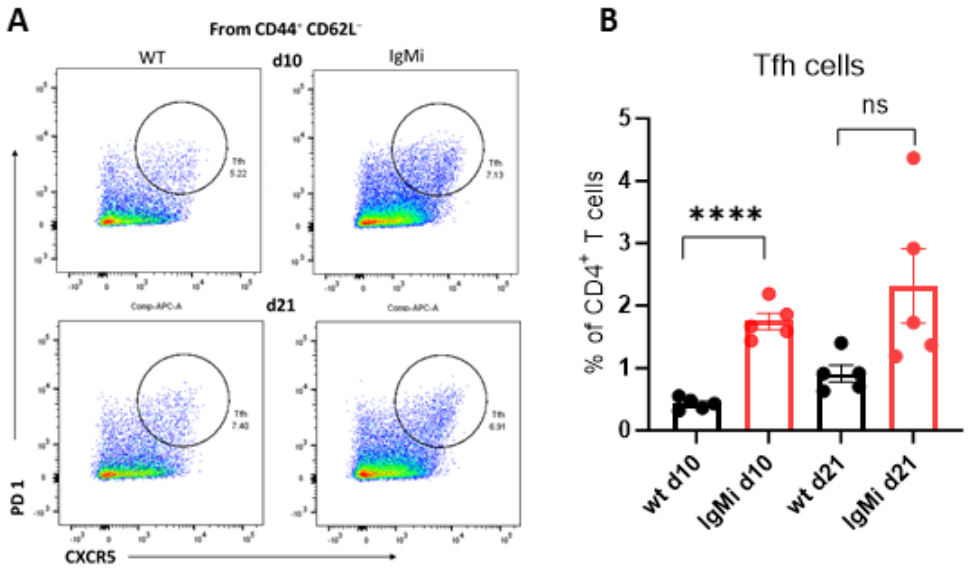

Figure 3.6 Tfh cells increased in IgMi mice after immunisation with IC

WT and IgMi mice were immunised with an immune complex composed of 10 µg of NP_{18}-CGG plus 90 µg low-affinity anti-NP IgM^a (clone Fab82), and spleen tissues were collected at two different time point at days 10 and 21. (A) Tfh population identified as $PD1^{high}$ $CXCR5^{high}$ were gated from CD4+CD62L-$CD44^+$ T cells. Upper plots represent Tfh cells of WT and IgMi mice at day 10 and lower plots at day 21. (B) Quantification of Tfh cells, showed as percentage of CD4 T cells. Data statistical tests were performed as mean ± SEM by a two-tailed unpaired T-test. (****P ≤ 0.0001, ns; not significant). Data from one experiment. Each symbol represents an individual mouse.

3.3.2. Effects of absence of Ig hypermutation, class switch recombination or IgM on GC B cell selection.

To further test the role of antibody affinity and switched antibody IgG for the regulation of GCs, we investigated two different models of mice: AID-deficient (AIDko), and IgG1M. AIDko mice lack class switch recombination (CSR) and somatic hypermutation (SHM) as both processes are dependent on the enzyme activation-induced cytidine deaminase (AID) (Muramatsu et al., 2000). As a result, AIDko mice produce IgM antibodies in response to antigen, but cannot switch to IgG or undergo somatic hypermutation to increase affinity. On the other hand, IgG1M B cells exclusively express IgG1 as BCR (Waisman et al., 2007). Further, IgG1M B cells secrete IgG1, but cannot produce any other class of soluble antibodies (Figure 3.7 A). All mice were primed with KLH precipitated with alum i.p and 4 weeks later received soluble NP-KLH i.p. Spleens were harvested at day 5 and 8 to analyse GC responses (Figure 3.7 B).

First, we checked the IgM+ and IgG1+ GC B cells populations in AIDko and IgG1M mice by FACS staining (Figure 3.8). The data confirmed that AIDko mice are only capable of producing immunoglobulin M (IgM) BCR and cannot undergo class switch recombination to immunoglobulin G1 (IgG1). In contrast, IgG1-only (IgG1M) mice exclusively express IgG1 as their B cell receptor, without IgM expression (Figure 3.8). To evaluate germinal centre (GC) kinetics in these different mice, we identified GCs as $B220^{+}CD38^{low}Fas^{high}$ populations by flow cytometry (Figure 3.9 A). Compared to immunised WT littermate control and IgG1M mice, AIDko mice exhibited significantly enlarged GC responses at days 5 and 8 post-immunization (Figure 3.9 B, and C). IgG1M mice developed a smaller GC compartment, similar to WT mice, and no significant difference in GC B cells was observed between IgG1M and WT mice at both d5 and d8 (Figure 3.9 B, and C). Frequencies of NP-specific GC B cells were markedly higher in

AIDko versus WT and IgG1M mice at d5, although IgG1M mice showed a modest but non-significant reduction compared to WT. By day 8, hapten-specific GC B cells declined in wt mice, similar to what was found in a previous study (Zhang et al., 2013). The same decline in hapten-specific B cells was seen in AIDko and IgG1M mice (Figure 3.9 C). Further, frequencies of dark zone (DZ) and light zone (LZ) B cells were investigated. Interestingly, GCs from AIDko mice displayed significantly reduced DZ frequencies and expanded LZ proportions compared to WT mice throughout the time course. In contrast, IgG1M GCs exhibited the opposite phenotype, with significantly decreased LZ and elevated DZ frequencies (Figure 3.10 A). The quantification of the ratio of DZ to LZ showed markedly reduced in AIDko GCs but significantly increased in IgG1M GCs relative to WT controls (Figure 3.10 B).

Overall, Soluble IgM, which is present in AIDko but not IgG1-only (IgG1M) mice, is crucial for complement fixation and immune complex formation via CD21 to provide stimulatory signals during the germinal centre response. Furthermore, no high affinity antibody restricting GC B cells selection and mutation is present in AIDko mice. Also, soluble IgG, which is a negative regulator of B cell activation, is absent in AIDko mice, resulting in larger GCs, and particularly more LZ B cells.

Another, IgG1 probably acts as a negative regulator by binding to the inhibitory Fc receptor CD32 (Getahun and Cambier, 2015). Therefore, the lack of IgM and presence of IgG1 in IgG1M mice may impair antigen retention on FDCs and deliver negative signals to GC B cells, resulting in slightly reduction of GC, particularly fewer LZ B cells. In summary, the differential GC phenotypes between AIDko and IgG1M mice may be explained by the distinct immunoglobulin isotypes produced, which have opposing roles in regulating GC responses via effects on antigen retention for selection and B cell receptor signalling.

Following immunisation with the T cell-dependent antigen (NP-KLH), we assessed the frequency of Tfh cells in AIDko, IgG1M, and WT control mice at days 5 and 8 post-immunization. Tfh cells were identified by flow cytometry as $CD44^{+}CXCR5^{+}PD\text{-}1^{hi}$ populations (Figure 3.11 A). Mirroring GC kinetics, AIDko mice exhibited expanded Tfh cell frequencies compared to IgG1M and WT mice at both timepoints, although this difference did not reach statistical significance (Figure 3. 11 B). In contrast, IgG1M mice showed similar Tfh cell proportions to WT controls. Together, these data demonstrate that aberrant GC reactions in AIDko mice are associated with moderate increases in Tfh cell numbers. A possible explanation would be lack of antibody feedback due to lack of high affinity antibody in AIDko mice, increasing access of germinal centre B cells to antigen and allowing better antigen-presentation of light zone B cells to Tfh cells.

3.3.3. Testing the function of IgM Vs. IgG1 during immune responses.

To evaluate the impact of impaired IgM secretion on antibody affinity maturation during the primary response, IgG1M mice, and WT controls were immunized with 4-hydroxy-3-nitrophenylacetyl hapten conjugated to ovalbumin (NP-OVA) precipitated in alum plus heated inactivated *Bordetella pertussis*. Blood samples were collected at d8 and d15 post-immunization. Enzyme-linked immunosorbent assays (ELISAs) were conducted to quantify total and high-affinity NP-specific IgG1 (Figure 3.12 A). Compared to WT mice, IgG1M mice exhibited significantly lower total NP-specific IgG1 titres at both timepoints (Figure 3.12 B). High-affinity NP-specific IgG1 levels were also markedly reduced in IgG1M versus WT mice (Figure 3.12 C). No significant differences in antibody affinity were observed between groups at d8, but a significant decrease in affinity was detected in IgG1M mice at day 15 (Figure 3. 12 D). In summary, these findings demonstrate impaired affinity maturation in IgG1M mice lacking secreted IgM, again highlighting the importance of IgM for optimal IgG1 antibody responses against T-dependent antigens. The reduction in high-affinity IgG1 may indicate the importance of IgM for IC formation, the induction GC response, and deposition of antigen on FDC. Class-switched IgG1 may have an intrinsic disadvantage in driving GC reactions necessary for affinity maturation without the action of IgM. In summary, the inability to produce soluble IgM in the IgG1M mice model negatively impacts multiple aspects of T-dependent antibody responses, likely due to reduced antigen retention due to defective immune complex trapping on FDCs.

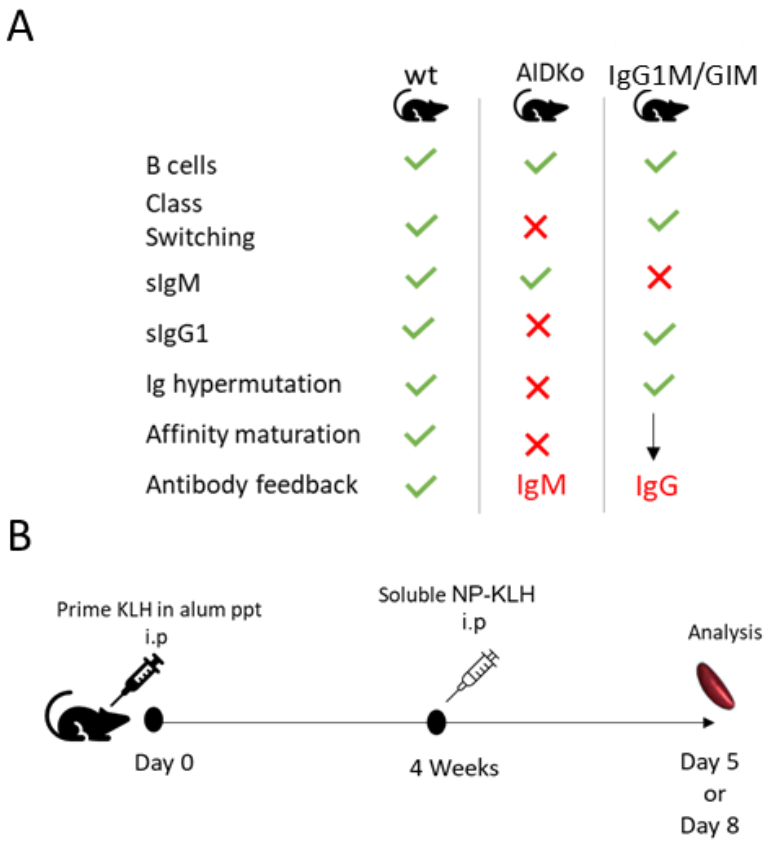

Figure 3.7 Summary of differences between WT, AIDko, and IgG1M mice
(A) To further test the role of affinity maturation and IgG for regulation of GCs, wt, AIDko, and IgG1M mice expressing only IgG1 (secreted or as BCR) were compared. (B) Mice were primed with precipitated KLH with alum via i.p and 4 weeks later all mice received soluble NP-KLH via i.p. Spleen tissues were collected at day 5 and 8 to perform flowcytometry.

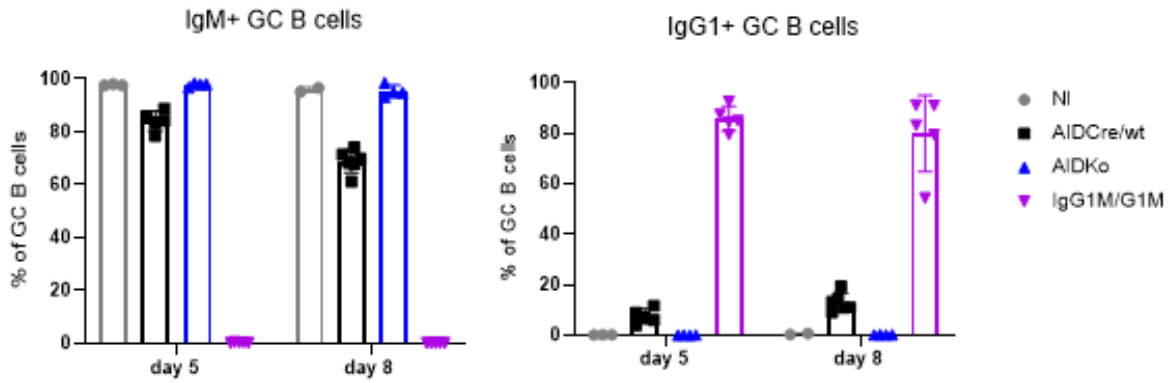

Figure 3.8 Absence of IgG in AIDko and IgM in IgG1M mice

WT, AIDko, and IgG1M were primed with KLH precipitated with alum i.p and 4 weeks later received soluble NP-KLH i.p. Spleens were harvested at day 5 and 8 to analyse GC responses Frequency of IgM and IgG1 as percentage of GC B cells in different type of mice; The data showed an absence of IgM, only IgG1+ GC in IgG1M only mice and no class switching (no IgG1) in AID ko mice. (NI) non-immunised WT. Data from one experiment. Each symbol represents an individual mouse.

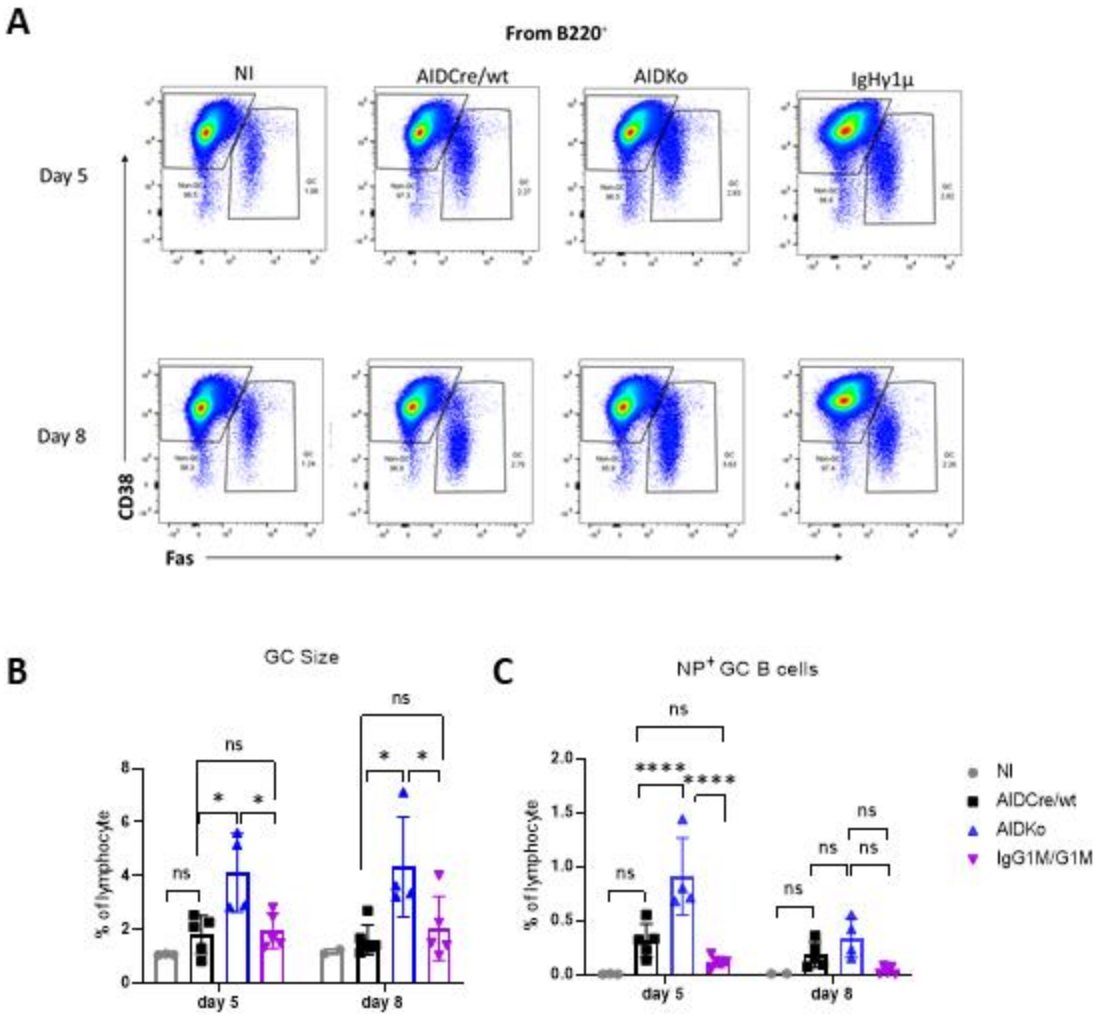

Figure 3.9 Increased GC response in AIDko, and reduced NP-specific GC response in IgG1M mice

WT, AIDko, and IgG1M were primed with KLH precipitated with alum i.p and 4 weeks later received soluble NP-KLH i.p. Spleens were harvested at day 5 and 8 to analyse GC responses. (A) Flow cytometry gating for GC B cells were identified as $B220^{+}CD138\text{-}\ CD38^{low}\ Fas^{+}$ on day 5 (upper plots) and day 8 (bottom plots) after immunisation with soluble NP-KLH in carrier primed mice. (B) GC size, showed as the percentage of GC from total lymphocytes. (C) NP specific GC size, showed as the percentage of NP specific GC B cells from total lymphocytes. Data statistical tests were performed as mean ± SEM performed by 2way ANOVA with Tukey's multiple comparison test. (*, $p < 0.05$;****, $p < 0.0001$; ns, not significant). Data from one experiment. Each symbol represents an individual mouse.

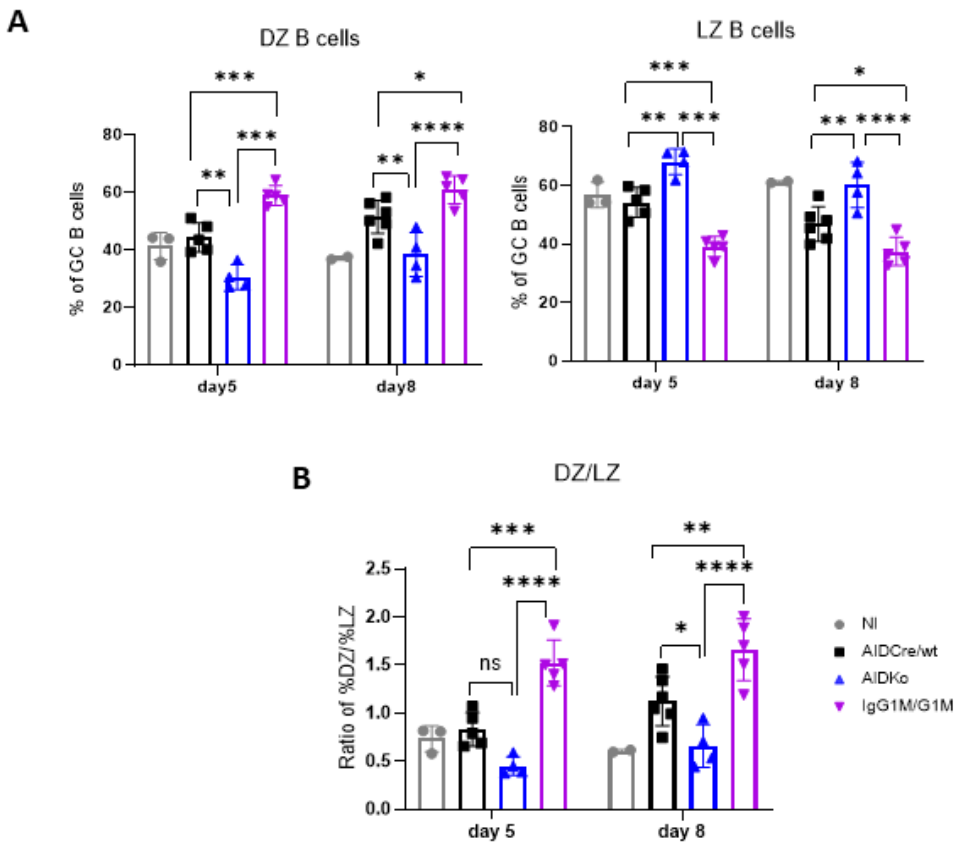

Figure 3.10 DZ/LZ ratio is reduced in AIDko and increased in IgG1M mice

WT, AIDko, and IgG1M were primed with KLH precipitated with alum i.p and 4 weeks later received soluble NP-KLH i.p. Spleens were harvested at day 5 and 8 to analyse GC responses. (A) DZ and LZ B cells, showed as as percentage of GC B cells. (B) Summary of the ratio of DZ to LZ B cells. Statistical tests were performed as mean ± SEM using 2-way ANOVA with Tukey's multiple comparison test. (*, $p < 0.05$; **, $p < 0.01$; ***, $p < 0.001$; ****, $p < 0.0001$; ns, not significant). Data from one experiment. Each symbol represents an individual mouse.

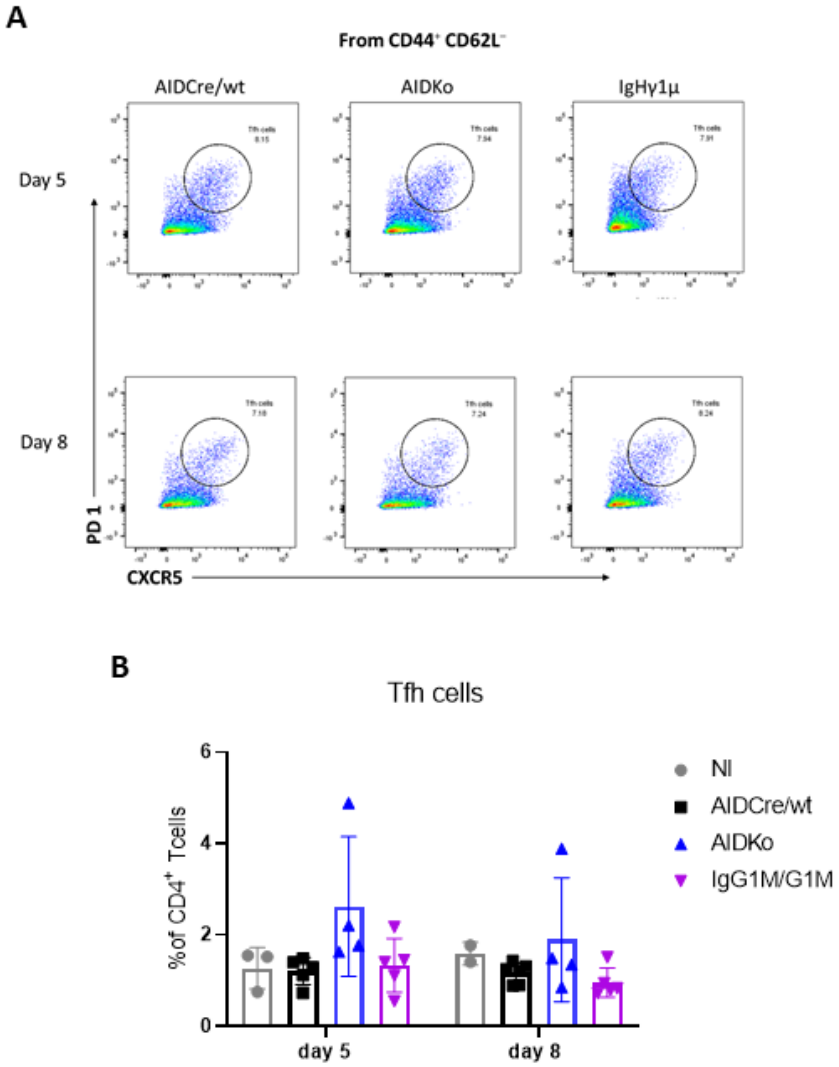

Figure 3.11 Tfh cell numbers correlate with GC sizes

WT, AIDko, and IgG1M were primed with KLH precipitated with alum i.p and 4 weeks later received soluble NP-KLH i.p. Spleens were harvested at day 5 and 8 to analyse GC responses. (A) Flow cytometry plots showing Tfh cells were gated as $PD1^{hi}$ $CXCR5^{hi}$ from $CD4^{+}CD62L^{-}CD44^{+}$ population for WT, AIDko, and IgG1M on d5 (upper plots) and d8 (bottom plots) after immunization. (B) Quantification of Tfh cells, showed as percentage of total CD4 T cells. Data from one experiment. Each symbol represents an individual mouse.

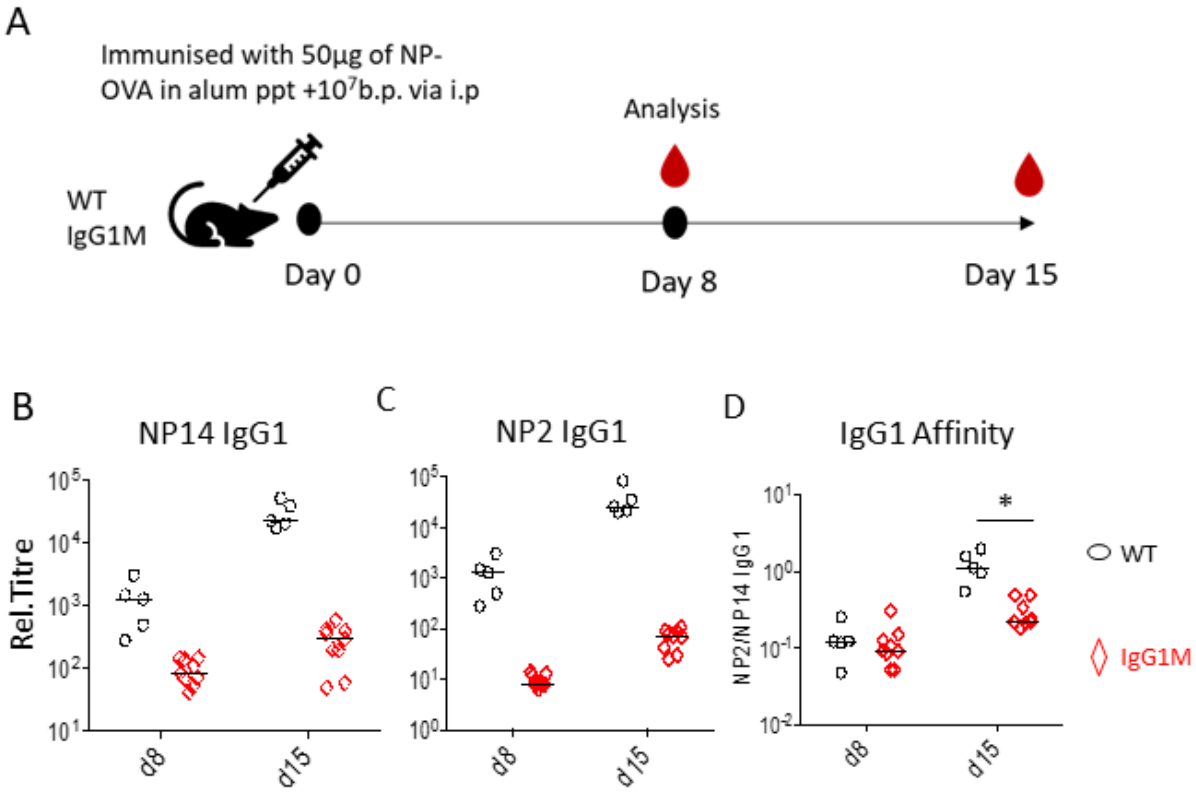

Figure 3.12 The titre of IgG1 high affinity reduced in IgG1M mice model.

(A)WT and IgG1M mice were immunised with 50µg of NP-OVA in alum ppt +10^7 b.p. via i.p. Blood samples were collected at d8 and d15 after the immunization. ELISA assay was performed to detect NP-specific IgG1 production in blood. Graphs shows (B) NP14-specific total IgG1 titre. (C) NP2-specific high affinity IgG1 titre, and (D) NP specific IgG1 affinity, showed as ratio of NP2/NP14.

3.3.4. Testing the impact of high avidity IgM on AIDKo and IgMi mice and the impact of this Ab class in these two strains.

An experiment was designed to test how antibody feedback regulates the germinal centre (GC) response. Three different mouse models were used in this experiment: 1) WT mice as a control, 2) AIDko mice, and 3) IgMi mice. All mice were immunized with immune complexes (IC) consisting of NP-CGG plus anti-IgM^a antibodies of low avidity (clone Fab82) injected intravenously (i.v.). At day 8, the mice were injected i.v. with either soluble high avidity anti-NP IgM^a (clone 1.197) or low avidity anti-NP IgM^a (clone Fab82). Spleen tissues were collected two days after receiving the soluble antibodies (i.e at day 10) (Figure 3.13).

Flow cytometry was used to identify GCs as B220$^+$ CD38^{low} Fas$^+$ (Figure 3.14 A) and the GC B cells examine 2 d after injection with the soluble antibodies. WT mice that received the high avidity IgM^a have slightly reduced GCs compared to the group that received the low avidity IgM^a, but no effect on NP-specific GC B cells (Figure 3.14 B, and C). This is different to the effect of high affinity Ab injection in a previous study (Zhang et al., 2013), where secondary responses were investigated. It is possible that the primary response to NP-CGG in the current experiment induced already higher affinity antibody formation. As the primary response develops slower than 2nd response, antibody injection was done significantly later in the current experiment. The optimal timing for antibody injection should to be tested in further pilot experiments. Also, IgM immune complex can improve GC response compared to antigen alone (our previous findings, unpublished). Hence, in the experiment described here, exogenous high avidity IgM^a may be unable to compete to regulate the GC B cell selection. As seen above (Figure 3.4, and 3.9). AIDko and IgMi all developed significantly bigger GC B cells , particularly NP-specific GC B cell numbers compared to WT controls.

Surprisingly there was also no significant effect of injection of high affinity antibody on GCs in AIDko or IgMi mice, nor on NP-specific GC B cell numbers (Figure 3.14 C). As expected, IgMi mice have higher GC B cells than wt, but similar to wt, should mutate their BCR receptor although they can't secret antibodies (Sahputra et al., 2018). Therefore, exogenous injected high avidity IgM^a antibody may not compete or have a strong effect on regulating BCR selection. Earlier research shows a B cell–intrinsic defect in apoptosis in GC in AID deficiency mice (Zaheen et al., 2009), which may explain why GC sizes in AIDko mice are bigger, also no effect for GC size from exogenous high avidity IgM^a, probably not antibody selection process. However, AIDko GC in the absence of extrinsic Ab injection, should be bigger compared to WT GC as seen in (Figure 3.9). This was not seen in the current experiment. Considering the large variance in AIDko GC sizes in this experiment, it would be good to repeat this experiment before discussing further conclusions

Plasma cell (PC) numbers were also assessed to investigate if introducing the high affinity antibodies had an effect on plasma cell outputs and NP-specific PCs. IgMi mice produced more plasma cells compared to WT mice after the IC immunisation (Figure 3.15 A). However, the total PC numbers did not significantly change after treatment with high avidity antibodies (Figure 3.15 A). Further, there was no change in the percentage of NP-specific PCs among $CD138^+$ PCs (Figure 3.15 B).

I then evaluated the dark zone (DZ) and light zone (LZ) compartments of the GC by flow cytometry (Figure 3.16 A). After injection of high avidity antibodies, DZ GC B cells were significantly reduced even the proportion of GC was same, LZ GC B cells were increased, and the ratio of DZ to LZ decreased significantly in WT mice compared to the group that received low avidity antibodies. This may indicate a higher selection threshold with lower B cells

circulation to the DZ in WT mice when exogenous high avidity antibodies were introduced. However, there was no significant change within AIDko and IgMi mice in either zone or the DZ/LZ ratio (Figure 3.16 B). The lack of an effect of high affinity antibody in AIDko mice further supports the hypothesis that the bigger GCs in AIDko mice are mainly due to the direct effects of AID on cell survival and/or apoptosis, and the bigger GC in AIDko are not mainly due to the lack of antibody feedback.

There was no effect on the frequency of IgM expressing unswitched GC B cells after addition of high avidity antibody in any of the genotypes (Figure 3.17 A). Similarly, there was no effect on seen class switched IgG1 expressing GC B cells (Figure 3.17 B).

The previous data showed that Tfh cell and GC B cells are highly interdependent during GC differentiation. GC B cells interact with Tfh cells by presenting antigen peptide on MHCII. Next, we examined whether different avidities of soluble antibody impact on the interaction of GC B cell - Tfh cells. We identified Tfh cells by flow cytometry as $CD44^{+}$ $PD1^{hi}$ $CXCR5^{hi}$ (Figure 3.18 A). Interestingly Injection of high avidity antibody strongly reduced Tfh cells. This data is reminiscent of previous findings that ICOS and Bcl6 mRNA are reduced in Tfh cells 24hr after high avidity antibody injection (Y. Zhang, unpublished). Bcl6 is master transcriptional factor for Tfh cells, and ICOS is required for the maintenance of Tfh cells. This may indicate that antibody-dependent restriction of antigen access of GC B cells inhibits antigen uptake and downstream T cell–B cell interaction, although GC sizes did not significantly change. Further, the populations of Tfh cells in AIDko and IgMi mice were similar as WT, but interestingly the same trends to reduced Tfh cell numbers were observed in AIDko and IgMi mice after giving exogenous high avidity antibody. When the ratio of Tfh to GC cells was calculated, there was an even clearer significant reduction of Tfh cells in AIDko mice (Figure 3.18 B). This confirms

that B cells may be unable to effectively capture the antigens on FDCs and presented to Tfh cells after exogenous high avidity antibody injection, which would restrain T cell–B cell interaction and Tfh cell survival.

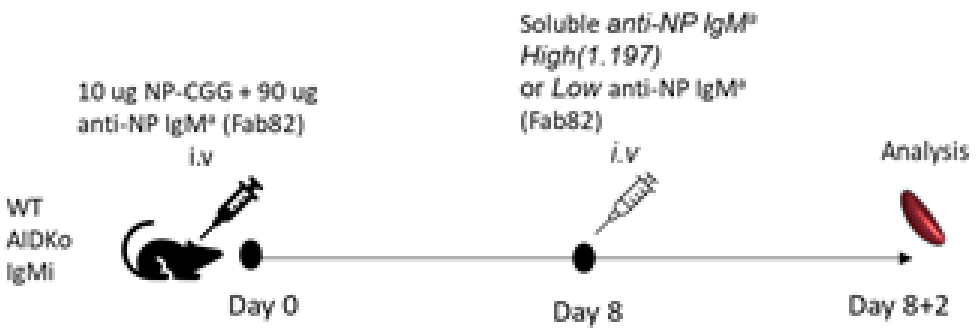

Figure 3.13 Experiment protocol of introducing the High or low avidity anti-NP IgM^a
WT (C57BL6), AIDko, and IgMi mice were immunised with immune complex 10 µg NP-CGG plus 90 µg anti-NP IgM^a of low avidity (clone Fab82) by i.v. Day 8 mice were injected with either soluble high avidity anti-NP IgM^a (clone 1.197) or low avidity anti-NP IgM^a (clone Fab82). Spleen tissues were collected two days after receiving the soluble antibodies.

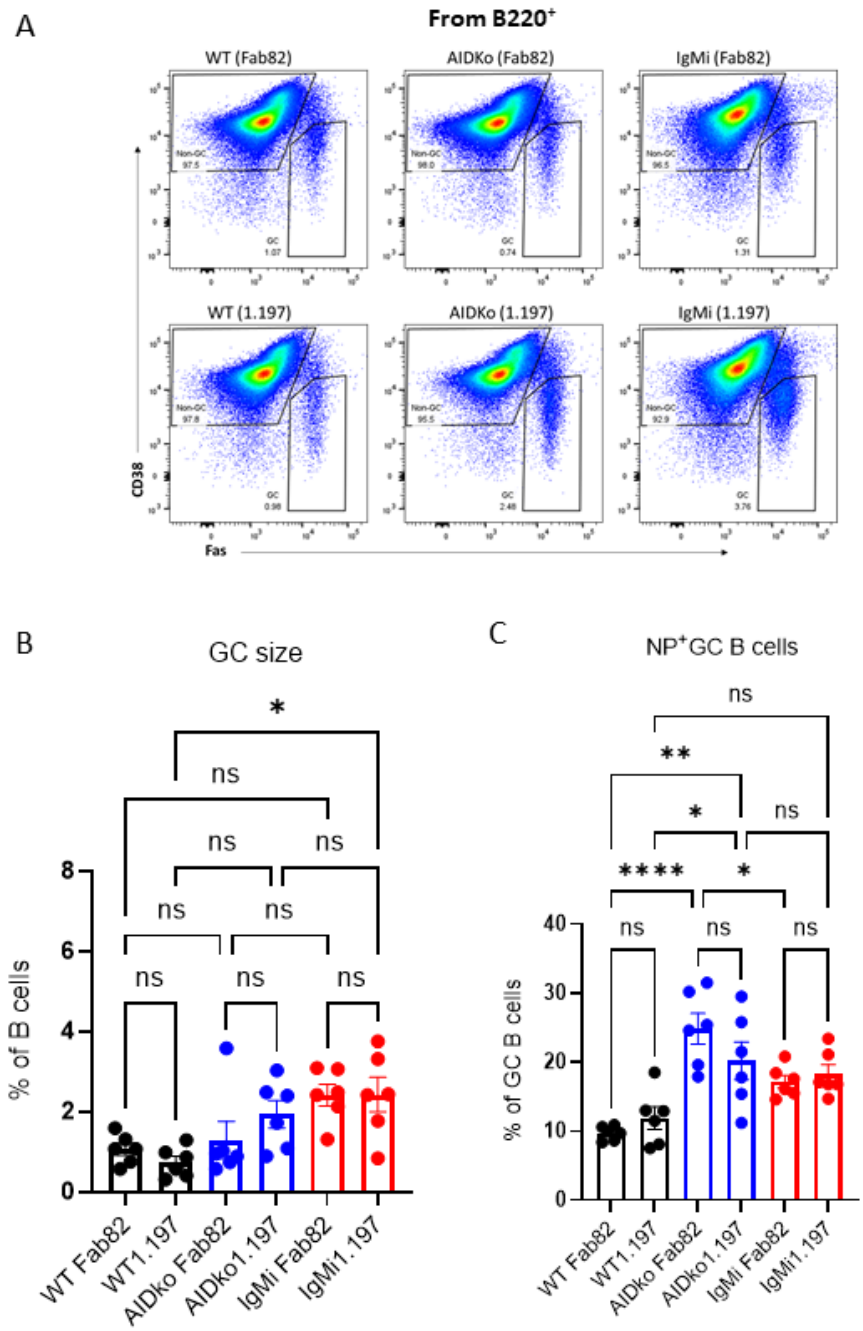

Figure 3.14 Injection of High avidity IgM does not reduce GC sizes in absence of secreted antibody.

WT (C57BL6), AIDko, and IgMi mice were immunised with immune complex 10 µg NP-CGG plus 90 µg anti-NP IgM^a of low avidity (clone Fab82) by i.v. Day 8 mice were injected with either soluble high avidity anti-NP IgM^a (clone 1.197) or low avidity anti-NP IgM^a (clone Fab82). Spleen tissues were collected two days after receiving the soluble antibodies. (A) Flowcytometry plot of GCs identified as CD38$^-$ Fas$^+$ from B cells population gate for WT, AIDko , and IgMi upper plots are GCs with low avidity anti-NP IgM^a (clone Fab 82) bottom plots are GCs with high avidity anti-NP IgM^a (clone 1.197). (B) GC size, showed as percentage of total B cells. (C) NP specific GC size, showed as percentage of GC B cells. Data statistical tests were performed as mean ± SEM performed by ordinary one-way ANOVA with Tukey's multiple comparison test (*, $p < 0.05$; **, $p < 0.01$; ***, $p < 0.001$; ****, $p < 0.0001$; ns, not significant). Data from one experiment. Each symbol represents one mouse.

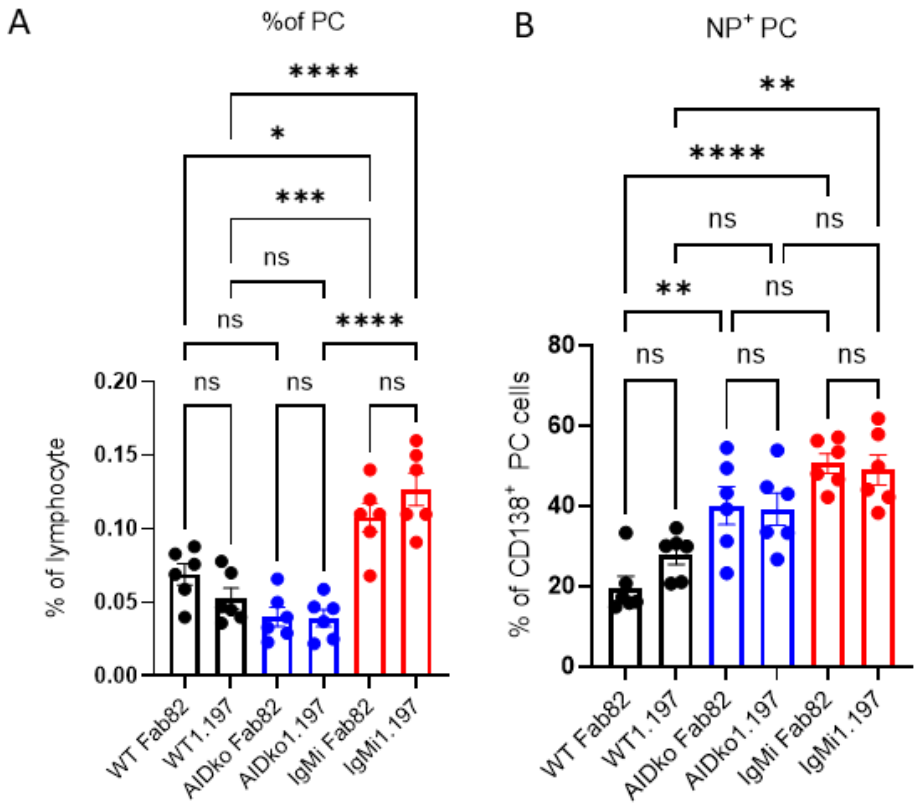

Figure 3.15 Plasma cells (PCs) and NP$^+$ PCs remain consistent disregarding varying antibodies administered

WT (C57BL6), AIDko, and IgMi mice were immunised with immune complex 10 µg NP-CGG plus 90 µg anti-NP IgM^a of low avidity (clone Fab82) by i.v. Day 8 mice were injected with either soluble high avidity anti-NP IgM^a (clone 1.197) or low avidity anti-NP IgM^a (clone Fab82). Spleen tissues were collected two days after receiving the soluble antibodies. (A)Plasma cells, shown as a percentage of total lymphocytes in WT, AIDko, and IgMi after injected with either low avidity (clone Fab 82) or high avidity (clone 1.197). (B) NP-specific PCs, showed as percentage of CD138$^+$ PCs. Data statistical tests were performed as mean ± SEM performed by ordinary one-way ANOVA with Tukey's multiple comparison test (*, $p < 0.05$; **, $p < 0.01$; ***, $p < 0.001$; ****, $p < 0.0001$; ns, not significant). Data from one experiment. Each symbol represents one mouse.

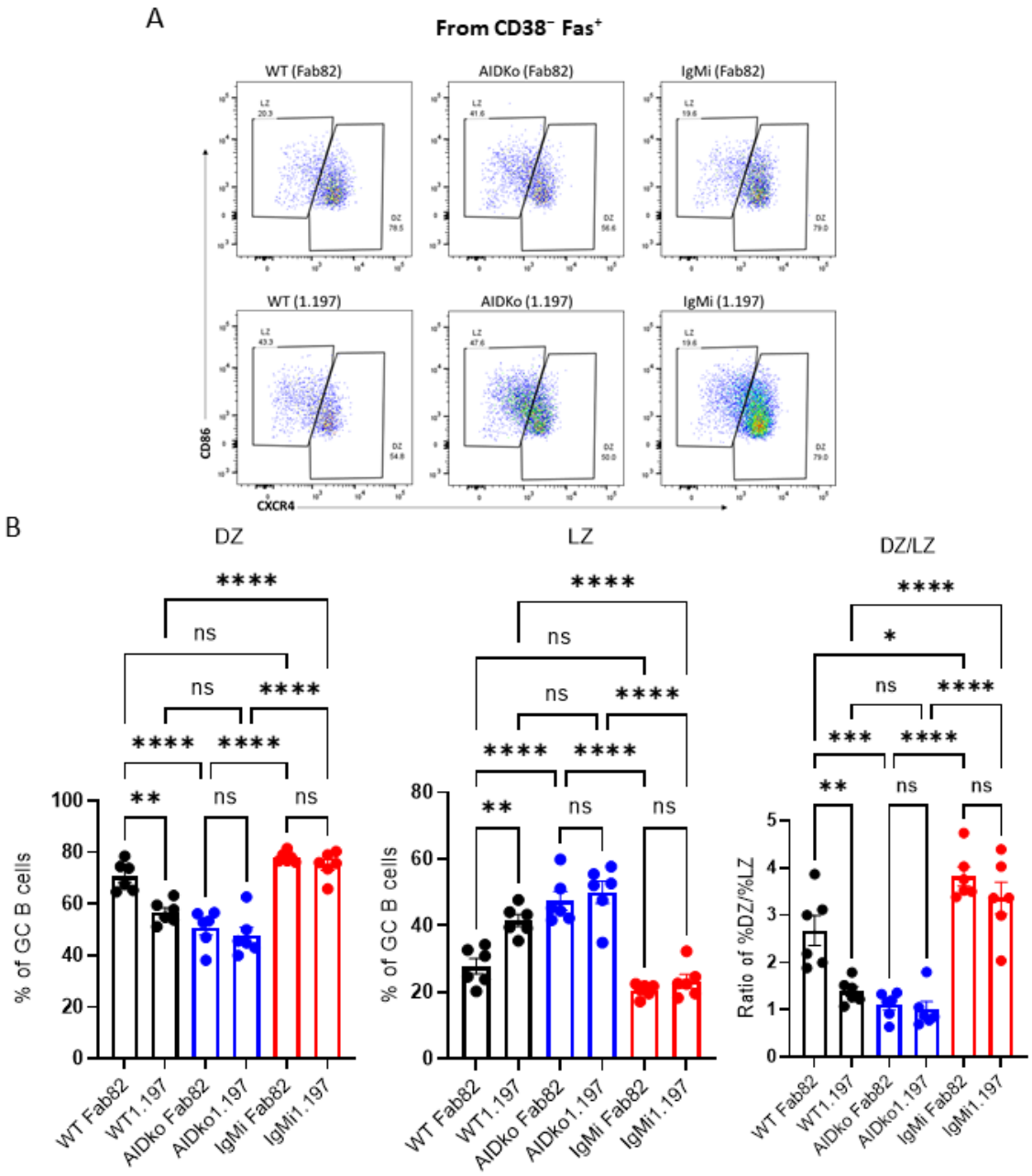

Figure 3.16 Injection of High avidity antibody reduced GC DZ B cells in WT mice

(A)Representative of FACS plot to identify CXCR4^{hi} CD86^{lo} DZ and CXCR4^{lo} CD86^{hi} LZ GC B cells for WT, AIDko, and IgMi upper plots are DZ and LZ with low avidity anti-NP IgM^{a} (clone Fab 82) bottom plots are DZ and LZ with high avidity anti-NP IgM^{a} (clone 1.197). (B) Percentage of DZ, LZ, and the ratio of DZ/LZ GC B cells. Data statistical tests were performed as mean ± SEM performed by ordinary one-way ANOVA with Tukey's multiple comparison test (*, $p < 0.05$; **, $p < 0.01$; ***, $p < 0.001$; ****, $p < 0.0001$; ns, not significant). Data from one experiment. Each symbol represents one mouse.

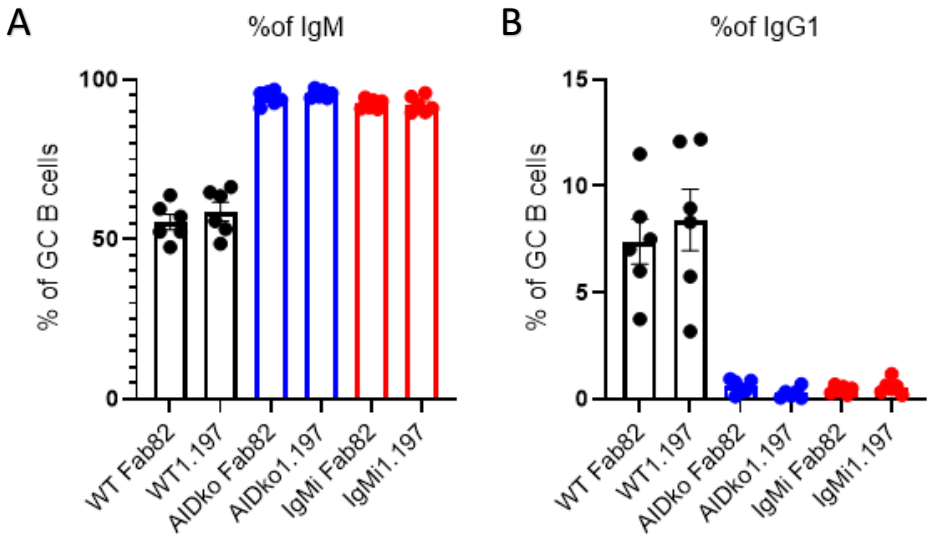

Figure 3.17 No effect in IgM and class switched IgG1 after administrated high avidity antibody

WT (C57BL6), AIDko, and IgMi mice were immunised with immune complex 10 µg NP-CGG plus 90 µg anti-NP IgM^a of low avidity (clone Fab82) by i.v. Day 8 mice were injected with either soluble high avidity anti-NP IgM^a (clone 1.197) or low avidity anti-NP IgM^a (clone Fab82). Spleen tissues were collected two days after receiving the soluble antibodies. (A)Percentage of IgM and IgG1 obtained from GCs in WT, AIDko and IgMi mice when administered with low avidity anti-NP IgM^a (clone Fab 82) or high avidity anti-NP IgM^a (clone 1.197). Data from one experiment. Each symbol represents one mouse.

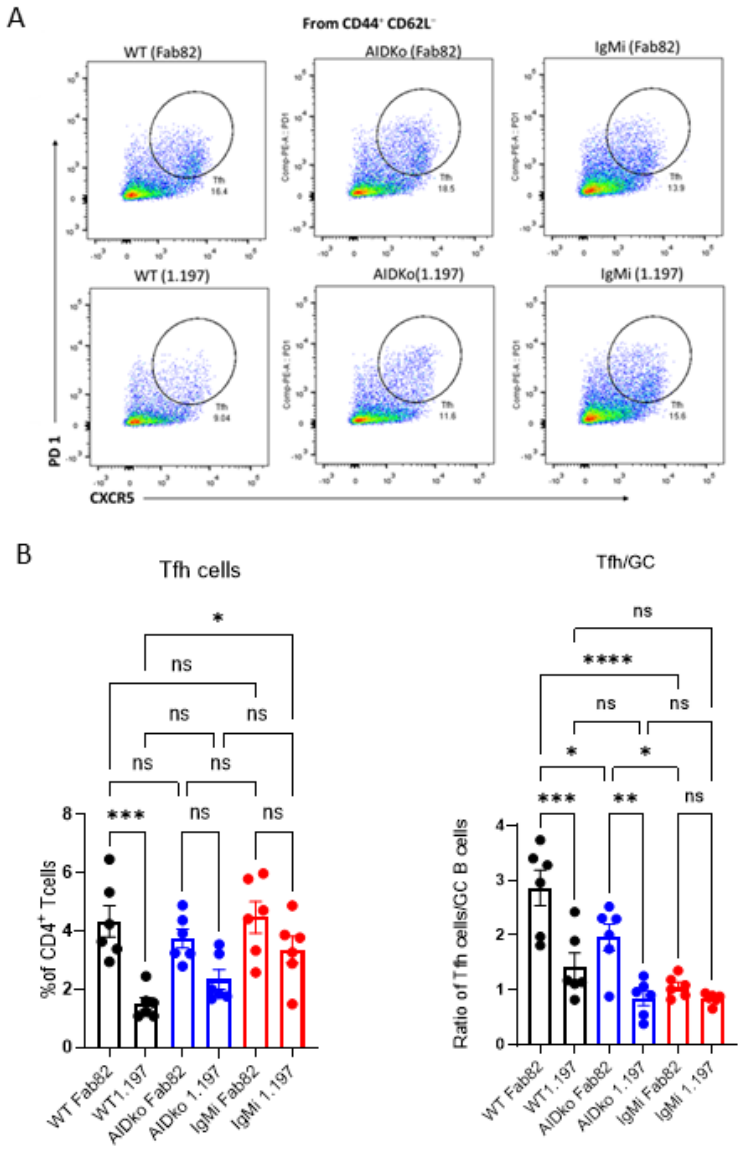

Figure 3.18 Tfh cells are strongly reduced after injection of low or high avidity antibody
WT (C57BL6), AIDko, and IgMi mice were immunised with immune complex 10 µg NP-CGG plus 90 µg anti-NP IgM^a of low avidity (clone Fab82) by i.v. Day 8 mice were injected with either soluble high avidity anti-NP IgM^a (clone 1.197) or low avidity anti-NP IgM^a (clone Fab82). Spleen tissues were collected two days after receiving the soluble antibodies. (A) Representative flow cytometry plots of Tfh cells identified as PD1^{hi} CXCR5^{hi} gated from activated T cells CD44$^+$; upper plots are Tfh cells with low avidity anti-NP IgM^a (clone Fab 82) and bottom plots are Tfh cells with high avidity anti-NP IgM^a (clone 1.197). (B) Frequency of Tfh population from total CD4$^+$ T cells and the ratio of Tfh cells to GC B cells. Statistical tests were performed as mean ± SEM performed by ordinary one-way ANOVA with Tukey's multiple comparison test (*, $p < 0.05$; **, $p < 0.01$; ***, $p < 0.001$; ****, $p < 0.0001$; ns, not significant). Data from one experiment. Each symbol represents one mouse.

3.3.5. Testing the impact of Intermediate low-avidity antibody (anti-NP IgM^a) in ongoing GC responses

In the previous experiment, our objective was to investigate the impact of injecting high-avidity antibodies on germinal centres (GCs) regulation. The previous experiment was done by administering low affinity immune complexes (IC) on day 0. Our data suggested that antigen-low avidity IgM immune complex could improve the GC response (Chapter 3.1.4). In this study, we aimed to explore the effects of intermediate low-avidity antibodies (anti-NP IgM^a) on GC regulation in mice that were solely administered NP-CGG precipitated in alum, without the initial IC administration on day 0. Consistent with the previous experiments, WT, AIDko, and IgMi were used.

All mice were intraperitoneal (i.p.) immunised with NP-CGG precipitated in alum. Subsequently, on day 10, groups of mice received an intravenous (i.v.) injection of soluble intermediate low-avidity anti-NP IgM^a antibodies (clone 2.315). Spleen tissue samples were collected two days following the administration of soluble antibodies, corresponding to day 12 of the experiment (Figure 3.19) as IgM^a immune complexed has been reported to localize on FDC in GC light zone 24 hour of antibody administration (Zhang et al., 2013).

Flow cytometry was employed to identify GC B cells as B220$^+$ CD38$^-$ Fas$^+$ (Figure 3.20 A) following the administration of soluble antibodies. In WT mice, there was no discernible effect on GC size compared to the control group (without antibody administration). It is likely that by day10 of primary response there was already some endogenous affinity matured antibody production, which explains why – different to earlier experiments in the early phases of secondary responses (Zhang et al., 2013) intermediate low-avidity anti-NP IgM did not have a strong effect on GC selection in wt mice. As expected, AIDko and IgMi mice developed

slightly bigger GC size after injection of antigen, similar to the results described above (Figure 3.4 B, and 3.9 B).

Bigger GC in AIDko mice is may be due to the absence of a negative effect of mutations induced by AID, leading to less B cells apoptosis during GC B cell differentiation, and accumulate in the light zone (Figure 3.10 A) and do not effectively differentiate into plasma cells in mixed bone marrow chimeras (Boulianne et al., 2013). After injection with soluble intermediate low affinity anti-NP antibody, AIDko mice exhibited a trend to reduced GC sizes, particularly NP specific GC B cells (Figure 3.20 B, and C). This result would support the hypothesis that absence of antibody feedback is responsible for the larger GCs in AIDko mice. AIDko cannot produce affinity matured antibodies, and therefore exogenous intermediate low-avidity anti-NP IgM can block partly access to antigen for GC B cells, resulting in decreased GC, albeit not statistically significant. In IgMi mice (Figure 3.20 B, and C), soluble exogenous intermediate low-avidity anti-NP IgM antibodies led to slightly reduced GC sizes and NP-specific GC B cells, however, this effect was not significant. IgMi B cells can undergo affinity mutation, but do not secrete antibody, therefore, exogenous intermediate antibody should be able to inhibit GC B cells access to antigen on FDC.

To gain further insight into the effects of introduction of antibody feedback during the GC response, the number of plasma cell (PC) was identified as $CD138^{+}$ $B220^{-}$ and quantified. Surprisingly, the percentage of PC was significantly increased in WT mice after injection of soluble intermediate low affinity antibodies (Figure 3.20 D). AIDko had similar number of total plasma cells, but IgMi mice had significantly reduced plasma cell numbers (Figure 3.20 D), slightly different with the previous data injected with immune complex. It is not clear why antibody feedback induced higher numbers of PC, as an earlier study found a reduction of PC

output from GC when antibody feedback was introduced (Zhang et al., 2013). This study, however, observed GC derived PC by immunohistology. As similar histological study on the tissues of the present experiment might be helpful.

Subsequently, we investigated the impact of injecting soluble intermediate low-avidity antibodies on the distribution of GC B cells into dark and light zones, as defined by the gates illustrated in (Figure 3.21 A). As described above (chapter 3.1.2), AIDko mice showed a significant reduction in the DZ compartment and a corresponding increase in the LZ compartment, while IgMi mice showed the opposite effect. There was no effect on DZ/LZ distribution after introduction of antibody feedback (Figure 3.21 B).

We subsequently investigated whether there were any alterations in the frequency of IgM among all mouse genotypes, as well as IgG1 levels in WT mice following soluble antibody injection. As expected, this did not reveal significantly changes in the proportion of IgM in the groups of treated mice when compared to their respective control groups without antibody injection (Figure 3.22 A and B).

To test whether raising the GC B cell selection threshold by introduction of antibody feedback feeds back onto Tfh cell activation, we quantified Tfh cells. Tfh cells were identified as $CD44^{+}$ $PD1^{hi}$ $CXCR5^{hi}$, as depicted in (Figure 3.23 A). As described above, AIDko and particularly IgMi mice contain significantly more Tfh cells after primary response to NP-CGG antigen compared to WT mice (Fig. 3.23 B), mainly due to a bigger GC compartment (Fig. 3.23 C). Injection of intermediate low-avidity antibodies led to a non-significant reduction in Tfh cell numbers in all genotypes, with a stronger effect in AIDko and IgMi mice (Fig. 3.23 B), although there was no major effect on the Tfh/GC ratios (Figure 3.23 C). This may indicate that immunisation with intermediate low avidity antibodies in ongoing GCs in AIDko and IgMi mice can reduce GC B

cell–T cell interaction, because no high affinity antibody production in these two types of mice. These experiments should be repeated to confirm the results and increase statistical power.

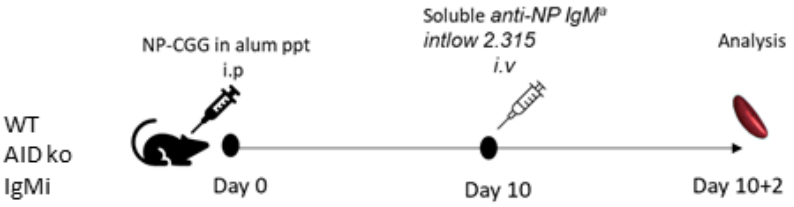

Figure 3.19 Experiment protocol of introducing the intermediate low avidity anti-NP IgM^a
WT, AIDko, and IgMi mice were immunised i.p with 50 µg NP-CGG precipitated in alum. Day 10 mice were i.v. injected with soluble intermediate low avidity anti-NP IgM^a (clone 2.315). Spleen tissues were collected two days after receiving the soluble antibodies.

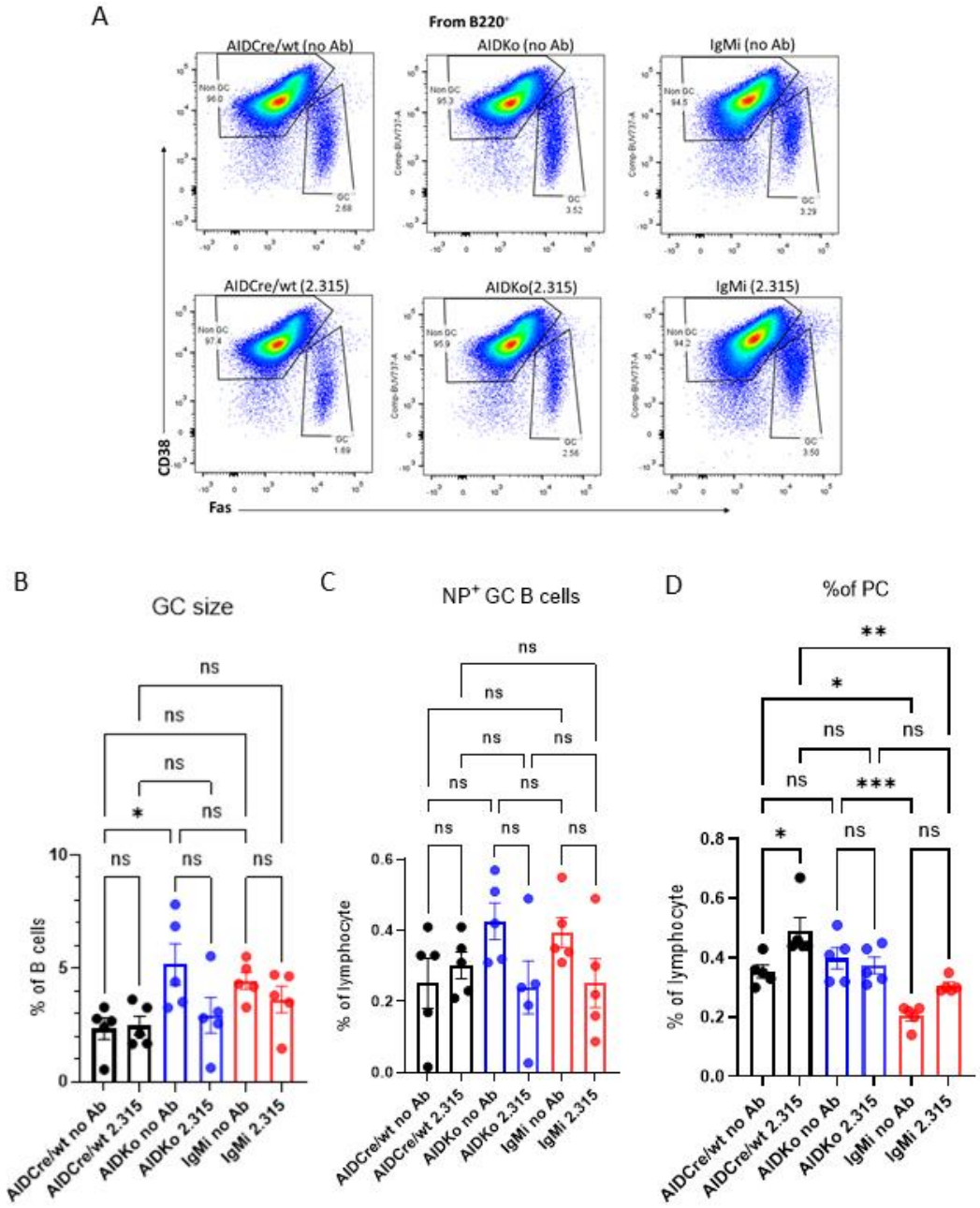

Figure 3.20 GC clearly reduced in AIDko mice After immunisation with intermediate low avidity antibody (clone 2.315) in ongoing GC response

WT, AIDko, and IgMi mice were immunised i.p with 50 µg NP-CGG precipitated in alum. Day 10 mice were i.v. injected with soluble intermediate low avidity anti-NP IgM^a (clone 2.315). Spleen tissues were collected two days after receiving the soluble antibodies. (A) Flow cytometry plots of GCs identified as CD38$^-$ Fas$^+$ from B cells population for WT, AIDko, and IgMi, upper plots are GCs with no soluble antibody as control, bottom plots are GCs after injected with intermediate avidity anti-NP IgM^a (clone 2.315). (B) GC Size, showed as percentage of total B cells. (C) NP- specific GC B cells, showed as percentage of total lymphocytes. (D) Plasma cells (PCs) showed as percentage of total lymphocytes. Data statistical tests were performed as mean ± SEM performed by ordinary one-way ANOVA with Tukey's multiple comparison test (*, $p < 0.05$; **, $p < 0.01$; ***, $p < 0.001$; ns, not significant). Data from one experiment. Each symbol represents one mouse.

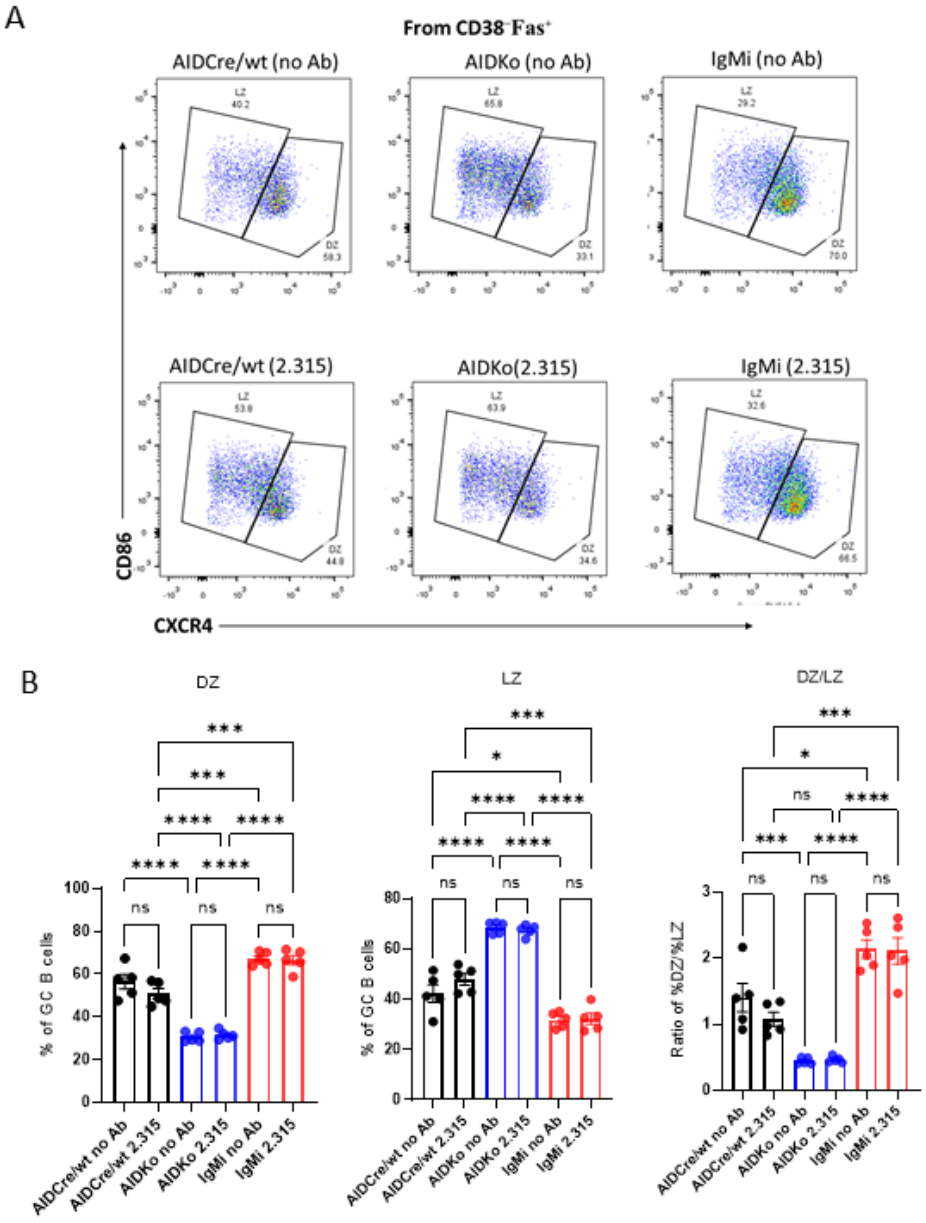

Figure 3.21 Injection of intermediate low avidity antibody in ongoing GC does not affect DZ
WT, AIDko, and IgMi mice were immunised i.p with 50 µg NP-CGG precipitated in alum. Day 10 mice were i.v. injected with soluble intermediate low avidity anti-NP IgM^{a} (clone 2.315). Spleen tissues were collected two days after receiving the soluble antibodies. (A) Representative of flow cytometry plot to identify DZ CXCR4^{hi} CD86^{lo} LZ CXCR4^{hi} CD86^{hi} from GC B cells population. (B) DZ, LZ GC B cells, showed as percentage of GC B cells, and the ratio of DZ and LZ. Data statistical tests were performed as mean ± SEM performed by ordinary one-way ANOVA with Tukey's multiple comparison test (*, $p < 0.05$; **, $p < 0.01$; ***, $p < 0.001$; ****, $p < 0.0001$; ns, not significant). Data from one experiment. Each symbol represents one mouse.

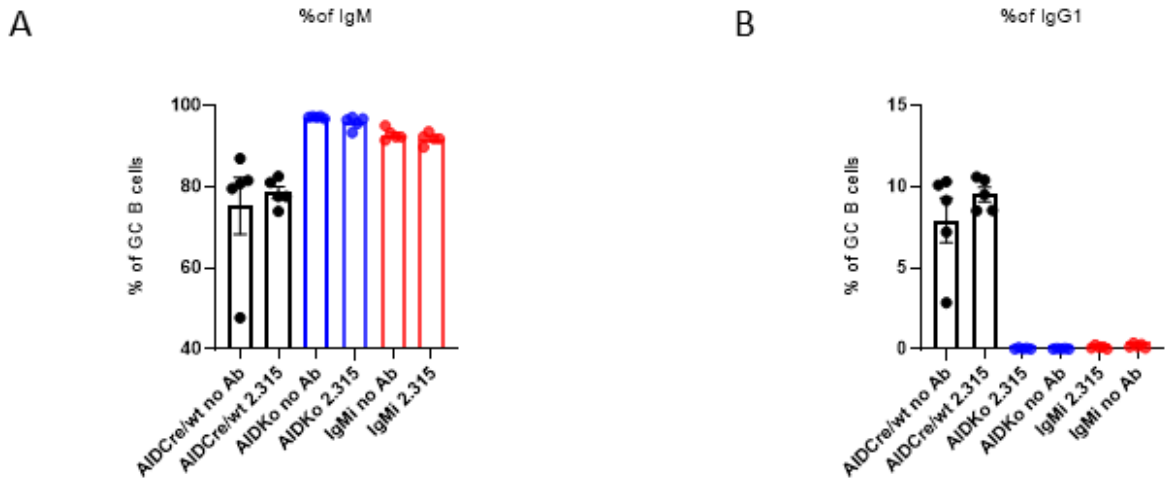

Figure 3.22 Injection of intermediate low avidity antibody does not affect the IgM in all mice genotype and WT IgG1

WT, AIDko, and IgMi mice were immunised i.p with 50 µg NP-CGG precipitated in alum. Day 10 mice were i.v. injected with soluble intermediate low avidity anti-NP IgM^a (clone 2.315). Spleen tissues were collected two days after receiving the soluble antibodies. From GC B cells, IgM$^+$ GC B cells were gated as IgM$^+$ IgG1$^-$ and IgG1$^+$ GC B cells were gated as IgM$^-$ IgG1$^+$. (A) IgM$^+$ GC B cells, showed as a percentage of GC B cells. (B) IgG1$^+$ GC B cells, showed as a percentage of GC B cells. Data from one experiment. Each symbol represents one mouse.

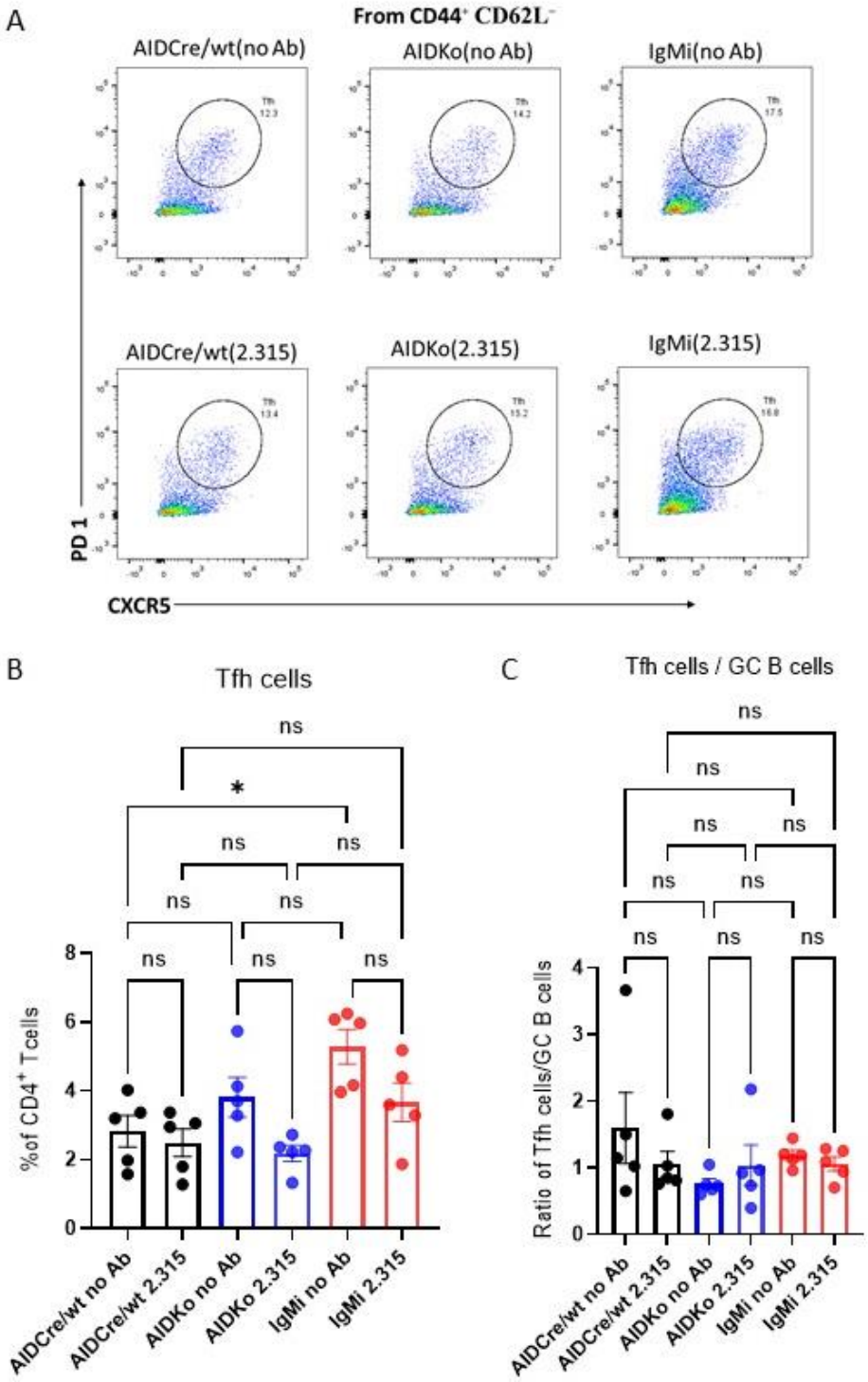

Figure 3.23 Tfh cells were reduced after injection of intermediate low avidity antibody in ongoing GC responses

(A) Representative of flow cytometry plots of Tfh cells PD1^{hi} CXCR5^{hi} gated from activated CD4 T cells CD44^{+} CD62L^{-} gate for WT, AIDko, and IgMi mice, upper plots are Tfh cells without soluble antibody treatment as control, bottom plots are Tfh cells with intermediate avidity anti-NP IgM^{a} (clone 2.315). (B) Tfh population, showed as percentage of total CD4^{+} T cells, and the ratio of Tfh cells and GC B cells. Data statistical tests were performed as mean ± SEM performed by ordinary one-way ANOVA with Tukey's multiple comparison test (*, $p < 0.05$; ns, not significant). Data from one experiment. Each symbol represents one mouse.

3.3.6. Testing the fitness of WT GC B cells in direct competition with AID deficient B cells

Next, we aimed to further investigate the effects of AID on GC B cell selection. Antigen NP-specific B cells from QM Cγ1Cre mTmG mice that were AIDWT were adoptively transferred into WT or AID deficient hosts, in order to compete with host WT or AID deficient B cells. The Cγ1-Cre x mTmG reporter strain induces constitutive expression of GFP in B cells after they have been activated by extrafollicular T cells, which is the first B cell - T cell interaction after antigen-contact inducing GC-lineage B cells (Toellner et al., 1998, Casola et al., 2006). Cγ1-Cre mice were crossed with QM mice expressing B cell receptors specific for the hapten 4-hydroxynitrophenyl (NP) (Cascalho et al., 1996a, Marshall et al., 2011) and a Cre-inducible eGFP reporter to get QM Cγ1Cre mTmG mice (Casola et al., 2006, Muzumdar et al., 2007, Marshall et al., 2011). As previously mentioned, AIDcre/cre (AIDko) mice are unable to undergo Ig hypermutation and class-switching due to a deficiency in the AID enzyme. Consequently, we hypothesised that B cells from AIDko mice would be unable to efficiently compete with antigen specific WT B cells in the GC environment.

Adoptively transferred dTomato^{+} cells can be tracked using flow cytometry. As soon as Cγ1-cre is expressed after the first T cell interaction, GFP expression induced marking most antigen-activated B cells, GC B cells and GC-derived memory B cells (Casola et al., 2006, Roco et al., 2019).

Donor NP-specific B cells from QM Cγ1Cre mTmG cells were transferred into AIDko and littermate control AIDcre/wt mice. 24 hr later, mice were immunized with NP-KLH in alum into the foot. Draining popliteal lymph nodes were harvested on days 8 and 12 for subsequent flow cytometric analysis (Figure 3.24 A). GC B cells were evaluated and identified through as CD138^{-}B220^{+}CD38^{low}Fas^{+} (Figure 3.24 B). GCs consistent of AIDwt and AIDko B cells

appeared by day 8. There was no clear difference in the size of the GC department dependent on whether the host was AIDwt or AIDko (Figure 3.25 A). From GCs further gates were employed to identify either donor GC B cells characterized as either GFP^+ or $dTomato^+$ or host GC B cells identified as $GFP^-dTomato^-$ (Figure 3.24 B). This showed that GCs at 8 d post immunisation contained more donor B cells than d 12 post immunization. Surprisingly, there were consistently fewer donor fluorescent protein $(FP)^+$ GC B cells present, if the host was AIDko (Fig. 3.25 B). Correspondingly, if the host was AIDko, host B cells made up almost 100% of GCs by 8 days after immunisation. Over time the process of host B cells taking over the GC response also happened if the host was AIDwt, but it occurred slower. By 12 days post immunisation AIDwt host B cells made up close to 100%, but the frequency was still lower than 4 d earlier if the host was AIDko (Figure 3.25 C).

The extent of GFP-induction in the donor B cell population was also evaluated. Being GC cells, GFP^{-ve} donor GC B cells should all have received Tfh help during the induction of the antibody response. However, these cells may either have received weaker signals from Tfh help, not efficiently inducing CSR, properly non-switched cells that express IgM, or recent immigrants into the GC that have only recently received Tfh signals and do not express GFP yet. More than 90% of donor GC B cells expressed GFP, although there was a trend to lower numbers 12 days post immunisation if the host was AIDko (Figure 3.25 D). Eight days post immunisation 80% of donor GC B cells were NP-specific B cells, regardless whether they were transferred into AIDwt and in AIDko hosts. By 12 days post immunisation there was a slight drop in NP-specificity in donor GC B cells when host GC B cells were AIDwt and could hypermutate. However, if the host GC B cells were AIDko, most of the remaining donor AIDwt GC B cells ceased to bind NP (Figure 3.25 E). This was different for the host GC B cells, where throughout the response around 20% of cells were NP-specific (Figure 3.25 F). Loss of NP-binding may

either indicate, that B cells were at DZ centroblasts stage and temporarily lost surface BCR expression, that GC B cells were very low affinity for NP, or that they became specific for a different epitope through Ig hypermutation, through immigration of GC founder B cells with different specificity, or through exit from the GC as effect cells such as PC or memory B cells. The different specificity could be either for another antigen, the carrier protein, or a random different specificity (i.e. non-specific).

These data indicate that QM donor B cell have some kind of problem competing with host BCR wt B cells. This is less pronounced when the host is AIDwt, but very pronounced if the host is AIDko, and donor QM B cells tend to loser their specificity to the hapten NP. As host BC outcompete donor BC and therefore should proliferate better, the hypothesis that loss of antigen-binding is due to a larger proportion of centroblasts being in the donor population is unlikely. In the following figures the proportions of DZ and LZ B cells in host and donor GC B cells will be tested.

The other explanation, that donor B cells mutate away from specificity while host B cells stay faithful to their original specificity, because they cannot mutate, is more likely, however, surprising, as it would mean that Ig hypermutation has an overwhelmingly negative effect on antigen-specificity. It is also possible that QM B cells are in a kind of mutational cul-de-sac, meaning the VDJ sequence of QM B cells may have good initial affinity for NP, but there are not sufficient options for mutations that would convert this sequence into a sequence coding for higher affinity BCR. This might explain why the proportion of NP-specific donor B cells reduces 12 d post immunisation, but not why the effect is bigger is host GC B cells are AIDko. Being AID-deficient, host GC B cells themselves cannot increase their affinity and gain a competitive advantage.

The last explanation, that donor B cells become replaced either through immigration of donor B cells specific for other epitopes, or through emigration of donor BC from the GC as effectors will be tested in the following figures. A final explanation might be that host AIDko BC have a selective advantage, because they can undergo proliferation without the associated off-target specific DNA-damaging mutational events (Zaheen et al., 2009).

Subsequently, the differentiation of FP^+ GC B cells from the donor or FP^- GC B cells from the host into the dark zone (DZ) and light zone (LZ) compartments was tested. The data reflect that donor FP^+ GC cells had lower potential for expansion when transferred into AIDko hosts, with on average half as many cells differentiating into DZ B cells (Figure 3.26 A) and correspondingly more GC B cells forming LZ B cells (Figure 3.26 B). Interestingly, although donor GC B cells, even in AIDwt hosts, tend to disappear from 8 d to 12 d post immunisation (Fig. 3.25 B), the percentage of donor DZ cells increases (Fig. 3.26 A). This may indicate that potentially donor QM cells start to recover by day 12. Further experiments on later timepoints should be done. Host B cells generally produced around 60% DZ B cells when the host was AIDwt, and fewer DZ B cells when the host was AIDko, as already described in chapter 3.1.2 (Fig. 3.26 B).

We also assessed the levels of IgM and IgG1 within both donor and host GCs. This showed that more donor GC B cells were non-switched when the host was AIDko and that in AIDko hosts the fraction of non-switched donor GC B cells increased over time (fig. 3.27 A). This corresponds to what was seen for GFP expression in donor B cells, with fewer donor BCs expression GFP when transferred into AIDko hosts (Fig. 3.25 D). It would confirm that donor GC B cells in AIDko hosts are less efficiently activated or receive less Tfh signals, potentially because they represent B cells that are recent immigrants into the GC, and not specific for the

main hapten NP (Fig. 3.25 E). For host GC B cells, it was seen that in AIDko hosts most were IgM expressing, which is expected as AIDko B cells can't do CSR (Fig. 3.27 B) When QM B cells were transferred into AIDwt hosts, the frequency of IgG1 switched host B cells increased over time, indicating that these cells were efficiently activated (Figure 3.27 B). As GCs are not structures where CSR is prevalent (Roco et al., 2019), this increase in class-switched host B cells may also be due to increased emigration of non-switched cells from the GC (Sundling et al., 2021).

In order to examine output from the GC, memory B cell (Bmem) production (Fig. 3.28) and PC production (Fig. 3.29) was tested. To evaluate Bmem production, memory B cells were gated as strong $B220^+$ $CD138^+$ NP-binding B cells. From there $CD38^+$ FAS^+ cells were gated and divided into FP^+ donor and FP^- host Bmem cells (Figure 3.28 A). This showed that the overall numbers of Bmem cells decreased over time, and more Bmem cells were generated when the host was AIDko (Fig. 3.28 B). Interestingly, there was an inverse relationship in donor B cells, which developed in smaller numbers when the host was AIDko (Fig. 3.28 C). This shows that the smaller numbers of donor GC B cells in AIDko hosts are not due to a loss from the GC due to an increased tendency of donor GC B cells to generate Bmem cells. Host GC B cells cells generated more memory B cells when the host was AIDko (Fig. 3.2 D), which is in line with the generally higher production of Bmem cells in AIDko hosts. Memory B cells generated from the GC tend to be the cells that are the less efficiently selected for affinity (Suan et al., 2017b), which would fit with AIDko B cells generating the main proportion of Bmem cells.

Plasma cell generation was also analysed to investigate effect of AID for the donor GC response (Fig. 3.29A, B). This showed that at later stages of the response plasma cell generation was mainly made up of host B cells (Fig. 3.29 C, and D). Plasma cells tend to be

more reliant on Tfh interaction and the cells that are more stringently selected for high affinity (Zhang et al., 2018). The fact that donor QM B cells do not produce plasma cells at later stages may indicate that the VDJ sequence of QM B cells is not able to mutate to high affinity. It may therefore be a good idea to repeat this experiment with a different VDJ combination that may have more potential for high affinity B cell generation. Donor AID deficiency had no effect on PC generation, however, there was an effect on the number of hapten-specific donor plasma cells. Reflecting what happens in GC B cells, fewer plasma cells were NP-binding when the host was AIDko (Fig. 3.29 E). This mirrors what is happening in donor GC B cells (Fig. 3.25 E). Testing host PC it was seen that in wt host BC the frequency of NP-binding B cells showed a tendency to increase, which would be in line with affinity maturation happening in the PC, however, in AIDko hosts, host PC seem to lose affinity for NP (Fig. 3.29 F). This is surprising as in absence of mutation there should be no increase in affinity, but also not a loss of affinity. It also does not reflect what happens in GC B cells (Fig. 3.25 F). Perhaps AIDko GC B cells produce plasma cell output only for a short time, and at later stages PC become replaced by PC specific for other antigens, e.g. from bystander GCs.

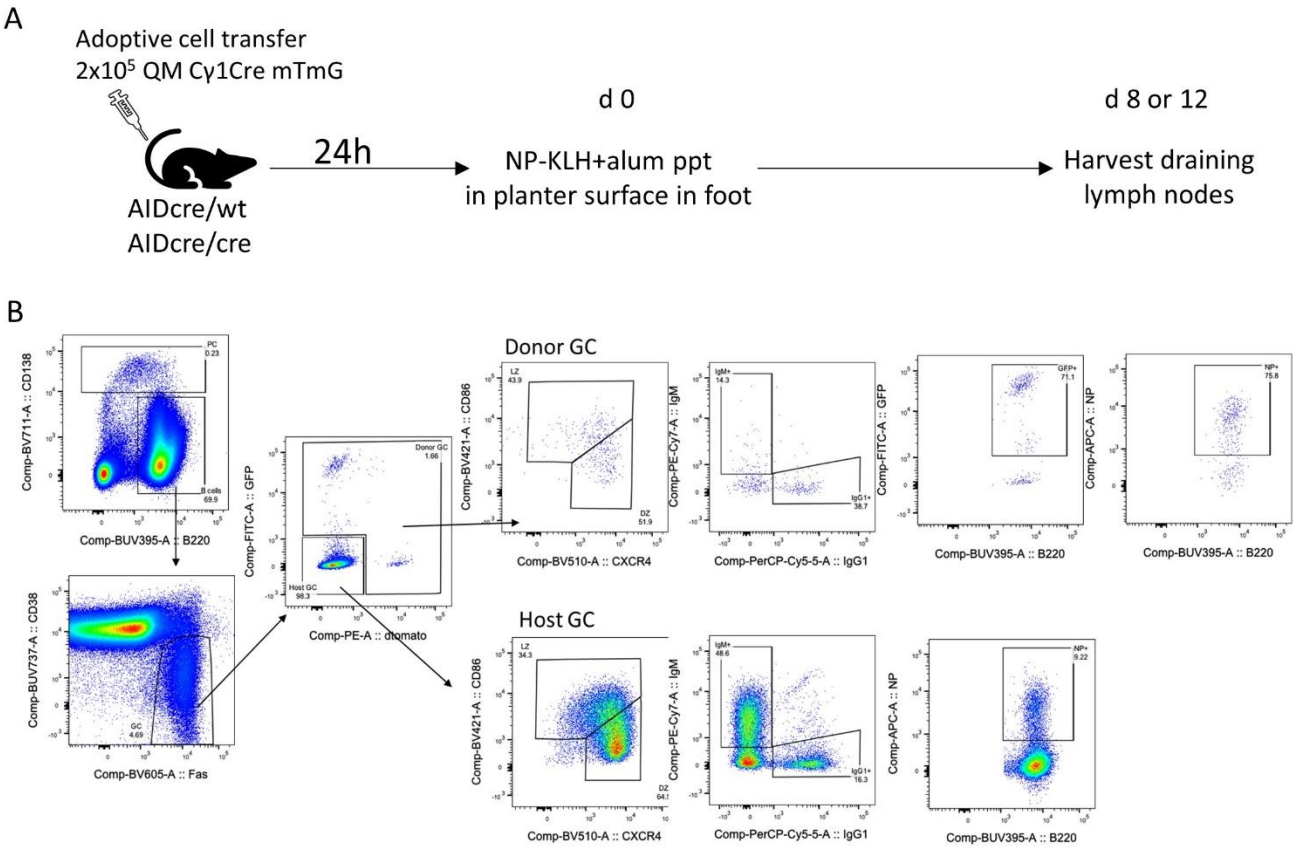

Figure 3.24 Gating strategy for identification of GFP+ donor cells and NP+ B cell host cells

(A) Schematic showing adoptive cell transfer of $2x10^5$ NP^+ B220 from QM Cγ1cre mTmG donor to AIDcre/cre (AIDko) or littermate AIDcre/wt (AIDwt) recipient mice injected i.v. 24 hours later, mice were immunised with 20 µg NP-KLH in alum into the plantar surface of one rear foot. Popliteal Lymph nodes were harvested at day 8 or day 12. (B) Gating strategy to identify GC as ($CD138^-$ $B220^+CD38^{low}$ Fas^+). From GC gate activated and IgG1 switched donor cells as (GFP^+ $dTomat^+$) or GFP^- host B cells (GFP^- dTomato-). From either donor GFP^+ or host $GFP^-dTomat^-$ GC B cells gates, DZ were identify as ($CXCR4^{hi}$ $CD86^o$), LZ as ($CXCR4^{lo}$ $CD86^{hi}$), donor GFP^+, non-switched as (IgM^+ $IgG1^-$), IgG1 class switched as (IgM^- $IgG1^+$), and NP-specific B cells.

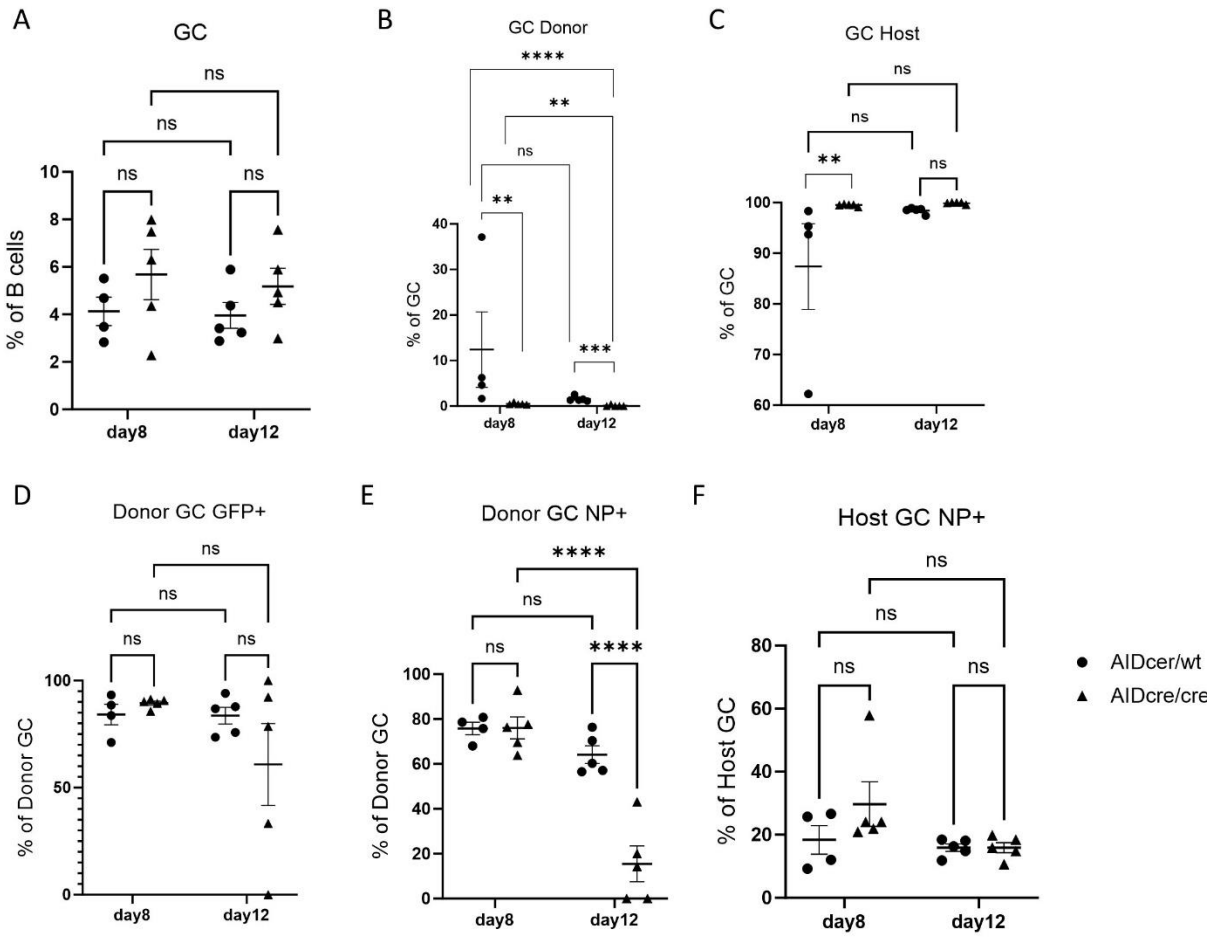

Figure 3.25 Selective disadvantage of QM Cγ1cre mTmG transferred cells in competition with endogenous AID deficient B-cells.

Analysis of donor and recipient GC responses by testing the fraction of donor (FP^+) vs recipient (FP^-) GC B cells. (A) The frequency of all GCs as percentage of total B cells. (B) The frequency of donor FP^+ GC B cells as percentage of all GC B cells. (C) The frequency of host FP^{-ve} GC B cells as percentage of GCs. (D) GFP^+ switched donor cells, quantified by gating on $B220^+$ Fas^+ GFP^+ B cells, shown as percentage of donor GC B cells. (E) Donor-derived FP^+ NP-specific GC B cells, showed as percentage of donor GC B cells. (F) Host NP-specific GC B cells, shown as a percentage of host GC B cells. Data statistical tests were performed as mean ± SEM Two-way ANOVA test mixed-effects analysis with Šídák's multiple comparisons test (*, $p < 0.05$; **, $p < 0.01$;****, $p < 0.0001$; ns, not significant). (B - C) logit Y transform. Data from one experiment. Each symbol represents one mouse.

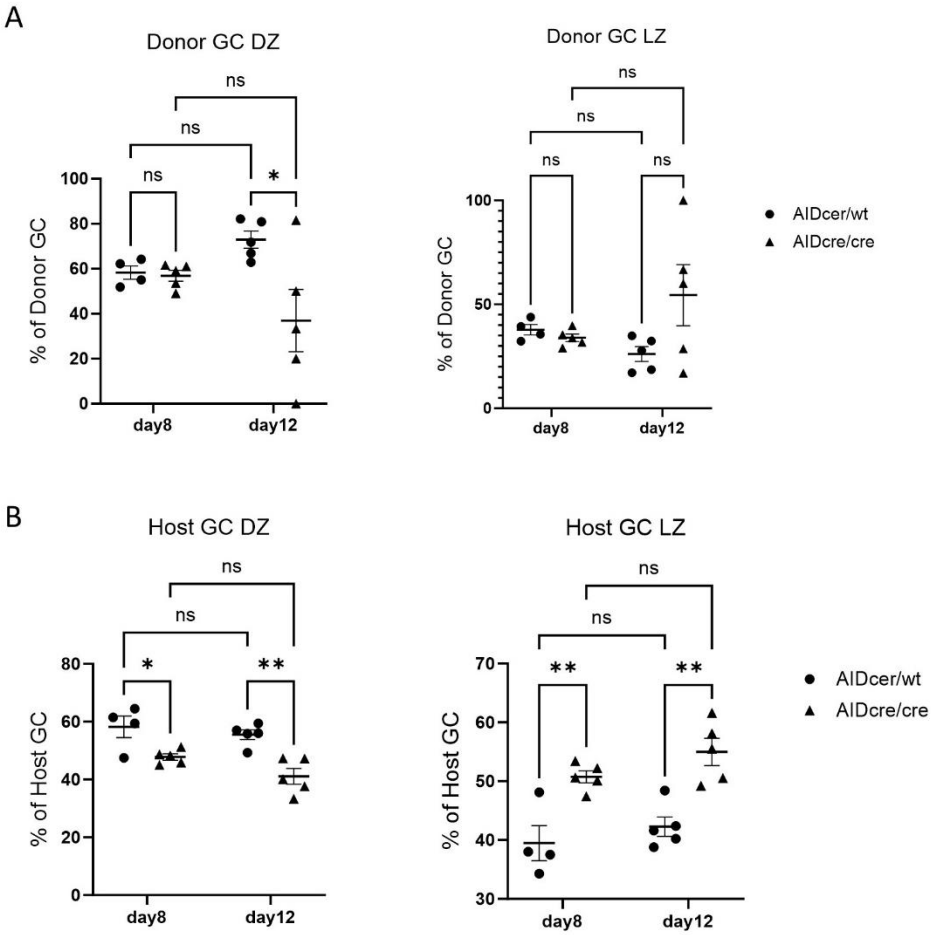

Figure 3.26 Cells transferred into AIDcre/cre (AIDko) produce similar proportion of DZ B cells.

Adoptive cell transfer of 2x105 NP+ B220 from QM Cγ1cre mTmG donor to AIDcre/cre (AIDko) or littermate AIDcre/wt (AIDwt) recipient mice injected i.v. 24 hours later, mice were immunised with 20 µg NP-KLH in alum into the plantar surface of one rear foot. Popliteal Lymph nodes were harvested at day 8 or day 12. (A) Donor DZ cells, and donor LZ cells, shown as a percentage of donor GC cells. (B) Host DZ and LZ cells, shown as a percentage of host GC cells. Data statistical tests were performed as mean ± SEM Two-way ANOVA test mixed-effects analysis with Šídák's multiple comparisons test (*, $p < 0.05$; **, $p < 0.01$, ns, not significant). Data from one experiment. Each symbol represents one mouse.

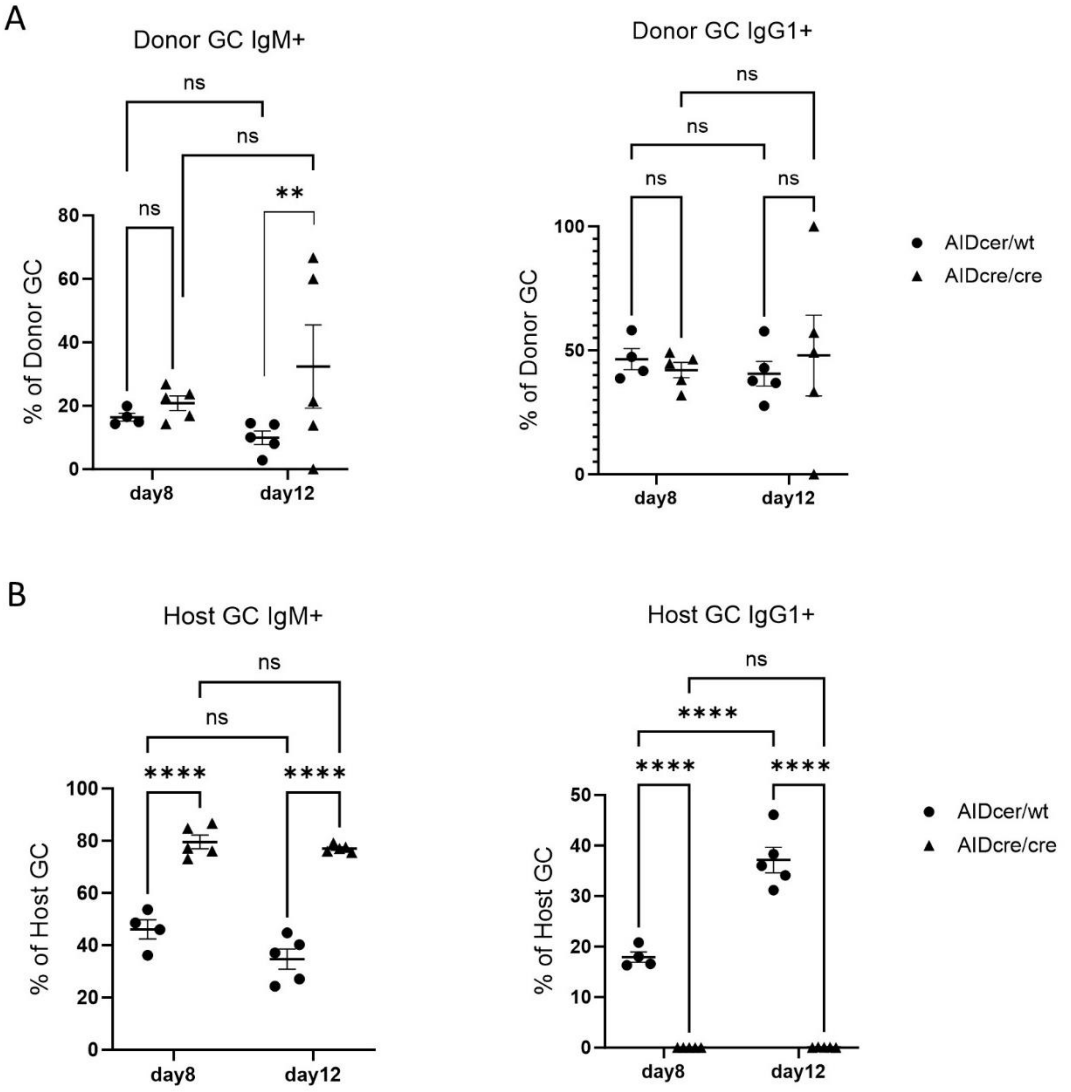

Figure 3.27 Quantification of donor and recipient unswitched IgM$^+$ and class switched IgG1$^+$.

Adoptive cell transfer of 2x105 NP+ B220 from QM Cγ1cre mTmG donor to AIDcre/cre (AIDko) or littermate AIDcre/wt (AIDwt) recipient mice injected i.v. 24 hours later, mice were immunised with 20 µg NP-KLH in alum into the plantar surface of one rear foot. Popliteal Lymph nodes were harvested at day 8 or day 12. (A) Donor IgM and class switched IgG1 GC cells, shown as a percentage of donor FP$^+$ GC B cells. (B) Percentage host IgM and IgG1 GC B cells, shown as a percentage of FP^{-ve} GC cells. Statistical tests were performed as mean ± SEM Two-way ANOVA test mixed-effects analysis with Šídák's multiple comparisons test (*, $p < 0.05$; ***, $p < 0.001$; ****, $p < 0.0001$; ns, not significant). (A) logit Y transform. Data from one experiment. Each symbol represents one mouse.

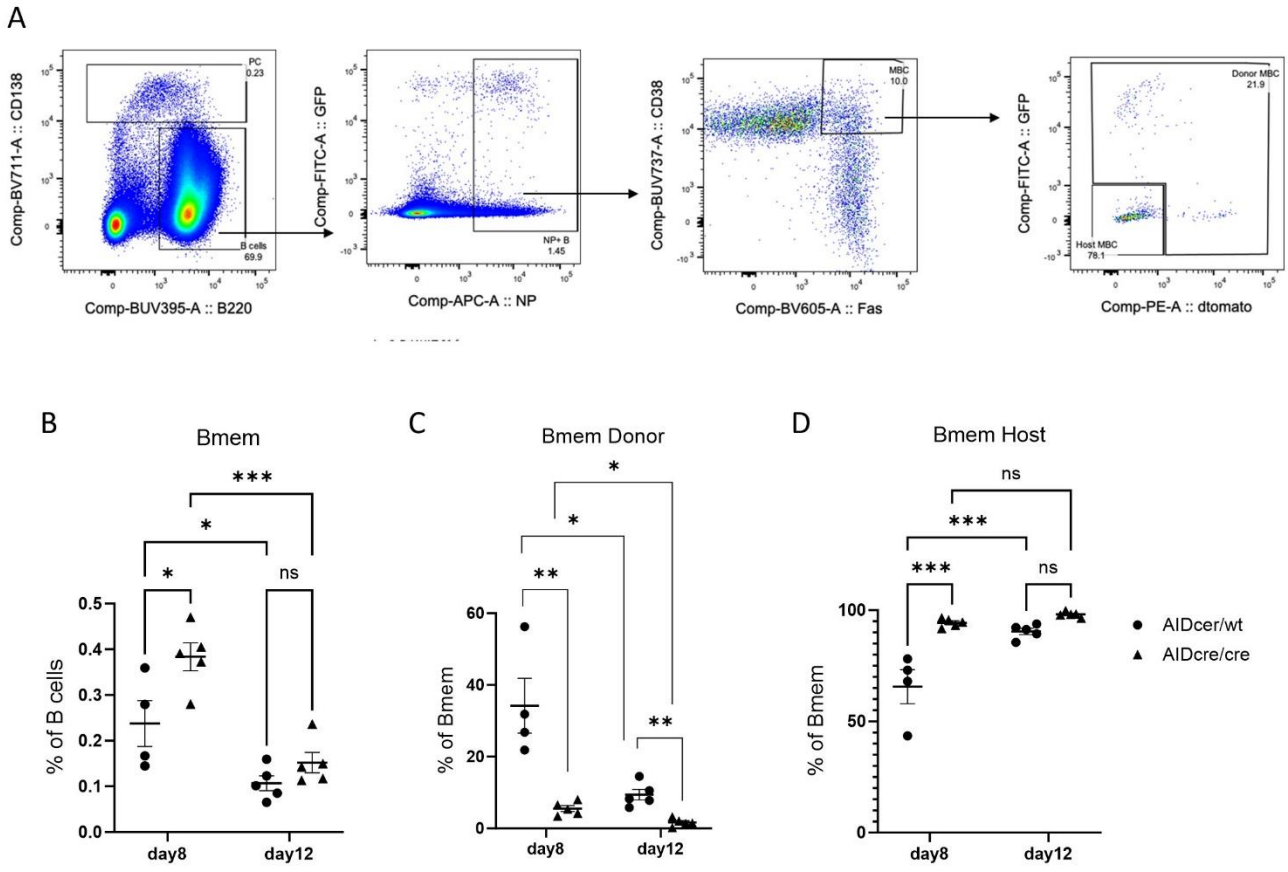

Figure 3.28 Donor memory B cells decrease in AIDko, while host Bmem increase.
Adoptive cell transfer of 2x105 NP+ B220 from QM Cγ1cre mTmG donor to AIDcre/cre (AIDko) or littermate AIDcre/wt (AIDwt) recipient mice injected i.v. 24 hours later, mice were immunised with 20 µg NP-KLH in alum into the plantar surface of one rear foot. Popliteal Lymph nodes were harvested at day 8 or day 12. (A) Gating strategy to identify donor and host memory B cells (Bmem). Bmem were gated as $CD138^{-}B220^{+}NP^{+}CD38^{high}Fas^{high}$ and from this population, either Bmem donor or host were characterized as $CD38^{high}Fas^{high}$ GFP^{+}/$dTomato^{+}$ or $CD38^{high}Fas^{high}$ $GFP^{-}dTomato^{-}$ respectively. (B) The frequency of NP+ $CD38^{high}Fas^{high}$ Bmem as a percentage of total B cells. (C) Donor $CD38^{+}$ GFP^{+} Bmem, shown as a percentage of total Bmem. (D) Frequency of host $CD38^{+}$ GFP-Bmem, shown as a percentage of total Bmem. Data statistical tests were performed as mean ± SEM Two-way ANOVA test mixed-effects analysis with Šídák's multiple comparisons test (*, $p < 0.05$; ***, $p < 0.001$; ns, not significant). (C) logit Y transform. Data from one experiment. Each symbol represents one mouse.

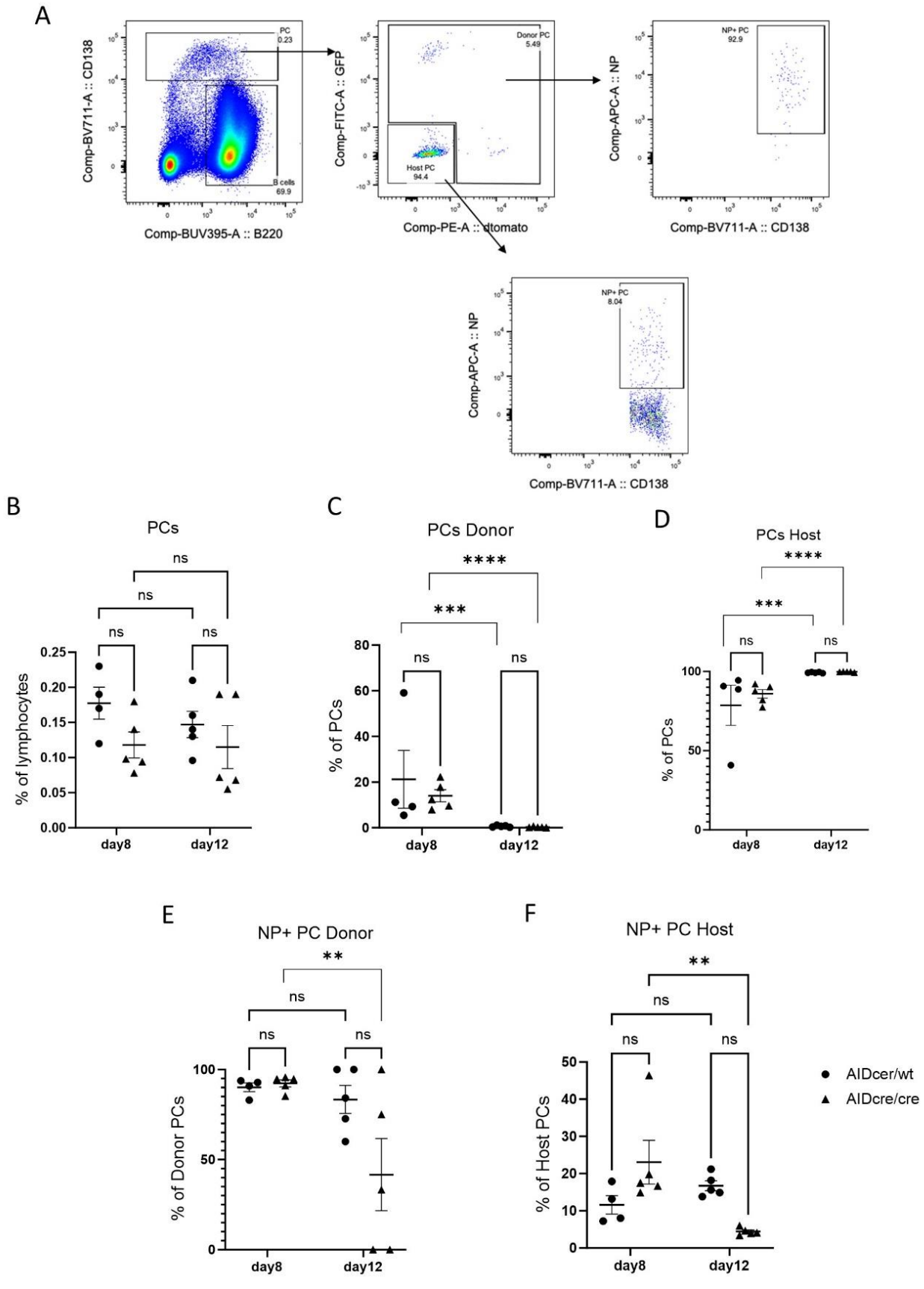
A
Comp-BV711-A :: CD138
Comp-BUV395-A :: B220
PC
0.23
B cells
69.9
Comp-FITC-A :: GFP
Comp-PE-A :: dtomato
Donor PC
5.49
Host PC
94.4
Comp-APC-A :: NP
Comp-BV711-A :: CD138
NP+ PC
92.9
NP+ PC
8.04
B
PCs
% of lymphocytes
C
PCs Donor
% of PCs
D
PCs Host
% of PCs
E
NP+ PC Donor
% of Donor PCs
F
NP+ PC Host
% of Host PCs
ns
day8
day12
AIDcer/wt
AIDcre/cre

Figure 3.29 Plasma cells were analysed 8 or 12 days after immunisation with NP-KLH in recipient AIDcre/wt and AIDcre/cre (AIDko) mice.

Adoptive cell transfer of 2x105 NP+ B220 from QM Cγ1cre mTmG donor to AIDcre/cre (AIDko) or littermate AIDcre/wt (AIDwt) recipient mice injected i.v. 24 hours later, mice were immunised with 20 µg NP-KLH in alum into the plantar surface of one rear foot. Popliteal Lymph nodes were harvested at day 8 or day 12. (A) Representative flow cytometry plots showing plasma cells (PCs) were gated as $CD138^{+}$ $B220^{-}$, from $CD138^{+}$ donor PCs were gated as GFP^{+} or $dTomato^{+}$ donor PCs, GFP^{-} $dTomato^{-}$ as host PCs, and NP-specific PCs from donor GFP^{+} $dTomato^{+}$ or host GFP^{-} $dTomato^{-}$ PC. (B) PCs, shown as a percentage of lymphocytes. (C) donor PCs, shown as a percentage of total plasma cells. (D) Host PCs, shown as a percentage of all plasma cells. (E) Donor NP-specific PCs showed as percentage of donor PCs. (F) Host NP-specific PCs, showed as percentage of host PCs. Data statistical tests were performed as mean ± SEM Two-way ANOVA test mixed-effects analysis with Šídák's multiple comparisons test (*, $p < 0.05$; **, $p < 0.01$, ns; not significant). (C – D – E) logit Y transform. Data from one experiment. Each symbol represents one mouse.

3.4. Discussion

In this study, we aimed to characterise GCs and Tfh cells and evaluate their regulation by antibodies. This was accomplished by testing the effect of absence of antibody or lack of class-switched immunoglobulins (Igs) using different mouse strains compared to wild-type (WT) controls. Specifically, we utilized IgMi, AIDko, and IgG1M mice to study GC regulation. The IgMi mice lack secreted antibody, and the B cells only have surface IgM expression as BCR. The AIDko mice lack activation-induced cytidine deaminase required for Ig somatic hypermutation and the B are unable to class-switch. The IgG1M mice have an IgG1 antibody as their B cell receptor instead of IgM and only produce IgG1. By comparing these strains, we can define the requirements for GC initiation, somatic hypermutation, and class switching. After characterising baseline GC responses, we then tested how soluble antibodies with varying affinities affect GC B cell and Tfh cell populations and their interactions. This approach provides insights into how antibody feedback shapes multiple aspects of the GC reaction and affinity maturation.

Natural IgM antibodies with low affinity help initiate and sustain GC reactions and act as bridge of innate and adaptive immune system (Baumgarth et al., 2000). Therefore, we tested whether absence of antibody in IgMi mice would affect the GC and Tfh cells compartment by introducing low avidity antibody complexed with antigen. IgMi mice had increased GC B cells (Figure 3.4) and increased NP-specific GC B cells in the spleen. This finding aligns with previous work by (Zhang et al., 2013) demonstrating that secreted high-affinity antibodies act as negative regulators of GCs by limiting B cell access to antigen on FDC. Without this antibody-mediated inhibition in IgMi mice, GC B cells can readily acquire antigen from FDCs, leading to expanded GC populations. In parallel with increased GC size, more Tfh cells were observed in IgMi spleens (Figure 3.6). Tfh cells are known to be maintained through stable interactions

with B cells (Qi et al., 2008). Thus, the accumulation of GC B cells in IgMi mice likely sustains the increase in Tfh cells. Furthermore, the ratio of dark zone (DZ) to light zone (LZ) B cells was increased in IgMi mice (Figure 3.5). This supports a model whereby LZ B cells positively selected based on their affinity can recycle back to the DZ for further somatic hypermutation (Allen et al., 2007b, Victora et al., 2010). Without competition from affinity matured antibodies, LZ B cell selection may ease, leading to more traffic of positively selected LZ B cells to the DZ. In summary, the absence of secreted antibody in IgMi mice results in deregulated GC responses, confirming a role for antibody feedback in GC regulation.

An experiment was conducted to investigate the role of affinity maturation and IgG feedback regulation of GCs. Genetically modified mice were used to address this question. Specifically, AID knockout (AIDko) mice, that do not class switch to IgG, and IgG1M mice that only express IgG1 were compared to WT control mice. We found that AIDko mice displayed enlarged GCs compared to WT mice. Despite the absence of affinity maturation in AIDko mice, there was an increased percentage of NP-specific GC B cells compared to controls. This may be because the lower affinity NP-specific B cells in AIDko mice were still able to bind the NP antigen (Figure 3.9 B and C), while the absence of hypermutation preserved the specificity of NP-specific GC B cells, causing less generation of GC B cells that have lost affinity to antigen. Additionally, flow cytometry analysis revealed an accumulation of $CD86^{hi}$ centrocytes in the light zone and a reduction in the ratio of dark zone to light zone cells in GCs of AIDko mice (Figure 3.10 A). Lack of IgG1 signalling via Fc receptors like FcγRIIB can reduce apoptosis of GC B cells (Boulianne et al., 2013), and this may allow accumulation of higher numbers of GC B cells in AIDko. Further, there was also slight increase in Tfh cells. This also may be caused by absence of antibody feedback, leading to better antigen access for GC B cells, which in turn

leads to stronger antigen presentation. Larger Tfh numbers could also simply be caused by the larger GCs, providing more space and more partners for cellular interactions.

IgG1M mice, which have IgG1 as BCR, have hyperreactive BCR signalling in response to BCR stimulation (Waisman et al., 2007). It has also been shown that IgG^{+ve} GC B cells have a selection advantage within GCs (Sundling et al., 2021). However, following immunisation IgG1M mice have similar numbers of total GC B cells as WT controls but showed strongly reduced NP-specific GC B cells (Figure 3.9 B and C) and similar numbers of Tfh cells than WT (Figure 3.11 B). Surprisingly, the DZ/LZ ratio of IgG1M GCs B cells was significantly higher compared to WT and AIDko mice (Figure 3. 10 B) suggesting that there was a defect in B cell selection in the LZ. IgG1M mice showed an impaired antibody response to NP-KLH at day 8 and day 15 post immunisation and the NP2/NP14 ratio of the IgG1 affinity was reduced by day 15. The reason for the impaired antibody response is not clear. However, secreted IgM has been shown to be important to form immune complex and has a function role in GC regulation and supporting antigen trapping on FDCs (Boes et al., 2000, Zhang et al., 2013). These findings are consistent with previous reports using the sIgM-/- mouse model, which lacks secreted IgM but retains membrane-bound IgM. Studies have demonstrated that sIgM-/- mice have impaired T-dependent antibody responses, indicating soluble IgM is important for GC development and IgG antibody production (Boes et al., 2000). Moreover, work by (Baumgarth et al., 2000) revealed sIgM-/- mice had reduced influenza-specific IgG2a titers compared to WT mice. Soluble IgM appears to enhance antigen presentation and T-B cell collaboration that are critical for antiviral IgG responses. Furthermore, immunization studies showed sIgM-/- mice had defects in memory B cell production, affinity maturation, and plasma cells (Ehrenstein et al., 1998).

In order to examine how GC B cell selection is affected by the absence of affinity maturation (AIDko mice) or absence of secreted soluble IgM (IgMi mice), antibody feedback through addition of intermediate affinity (clone 1.197) or high affinity (clone 2.315) anti-NP IgM^a variants were introduced. There was no major effect on GC size in wildtype mice receiving intermediate affinity antibody, while higher affinity antibody was able to reduce the size of WT GCs, although this was not statistically significant. This confirms a role of antibody feedback and antibody affinity in setting the selection threshold for GC B cells, as shown in our earlier study (Zhang et al., 2013). Mice unable to undergo affinity maturation or secrete IgM showed a stronger effect on GC size and antigen-specific GC B cells when given soluble intermediate affinity antibody, confirming that B cells that do not affinity mature or secrete antibody are quite sensitive to antibody feedback regulation by extrinsic antibody. These results were not reproduced in the high affinity antibody experiment, most likely due to experimental variation. Some of the experiments presented here should reproduced which was not possible due to time constraints due to the pandemic and the insufficient availability of monoclonal antibodies to NP. There were no significant changes in dark zone/light zone ratios.

Other factors that may be involved in the increased AIDko GCs may include genotoxic stress form AID expression without further apoptosis, and lack of IgG feedback inhibition to inhibit GC B cells. In IgMi mice affinity maturation through somatic hypermutation may occur as cells recirculate between light and dark zones. However, without antibody feedback inhibition from soluble IgM or negative regulation from IgG through Fc receptors, GC B cells are not inhibited and can expand better.

Both antibody feedback experiments showed a reduction in T follicular helper (Tfh) cells after injecting antibody, which may be attributed to B cells being inhibited by antibodies from taking up antigen from FDC and presenting this to Tfh cells. Tfh cells play an important role in B cell selection, so the lower percentage of light zone B cells in AID-Ko mice is not fully clear. LZ B cells capture antigens bound to follicular dendritic cells through their B cell receptors, process and present them as peptide-MHC class II complexes, with BCR-antigen engagement signaling allowing survival. Higher affinity germinal centre B cells more efficiently obtain Tfh signals because they acquire more antigen, present higher peptide-MHCII levels, and thereby stimulate greater Tfh activation (Schwickert et al., 2011, Victora et al., 2010). Therefore, lower LZ B cell percentages may result from deficient antigen acquisition and presentation to Tfh cells. Overall, the experiments demonstrate that enabling or restricting antigen access in the GC impacts on Tfh-B cell interactions, can reduce Tfh frequency and alter GC B cell subset proportions.

In the dark zone of GCs, activated B cells undergo a process called SHM, resulting in the generation of mutant clones with a wide range of BCR affinities for antigens. The selection of high-affinity BCRs is a critical step that takes place in the light zone of the GC It was believed that the primary mechanism for selecting high-affinity BCRs involved competition for antigens obtained from FDCs (MacLennan, 1994). However, an alternative factor comes into play within the light zone-the Tfh cells. They also play a significant role in selecting B cells based on their affinity for antigens (Victora et al., 2010). B cells with high-affinity BCRs compete in this environment because they more effectively capture and present antigens on major histocompatibility complex (MHC) molecules to Tfh cells compared to B cells with lower-affinity BCRs. Therefore, we studied the affinity dependent competition occurs in GCs by adoptively transferred QM cg1cre mTmg cells to either AIDcre/wt which can hypermutate or

AIDcre/cre which lack hypermutation recipients' mice. The donor GCs size are not significantly changed at day 8 in AIDcre/cre mice while 2 mice out of 4 were not detected by day 12 (Figure 3.25 B). Furthermore, the amounts of antigens in donors GCs are not altered by competition with high-BCR (Figure 3.25 E), while there is a slight increase in both AIDcre/cre host GCs and antigen-specific GC B cells. The explanation behind that, as reported previously, is that when AID activity is absent, it delays DNA damage responses and maintains the antigen-reactivity of GC B cells. This, in turn, preserves their reactivity to antigens, potentially giving B cells with AID deficiencies a competitive advantage. A malfunctioning GC response can slow down the clearance of antigens, leading to prolonged immune activation. Consequently, this delay may disrupt the normal tolerance mechanisms and trigger the production of self-reactive antibodies in both mice and individuals who lack functional AID, leading to potential autoimmune reactions (Kuraoka et al., 2011, Meyers et al., 2011).

This experiment did not clearly allow us to test GC B cell competition and affinity maturation. However, it may be possible to better test this in future by adoptively transferring B1-8^{lo} cells into AID knockout (AIDko) mice and using B1-8^{hi} cells transferred into AID wildtype (AIDwt) mice as a control. Our prediction is that transferring B1-8^{hi} cells into the competitive environment of AIDwt mice will allow them to predominate in GCs and outcompete endogenous polyclonal B cells. In contrast, transferring B1-8^{lo} cells into AIDko recipient mice could reveal whether these low affinity antigen-specific B cells can compete efficiently and undergo GC selection in a host. Thus, this approach may allow us to determine if the relative affinity of the B cell receptor determines its ability to dominate the GC reaction.

Chapter 4. Using Nr4a3 Tocky reporter mice, to characterise B cell responses and follicular helper T (Tfh) cell activation in mouse models with altered B cell receptor (BCR) signalling.

4.1. Introduction

B cell receptor (BCR) signalling plays an essential role in B cells development, activation and differentiation. The BCR complex's Igα and Igβ signalling subunits phosphorylate immunoreceptor tyrosine-based activation motifs (ITAMs) when antigen binds to the BCR immunoglobulin, initiating BCR signalling (Yao et al., 1995). Src-family kinase (SFK), binding through its SH2 domains, and recruits SYK leading to the activation of ITAMS through trans-autophosphorylation once ITAMS has been phosphorylated (Johnson et al., 1995). A signalling complex is created when downstream adaptor proteins like BLNK are phosphorylated by activated SYK (Kabak et al., 2002). This initiate signalling cascades through MAP kinase signalling, calcium flux, and PI3K/AKT activation (Guo et al., 2004, Hogan et al., 2010), throughout additional pathways. These pathways initiate the activation of B cells in response to stimuli.

IgM and IgD are two of the five known antibody isotypes, and they are co-expressed on the surface of naive B cells. Following activation, B cells will be downregulating expression of IgM and IgD and undergo class-switching of the BCRs to IgG, IgA or IgE isotype dependent on type of antigens (Toellner et al., 1998). BCR isotypes significantly differ substantially in the length of their cytoplasmic regions which influences their signalling strength and trafficking. Most BCR isotypes like IgM and IgD signal through the Igα/β heterodimer. However, IgG1 contains 28 amino acids in the cytoplasmic region while there are only 3 amino acids in the IgM cytoplasmic region (Todo et al., 2014), which give IgG1 stronger downstream BCR signalling independently of Igα/β. The IgG1 cytoplasmic domain helped to substantially rescue B cell

development defects in a mouse model with shortened Igα tail (Waisman et al., 2007). Other studies have genetically modified B cells to express an engineered chimeric BCR enhancing BCR signalling and activation. These modified BCR show increased calcium flux upon antigen stimulation, prolonged cell surface BCR half-life, and rapid plasmablast differentiation (Martin and Goodnow, 2002, Horikawa et al., 2007). Our lab has generated a mouse model to alter BCR signalling by replacing the cytoplasmic tail of IgM with that of IgG1 by targeted insertion of the Ighg1 cytoplasmic tail into the Ighm gene, leaving the immunoglobulin heavy chain VDJ area in germline configuration. Against expectation mice with this modification showed an anergic phenotype characterized by reduced BCR signalling capacity. Anergy is induced during bone marrow B cell development, likely because of the inappropriately strong signalling of this modified B cell receptor. Specifically, these IgMg1 B cells display diminished surface BCR expression and calcium mobilization upon BCR ligation compared to normal wild type B cells. Additionally, analysis of BCR-induced phosphorylation events reveals impaired activation of downstream signalling proteins (Zhang, 2019).

Binding of antigen by the BCR and subsequent BCR signalling are essential processes the regulate B cell activation and differentiation, and play crucial roles in GC reactions, allowing B cells to proliferate and improve receptors via affinity maturation (Yam-Puc et al., 2018). In a model of antibody feedback, antigen-antibody complexes deposited on FDCs can be used to kinetically test BCR affinity. The antibodies in these immune complexes mask antigen access in a competitive manner based on BCR binding strength. Antigen-antibody complexes selectively allow higher affinity BCR variants to access antigen (Zhang et al., 2013). BCRs with high binding affinity for a specific antigen are able to recruit help from Tfh cells by enabling B cells to obtain and present more antigen, fostering increased B-Tfh interaction. Interaction

and signalling from cognate B cells have been demonstrated to sustain and enhance Tfh cell proliferation in GC (Coffey et al., 2009, Baumjohann et al., 2013).

Within GCs, Tfh cells require sustained stimulation from B cells through several interactions: engagement of the T cell receptor (TCR) by B cell-presented antigen peptides and co-stimulation signals exchanged between the two cell types. Sustained antigen-driven TCR signalling, CD28 ligation, and CD40 ligation are essential for enabling Tfh cells to fully mature, expand, and persist over time (Johnston et al., 2009, Deenick et al., 2010). Furthermore, GC B cells expressing ICOSL provide crucial stimulation of the inducible co-stimulator (ICOS) receptor on Tfh cells. Ligation of ICOS by B cells results in the activation of the PI3Kδ signalling, controlling lineage commitment, which increases expression of the Tfh-defining molecules BCL6 and CXCR5 and exaggerates differentiation of Tfh cells (Stone et al., 2015). Without these reciprocal signals from GC B cells, Tfh cells cannot maintain or acquire their specialised phenotype and function.

The generation of Tfh cells is a critical step in the development of robust, protective humoral immunity following immunization. Tfh cells can be identified in mice as $CD4^+$ $CD44^+$ $CD62L^{low}$ activated T cells which express high levels of PD1, CXCR5 and ICOS. The recently developed Nr4a3-Tocky transgenic mouse model offers a novel system to visualize/track TCR stimulation elicited by peptide antigens presented by APC cells (Bending et al., 2018). Nr4a3, a gene induced in T cells, is triggered by calcineurin and NFAT activation after TCR binding to MHC II on antigen-presenting cells. Within 30 minutes, calcineurin/NFAT signalling leads to robust upregulation of Nr4a3 expression (Bending et al., 2018). The Nr4a3-Tocky mouse utilizes a fluorescent Timer reporter to analyse dynamic changes in TCR signalling strength in individual T cells in vivo by linking timer expression to Nr4a3, which is rapidly induced downstream of

TCR stimulation. This model includes an unstable timer protein, which undergoes an irreversible shift in fluorescence emission from blue to red over time. In Nr4a3-Tocky mice, newly activated T cells will initially express the blue version of the timer protein due to strong Nr4a3 induction. Over approximately 7 hours, the timer protein matures to red fluorescence (Bending et al., 2018, Elliot et al., 2021). The status of Timer colour in each T cell offers a readable output indicating recent or past TCR signalling strength. Figure 4.1 provides a simulated scatter plot profiling the Timer fluorescent phenotypes of T cells from Nr4a3-Tocky mice.

IgMg1 and IgG1M models were chosen to compare the IgMg1 mouse with a mouse where the whole IgG1 BCR is expressed during B cells development. This may allow differentiating between the signalling effect from the IgG1 cytoplasmic chain and effects from the outer part of the IgG BCR. However, there things are more complex: IgG1M mice do not make soluble IgM, and they also do not make IgD. There is also no anergy in IgG1M.

4.2. Chapter aims.

In this chapter, the aim is to characterise B cell and Tfh cell responses mouse models with altered B cell receptor (BCR) signalling, especially in IgMg1 and IgG1M mice after the stimulation with T-dependent antigens. These mice, along with WT controls, were crossed with Nr4a3-Tocky mice to evaluate the impact of modulated BCR signalling on the development and reactivation of Tfh cells. The crossed of WT, IgMg1 and IgG1M to Nr4a3-Tocky mouse model also provides an opportunity to evaluate B cell-T cell interactions in AID knockout mice when B cells can't do class switch or affinity mature after the TD antigen stimulation.

The detailed aims of this chapter are:

1) Analysis of B cell responses and evaluation of Tfh cell stimulation at different time points after antigen boosting. This will test B cell and Tfh activation in T cell-dependent antigen responses in IgMg1, IgG1M-Nr4a3-Tocky mice.
2) Analysis of B cell responses to T cell-dependent antigens and evaluation of Tfh cell after stimulation with soluble antigen in AID knockout Nr4a3-Tocky mice.
3) Preliminary analysis of Nur77-Tempo mice to test for a function of the Nr4a1 gene following B cell responses.

4.3. Results

4.3.1. Analysis of GC B cell response and Tfh cell Nr4a3-expression in mouse models with altered BCR signalling

To analyse the role of GCs B for Tfh cells activation in altering BCR mouse model during TD-antigen response, we used the Nr4a3-Tocky reporter system. This allowed investigation of early TCR signalling in Tfh cells during an in vivo immune response. WT, IgMg1/g1, and IgG1M/G1M Nr4a3-Tocky mice were immunised with 10µg NP-KLH in alum precipitation into the plantar surface of one rear foot. At day 5 or 8, mice were boosted with 10 µg soluble NP-KLH in the same foot. Popliteal lymph nodes as draining lymph nodes (DrLN) were collected at 4 hr after antigen boost (Figure 4.2 A). Four hours is sufficient time for antigen-specific memory B cells to access antigen arriving in the subcapsular sinus and to transport it back into the GC (Zhang et al., 2022). It was estimated that this is also sufficient time for these B cells to present the antigen to Tfh cells and induce a Nr4a3-Tocky signal.

To test the impact of the BCR on antigen capture and presentation to Tfh cells, Tfh cells were analysed and identified as $CD3^{+}CD4^{+}CD44^{+}$ $CD62L^{-}PD1^{hi}CXCR5^{hi}$ on days 5 and 8 and this gated as shown in (Figure 4.5 B). Without additional stimulation all three genotypes contained similar numbers of Tfh cells in GCs. Following boost with soluble antigen 5 d post immunisation, the percentage of Tfh cells stayed similar in wt mice, but increased significantly in IgMg1 mice while IgG1M GCs lost Tfh cells (Figure 4.2 C). At day 8 a similar picture showed as on day 5, with larger numbers of Tfh cells in IgMg1 GCs, but lower Tfh cell numbers in IgG1M GCs. In general, there was a stronger loss of Tfh cells after antigen administration 8 days after immunisation than 5 days after immunisation. All these data have weak statistical significance because of the low numbers of animals that were available, however, the similar

pattern 5 and 8 days post immunisation makes it likely that these changes are reproducible (Figure 4.2 C).

The GC reaction in dependent on the ability of Tfh to interact with GC B cells (de Vinuesa et al., 2000). On the other hand, B cells play an important role for supporting Tfh cell differentiation. Antigen capture by B cells in the GC predominantly re-activates Tfh cells, leading to Nr4a3 expression indicating TCR signalling strength. We therefore evaluated Nr4a3 blue reporter expression in newly activated Tfh cells after 4 hours of stimulation with soluble antigen. In WT mice, Nr4a3 blue expression was significantly higher in antigen-boosted groups compared to non-boosted controls at d5 and d8 (Figure 4.3 A). Furthermore, Nr4a3 blue expression (the percentage of $blue^{+}red^{-}$ Tfh cells) was higher at d5 than the expression at d8, which indicates higher TCR signalling strength or better antigen-presentation by B cells in newly formed GCs than matured GCs. There was a slight increase in the proportion of Nr4a3 blue expressing Tfh cells in IgG1M mice compared to WT and IgMg1 mice at d 5, becoming a significant increase by d8. However, no difference was observed between IgMg1 and WT mice (Figure 4.3 B). A significant increase was observed in the frequency of persistent signalling $blue^{+}red^{+}$ cells in IgMg1 and IgG1M mice compared to WT at day 5, indicating stronger TCR signalling in later stage of GCs. Persistent $blue^{+}red^{+}$ expression was similar between IgMg1 and WT by day 8, but remained significant higher in IgG1M compared to WT. Arrested $blue^{-}red^{+}$ Tfh cell increased also at day 8 by comparing to day 5 without additional stimulation, probably reflecting that Tfh activity in mature GCs was past its peak. No difference in arrested $blue^{-}red^{+}$ Tfh cell frequencies were detected in IgMg1 and IgG1M mice (Figure 4.3 C, and D). Figure 4.3E shows alterations in non-activated Nr4a3-negative populations before and after stimulation, confirming a loss of non- activated cells due to generation $blue^{+}red^{-}$ or arrested $blue^{-}red^{+}$ Tfh cells.

Further, the analysis of Nr4a3 blue and red reporter expression intensity (MFI) revealed increased TCR signalling in newly activated Tfh cell in IgMg1 versus WT mice after antigen boost, which was even higher in Tfh cells of IgG1M mice, again indicating stronger TCR signalling than in WT (Figure 4.3 F). No changes were observed in Tfh red^{+} cell MFIs (Figure 4.3 G). These data suggest that altering the BCR in IgMg1 and IgG1M mice captures antigen for presentation to Tfh cells inducing stronger TCR signalling compared to WT mice.

Next, we evaluated germinal centre (GC) B cells, antigen-specific GC B cells, and plasma cells (PCs) by flow cytometry. Following from 5 d post immunisation to 8 d, total GC B cells increased in all mice (Fig 4.4 A), but the percentage of antigen NP-specific GC B cells reduced from d5 to d8 if related to total GC B cells (Figure 4.4 B), perhaps due to bigger DZ compartments in more mature GC, as DZ B cells downregulate their BCR. As described by others, total GC B cells were significantly reduced in IgMg1 mice at d5 and d8 compared to WT mice before antigen boost, however antigen NP-specific GC B cells were similar as WT (Lingling, thesis 2019). Total GC B cells were significantly reduced in IgG1M mice at d5 compared to WT and IgMg1 mice, but recovered to numbers similar to WT mice at d8. NP-specific GC B cells were significantly decreased in IgG1M mice at d5 and d8. The initially smaller GC in IgG1M mice may be due to the absence of IgM antibody and negative effect from IgG, as discussed above (Figure 3.12). After antigen boost, total GC B cells slightly reduced in all genotypes. NP-specific GC B cells did not change after boost in WT mice and IgMg1 mice, but were significantly reduced in IgG1M, particularly at d8 (Figure 4.4 B). Despite the reduction in overall GC B cells and an increased percentage of Tfh cells, the frequency of NP-specific GC B cells was elevated in IgMg1 mice compared to WT or IgG1M mice. In contrast, IgG1M mice exhibited a strong reduction in NP-specific GC B cells after administration of soluble antigen at days 5 and 8.

Plasma cells increased in WT mice following the time point d5 to d8 (Fig 4.4 C). At day 5, IgMg1 and IgG1M mice showed plasma cell (PC) responses equivalent to WT mice. By day 8, PCs was increased in IgMg1 mice. Surprisingly, IgG1M mice exhibited impaired PC responses compared to WT and IgMg1 mice. In addition, antigen boost resulted in a decrease in plasma cell numbers in all mice (Figure 4.4 C).

Overall, these data suggest that altering the BCR affects the GC reaction, probably changes antigen presentation by B cells to Tfh cells, and therefore resulting in different TCR singling strength.

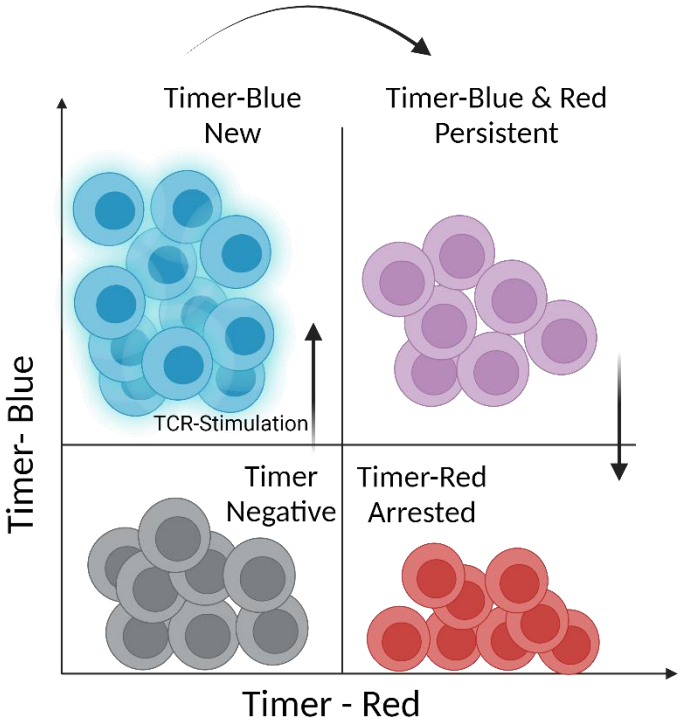

Figure 4.1 Dynamic of Tocky mice Nr4a3-blue and Nr4a3-red expression after TCR stimulation.

The plot displays Timer-red fluorescence on the x-axis and Timer-blue fluorescence on the y-axis. This allows visualization of the heterogeneous Timer expression patterns among T cells, with cell populations falling into distinct subsets based on their fluorescence. Cells with strong recent TCR signals will cluster in the upper left with high Timer-blue levels (blue). Intermediate populations with mixed Timer colours are the persistent T cells (purple). Cells with past TCR signals but no recent induction will localize to the lower right with predominant Timer-red (red). Created by Biorender. Adopted from (Bending et al., 2018).

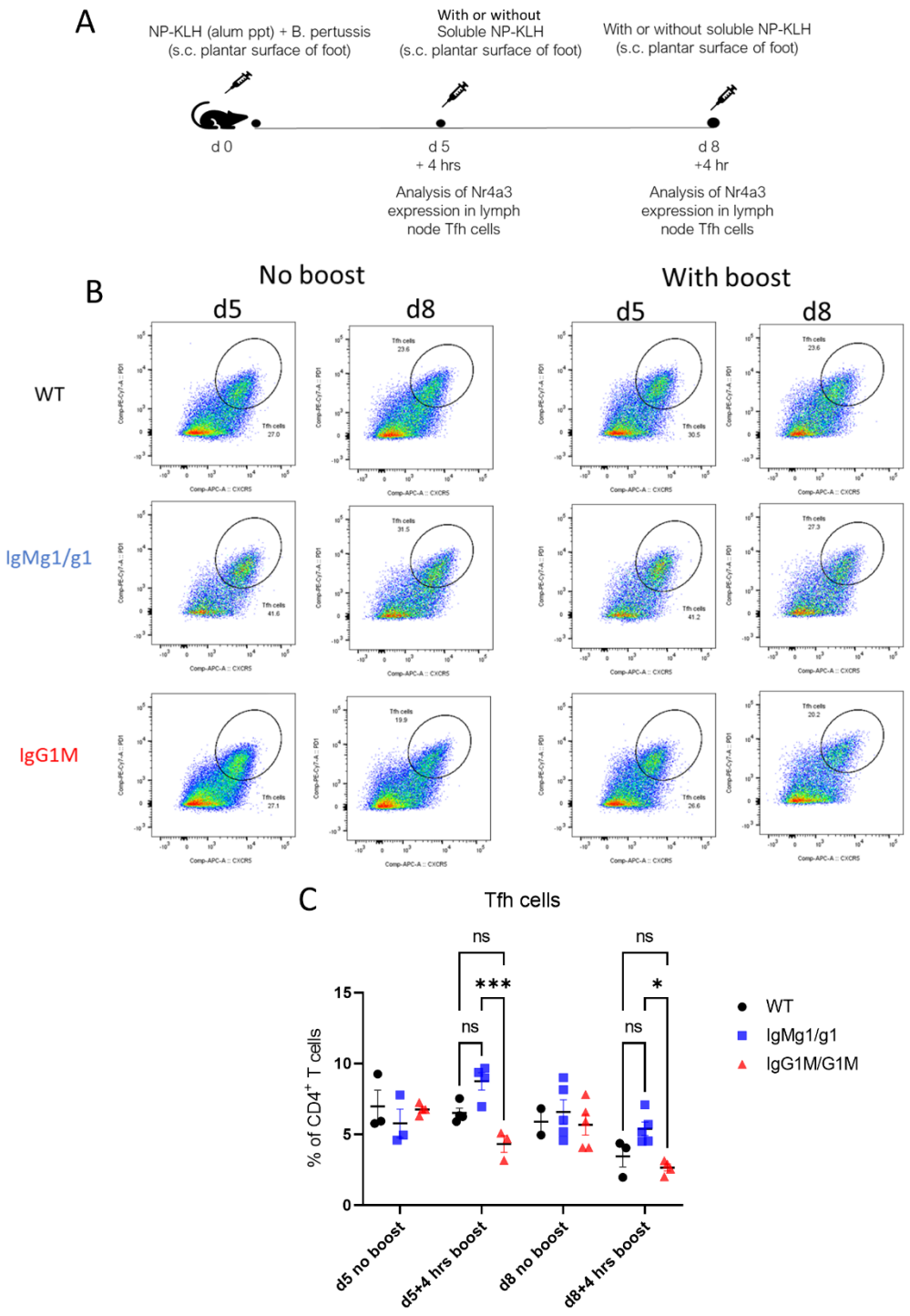

Figure 4.2 Tfh cells population decreased in IgG1M over time when received soluble NP-KLH

WT, IgMg1, and IgG1M Nr4a3-Tocky mice were immunised with 10 µg NP-KLH plus alum precipitation and heat-inactivated *B. pertussis* s.c. on the plantar surface of one rear foot. At day 5 or 8 mice were boosted with 10 µg soluble NP-KLH, and draining lymph nodes were harvest at 4hrs later. analysed by flow cytometry. (B) Representative flow cytometry plots showing Tfh cells. From lymphocytes, T cells were gated as $CD3^+$ $CD19^-$. From T cells, $CD4^+$ T cells were gated as $CD4^{+,}$ and then $CD44^+$ $CD62L^-$ gated as activated T cells. From activated cells, Tfh cells were gated as PD-1^{hi} $CXCR5^{hi}$. (C) Tfh cells, plotted as percentage of $CD4^+$ T cells. Stated as mean ± SEM Two-way ANOVA Within each row, compare columns (simple effects within rows) Data from one experiment. Each symbol represents one mouse.

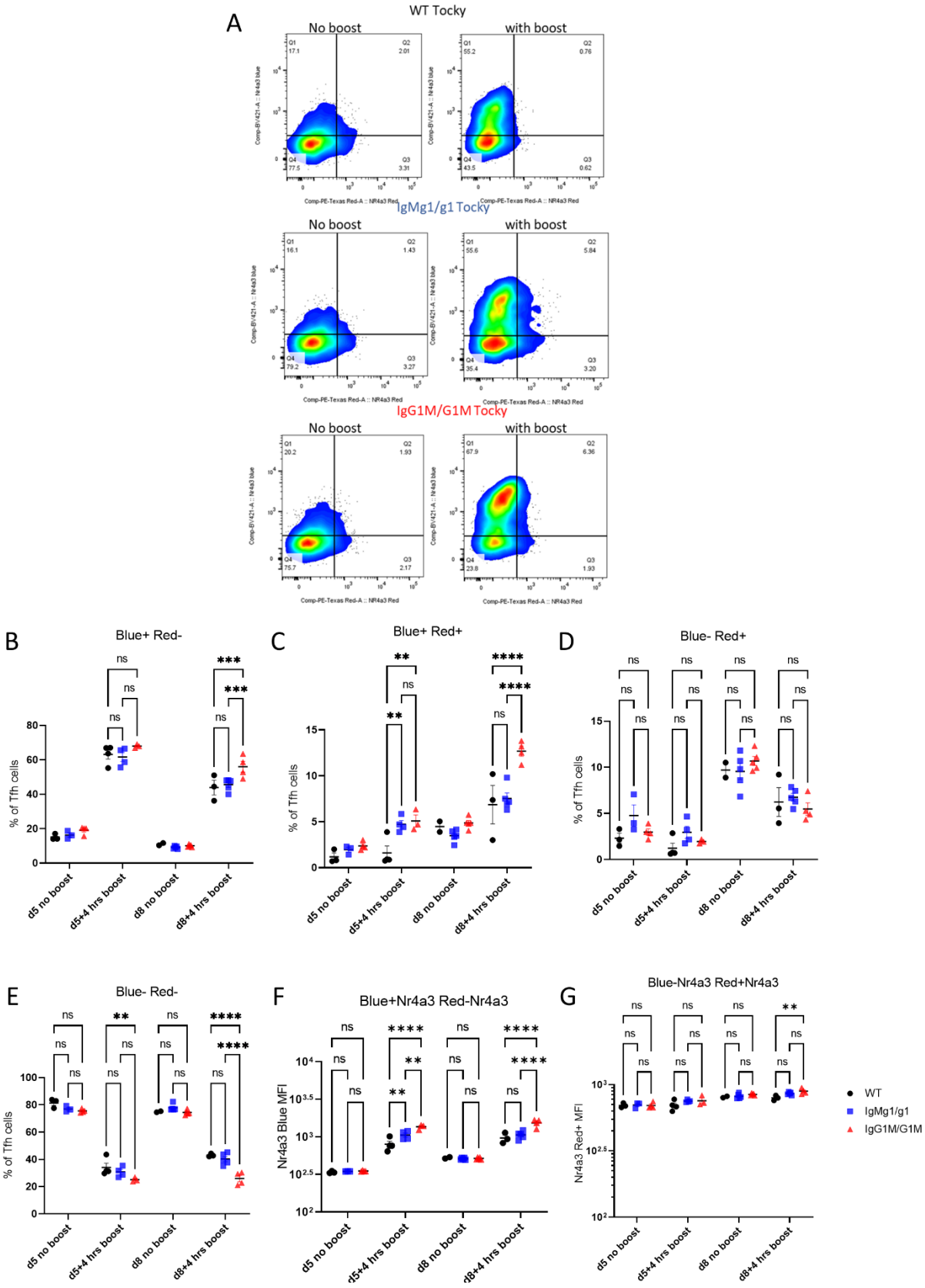
A
WT Tocky
No boost
with boost
IgMg1/g1 Tocky
IgG1M/G1M Tocky
B
Blue+ Red-
C
Blue+ Red+
D
Blue- Red+
E
Blue- Red-
F
Blue+Nr4a3 Red-Nr4a3
G
Blue-Nr4a3 Red+Nr4a3
% of Tfh cells
Nr4a3 Blue MFI
Nr4a3 Red+ MFI
d5 no boost
d5+4 hrs boost
d8 no boost
d8+4 hrs boost
WT
IgMg1/g1
IgG1M/G1M

Figure 4.3 Nr4a3-blue expression induced by the boost 4 hours of stimulation involved BCR-mediated Ag captured by B cells

WT, IgMg1, and IgG1M Nr4a3-Tocky mice were immunised with 10 μg NP-KLH plus alum precipitation and heat-inactivated *B. pertussis* s.c. on the plantar surface of one rear foot. At day 5 or 8 mice were boosted with 10 μg soluble NP-KLH, and draining lymph nodes were harvest at 4hrs later. (A) Flow cytometry plots showing Nr4a3-blue and Nr4a3-red expression, gated from PD-1^{hi} $CXCR5^{hi}$ Tfh cells. (B) Nr4a3-$blue^{+}$ red^{-} Tfh cells, shown as percentages of Tfh cells; (C) Nr4a3-$blue^{+}$ red^{+} Tfh cells shown as percentages of Tfh cells; (D) Nr4a3-$blue^{-}$ red^{+} Tfh cells shown as percentages of Tfh cells; (E) Nr4a3-blue- red- Tfh cells shown as percentages of Tfh cells; (F) Nr4a3 blue+ MFI in Nr4a3-$blue^{+}$ red^{-} Tfh cells; (G) Nr4a3 red^{+} MFI in Nr4a3-$blue^{-}$ red^{+} Tfh cells. Stated as mean ± SEM Two-way ANOVA. Each symbol represents one animal. MFI: mean fluorescence intensity. Data from one experiment. Each symbol represents one mouse.

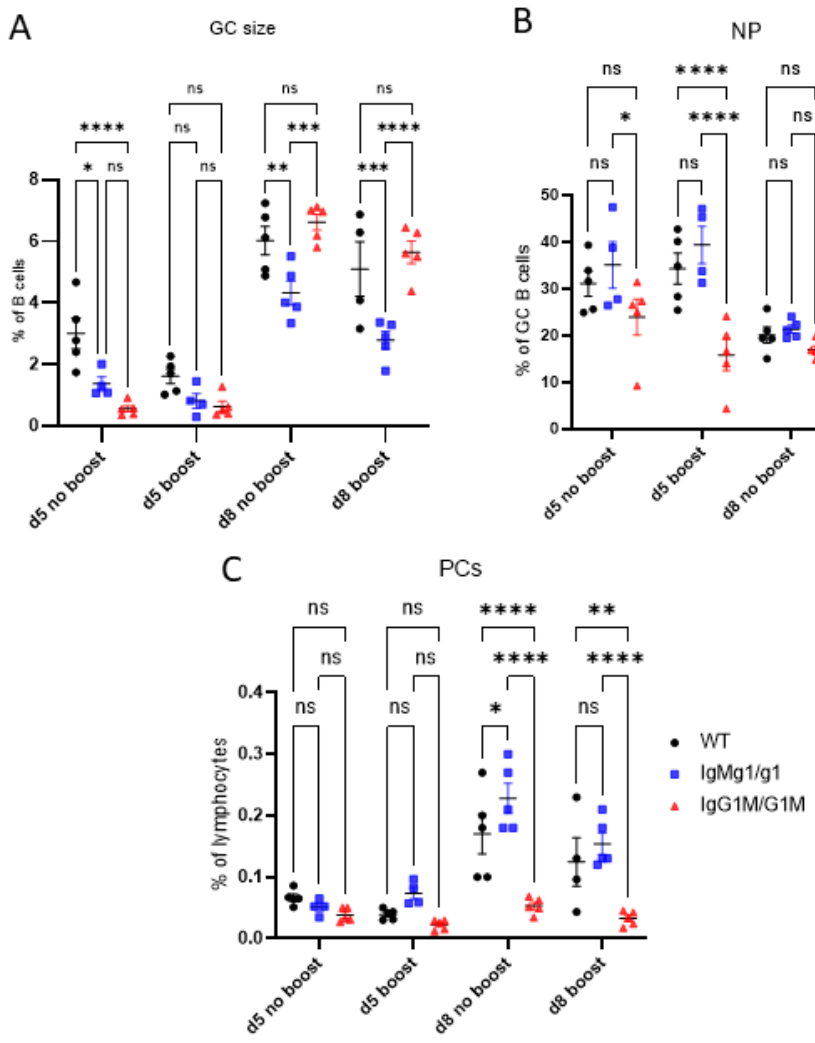

Figure 4.4 IgG1M mice have larger GC but showed an impaired of NP-specific and PCs frequency.

WT, IgMg1, and IgG1M Nr4a3-Tocky mice were immunised with 10 µg NP-KLH plus alum precipitation and heat activated *B. pertussis* s.c. on the plantar surface of foot. At day 5 and 8, mice were boosted with 10 µg soluble NP-KLH on the same foot. Mice were culled 4 hours later, and lymph nodes analysed by flow cytometry. (A) GC B cells, presented as percentage of total B cells. (B) NP-specific GC B cells, presented as percentage of GC B cells. (C) Plasma cells (PCs), presented as percentage of total lymphocytes. Stated as mean ± SEM Two-way ANOVA Within each row, compare columns (simple effects within rows), each symbol represents one animal. Data from one experiment. Each symbol represents one mouse.

4.3.2. Analysis of antigen presentation to Tfh cells in DrLN after stimulation with antigen for 18 hours in altered BCR mouse models.

In the previous experiment, IgMg1 and IgG1M mice showed strong Nr4a3 expression in recently activated Tfh cells after stimulation with soluble antigen for 4 hours. This indicated increased antigen capture in the modified BCR mouse models, particularly in IgG1M mice. In the next step, GC responses and TCR signalling dynamics were measured in the IgMg1 and IgG1M by extending the antigen re-exposure duration, with the aim of potentially finding a stronger signal after overnight incubation.

WT, IgMg1, and IgG1M Nr4a3-Tocky mice were immunised with 10 µg NP-KLH in alum precipitation plus heat-inactivated *B. pertussis* s.c. on the plantar surface of the foot. At day 8, mice were boosted with 10 µg of soluble NP-KLH on the same foot. Mice were culled 18 hours later, and draining lymph nodes were analysed by flow cytometry (Figure 4.5 A). Nr4a3 expression within Tfh cells was identified as $PD1^{hi}CXCR5^{hi}$ Nr4a3-$blue^{+}$ or red^{+} (Figure 4.5 B). Tfh cells were gated as $CD4^{+}CD62L^{-}CD44^{+}PD1^{hi}CXCR5^{hi}$ before and after boosting with soluble NP-KLH (Figure 4.6 A). In the primary response to antigen, there was no significant difference in the percentage of Tfh cells among all mouse genotypes (Figure 4.6 B). Following boost with soluble antigen, total Tfh cells didn't show any difference in WT mice. In IgMg1 mice Tfh cells showed a similar trend as those in WT mice, while Tfh cells presented a clear but not significant reduction in IgG1M mice compared to WT mice.

In the next step, persistence of TCR signal strength in re-activated antigen-specific Tfh cells after 18 hours of stimulation with soluble antigen were characterised by evaluating Nr4a3 expression (Figure 4.7 A). Compared to 4 h stimulation, following 18 hr stimulation there were not many Timer-blue (newly activated) Tfh cells detectable. Numbers increased after

stimulation in WT mice, but there was not major difference in IgMg1 and IgG1M mice compared to their respective unchallenged controls. Comparing to WT Tfh cells after stimulation, there was a minor reduction in IgMg1 and a significant reduction of Nr4a3-blue expressing Tfh cells in IgG1M mice (Figure 4.8 A). As expected, after extending the antigen exposure time (Elliot et al., 2021). Timer blue^{+} red^{+} (persistent) cells were significantly higher in all challenged groups compared to the unchallenged groups. There were no significant differences in blue^{+} red^{+} or blue^{-} red^{+} arrested Tfh cells among the challenged WT, IgMg1 and IgG1M groups (Figures 4.8 B and C), and a corresponding reduction of timer protein negative cells (Figure 4.8 D). Additionally, the MFI of timer blue^{+} Tfh cells and MFI of red were unchanged in the boosted groups (Figures 4.8 E and F). Then the MFI of blue and red within blue^{+} red^{+} Tfh cells were measured. Nr4a3-blue MFI did not change (Figure 4.8 G) in all groups after 18hr challenge. Nr4a3-red MFI significantly increased in the groups challenged with antigen (Figure 4.8 H), but no difference was detected in all challenged groups. These data show that 18 h is a long time in terms of Tfh stimulation, and most freshly activated Timer-blue Tfh cells have differentiated into blue-red double positive cells. The differences in TCR signal strength of the different genotypes seen after 4 hr tend to get lost after 18 h.

To determine how extended antigen stimulation affected the differentiation of GC B cells in the mouse models, GC B cells were assessed by flow cytometry (Figure 4.9 A). Total GC populations were identified as B220^{+}Fas^{+}CD38^{-} before and after boosting with soluble NP-KLH (Figure 4.10 A). Before boosting with soluble antigen, GC sizes all groups are largest in IgG1M mice, and smallest in WT mice. After the introduction of soluble NP-KLH for 18 hours, GCs markedly impaired in all groups, particularly in IgMg1 and IgG1M groups (Figure 4.10 B).

BCR engagement and interaction with Tfh cells in the LZ supports high-affinity B cells that receive positive selection signals and determines the positioning of the B cells within the GC. To assess this, we analysed the GC B cells in the dark zone (DZ) and light zone (LZ) which can be identified by flow cytometry as $CXCR4^{+}CD86^{-}$ for DZ B cells and $CXCR4^{-}CD86^{+}$ for LZ B cells (Figure 4.11 A). There were no major differences in DZ/LZ distribution between the different genotypes, or after antigen stimulation (Figures 4.11 B and C).

Then the GC B cells to bind antigen were analysed. NP-binding GCs B cells were identified as $B220^{+}Fas^{+}NP^{+}$ (Figure 4.12 A). The frequency of NP-specific GC B cells presented as a percentage of GC B cells showed no significant change after boost antigen for 18hrs. However, a slight reduction in IgG1M mice was observed by comparing to WT before antigen boost but this was not significant even after immunisation with soluble antigen (Figure 4.12 B). These data suggest that expanding the time of antigen exposure did not affect number of antigen-specific GC B cells nor DZ/LZ ratios in mice with modified BCRs.

There were no apparent changes in NP-specific GC B cells between different genotypes or after injection of antigen. This could be because the antigen used for flow cytometry staining – NP-APC - only detects NP-binding of higher affinity B cells (Viant et al., 2020). Therefore, the frequency of IgM and class-switched IgG1-positive GC B cells were assessed as another measure of GC B cell activation. IgM^{+} GC B cells were identified as IgM^{+} $IgG1^{-}$ and $IgG1^{+}$ GC B cells were identified as IgM^{-} $IgG1^{+}$ from the GC B cell population (Figure 4.13 A). As published earlier, the frequency of IgM expressing cells was reduced in IgMg1 mice compared to WT (Lingling thesis, 2019), even after challenge with soluble antigen. Correspondingly, IgMg1 mice showed an increased frequency of class-switching to IgG1 compared to WT (Figures 4.13 B and C).

From the IgM^+ or $IgG1^+$ cells, the affinity of the BCR in GC B cells were estimated by gating on IgM^+ NP^{hi} high affinity and NP^{lo} low affinity B cells as illustrated (Figure 4.14 A) or $IgG1^+$ NP^{hi} or NP^{lo} as illustrated (Figure 4.15 A). in IgM^+ cells, there were fewer significantly fewer NP-specific high affinity or low affinity B cells in IgMg1 GCs, with a similar distribution between high and low affinity GC B cells (Fig. 4.15 B, and C). IgG1M mice could not be analysed, as they do not express IgM. Giving soluble antigen did not change this distribution significantly (Figures 4.14 B and C). IgMg1 and IgG1M mice contained more $IgG1^+$ GC B cells that wt. Again, there were no significant differences in the distribution of high and low affinity cells, and immunisation with soluble antigen did not change this (Figures 4.15 B and C). However, to improve the system for measuring the affinity of antigen-specific GC B cells, as well as GC IgM^+ or IgG^+ with low or high BCR affinity, use of hapten-chromophore proteins with varying numbers of hapten molecules—such as NP^{hi}- or NP^{lo}-allophycocyanin (APC)—to estimate the relative affinities of BCRs (Nishimura et al., 2011).

Finally, plasma cell (PC) production was measured when re-challenged with soluble antigen. IgMg1 mice showed a slight increase in PCs compared to WT and IgG1M mice, however, this was not significant. This difference was lost after re-challenge with soluble NP-KLH (Figure 4.16 A). The frequency of NP-specific PCs showed a similar trend across all genotypes but was decreased in response to soluble NP-KLH (Figure 4.16 B).

Overall, stimulation with soluble NP-KLH for 18 hours didn't affect GC size and NP-specific GC B cells, or TCR timer blue and red in the altered BCR model mice compared to WT. Therefore, increasing the time of antigen exposure may miss the best time for the evaluation of the effect of antigen presentation on GC B cells to Tfh cells.

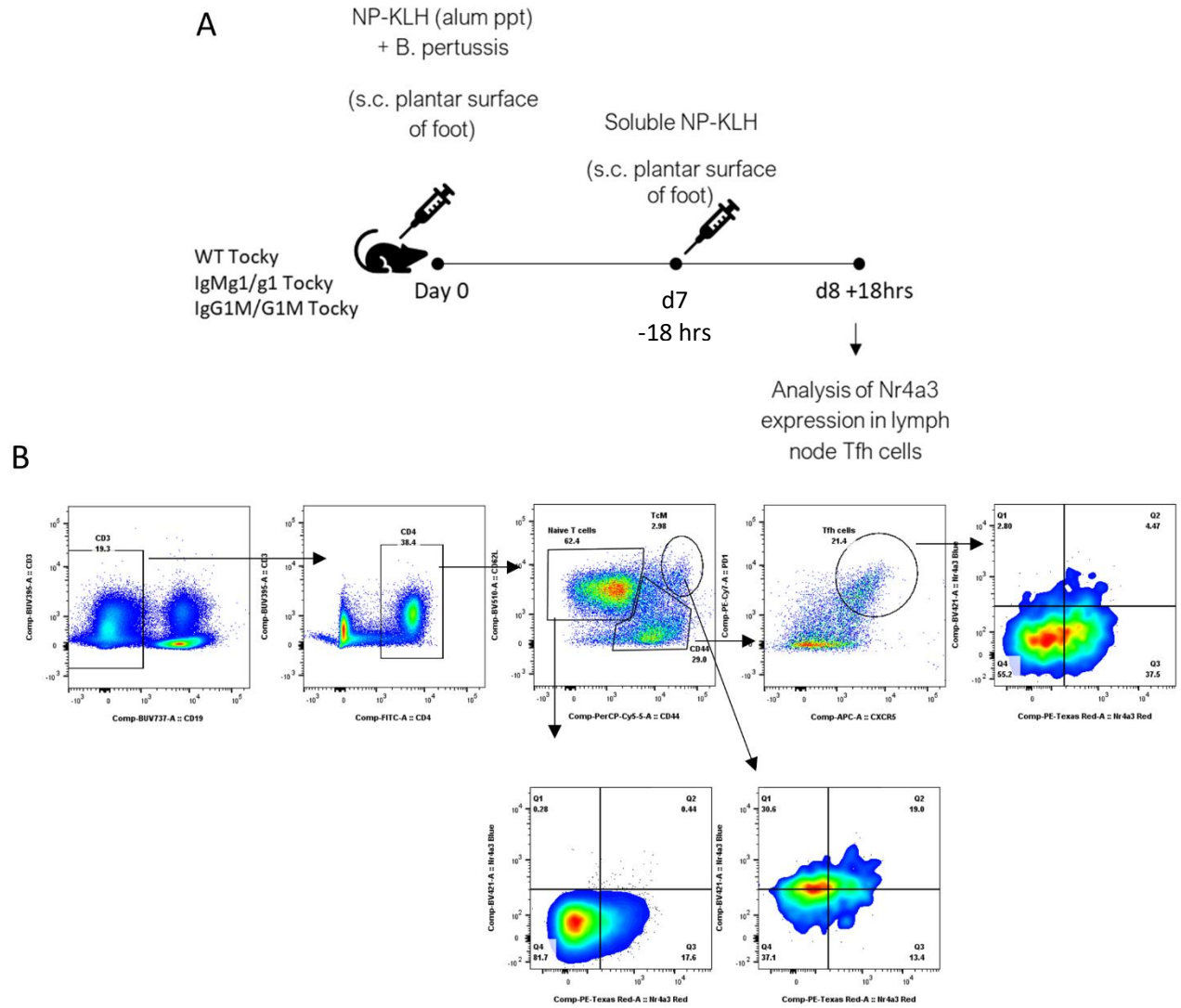

Figure 4.5 To determine the Nr4a3-expression in Tfh cells by using Nr4a3 Tocky mice after immunisation with soluble antigen for 18 hours.

(A)WT, IgMg1, and IgG1M Nr4a3-Tocky mice were immunised with 10µg NP-KLH in alum precipitation plus heat-inactivated *B. pertussis* on the plantar surface of foot. At day 8 mice were boosted with 10 µg soluble NP-KLH on the same foot. Mice were culled 18 hours later, and lymph nodes analysed by flow cytometry. (B) Gating strategy and representative flow cytometry plots showing Nr4a3-blue and Nr4a3-red expression in naive $CD4^+$ T cells and Tfh cells. From lymphocytes, T cells were gated as $CD3^+$ $CD19^-$. From CD3 T cells, $CD4^+$ T cells were gated as $CD4^+$. From $CD4^+$ T cells, $CD62L^+$ $CD44^-$ was gated as naïve CD4+ T cells, CD62L+CD44+ was gated as central memory T cells, and $CD62L^-CD44^+$ was gated as activated cells. From activated cells, Tfh cells were gated as PD-1^{hi} $CXCR5^{hi}$.

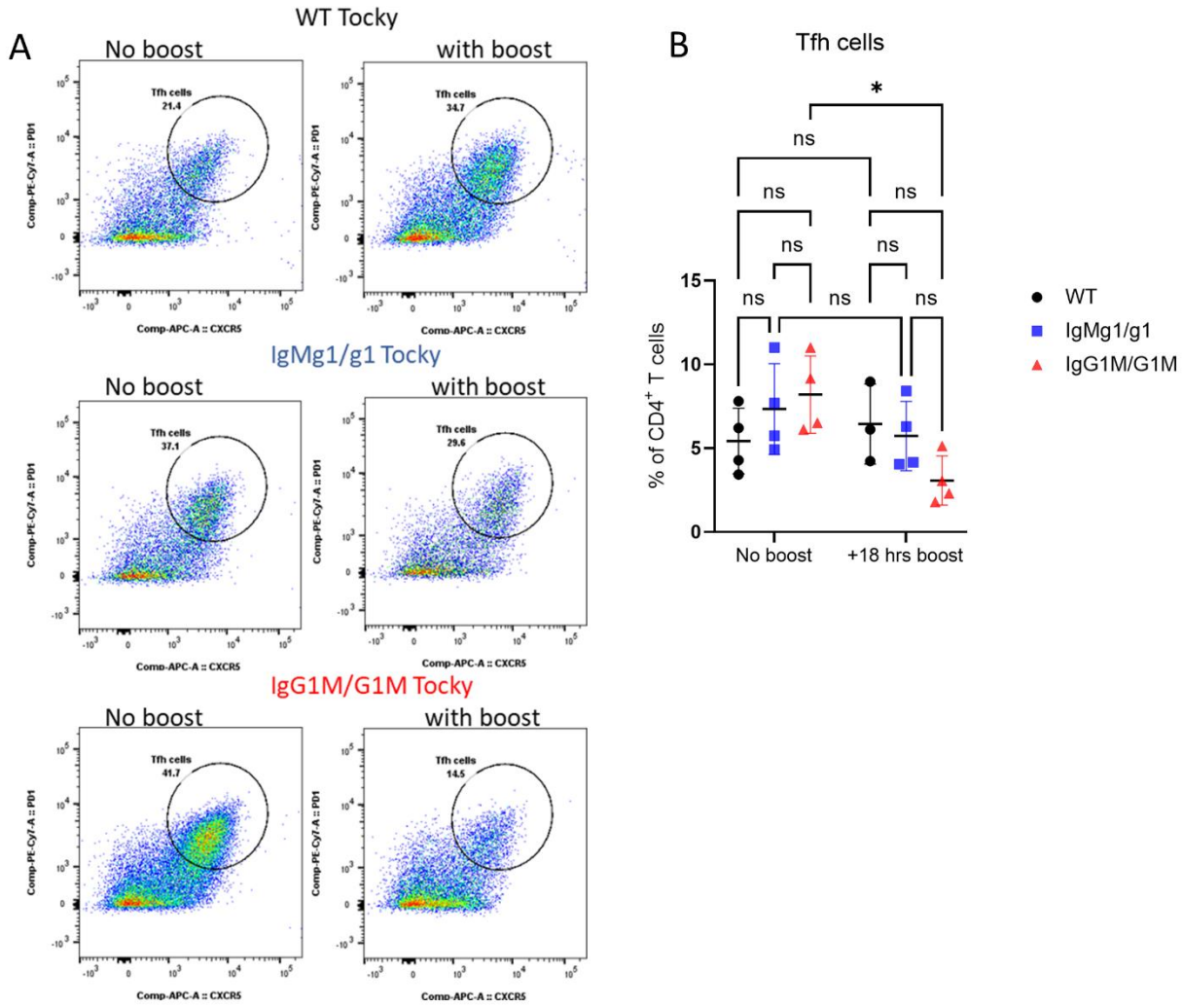

Figure 4.6 Tfh cells in DrLN were reduced in IgG1M after boost with soluble antigen.
WT, IgMg1, and IgG1M Nr4a3-Tocky mice were immunised with 10µg NP-KLH in alum precipitation plus heat-inactivated *B. pertussis* on the plantar surface of foot. At day 8 mice were boosted with 10 µg soluble NP-KLH on the same foot. Mice were culled 18 hours later. (A) Representative flow cytometry plots showing Tfh cells. From lymphocytes, T cells were gated as $CD3^+$ $CD19^-$. From CD3 T cells, $CD4^+$ T cells were gated as $CD4^+$. From $CD4^+$ T cells, naïve CD4+ T cells were gated as $CD62L^+$ $CD44^-$ and activated cells were gated as $CD44^+$ $CD62L^-$. From activated cells, Tfh cells were gated as PD-1^{hi} $CXCR5^{hi.}$ (B) Tfh cells presented as percentage of total $CD4^+$ T cells. Stated as mean ± SEM Two-way ANOVA Within each row, compare columns (simple effects within rows). Data from one experiment. Each symbol represents one mouse.

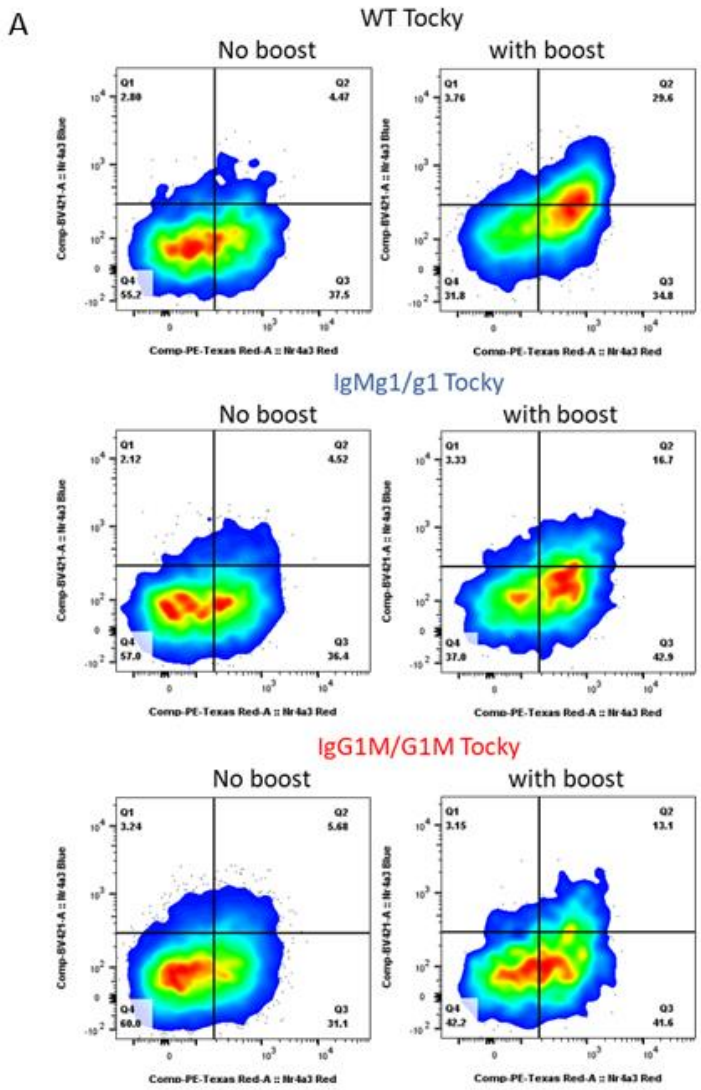

Figure 4.7 Tfh cells Nr4a3 blue and red expression after boost with soluble NP-KLH
WT, IgMg1, and IgG1M Nr4a3-Tocky mice were immunised with 10µg NP-KLH in alum precipitation plus heat-inactivated *B. pertussis* on the plantar surface of foot. At day 8 mice were boosted with 10 µg soluble NP-KLH on the same foot. Mice were culled 18 hours later. (A) Representative flow cytometry plots showing Nr4a3-blue and Nr4a3-red expression in Tfh cells identified as $PD1^{hi}$ $CXCR5^{hi}$ in drLN.

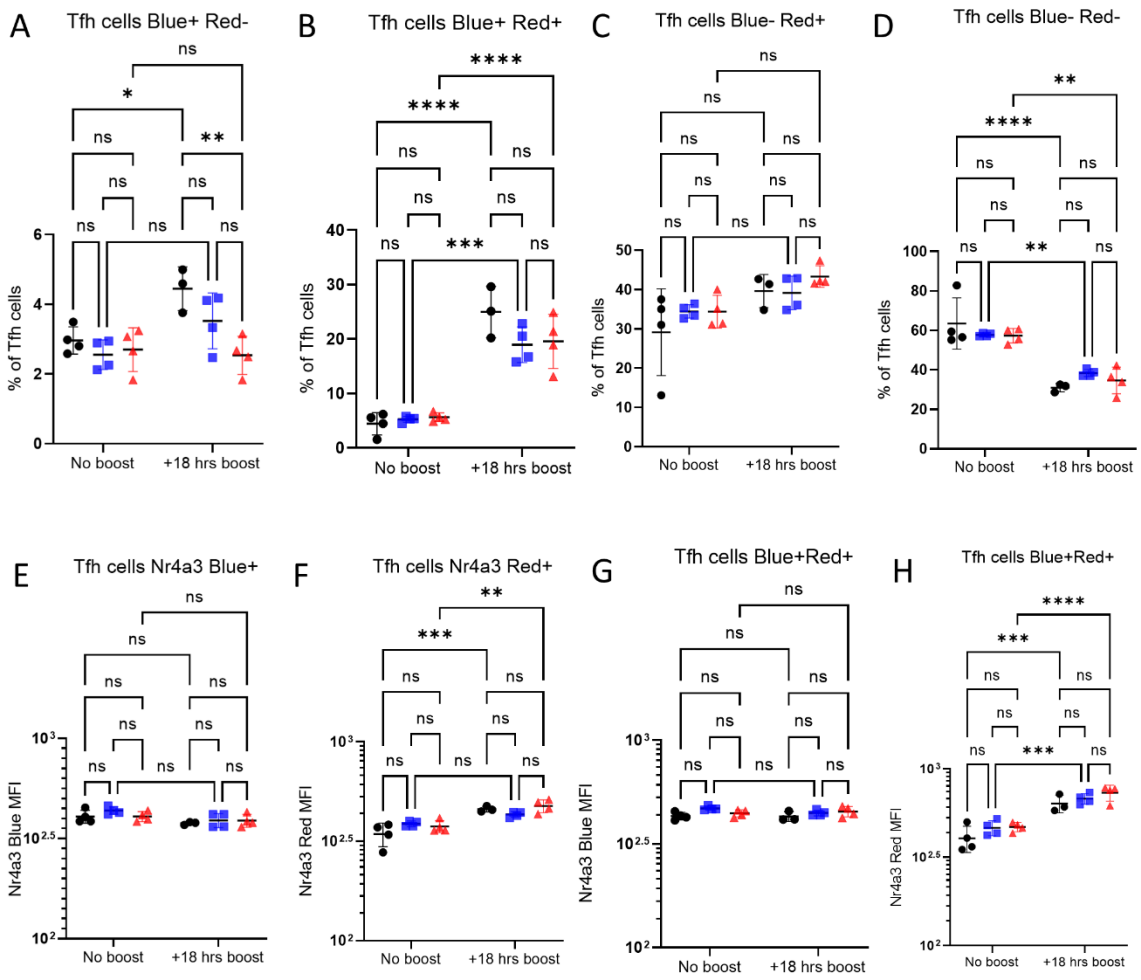

Figure 4.8 Nr4a3-blue and Nr4a3-Red expression in Tfh cells 8 days after NP-KLH immunisation of Nr4a3-Tocky mice.

WT, IgMg1, and IgG1M Nr4a3-Tocky mice were immunised with 10µg NP-KLH in alum precipitation plus heat-inactivated *B. pertussis* on the plantar surface of foot. At day 8 mice were boosted with 10 µg soluble NP-KLH on the same foot. Mice were culled 18 hours later. (A) Nr4a3-blue+ red- Tfh cells presented as percentage of Tfh cells; (B) Nr4a3-blue+ red+ Tfh cells presented as percentage of Tfh cells; (C) Nr4a3-blue- red+ Tfh cells presented as percentage of Tfh cells;(D) Nr4a3-blue- red- Tfh cells presented as percentage of Tfh cells; (E) Nr4a3 blue+ MFI in Nr4a3-blue+ red- Tfh cells; (F)) Nr4a3 red+ MFI in Nr4a3-blue- red+ Tfh cells;(G) Nr4a3 blue+ and red+ MFI in Nr4a3-blue+ red- Tfh cells; (H) Nr4a3 blue+ and red+ MFI in Nr4a3-blue- red+ Tfh cells. (Black circle WT, Red square IgMg1, Red tringle IgG1M). Stated as mean ± SEM Two-way ANOVA Within each row, compare columns (simple effects within rows). MFI: Median Fluorescence Intensity. Data from one experiment. Each symbol represents one mouse.

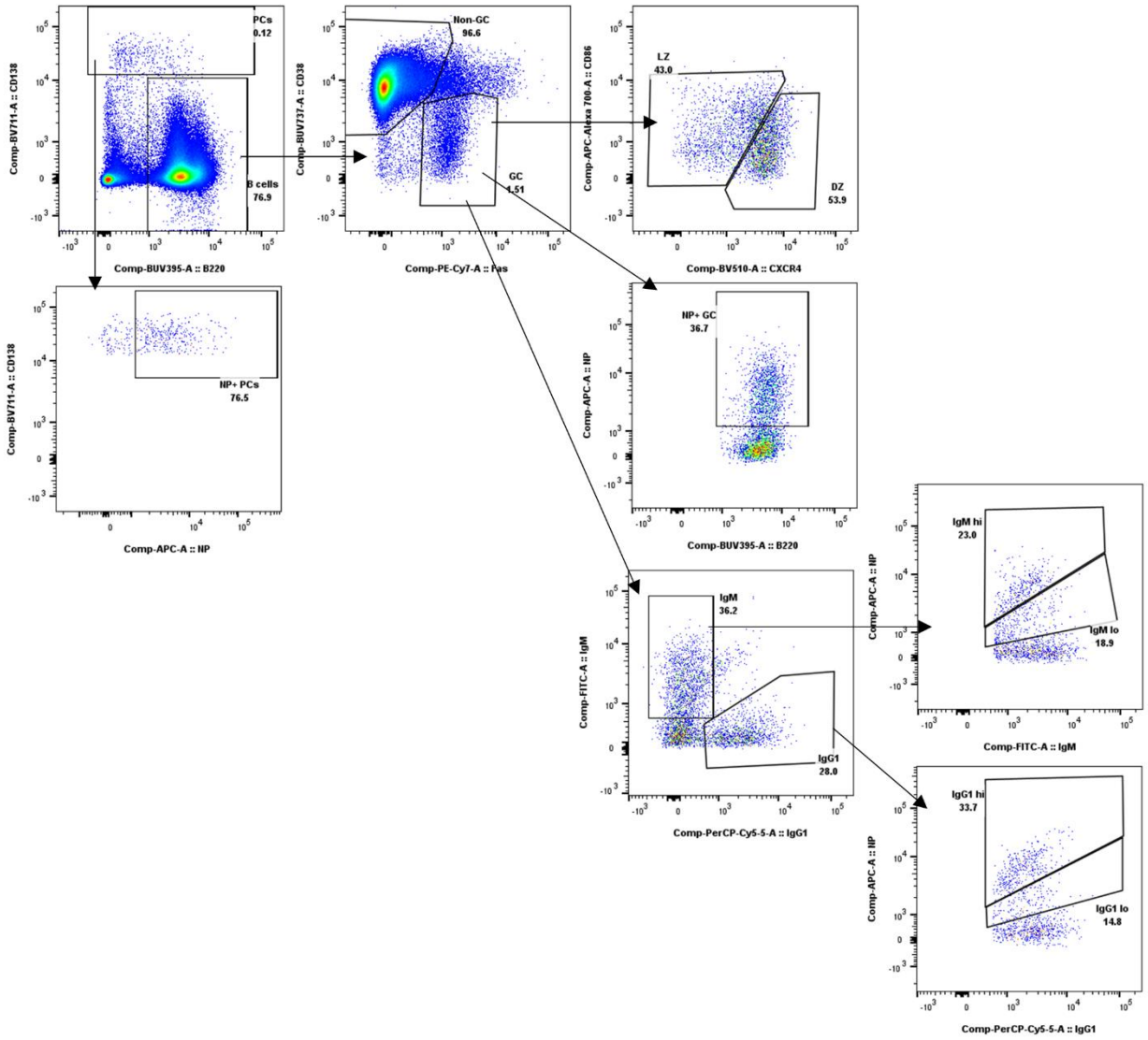

Figure 4.9 GC B cells and BCR NP-affinity assessed by flow cytometry in Nr4a3 Tocky mice.
WT, IgMg1, and IgG1M Nr4a3-Tocky mice were immunised with 10µg NP-KLH in alum precipitation plus heat activated *B. pertussis* on the plantar surface of foot. At day 8, mice were boosted with 10 µg soluble NP-KLH on the same foot. Mice were culled 18 hours later, and lymph nodes analysed by flow cytometry. Gating strategy for plasma cells, NP-specific plasma cells, GC B cells, DZ GC B cells, LZ GC B cells, NP-specific GC B cells, IgM GC B cells and IgG1 GC B cells. From live lymphocytes, plasma cells (PCs) were gated as $CD138^{+}$ and B cells were gated as $B220^{+}$ $CD138^{-}$. From B cells, GC B cells were gated as Fas^{+} $CD38^{-}$. DZ were gated as $CXCR4^{+}$ $CD86^{-}$ and LZ were gated as $CXCR4^{-}$ $CD86^{+}$. NP-specific GC B cells were gated as NP-APC^{+}. From GC B cells, IgM^{+} GC B cells were gated as IgM^{+} $IgG1^{-}$ and $IgG1^{+}$ GC B cells were gated as IgM^{-} $IgG1^{+}$. IgM^{+} GC B cells NP^{hi} cells were gated as NP-APC^{hi} IgM^{+} cells and NP^{lo} cells were gated as NP-APC^{lo} IgM^{+}. $IgG1^{+}$ GC B cells NP^{hi} cells were gated as NP-APC^{hi} $IgG1^{+}$ cells and NP^{lo} cells were gated as NP-APC^{lo} $IgG1^{+}$.

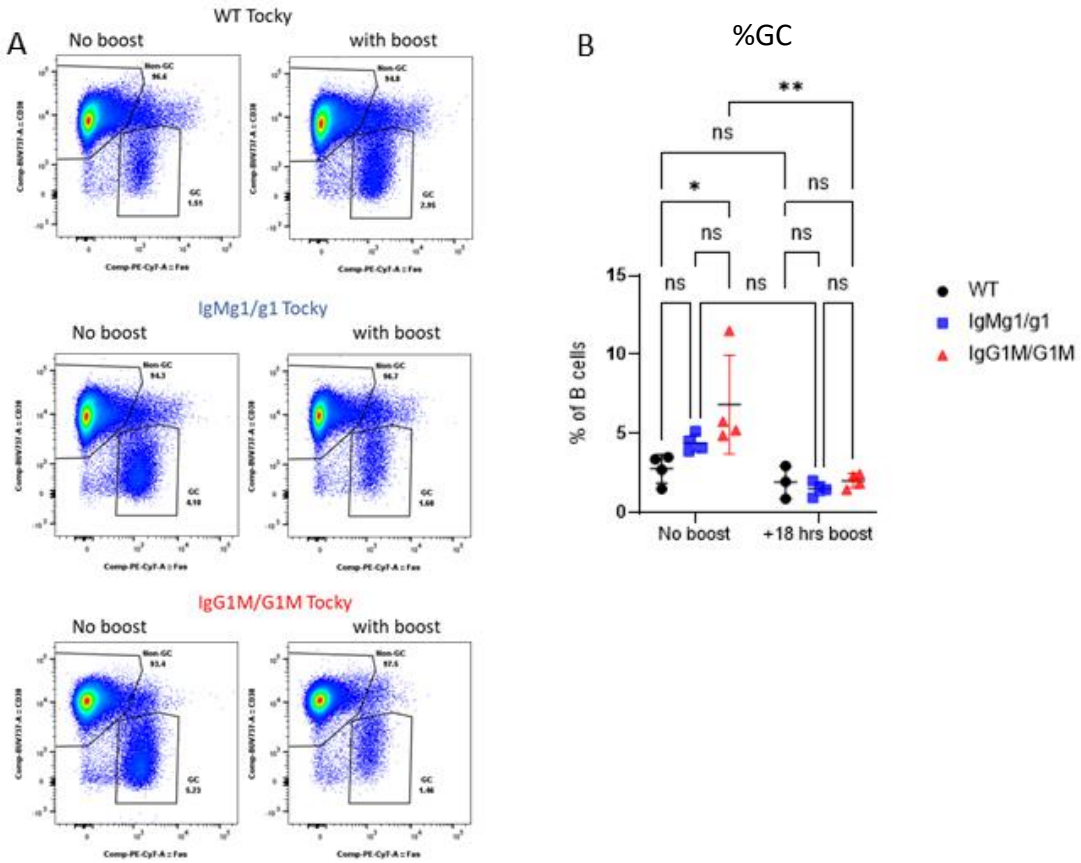

Figure 4.10 GC B cells are reduced after re-challenge with soluble Ag.
WT, IgMg1, and IgG1M Nr4a3-Tocky mice were immunised with 10µg NP-KLH in alum precipitation plus heat activated *B. pertussis* on the plantar surface of foot. At day 8, mice were boosted with 10 µg soluble NP-KLH on the same foot. Mice were culled 18 hours later. (A) Representative flow cytometry plots showing GCs identified as $B220^{+}Fas^{+}CD38^{-}$. (B) Frequency of GC B cells as percentage of total B cells. Stated as mean ± SEM Two-way ANOVA Within each row, compare columns (simple effects within rows). Data from one experiment. Each symbol represents one mouse.

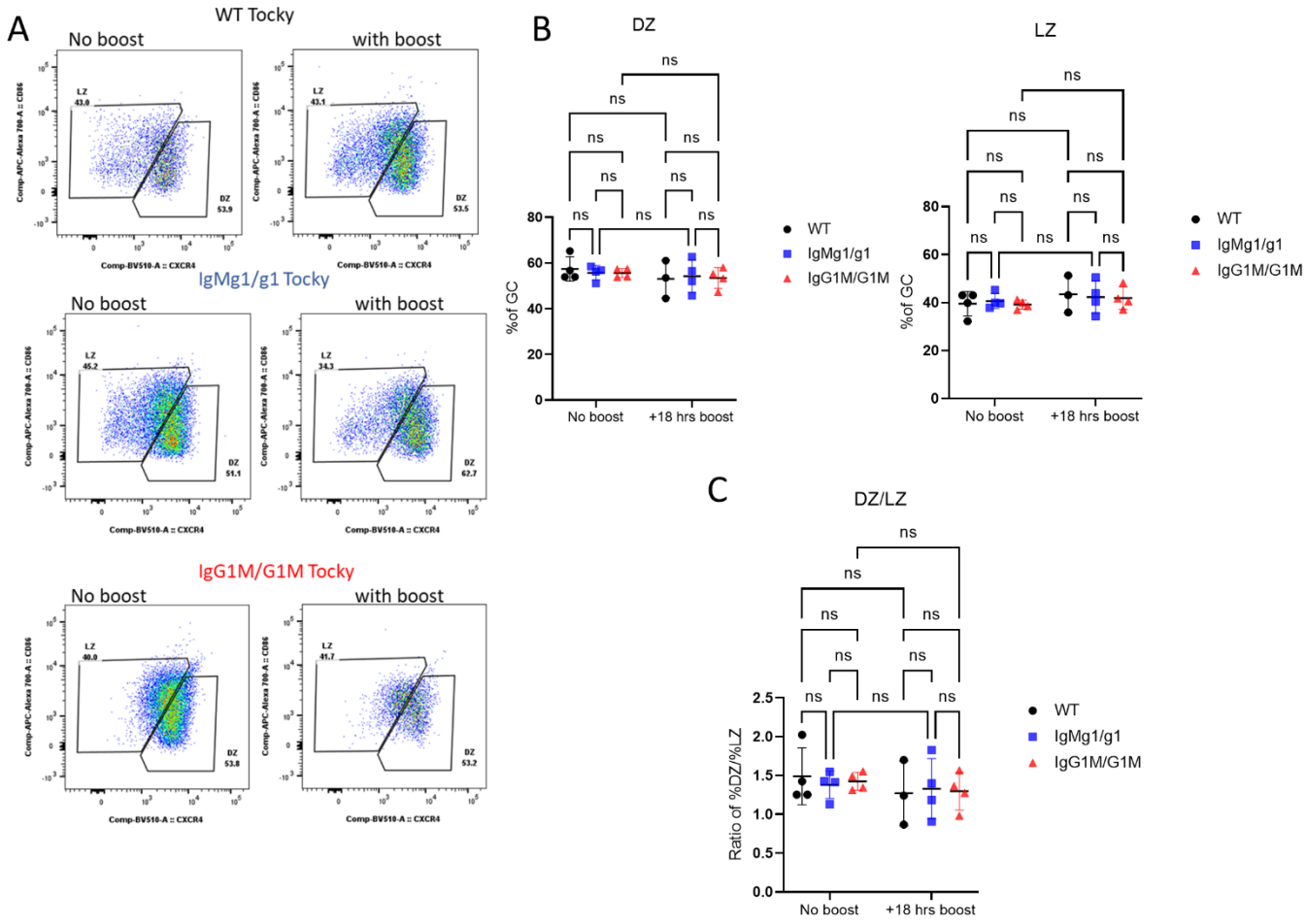

Figure 4.11 Similar trend of DZ/LZ ratio before and after injection of soluble antigen.
WT, IgMg1, and IgG1M Nr4a3-Tocky mice were immunised with 10µg NP-KLH in alum precipitation plus heat activated *B. pertussis* on the plantar surface of foot. At day 8, mice were boosted with 10 µg soluble NP-KLH on the same foot. Mice were culled 18 hours later. (A)Representative flow cytometry plots showing DZ was identified as $CXCR4^{+}CD86^{-}$ and LZ was identified as $CXCR4^{-}CD86^{+}$. (B) DZ and LZ GC B cells presented as percentage of GC. (C) Summary statistics showing DZ/LZ ratio. Stated as mean ± SEM Two-way ANOVA Within each row, compare columns (simple effects within rows). Data from one experiment. Each symbol represents one mouse.

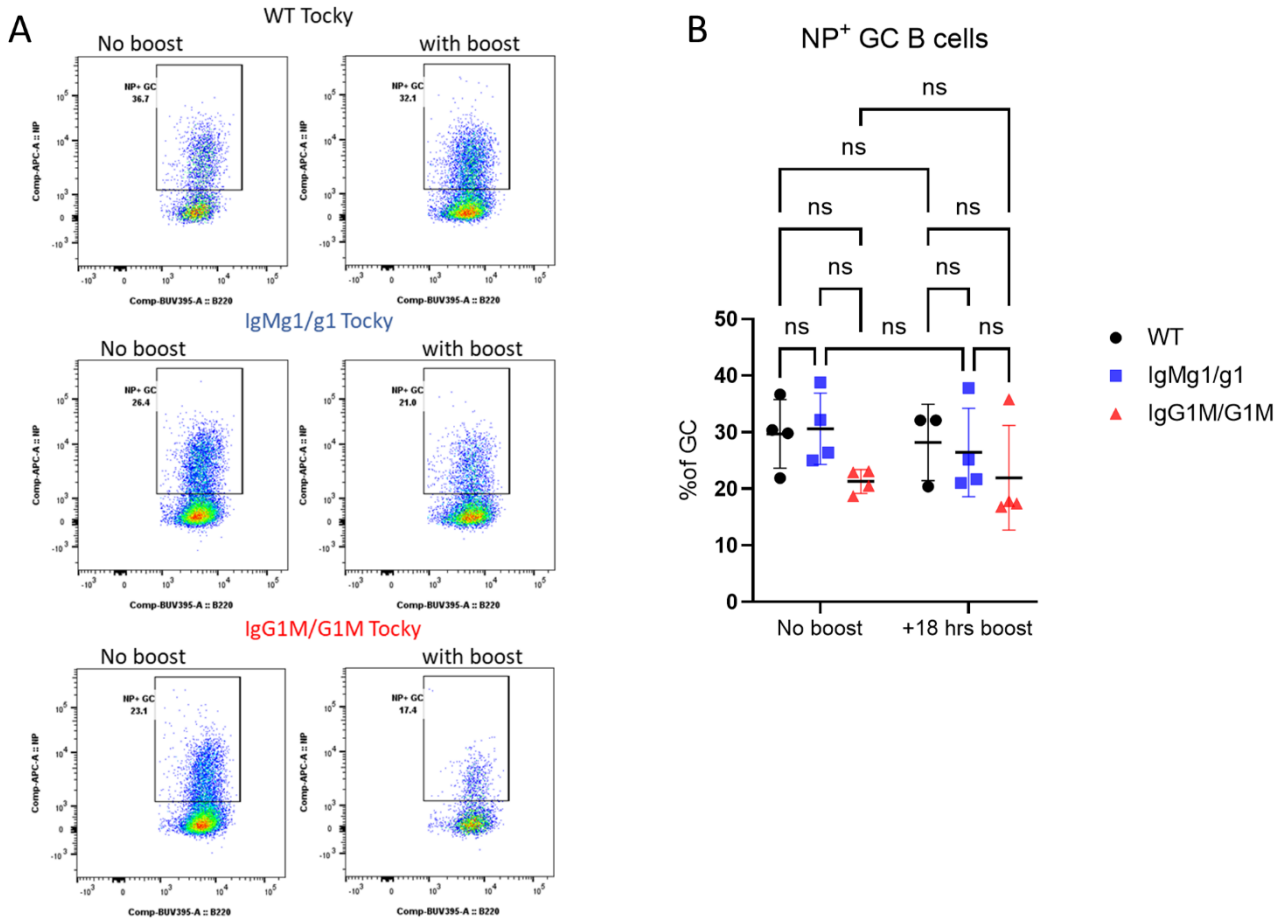

Figure 4.12 The frequency of NP-specific GC B cells following injection of soluble NP-KLH is unchanged in IgMg1 mice compared with WT, but slightly reduced in IgG1M mice.
WT, IgMg1, and IgG1M Nr4a3-Tocky mice were immunised with 10µg NP-KLH in alum precipitation plus heat activated *B. pertussis* on the plantar surface of foot. At day 8, mice were boosted with 10 µg soluble NP-KLH on the same foot. Mice were culled 18 hours later. (A) Representative flow cytometry plots showing NP+ GCs B cells. (B) NP-specific GCs B cells presented as percentage of GC B cells. Stated as mean ± SEM Two-way ANOVA Within each row, compare columns (simple effects within rows). Data from one experiment. Each symbol represents one mouse.

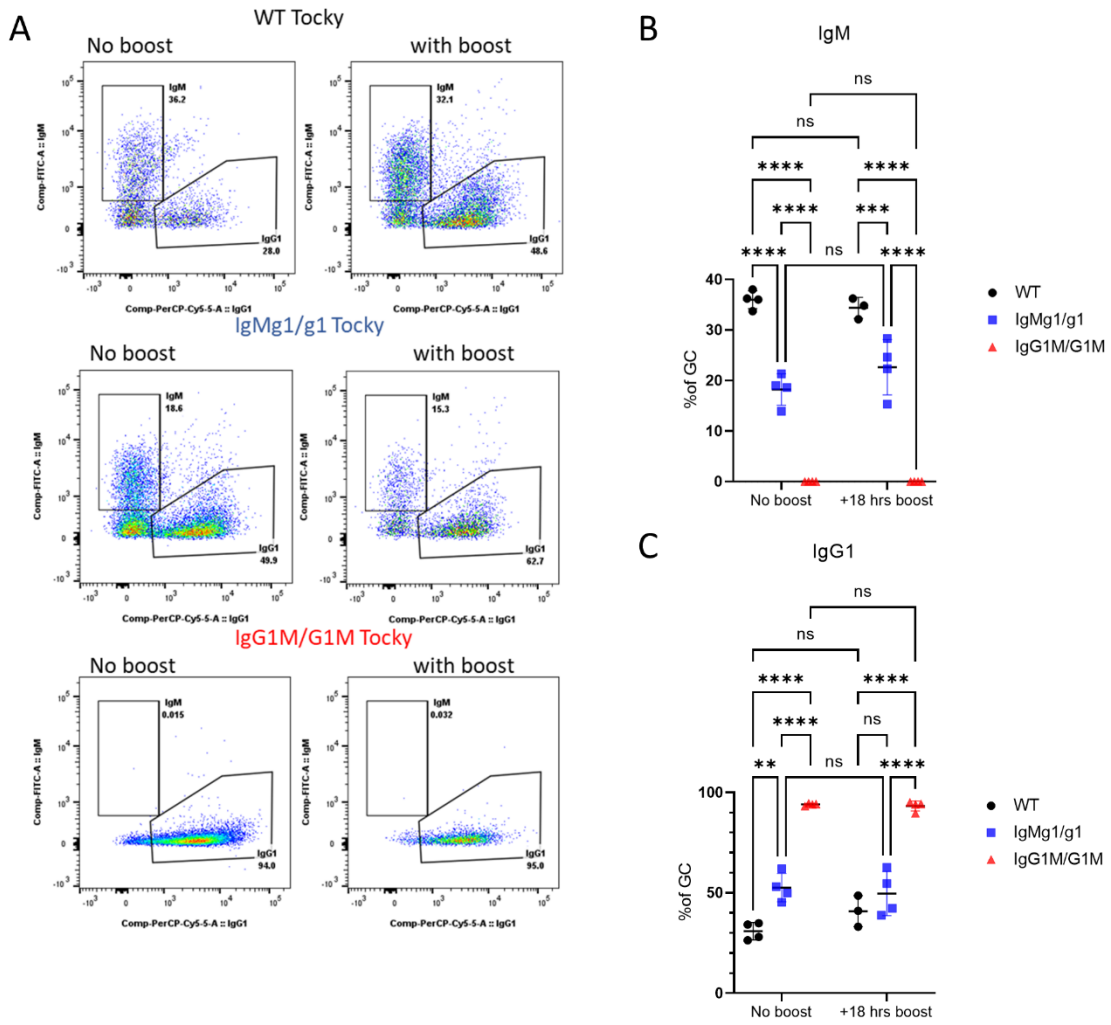

Figure 4.13 The percentage of IgM+ cells is reduced and percentage of IgG1+ cells is increased in GCs of IgMg1 mice.

WT, IgMg1, and IgG1M Nr4a3-Tocky mice were immunised with 10µg NP-KLH in alum precipitation plus heat activated *B. pertussis* on the plantar surface of foot. At day 8, mice were boosted with 10 µg soluble NP-KLH on the same foot. Mice were culled 18 hours later. (A) Representative of flow cytometry plots showing IgM and IgG1. From GC B cells, IgM^+ GC B cells were gated as IgM^+ $IgG1^-$ and $IgG1^+$ GC B cells were gated as IgM^- $IgG1^+$. (B) IgM^+ cells presented as percentage of GC B cells. (C) $IgG1^+$ cells presented as percentage of GC B cells. Stated as mean ± SEM Two-way ANOVA Within each row, compare columns (simple effects within rows). Data from one experiment. Each symbol represents one mouse.

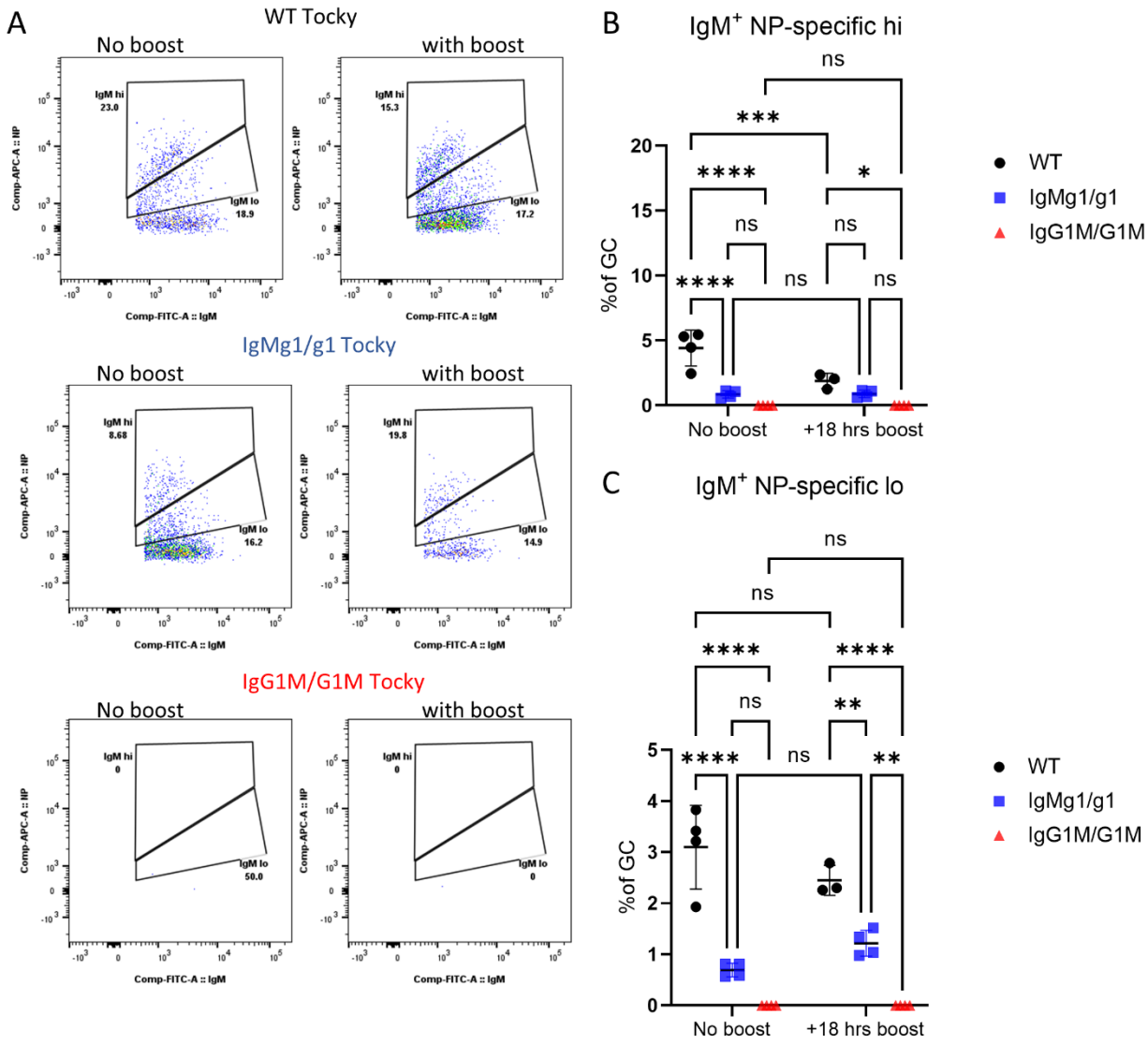

Figure 4.14 Analysis of IgM NP-affinity by flow cytometry

(A)Representative of flow cytometry plots. From GC B cells, NP^{hi} cells were gated as NP-APC^{hi} IgM^+ cells and NP^{lo} cells were gated as NP-APC^{lo} IgM^+. (B) IgM^+ NP^{hi} presented as percentage of GC B cells. (C) IgM^+ NP^{lo} presented as percentage of GC B cells. Stated as mean ± SEM Two-way ANOVA Within each row, compare columns (simple effects within rows). Data from one experiment. Each symbol represents one mouse.

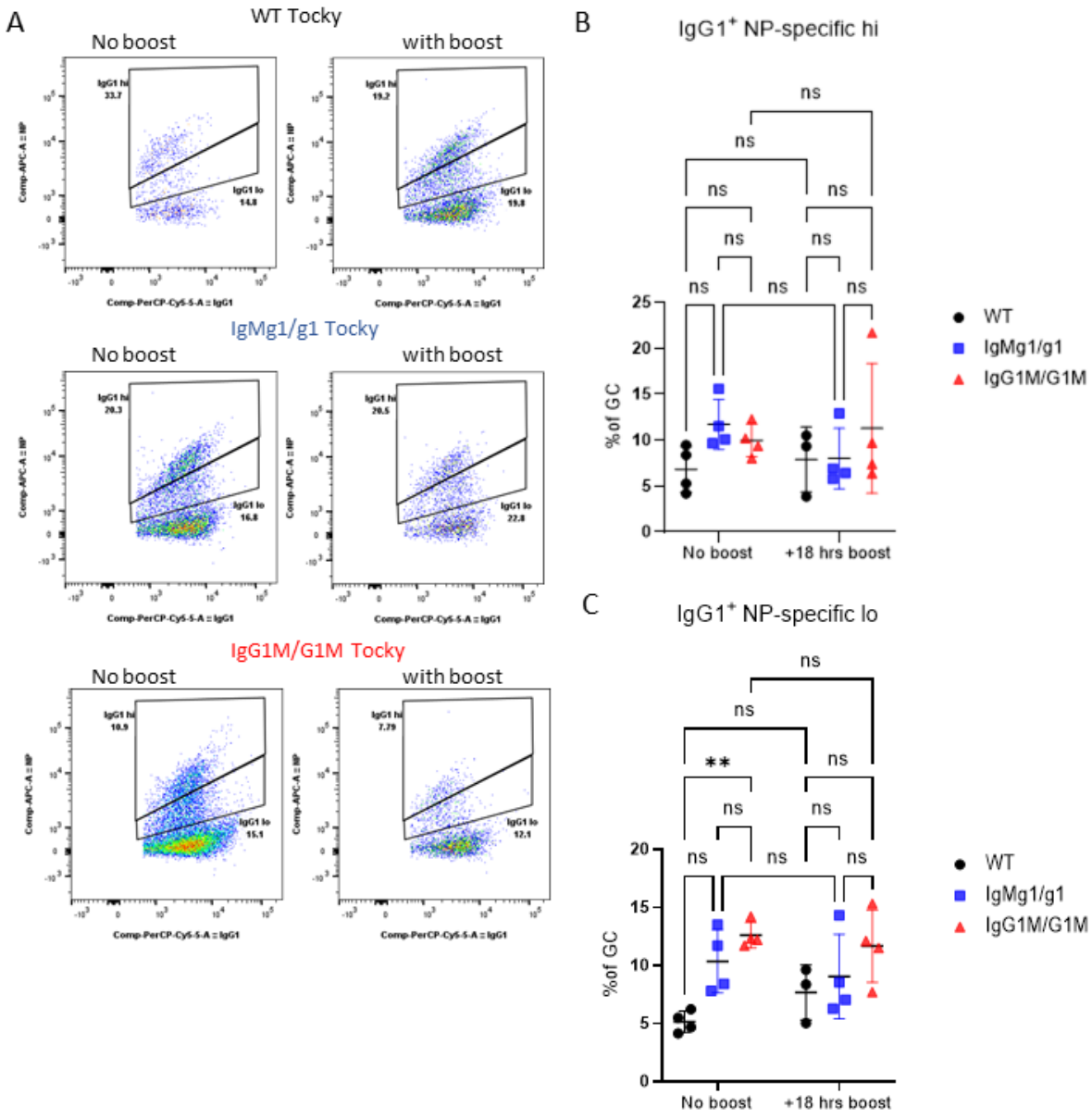

Figure 4.15 Analysis of IgG1 NP-affinity by flow cytometry

(A) Representative of flow cytometry plots. From GC B cells, NP^{hi} cells were gated as NP-APC^{hi} $IgG1^{+}$ cells and NP^{lo} cells were gated as NP-APC^{lo} $IgG1^{+}$.(B) $IgG1^{+}$ NP^{hi} as percentage of GC B cells. (C) $IgG1^{+}$ NP^{lo} presented as percentage of GC B cells. Stated as mean ± SEM Two-way ANOVA Within each row, compare columns (simple effects within rows). Data from one experiment. Each symbol represents one mouse.

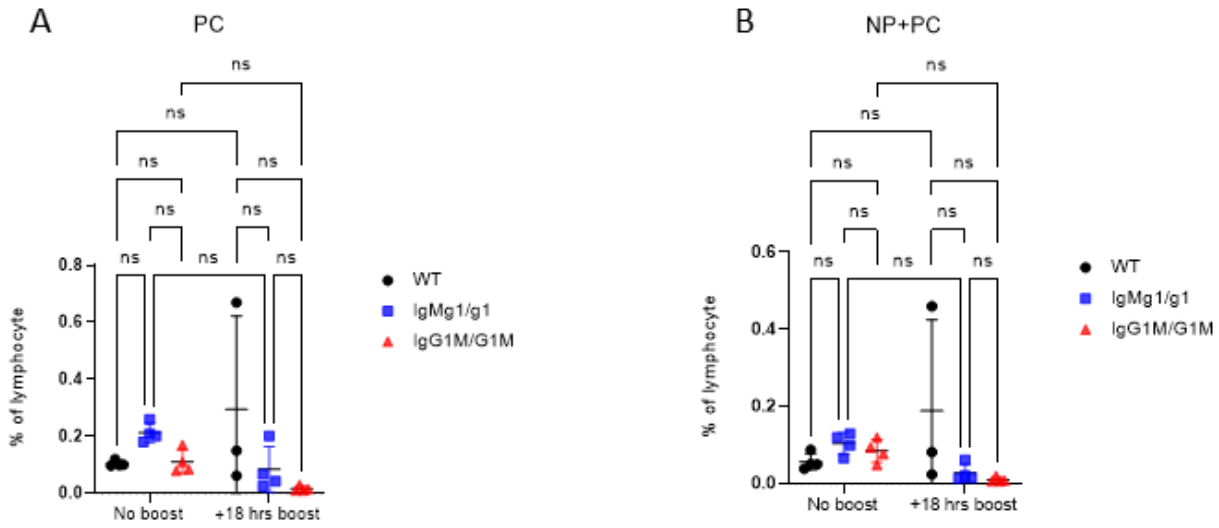

Figure 4.16 PCs and NP+ PCs are slightly reduced in IgG1M mice.
WT, IgMg1, and IgG1M Nr4a3-Tocky mice were immunised with 10µg NP-KLH in alum precipitation plus heat activated *B. pertussis* on the plantar surface of foot. At day 8, mice were boosted with 10 µg soluble NP-KLH on the same foot. Mice were culled 18 hours later. (A) total Plasma cells $B220^{-}CD138^{+}$ (PCs) presented as percentage of total lymphocytes. (B) NP-specific PCs presented as percentage of total lymphocytes. Stated as mean ± SEM Two-way ANOVA Within each row, compare columns (simple effects within rows). Data from one experiment. Each symbol represents one mouse.

4.3.3. Stimulation with soluble antigen increased central memory T cells in DrLN within 4 hours of stimulation with soluble-NP-KLH

Central memory T cells (TcM) are a subset of $CD4^+$ T cells that are characterised by the expression of homing markers L-selectin (CD62L) and CC chemokine receptor-7 (CCR7) that preferentially reside and circulate in secondary lymphoid organs (SLO). They can be identified as $CD62L^{hi}$ $CD44^{hi}$ CD4 T cells, and these cells are able to rapidly differentiate into effectors in response to secondary antigenic challenges (Pepper and Jenkins, 2011).

To determine the population of TcM and assess Nr4a3 Timer blue and red cells in TcM in draining lymph nodes (DrLN), mice were immunized as previously described (Figure 4.2 A). TcM were identified by flow cytometry as $CD4^+CD44^{hi}CD62L^{hi}$ (Figure 4.17 A). The frequency of TcM within CD4+ T cells after re-challenge with soluble NP-KLH for 4hrs more than doubled in all strains of mice. On day 5, IgG1M mice had a greater increase in TcM cells than IgMg1 and WT mice. After antigen boost on day 8, both IgMg1 and IgG1M mice had significantly more TcM cells than WT mice (Figure 4.17 B). This indicates that antigenic challenge can rapidly mobilise TcM cells.

Next, the TcM population was evaluated for TCR signalling by using the Nr4a3 Timer blue and red reporter (Figure 4.18 A). Re-exposure to soluble antigen for 4hr increased the frequency of Timer blue+ cells in all strains. Interestingly, while in IgMg1 mice the frequency of Timer $blue^+$ cells after antigen preexposure displayed comparable level to WT on day5, there were significantly more time Blue+ cells in IgG1M mice (Figure 4.18 B). On day 8, both IgMg1 and IgG1M mice showed significant increases in Timer $blue^+$ cells over WT mice (Figure 4.18B). Similar observations were made for persistently activated TcM ($blue^+red^+$) in

IgMg1 and IgG1M mice, and also for amount recently inactivated (TcM blue^{-}red^{+}), and negatively staining Timer (TcM blue^{-}red^{-}) cells in IgMg1 and IgG1M mice (Figures 4.18 C, D, and E). These data suggest that within the TcM population, soluble antigen triggers TCR signalling through newly activated Nr4a3-blue cells and remaining active Nr4a3-red cells. The sustained expression of Nr4a3-red may be due to extensive proliferation upon antigen stimulation, when these cells home to secondary lymphoid organs and secrete IL-2.

4.3.4. Evaluation of the TcM population within the DrLN and spleen after 18 hours of stimulation with soluble-NP-KLH

Previously, we demonstrated that the TcM population increases after a 4-hour antigenic boost. The aim here was to investigate this population in both the DrLN and the distant lymphoid organ spleen. We also evaluated the T follicular helper (Tfh) cell population within the spleen.

To investigate the TcM population and assess Nr4a3 Timer blue and red cells in the DrLN and spleen, all mice were immunized as described on Figure 4.5 A. At day8, after a boost with same soluble antigen for 18hrs, TcM were clearly identified as CD62L^{hi} CD44^{hi} CD4^{+} T cells (Figure 4.19 A) in drLN. The frequency of TcM was significantly increased 18 hours after boosting with soluble antigen compared to non-boosted controls as a percentage of total TcM cells. IgMg1 had comparable level of TcM as WT control after boost antigen. IgG1M mice displayed reduced TcM after re-challenge with soluble antigen compared to IgMg1 and WT mice (Figure 4.19 B). The expression of TcM Timer blue showed similar trends before and after boosting with soluble antigen in all mouse genotypes (Figure 4.20 B). However, since these mice were stimulated for 18 hours, cells may have been in the Timer red persistent phase. Thus, WT mice displayed significant increased expression of Timer blue and red compared to non-boosted respective controls, IgG1M and IgMg1 mice presented slight but non-significant

increases in Timer blue and red cells after boosting. There was no change in TcM blue^{+}red^{+} cells in any mouse genotype after re-challenge with soluble antigen (Figure 4.20 C). In the Timer red arrested phase, WT mice showed a clear but non-significant reduction after boosting compared to the primary response, while there was no change in IgMg1 and IgG1M mice compared to non-boost respective controls (Figure 4.20 D). Negative Timer cells were clearly reduced after boosting soluble antigen, indicating that TcM were reactivated in response to the soluble antigen (Figure 4.20 E).

We next assessed central memory CD4+ T cells in the spleen as a distant secondary lymphoid organ. TcM in the spleen were quantified by the expression of CD62L^{hi} CD44^{hi} on CD4^{+} T cells (Figure 4.21 A). The frequency of TcM in WT mice was similar between non-boosted and boosted groups. TcM in IgMg1 mice slightly reduced after boost antigen. However, the IgG1M in the re-challenged group showed a significant increase compared to IgMg1 mice (Figure 4.21 B). This suggests that TcM are able to circulate through lymphoid organs and home there.

The expression of Nr4a3 Timer blue and red was assessed to determine if TcM in the spleen were able to recognise soluble antigen and re-activate TCR signalling (Figure 4.22 A). WT and IgMg1 mice did not show any difference in Timer blue^{+} TcM before or after receiving soluble antigen. However, IgG1M mice displayed significant increase in newly activated Timer blue+ cells in both non-boosted and boosted groups as a percentage of total TcM cells (Figure 4.22 B). In contrast, persistently activated Timer blue^{+}red^{+} TcM were elevated in WT and IgMg1 mice regardless of soluble antigen exposure, while Timer blue^{+}red^{+} cells were reduced in IgG1M mice after restimulation of soluble antigen for 18hr (Figure 4.22 C). There was no change in the frequency of arrested Timer blue^{-}red^{+} or negative Timer blue-red- cells (Figures 4.22 D and E) in all groups. These data suggest that TcM in WT and IgMg1 mice were strongly

reactivated by both the primary and secondary responses, as evidenced by increased Timer blue^{+}red^{+} expression.

We next investigated the proportion of Tfh cells and their TCR signalling through Nr4a3-Tocky mice in the spleen. As expected, the frequency of Tfh cells was detected but at a lower proportion compared to Tfh cells in the DrLN, probably because there was less antigen capture in the spleen (Figures 4.23 A and B). With fewer effector Tfh cells, there was minimal observable TCR signalling within splenic Tfh cells (Figure 4.24 A), and most of these cells appeared to be in an arrested phase, making it difficult to measure and interpret Nr4a3 Timer blue^{+} or red^{+} cells (Figures 4.24 B, C, D, and E).

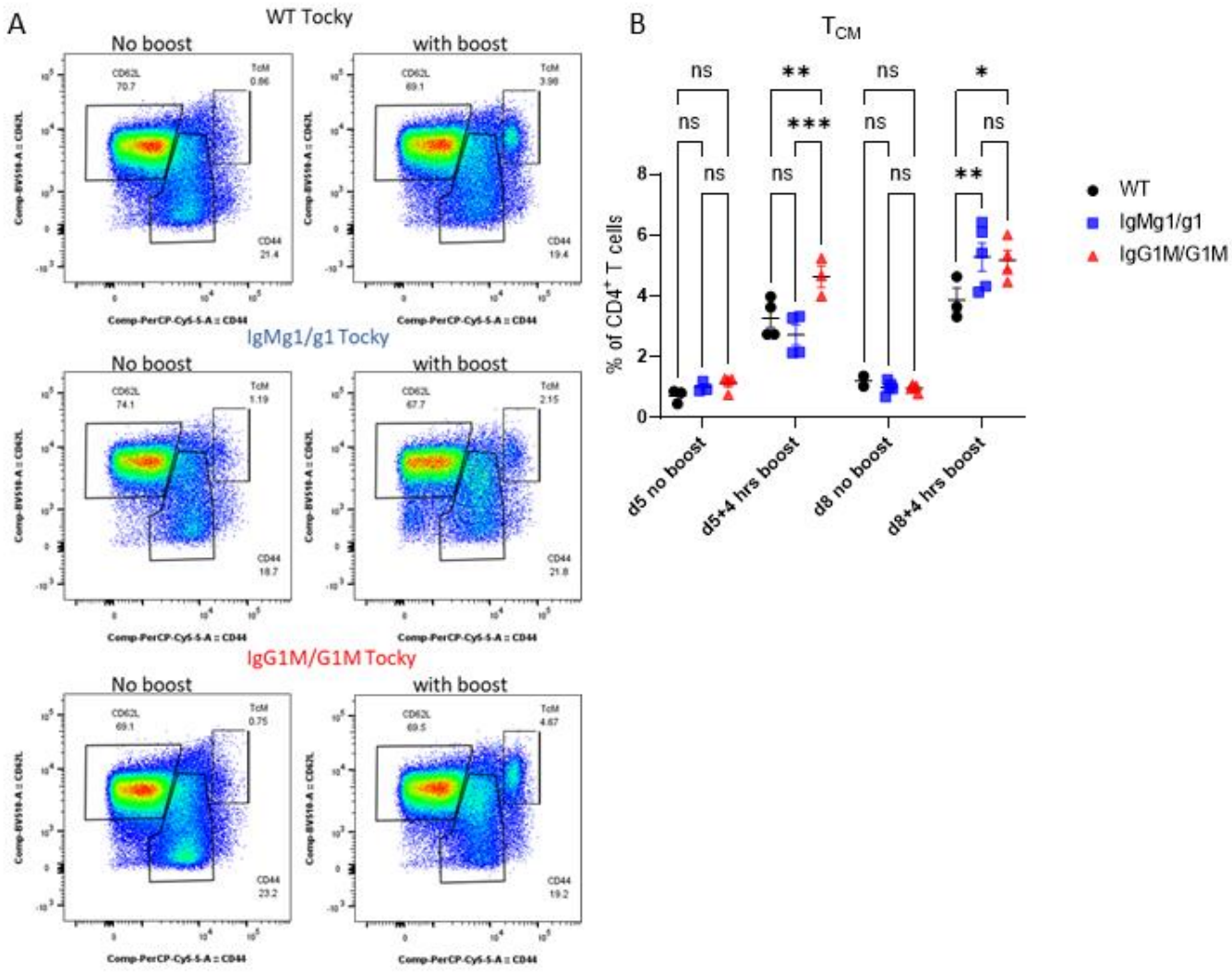

Figure 4.17 Increased percentage of TcM in DrLN after 4 hrs of stimulation with soluble Ag. (A) Representative flow cytometry plots showing TcM population gated from $CD4^+$T cells and identified as $CD62L^+$ $CD44^+$.Naive CD4+ T cells identified as $CD62L^+$ $CD44^-$. Activated $CD4^+$T cells identified as $CD62L^-$ $CD44^+$. TcM population were gated as shown in Figure 4.5 (B) Frequency of TcM as percentage of total CD4+T cells. Stated as mean ± SEM Two-way ANOVA Within each row, compare columns (simple effects within rows). Data from one experiment. Each symbol represents one mouse.

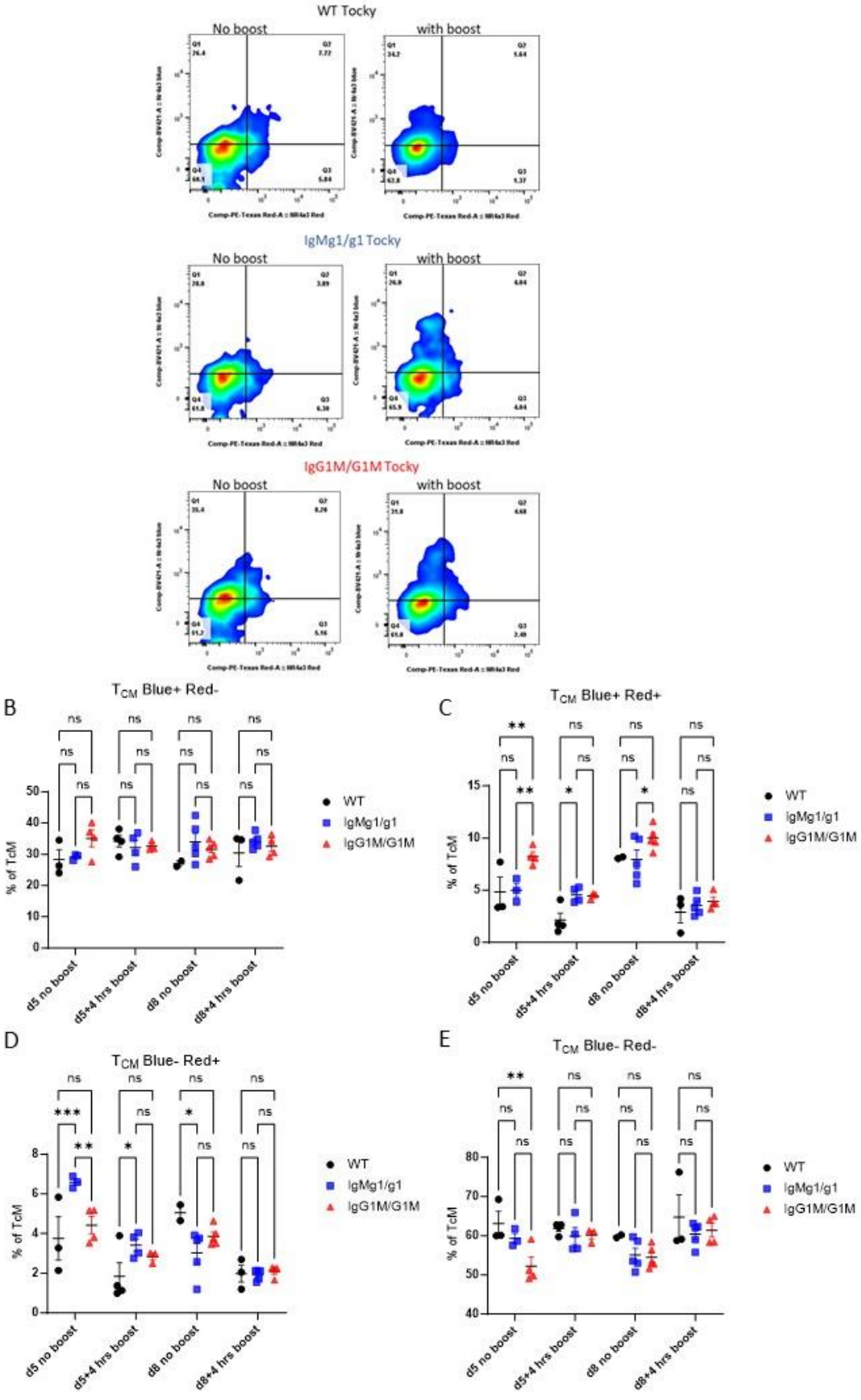
WT Tocky
No boost
with boost
IgMg1/g1 Tocky
No boost
with boost
IgG1M/G1M Tocky
No boost
with boost
B
TCM Blue+ Red-
% of TcM
WT
IgMg1/g1
IgG1M/G1M
d5 no boost
d5+4 hrs boost
d8 no boost
d8+4 hrs boost
C
TCM Blue+ Red+
D
TCM Blue- Red+
E
TCM Blue- Red-

Figure 4.18 TcM Nr4a3-blue and Nr4a3-red expression in DrLN is increased after boosting with soluble antigen.

(A) Representative flow cytometry plots showing Nr4a3-blue and Nr4a3-red expression in TcM cells which were identified as $CD62L^+$ and $CD44^+$. (B) Frequency of Nr4a3-$blue^+$ red^- TcM cells as percentage of TcM(C) Frequency of Nr4a3-$blue^+$ red^+ TcM cells as percentage ofTcM. (D) Frequency of Nr4a3-$blue^-$ red^+ TcM cells as percentage of TcM. (E) Frequency of Nr4a3-$blue^-$ red^- TcM cells as percentage of TcM. Stated as mean ± SEM Two-way ANOVA Within each row, compare columns (simple effects within rows). Data from one experiment. Each symbol represents one mouse.

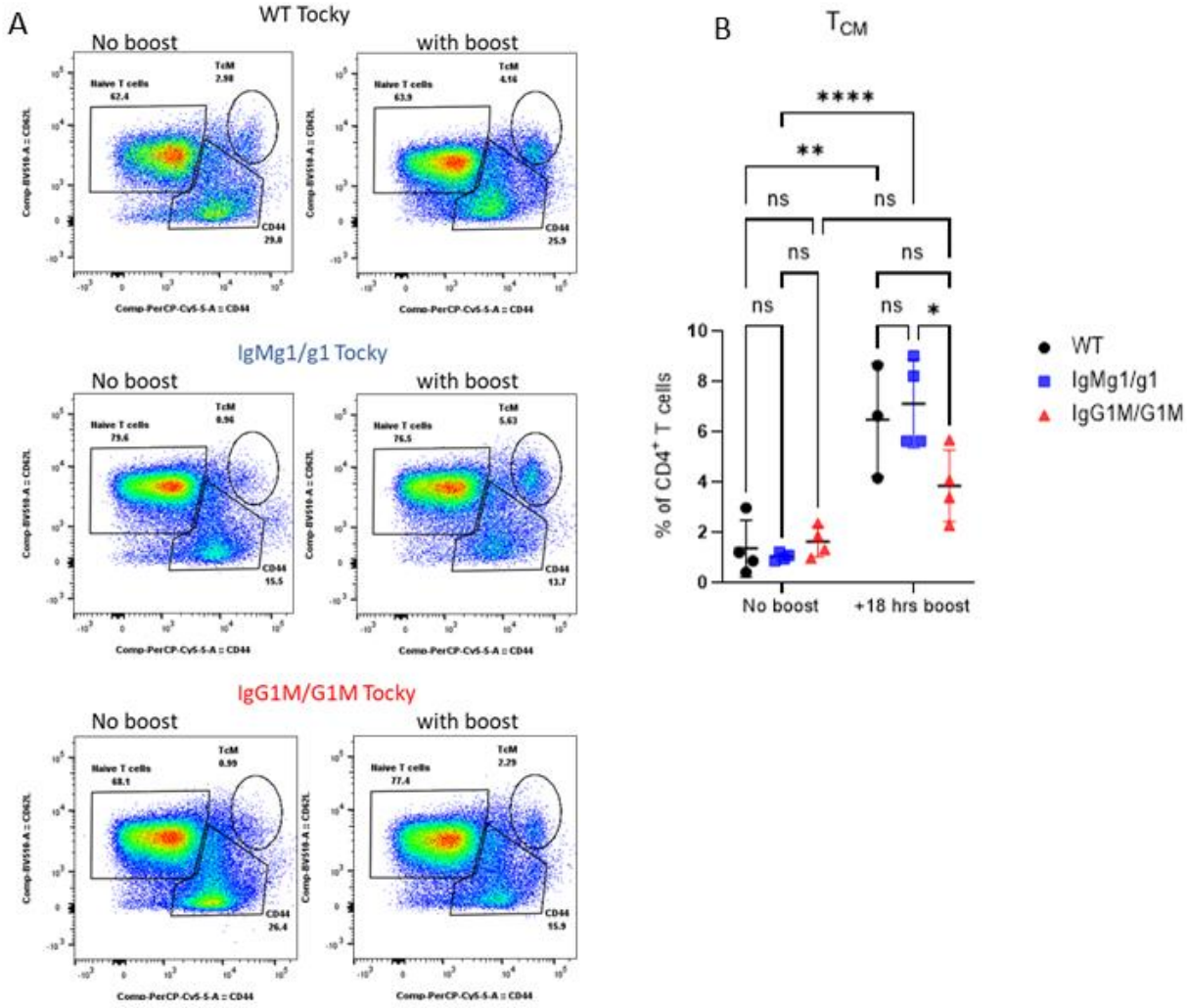

Figure 4.19 Increased percentage of TcM in DrLN after stimulation with soluble antigen for 18 hours.

WT, IgMg1, and IgG1M Nr4a3-Tocky mice were immunised with 10µg NP-KLH in alum precipitation plus heat-inactivated B. pertussis on the plantar surface of foot. At day 8 mice were boosted with 10 µg soluble NP-KLH on the same foot. Mice were culled 18 hours later, and lymph nodes analysed by flow cytometry. (A) Representative flow cytometry plots showing TcM population gated from $CD4^+$T cells and identified as $CD62L^+$ $CD44^+$.Naive $CD4^+$ T cells identified as $CD62L^+$ $CD44^-$. Activated $CD4^+$T cells identified as $CD62L^-$ $CD44^+$. (B) Frequency of TcM as percentage of total $CD4^+$T cells. Stated as mean ± SEM Two-way ANOVA Within each row, compare columns (simple effects within rows). Data from one experiment. Each symbol represents one mouse.

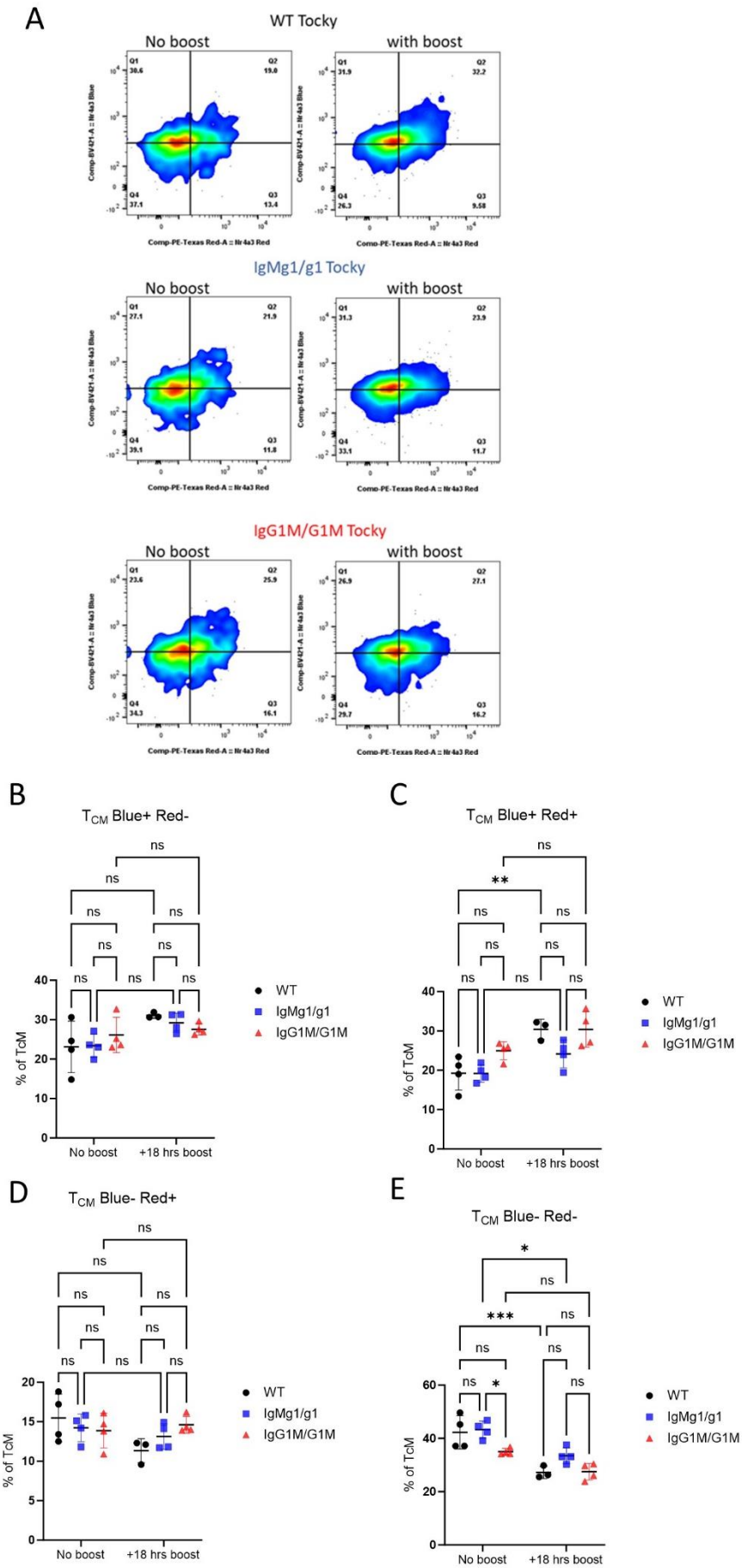
A
WT Tocky
No boost
with boost
IgMg1/g1 Tocky
No boost
with boost
IgG1M/G1M Tocky
No boost
with boost
B
TCM Blue+ Red-
% of TcM
No boost
+18 hrs boost
WT
IgMg1/g1
IgG1M/G1M
C
TCM Blue+ Red+
% of TcM
No boost
+18 hrs boost
WT
IgMg1/g1
IgG1M/G1M
D
TCM Blue- Red+
% of TcM
No boost
+18 hrs boost
WT
IgMg1/g1
IgG1M/G1M
E
TCM Blue- Red-
% of TcM
No boost
+18 hrs boost
WT
IgMg1/g1
IgG1M/G1M

Figure 4.20 WT mice had an increase in persistently activated TcM Timer blue^{+}red^{+} following an 18-hour boost with soluble antigen in DrLN.

WT, IgMg1, and IgG1M Nr4a3-Tocky mice were immunised with 10µg NP-KLH in alum precipitation plus heat-inactivated B. pertussis on the plantar surface of foot. At day 8 mice were boosted with 10 µg soluble NP-KLH on the same foot. Mice were culled 18 hours later, and lymph nodes analysed by flow cytometry. (A) Representative flow cytometry plots showing Nr4a3-blue and Nr4a3-red expression in TcM cells were identified as CD62L^{+} and CD44^{+}. (B) Frequency of Nr4a3-blue^{+} red^{-} TcM cells as percentage of CD4^{+} T cells. (C) Frequency of Nr4a3-blue^{+} red^{+} TcM cells as percentage of CD4^{+}T cells. (D) Frequency of Nr4a3-blue^{-} red^{+} TcM cells as percentage of CD4^{+}T cells. (E) Frequency of Nr4a3-blue^{-} red^{-} TcM cells as percentage of CD4^{+}T cells. Stated as mean ± SEM Two-way ANOVA Within each row, compare columns (simple effects within rows). Data from one experiment. Each symbol represents one mouse.

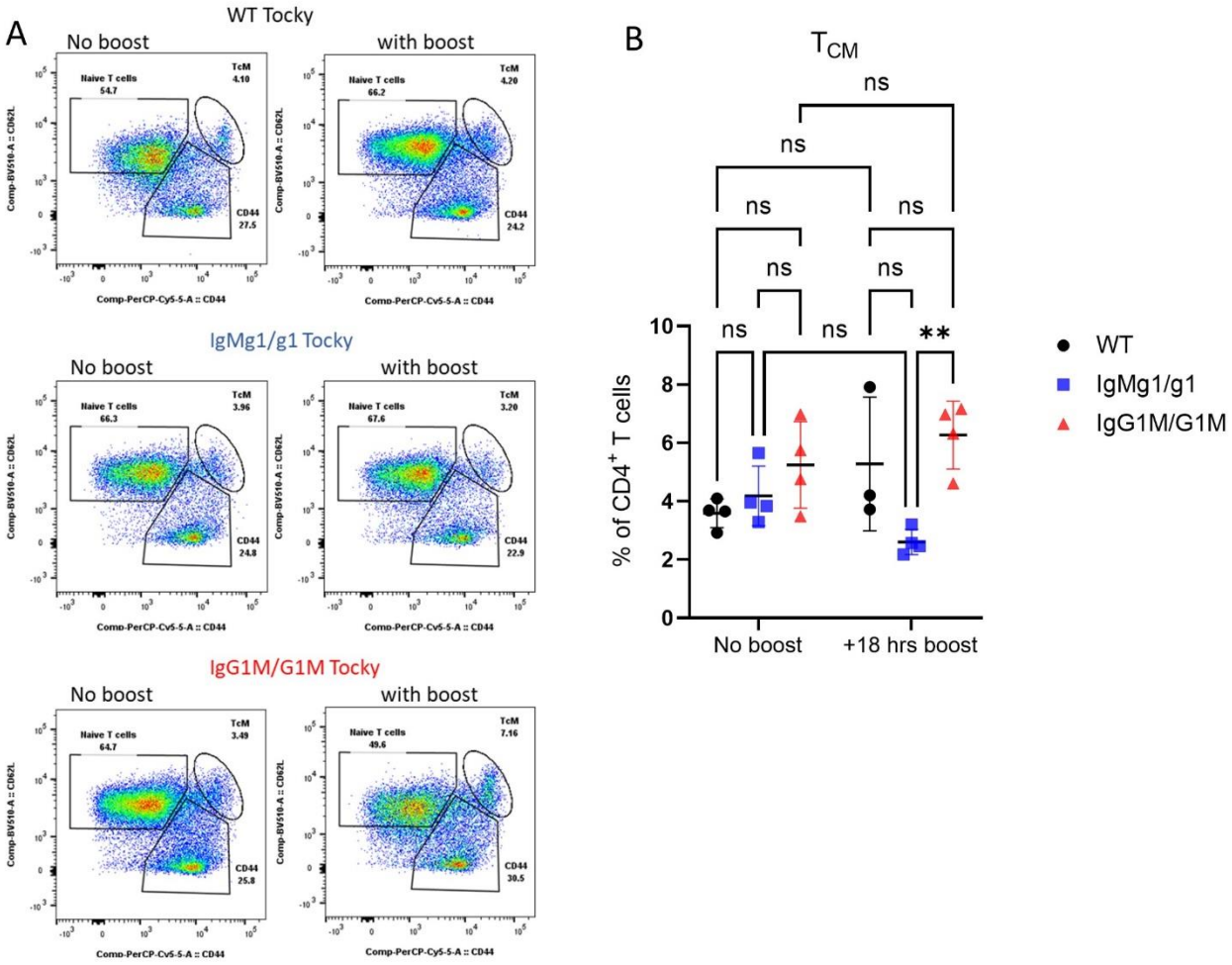

Figure 4.21 IgG1M mice have increased circulation of TcM to the spleen.
WT, IgMg1, and IgG1M Nr4a3-Tocky mice were immunised with 10µg NP-KLH in alum precipitation plus heat-inactivated B. pertussis on the plantar surface of foot. At day 8 mice were boosted with 10 µg soluble NP-KLH on the same foot. Mice were culled 18 hours later, and spleen tissues analysed by flow cytometry. (A) Representative flow cytometry plots showing TcM population in spleen gated from $CD4^+$T cells and identified as $CD62L^+$ $CD44^+$.Naive $CD4^+$ T cells identified as $CD62L^+$ $CD44^-$. Activated $CD4^+$T cells identified as $CD62L^-$ $CD44^+$. (B) Frequency of TcM as percentage of total $CD4^+$T cells. Stated as mean ± SEM Two-way ANOVA Within each row, compare columns (simple effects within rows). Data from one experiment. Each symbol represents one mouse.

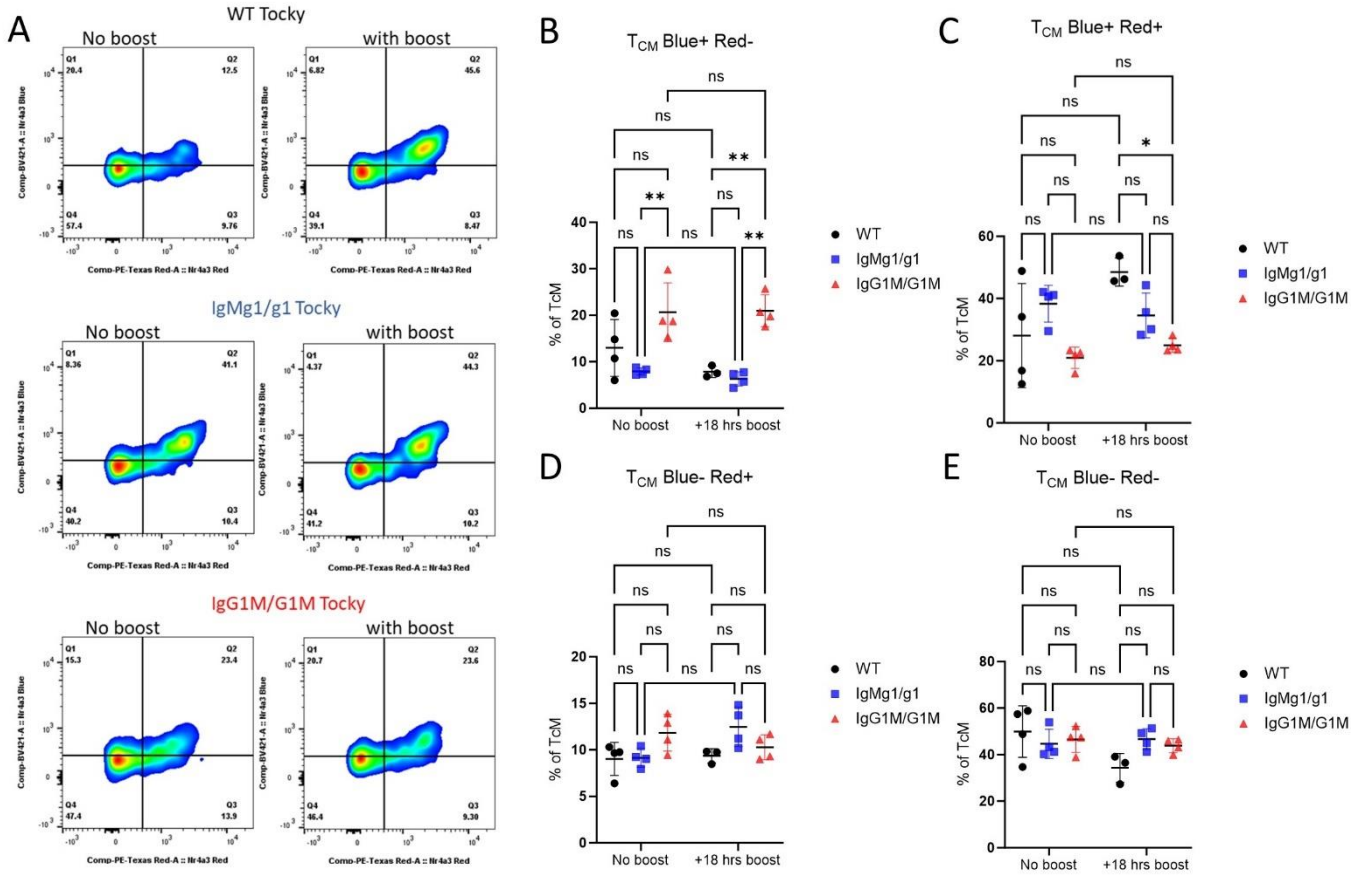

Figure 4.22 Nr4a3-blue and Nr4a-red expression in spleen TcM cells.

WT, IgMg1, and IgG1M Nr4a3-Tocky mice were immunised with 10µg NP-KLH in alum precipitation plus heat-inactivated B. pertussis on the plantar surface of foot. At day 8 mice were boosted with 10 µg soluble NP-KLH on the same foot. Mice were culled 18 hours later, and spleen tissues analysed by flow cytometry. (A) Representative flow cytometry plots showing Nr4a3-blue and Nr4a3-red expression in spleen TcM cells were identified as $CD62L^+$ and $CD44^+$. (B) Frequency of Nr4a3-$blue^+$ red^- TcM cells as percentage of $CD4^+$ T cells. (C) Frequency of Nr4a3-blue+ red+ TcM cells as percentage of $CD4^+$T cells. (D) Frequency of Nr4a3-$blue^-$ red^+ TcM cells as percentage of $CD4^+$T cells. (E) Frequency of Nr4a3-$blue^-$ red^- TcM cells as percentage of $CD4^+$T cells. Stated as mean ± SEM Two-way ANOVA Within each row, compare columns (simple effects within rows). Data from one experiment. Each symbol represents one mouse.

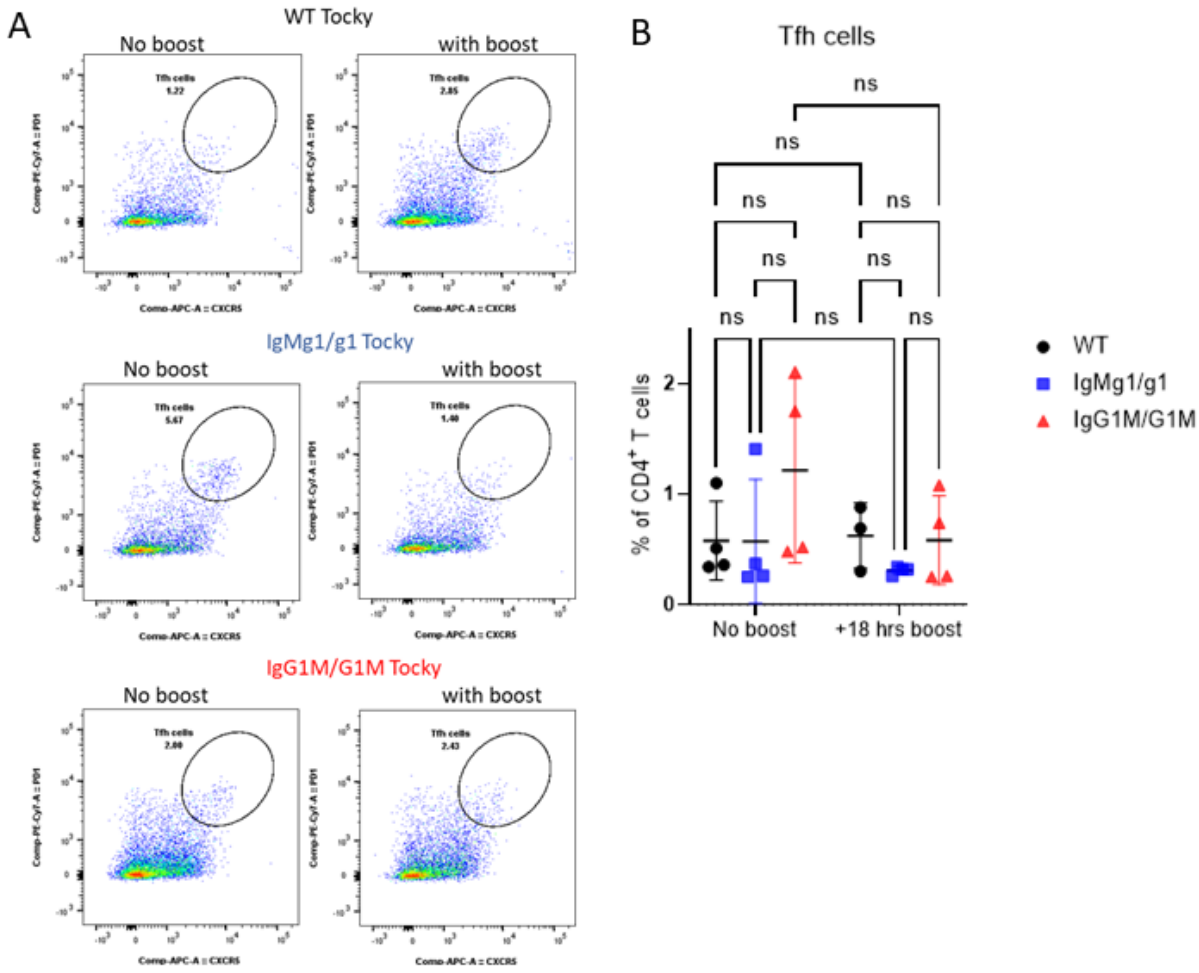

Figure 4.23 Analysis of Tfh cells in spleen.

WT, IgMg1, and IgG1M Nr4a3-Tocky mice were immunised with 10µg NP-KLH in alum precipitation plus heat-inactivated B. pertussis on the plantar surface of foot. At day 8 mice were boosted with 10 µg soluble NP-KLH on the same foot. Mice were culled 18 hours later, and spleen tissues analysed by flow cytometry. (A) Representative flow cytometry plots showing Tfh cells. From lymphocytes, T cells were gated as $CD3^+$ $CD19^-$. From $CD3^+$ T cells, $CD4^+$ T cells were gated as $CD4^+$. From $CD4^+$ T cells, naïve $CD4^+$ T cells were gated as $CD62L^+$ $CD44^-$ and activated cells were gated as $CD44^+$ $CD62L^-$. From activated cells, Tfh cells were gated as PD-1^{hi} $CXCR5^{hi}$. (B) Frequency of Tfh cells as percentage of total $CD4^+$ T cells. Stated as mean ± SEM Two-way ANOVA Within each row, compare columns (simple effects within rows). Data from one experiment. Each symbol represents one mouse.

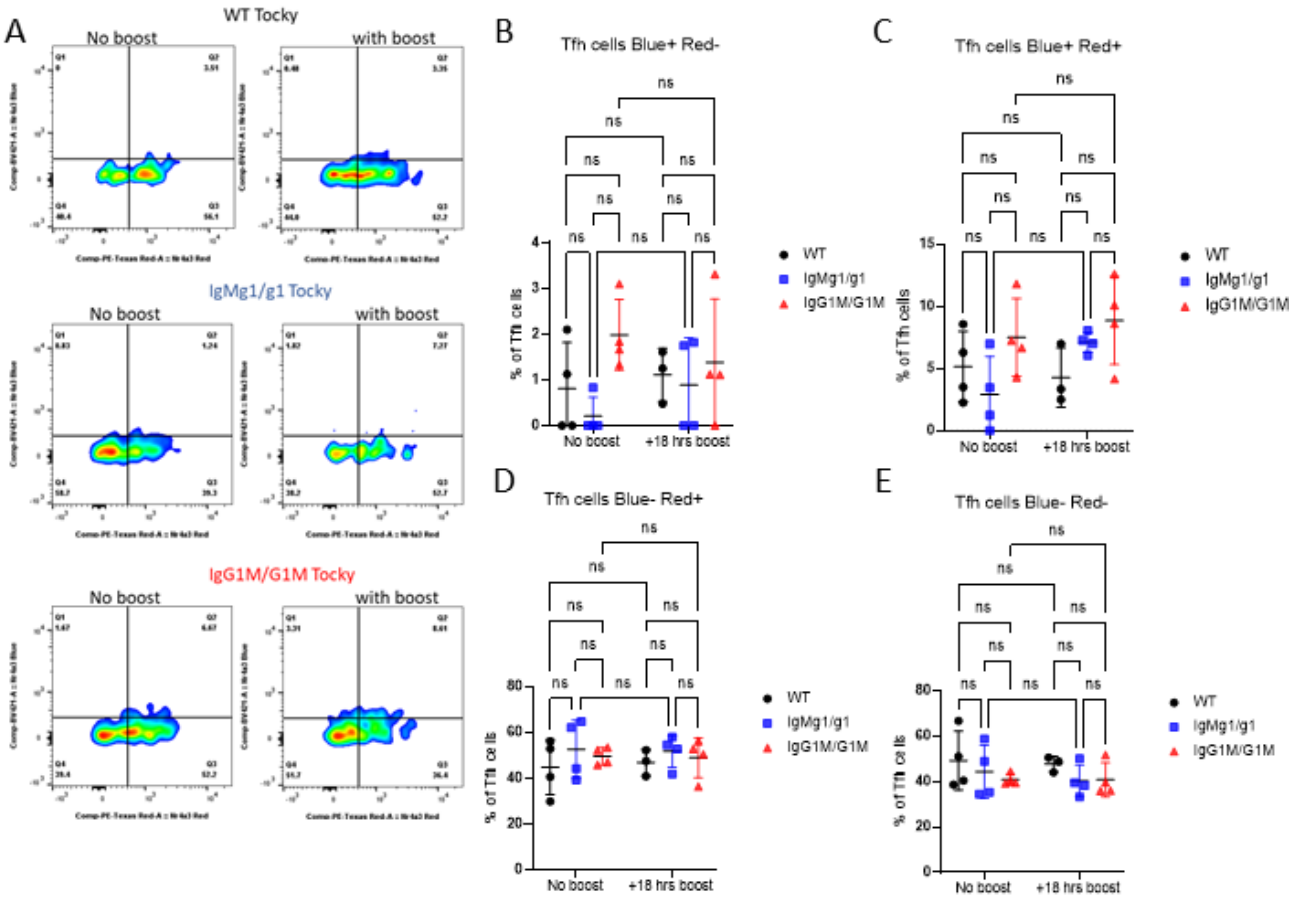

Figure 4.24 Nr4a3-blue and Nr4a3-Red expression in spleen Tfh cells.

WT, IgMg1, and IgG1M Nr4a3-Tocky mice were immunised with 10µg NP-KLH in alum precipitation plus heat-inactivated B. pertussis on the plantar surface of foot. At day 8 mice were boosted with 10 µg soluble NP-KLH on the same foot. Mice were culled 18 hours later, and spleen tissues analysed by flow cytometry. (A) Representative flow cytometry plots showing Nr4a3-blue and Nr4a3-red expression in spleen Tfh cells identified as PD-1^{hi} $CXCR5^{hi}$. (B) Frequency of Nr4a3-blue+ red- Tfh cells as percentage of Tfh cells. (C) Frequency of Nr4a3-$blue^{+}$ red^{+} Tfh cells as percentage of Tfh cells. (D) Frequency of Nr4a3-$blue^{-}$ red^{+} Tfh cells as percentage of Tfh cells. (E) Frequency of Nr4a3-$blue^{-}$ red^{-} Tfh cells as percentage of Tfh cells. Stated as mean ± SEM Two-way ANOVA Within each row, compare columns (simple effects within rows). Data from one experiment. Each symbol represents one mouse.

4.3.5. Investigate the B-T cells interaction in absence of affinity maturation by using AIDcre/cre Nr4a3-Tocky mice.

During a T-dependent immune response, activated B cells undergo class switch and affinity maturation, before differentiating into plasma cells which produce antibodies against the antigen. This process of class switch and affinity maturation requires enzyme AID (activation-induced cytidine deaminase). These antibodies should hypermutate at a very high rate and diversify through SHM and CSR. Without AID, B cells cannot undergo class switching or hypermutation, which leads to a loss of affinity maturation. Here, we aim to study how the absence of AID affects the ability of GC B cells to present antigen peptides to Tfh cells, a process essential for receiving helper signals. Without AID, the lower affinity and diversity of B cell receptors may result in less effective antigen processing and presentation. To evaluate this, we measured the expression of the Nr4a3 Tocky reporter in AIDcre/cre (AIDko) mice.

Without AID, B cells fail to undergo class switching and hypermutate resulting in the loss of affinity maturation. Here, we aim to examine the effect of absence of AID on the ability of GC B cells to present antigen peptide to Tfh cells, which is necessary to receive helper signals from Tfh cells. Without AID, the reduced affinity and diversity of B cell receptors may lead to suboptimal antigen processing and presentation. This was evaluated by measuring the expression of the Nr4a3 Tocky reporter in AIDcre/cre (AIDko) mice.

To test this, AIDcre/wt and AIDcre/cre Nr4a3-Tocky mice were immunized with 10 µg NP-KLH precipitated in alum plus heat-inactivated *B. pertussis* into the plantar surface of the rear foot. At day 5, mice were boosted with 10 µg of soluble NP-KLH on the same foot. Mice were culled 4 hours later, and lymph nodes were analysed by flow cytometry (Figure 4.25 A). Tfh cells were identified by flow cytometry as $CD4^+$ $CD62L^-$ $CD44^+$ $PD1^{hi}$ $CXCR5^{hi}$. The expression of the

Nr4a3 timer protein in blue and red florescent states was measured in these Tfh cells (Figure 4.25 B). As shown in chapter 3, the frequency of Tfh cells is slightly higher in AIDko mice compared to WT. The frequency of recently activated timer blue+ red- cells within Tfh cells increased slightly, but not significantly in AIDcre/cre mice (Figure 4.26 B). There was not significant change in the frequencies of the other timer timer populations (Figures 4.26 C, D, and E). Furthermore, the blue MFI of Nr4a3^{-}blue^{+} Tfh cells and the red MFI of Nr4a3^{-}red^{+} Tfh cells are not significantly different in AIDcre/cre mice, suggesting equal Nr4a3 expression in the Nr4a3+ cells (Figures 4.26 F, and G). While there was no change in Tfh cell Nr4a3 expression, GC size and frequency of NP-specific GC B cells were significantly increased in AIDcre/cre mice compared to AIDcre/wt (Figures 4.27 A, and B), consistent with has been shown in chapter 3.

To further examine the kinetics of Tfh activation in these models at a more mature stage of the GC response, the experiment was repeated by injecting antigen 8 days post primary immunisation. AIDcre/wt and AIDcre/cre Nr4a3-Tocky mice were immunized with 10 µg NP-KLH precipitated in alum with heat-inactivated *B. pertussis* on the plantar surface of the foot. At day 8, mice were boosted with 10 µg soluble NP-KLH into the same foot. Lymph nodes were taken 4 hours later and analysed by flow cytometry (Figure 4.28 A). Tfh cells were identified by flow cytometry, and the Nr4a3 timer in blue and red fluorescent states was measured (Figure 4.28 B). In this experiment the frequency of Tfh cells was comparable between both groups (Figure 4.28 C). There were no significant differences in the frequencies of persistent Nr4a3 timer blue^{+}red^{+} Tfh cells or arrested Nr4a3 timer blue^{-}red^{+} Tfh cells, and the frequency of recently activated Nr4a3 timer blue^{+}red^{-} Tfh cells also did not exhibit significantly different between groups (Figures 4.28 D, E, F, and G). Moreover, the blue MFI of Nr4a3-blue^{+} Tfh cells and the red MFI of Nr4a3-red^{+} Tfh cells were similar between

AIDcre/cre and AIDcre/wt control mice. This shows that at a more mature stage GC development at day 8, it seems that absence of AID has a minor effect on TCR signal Nr4a3 expression in Nr4a3^{+} Tfh. Also, and surprisingly, in contrast to the day 5 timepoint, there were no differences observed in GC size or frequency of NP-specific GC B cells between groups at this stage (Figures 4.29 A, and C). Also, the MFI of Nr4a3-blue^{+} Tfh cells was similar between AIDcre/cre and AIDcre/wt mice.

Overall, this indicates that Tfh cell activation was not defective in response to B cells lacking AID activity and somatic hypermutation. Therefore, the increased GC response observed in AIDcre/cre mice appears to be driven by enhanced B cell survival and antigen presentation capacity due to lack of AID activity, rather than derived by altered Tfh cell activation. AID-deficiency probably results in delayed antigen clearance and chronic immune activation, and the increased Tfh cell numbers seen in AIDko mice may be just due to an increased space for Tfh cell survival, as GCs tend to be larger with bigger numbers of GC B cells available for interactions with Tfh cells.

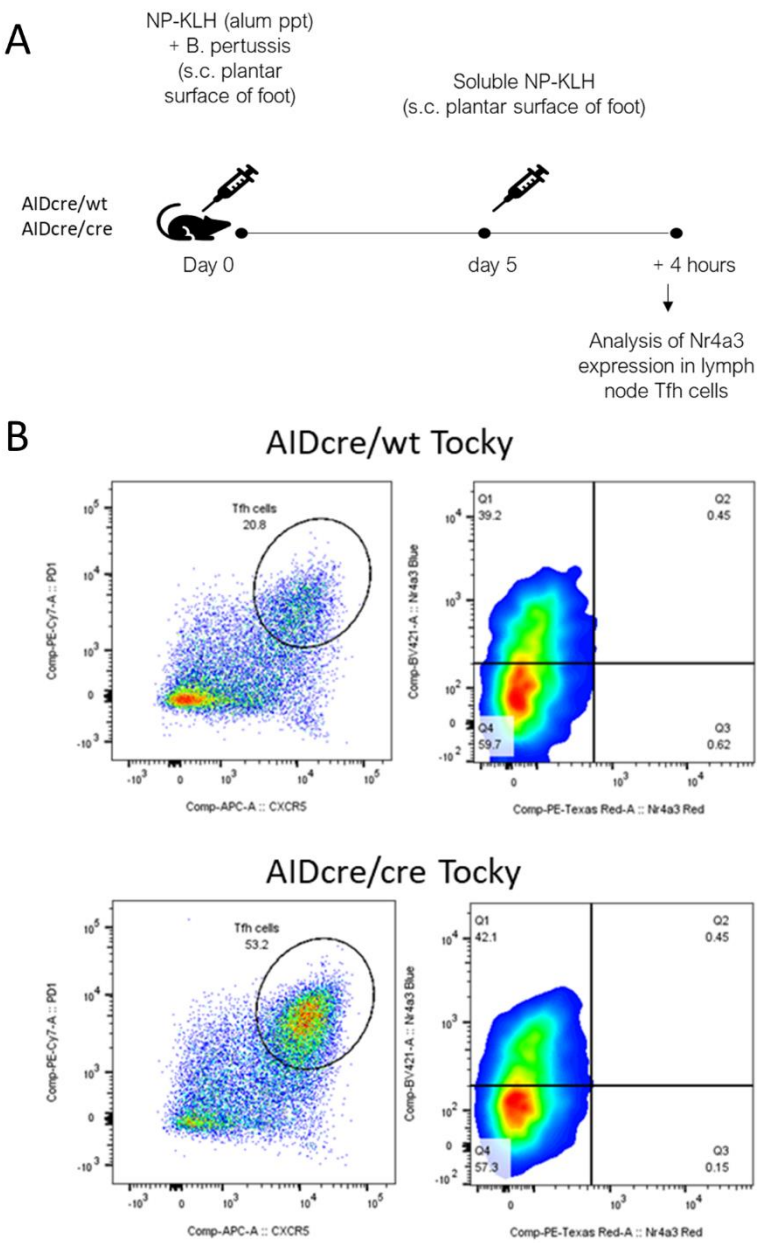

Figure 4.25 Analysis of Nr4a3 blue and red expression on AIDcre/wt Tocky and AIDcre/cre Tocky mice 4 hours stimulation by soluble antigen during early GC formation.

(A)AIDcre/wt and AIDcre/cre Nr4a3-Tocky mice were immunised with 10µg NP-KLH in alum precipitation plus heat-inactivated *B. pertussis* on the plantar surface of foot. At day 5 mice were boosted with 10µg soluble NP-KLH. Mice were culled 4 hours later, and lymph nodes analysed by flow cytometry. (B) Representative flow cytometry plots showing Tfh cells and Nr4a3-blue and Nr4a3-red expression in Tfh cells. From lymphocytes, T cells were gated as $CD3^+$ $CD19^-$. From T cells, $CD4^+$ T cells were gated as $CD4^+$. From $CD4^+$ T cells, activated cells were gated as $CD44^+$ $CD62L^-$. From activated CD4 T cells, Tfh cells were gated as PD-1^{hi} $CXCR5^{hi}$. From Tfh cells, timer blue and red were gated as BV421-Nr4a3 $blue^+$ and PE-Texas Red Nr4a3 red^+.

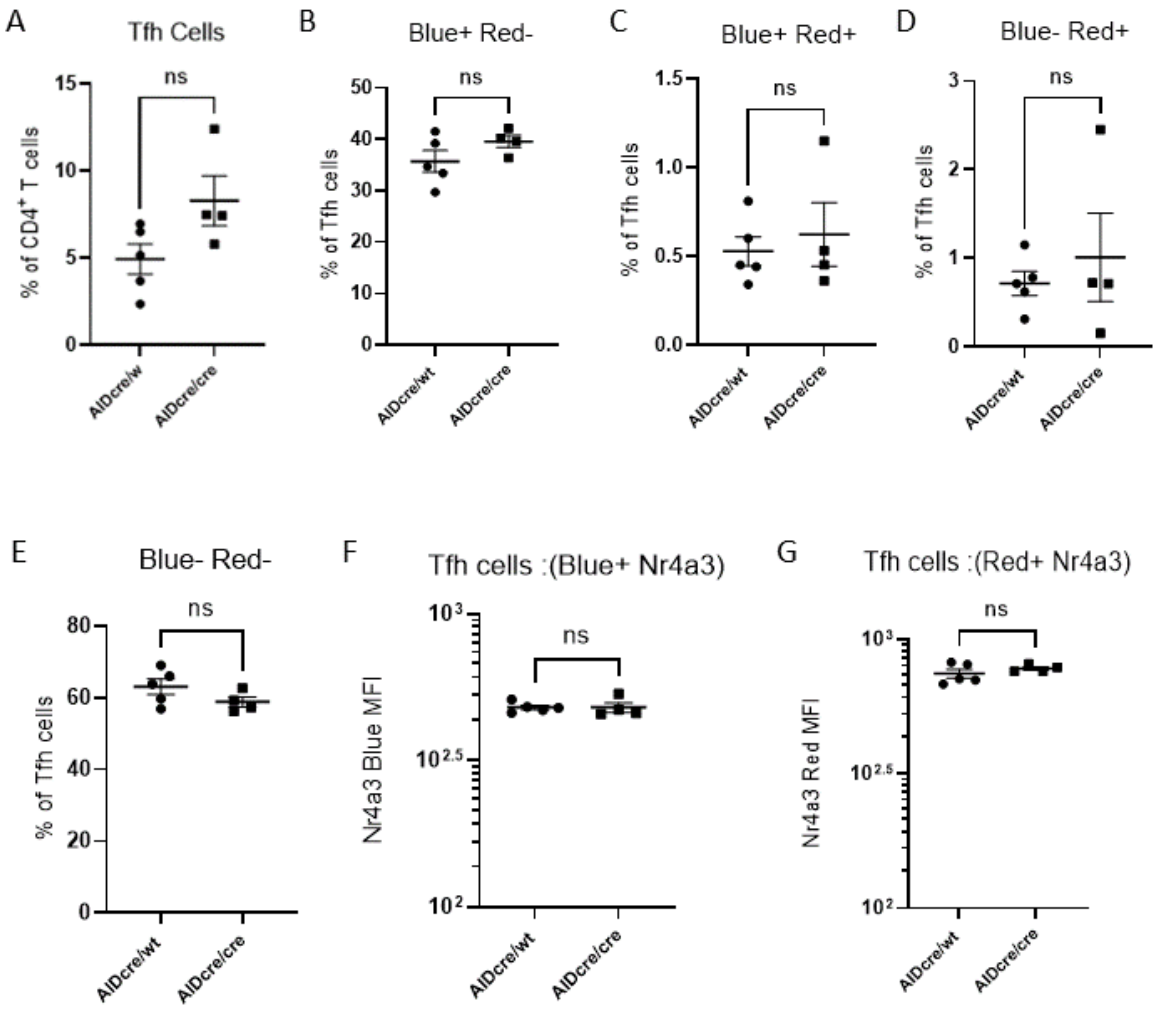

Figure 4.26 Tfh cells were increased in AIDcre/cre-Tocky mice, but there was no increase in recently activated Nr4a3-blue$^+$ Tfh cells.

(A) Frequency of Tfh cells as percentage of total CD4$^+$ T cells. (B) Frequency of Nr4a3-blue$^+$ red$^-$ Tfh cells as percentage of Tfh cells; (C) frequency of Nr4a3-blue$^+$ red$^+$ Tfh cells as percentage of Tfh cells; (D) frequency of Nr4a3-blue$^-$ red$^+$ Tfh cells as percentage of Tfh cells;(E) frequency of Nr4a3-blue$^-$ red$^-$ Tfh cells as percentage of Tfh cells; (F) Nr4a3 blue$^+$ MFI in Nr4a3-blue$^+$ red$^-$ Tfh cells; (G)) Nr4a3 red$^+$ MFI in Nr4a3-blue$^-$ red$^+$ Tfh cells. Stated as mean ± SEM (error bars; unpaired two-tailed t-test. ns no significant. Data from one experiment. Each symbol represents one mouse.

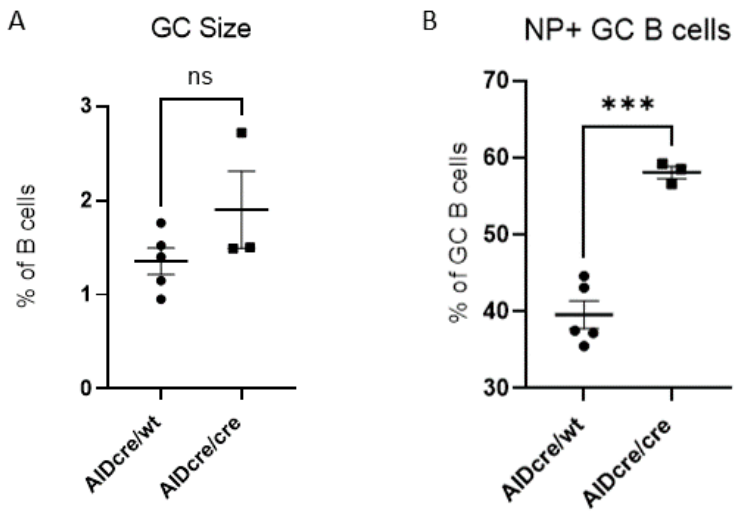

Figure 4.27 AIDcre/cre-Tocky mice had higher frequency of NP specific GC B cells.
AIDcre/wt and AIDcre/cre Nr4a3-Tocky mice were immunised with 10µg NP-KLH in alum precipitation plus heat-inactivated *B. pertussis* on the plantar surface of foot. At day 5 mice were boosted with 10µg soluble NP-KLH. Mice were culled 4 hours later, and lymph nodes analysed by flow cytometry. (A) Frequency of GC as percentage of total B cells. (A) Frequency of NP-specific B cells as percentage of GC B cells. Stated as mean ± SEM (error bars; unpaired two-tailed t-test). **P < 0.01, ***P < 0.001, ns: no significant. Data from one experiment. Each symbol represents one mouse.

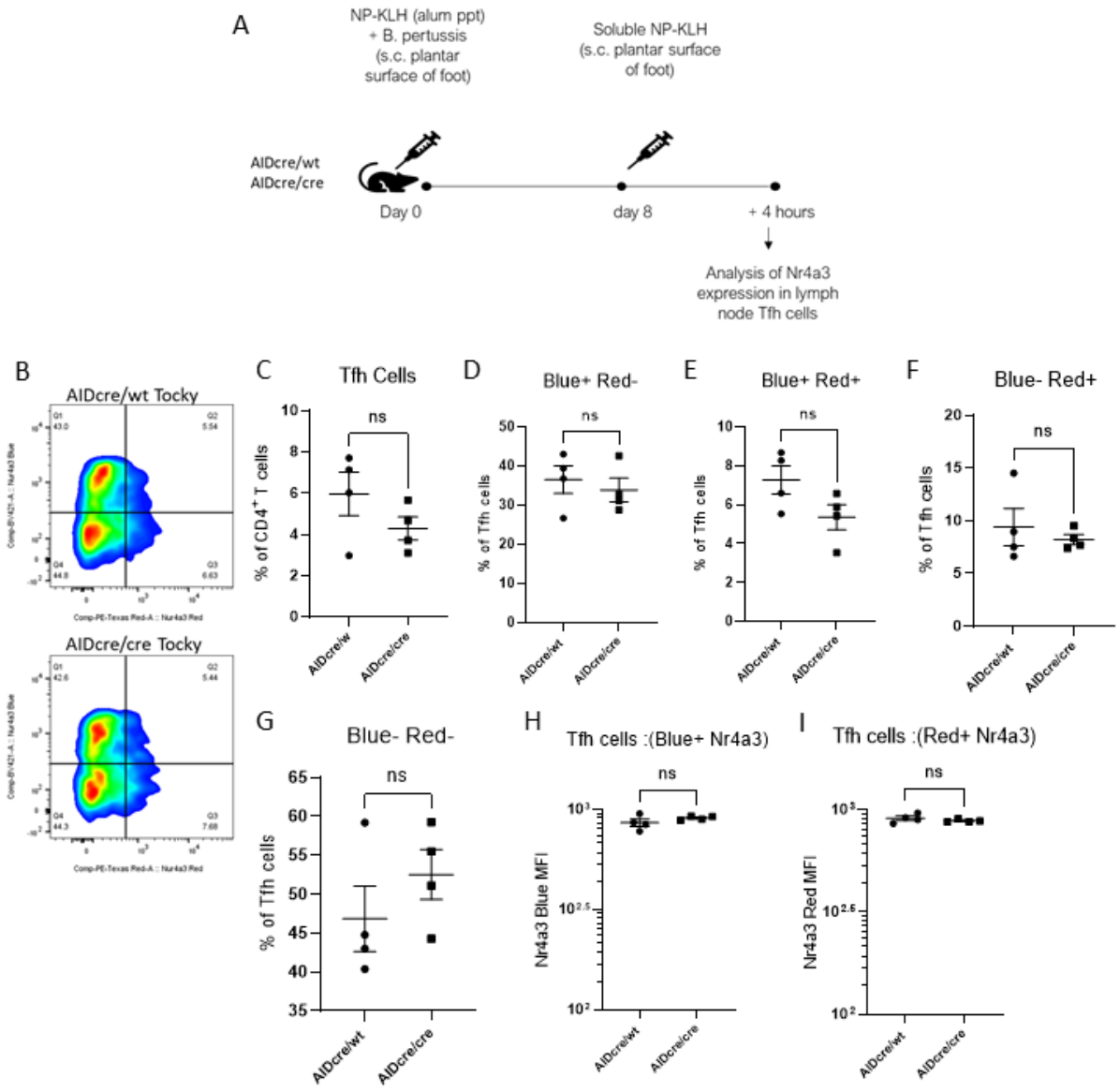

Figure 4.28 No difference in Nr4a3-Tocky expression in AIDcre/wt and AIDcre/cre at day 8 after 4-hour boost with soluble NP-KLH.

(A)AIDcre/wt and AIDcre/cre Nr4a3-Tocky mice were immunised with 10µg NP-KLH in alum precipitation plus heat-inactivated *B. pertussis* on the plantar surface of foot. At day 8 mice were boosted with 10 µg soluble NP-KLH. Mice were culled 4 hours later, and lymph nodes analysed by flow cytometry. (B) Flow cytometry plots of Nr4a3-blue and Nr4a3-red expression in Tfh cells. (C) Frequency of Tfh cells as percentage of total $CD4^+$ T cells. (D) Frequency of Nr4a3-$blue^+$ red^- Tfh cells as percentage of Tfh cells; (E) frequency of Nr4a3-$blue^+$ red^+ Tfh cells as percentage of Tfh cells; (F) frequency of Nr4a3-$blue^-$ red^+ Tfh cells as percentage of Tfh cells;(G) frequency of Nr4a3-$blue^-$ red^- Tfh cells as percentage of Tfh cells; (H) Nr4a3 $blue^+$ MFI in Nr4a3-$blue^+$ red^- Tfh cells; (I) Nr4a3 red^+ MFI in Nr4a3-$blue^-$ red^+ Tfh cells. Stated as mean ± SEM (error bars; unpaired two-tailed t-test). ns: no significant. Data from one experiment. Each symbol represents one mouse.

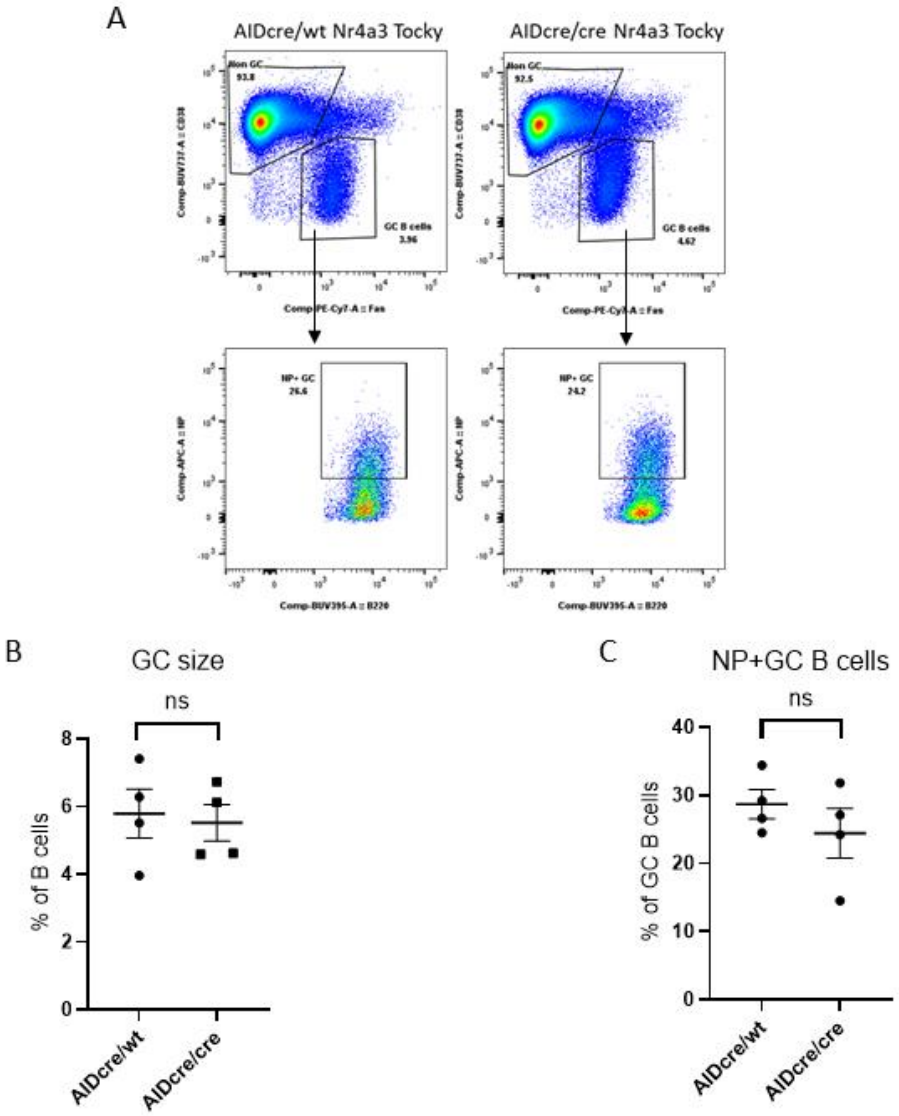

Figure 4.29 AIDcre/wt and AIDcre/cre mice had similar GC size and frequency of NP-specific GC B cells at day8 after 4hr stimulation with soluble antigen for 4 hours.

AIDcre/wt and AIDcre/cre Nr4a3-Tocky mice were immunised with 10µg NP-KLH in alum precipitation plus heat-inactivated *B. pertussis* on the plantar surface of foot. At day 8 mice were boosted with 10 µg soluble NP-KLH. Mice were culled 4 hours later, and lymph nodes analysed by flow cytometry. (A) Flow cytometry plots of GCs were gated as $Fas^{+}CD38^{-}$ and NP-specific GC B cells gated as $NP\text{-}APC^{+}$. (B) Frequency of GC as percentage of total B cells. (C) Frequency of NP-specific B cells as percentage of GC B cells. Stated as mean ± SEM (error bars; unpaired t-test, two-tailed test). ns; no significant. Data from one experiment. Each symbol represents one mouse.

4.3.6. Soluble antigen booster immunisation induces Nr4a1 (Nur77)-Tempo reporter protein antigen-reactive Tfh cells, but not in B cells.

The previously described experiments used Nr4a3, a subunit of the Nr4a family of orphan nuclear receptors, to measure TCR signalling in T cells. Here we had the opportunity to test the same reporter timer protein driven by the regulatory elements of another subunit called Nur77, encoded by the Nr4a1 gene. Both genes were previously reported as primary response genes that are rapidly upregulated in response to antigen receptor stimuli (Tan et al., 2020). However, due to weaker expression of Nr4a3 in T cells, the timer protein in Nr4a3-Tocky mice could not be detected in B cells and was only useful as a reporter of TCR signalling. Therefore, we tried to use the alternative Nur77-Tempo (Nr4a1) reporter mouse to allow analysis of BCR and TCR signalling, which recently has been developed by the group of David Bending in our Institute (Elliot et al., 2022). Due to time constraints of this project, Nur77-Tempo mice were crossed with either WT or IgMg1 mice to obtain mice that were either WT or contained one IgMg1 allele and were heterozygous for Nr4a1-Tempo allele. IgMg1/wt heterozygous mice should contain a mix of BCR WT and IgMg1 B cells. T cell populations in Nr4a1-Tempo mice can be identified by flow cytometry, similar to Nr4a3-Tocky mice as illustrated in (Figure 4.1). Nr4a1-Tempo mice contain the same blue/red timer protein as Nr4a3-Tocky mice, showing the maturation of TCR signalling from lymphocytes recently activated in response to stimuli. Timer-blue represents recently activated, and Timer red cells in arrested phase, whereas double positive cells are recently activated cells that have started acquiring red proteins, or are reactivated timer red positive cells.

To assess Nr4a1 expression B cells and Tfh cells of mice with IgMg1 BCR following in vivo stimulation, WT Nur77 and IgMg1/wt Nur77 Nr4a1-Tempo mice were immunized with NP-KLH in alum plus heat-inactivated *B. pertussis* s.c. into the plantar surface of the rear foot. At

day 5, mice were boosted with either soluble NP-KLH or NP-CGG in the same foot. Lymph nodes were taken 4 hr later and analysed by flow cytometry (Figure 4.30 A). Gating schemes for identification of Tfh and TcM populations and their Nr4a1 expression of TCR timer blue and red were adjusted according to CD62L expression on naive $CD4^+$ T cells (Figure 4.30 B). Tfh cells were identified as $CD44^+$ $PD1^{hi}$ $CXCR5^{hi}$ (Figure 4.31 A). Analysis of Tfh cells in draining lymph nodes (DrLN) showed that boosting with either the same primed protein NP-KLH or the control protein NP-CGG resulted in similar frequencies of Tfh cells as a percentage of $CD4^+$ T cells (Figure 4.31 B).

The TCR stimulation dependent Nr4a1-blue and Nr4a1-red expression was assessed after gating on Tfh cells (Figure 4.32 A). Newly reactivated Tfh cells expressing timer $blue^+red^-$ and persistent Tfh cells expressing timer $blue^+red^+$ were significantly increased in mice that received the same soluble antigen. However, there was no difference in the frequency of timer $blue^+$ Tfh cells between IgMg1 and WT control mice treated with the same antigen (Figure 4.32 B, and C). The frequency of timer red^+ arrested T cells was slightly reduced, though not significantly, within the group immunised with the same primed NP-KLH antigen (Figure 4.32 D). Correspondingly, the frequency of negative timer $blue^-red^-$ Tfh cells was reduced in mice immunised with NP-KLH (Figure 4.32 E). Additionally, the MFI of Nr4a1-blue in newly activated Tfh cells was increased in mice immunised with the same primed NP-KLH protein compared to NP-CGG, while there was no significant difference in Nr4a1-red^+ MFI (Figure 4.32 F, and G). These data suggest that re-challenge with the same soluble antigen protein induces Nr4a1 in T cells that bind cognate antigen presented by B cells. As there was not change in Tfh cell activation, it is likely that there was no change in the amount of antigen presented to Tfh cells by IgMg1 BCR B cells in this experiment. This is different from IgMg1/Mg1 homozygous data (Fig. 4.3B), which showed that IgMg1 B cells induce more

persistent signalling in Tfh cells. It is possible that in the IgMg1/wt heterozygous situation the impact from IgMg1 B cells on Tfh TCR signalling is too low to be detected with this method.

We assessed Nr4a1 expression in central memory T (TcM) cells, identified as $CD4^+$ $CD62L^+$ $CD44^{high}$ T cells. Nr4a1 blue and red expression in TcM cells was evaluated by flow cytometry (Figure 4.33 A). At 4 hours after challenge with either the primed protein (NP-KLH) or a different carrier protein (NP-CGG), the proportion of DrLN TcM cells did not change in groups immunized with either the same or different antigens. Additionally, there was no difference in the TcM population was detected in altered BCR IgMg1 compared to WT controls (Figure 4.33 B). However, after re-challenge with the same primed antigen, WT mice showed a significant increase in Nr4a1-$blue^+$ TcM cells, indicating newly activated cells upon re-encountering antigen, compared to IgMg1 mice (Figure 4.33 C). Within the Nr4a1-$blue^+red^+$ persistent TcM population, there was an increase in WT mice after re-challenged with NP-CGG, potentially suggesting TcM in WT mice respond to NP in some manner. However, the persistent Nr4a1-$blue^+red^+$ TcM population did not change between WT and IgMg1 mice after immunisation with the same primary antigen (Figure 4.33 D). IgMg1 mice had an increased frequency of Nr4a1-red^+ arrested TcM cells compared to WT (Figure 4.33 E). The frequency of Nr4a1-negative TcM cells, indicating no stimulation, was reduced in mice after injection with the same antigen NP-KLH while it was increased in the group after immunisation with the different carrier protein NP-CGG (Figure 4.33 F).

As mentioned earlier, the Nr4a1 gene rapidly responds in B cells after stimulation with antigen. To further investigate this, we assessed Nr4a1 timer expression in different B cell subsets during an immune response. Timer blue and red were measured on $CD38^+Fas^-$ as non-GC B cells and $CD38^{low}Fas^+$ as GC B cells after responding to soluble antigen (Figures 4.34

A, and B). Non-GC B cells had low background levels of timer blue fluorescence that were not clearly distinguishable by flow cytometry, even with increased expression after stimulation with the same primary antigen (Figure 4.34 C). The GC size did not change significantly between IgMg1 and WT mice under either boosted with NP-KLH or NP-CGG. There was no detectable increase in GC B cells expressing timer blue+, indicating newly activation (Figures 4.34 D, and E).

To increase sensitivity, we examined NP-specific GC B cells, identified as Fas^{+} NP^{+}. These were further gated to assess timer blue and red expression (Figure 4.35 A, and B). Despite IgMg1 mice showing a clear but not statistically significant increase in the frequency of NP-binding GC B cells compared to WT, Nr4a1 $blue^{+}$ expression was not strong enough to robustly detect expression, as seen in Tfh cells. Therefore, there was no detectable change between IgMg1 and WT mice after booster immunisation with antigen (Figure 4.35 B and C).

Overall, newly activated Tfh cells increased equivalently in IgMg1 and WT mice in response to soluble antigen, suggesting normal antigen presentation to Tfh cells by B cells. No differences were detected in Nr4a1 expression on GC B cells or NP-binding GC B cells. This could be because the mice used were double heterozygous, which may not provide a strong enough Nr4a1 signal. Using homozygous mice would likely make the signals more sensitive, as having two copies of the gene produces more protein than just one. Further experiments using homozygous mice will be needed to determine.

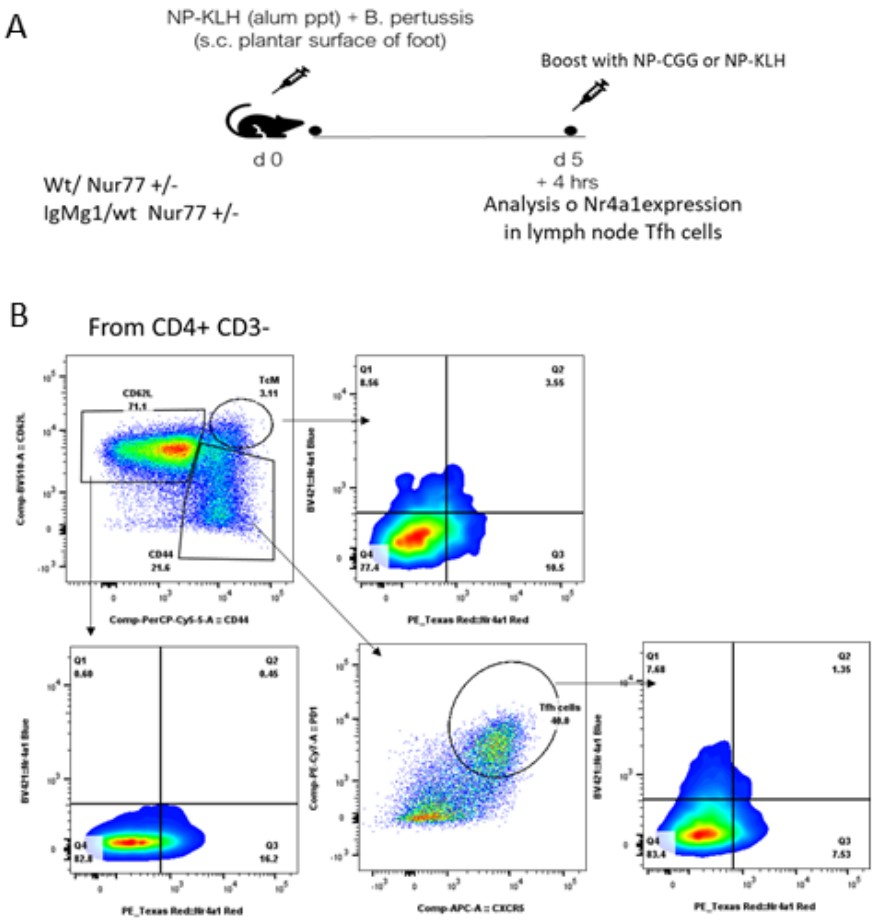

Figure 4.30 Immunization Protocol and Tfh cells and TcM in Nur77 (Nr4a1) WT and IgMg1 mice.

(A) Wt Nur77 or IgMg1/wt Nur77 Nr4a1-Tempo mice were immunised with 10µg NP-KLH in alum plus heat-inactivated *B. pertussis* s.c. on the plantar surface of foot. At day 5 mice were boosted with either 10 µg soluble NP-KLH or NP-CGG. Mice were culled 4 hours later, and lymph nodes analysed by flow cytometry. (B) Gating strategy of Tfh cells and their Nr4a1 blue and red expression. From live cells, T cells were gated as $CD3^+$ $CD19^-$. From CD3 T cells, $CD4^+$ T cells were gated as $CD4^+$. From $CD4^+$ T cells, naïve $CD4^+$ T cells were gated as $CD62L^+$ $CD44^-$ and activated T cells were gated as $CD44^+$ $CD62L^-$. From activated T cells, Tfh cells were gated as PD-1^{hi} $CXCR5^{hi}$. From Tfh cells gating Nr4a1-blue and Nr4a1-red expression in Tfh cells.

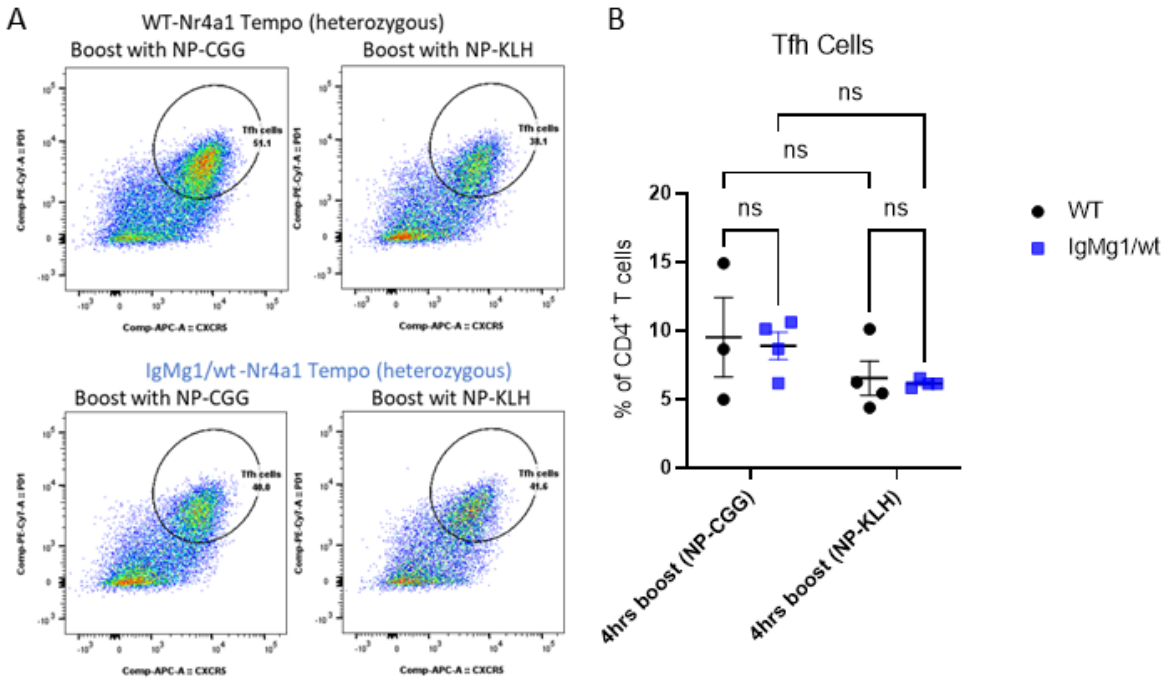

Figure 4.31 Tfh Cells from WT and IgMg1 mice showed similar percentages after stimulation with the same Carrier-Primed Protein (NP-KLH).

(A) Representative flow cytometry plots showing Tfh cells were gated from $CD4^+$ T cells, activated T cells were gated as $CD44^+$ $CD62L^-$. From activated T cells, Tfh cells were gated as $PD\text{-}1^{hi}$ $CXCR5^{hi}$. (B) Frequency of Tfh cells as percentage of $CD4^+$ T cells. Data statistical tests were performed as mean ± SEM Two-way ANOVA test mixed-effects analysis with Šídák's multiple comparisons test (ns, not significant). Data from one experiment. Each symbol represents one mouse.

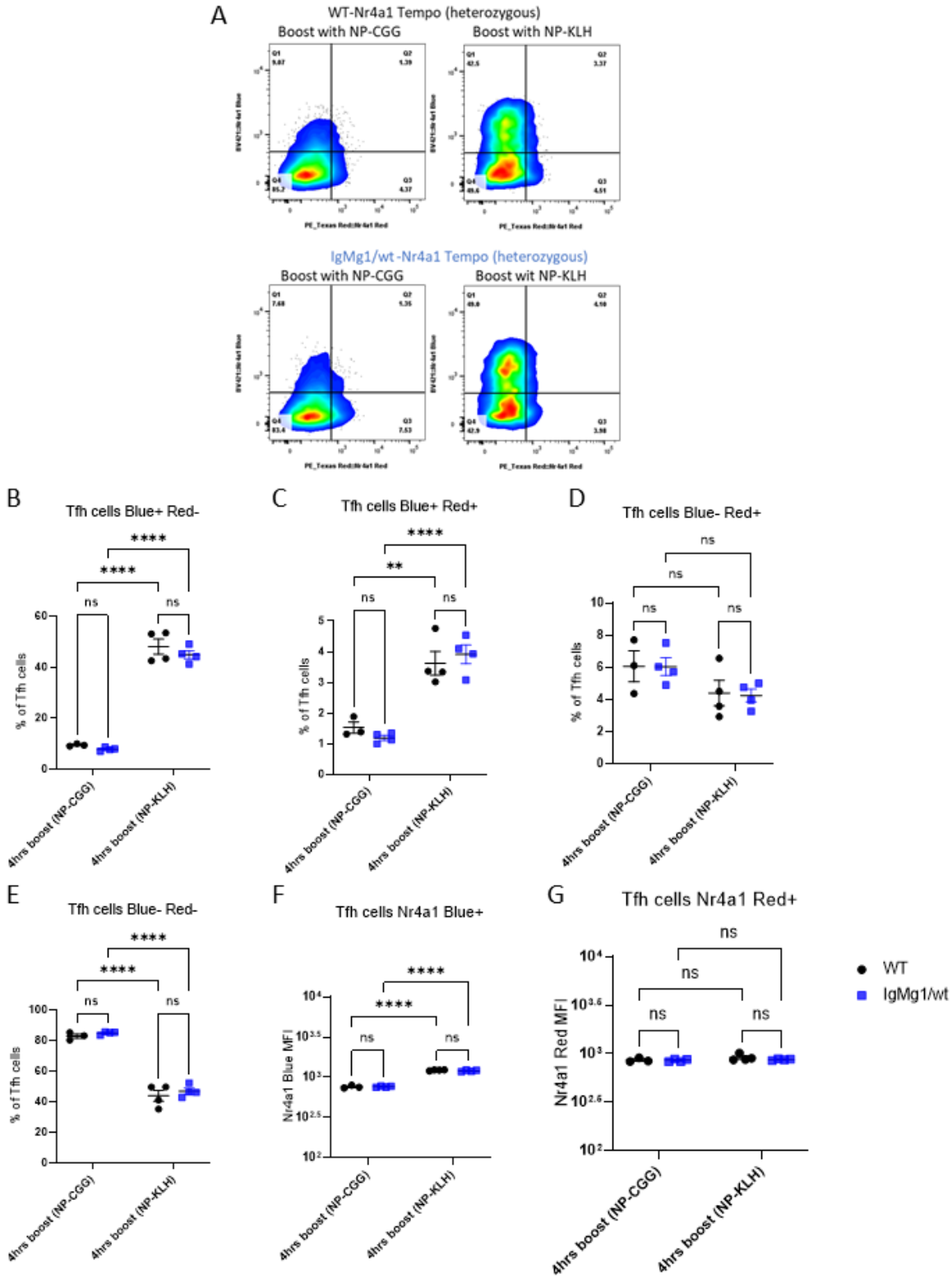

Figure 4.32 Nr4a1 expression shows strongly increased in same carrier primed protein (NP-KLH) but no significant differences between WT and IgMg1 mice.

(A) Flow cytometry plots of Nr4a1-blue and Nr4a1-red expression in Tfh cells. (B) Frequency of Nr4a1-blue$^+$ red$^-$ Tfh cells as percentage of Tfh cells; (C) frequency of Nr4a1-blue$^+$ red$^+$ Tfh cells as percentage of Tfh cells; (D) frequency of Nr4a1-blue$^-$ red$^+$ Tfh cells as percentage of Tfh cells;(E) frequency of Nr4a1-blue$^-$ red$^-$ Tfh cells as percentage of Tfh cells; (F) Nr4a1- blue$^+$ MFI in Nr4a1-blue$^+$ red$^-$ Tfh cells; (G) Nr4a1- red$^+$ MFI in Nr4a1-blue$^-$ red$^+$ Tfh cells**.** Data statistical tests were performed as mean ± SEM Two-way ANOVA test mixed-effects analysis with Šídák's multiple comparisons test (*, $p < 0.05$; **, $p < 0.01$; ***, $p < 0.001$; ****, $p < 0.0001$; ;ns, not significant). Data from one experiment. Each symbol represents one mouse.

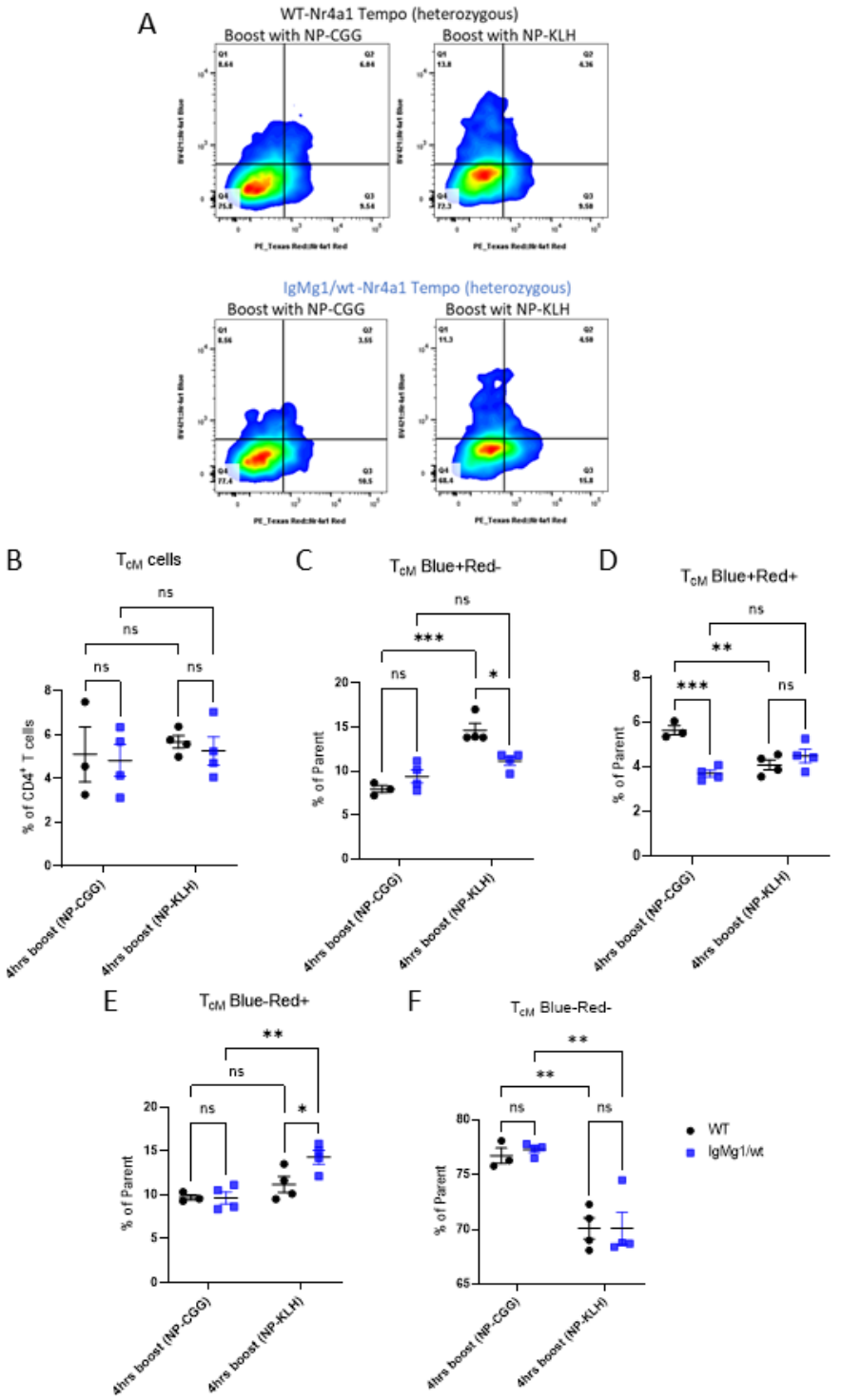

Figure 4.33 Central memory T cells in WT has strong expression of Nur77 compared with IgMg1 mice.

(A) Flow cytometry plots of Nr4a1-blue and Nr4a1-red expression in TcM cells. (B) Frequency of TcM cells as percentage of $CD4^+$ T cells. (C) Frequency of Nr4a1-$blue^+$ red^- TcM cells as percentage of TcM cells; (D) frequency of Nr4a1-$blue^+$ red^+ TcM cells as percentage of TcM cells; (E) frequency of Nr4a1-$blue^-$ red^+ TcM cells as percentage of TcM cells;(F) frequency of Nr4a1-$blue^-$ red^- TcM cells as percentage of TcM cells. Data statistical tests were performed as mean ± SEM Two-way ANOVA test mixed-effects analysis with Šídák's multiple comparisons test (*, $p < 0.05$; **, $p < 0.01$; ***, $p < 0.001$; ****, $p < 0.0001$; ns, not significant).Data from one experiment. Each symbol represents one mouse.

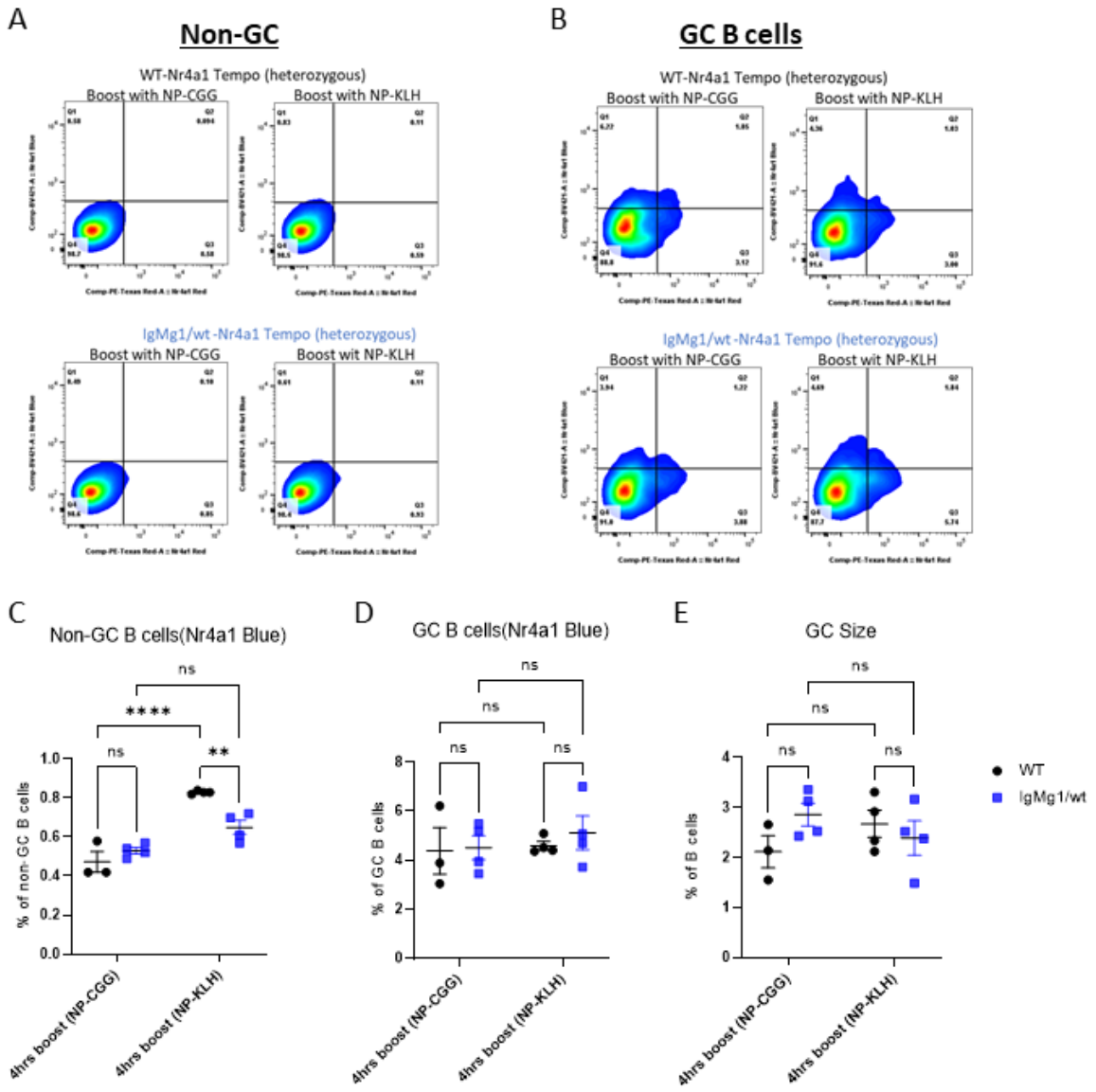

Figure 4.34 Nur77 Tempo GC B cells have no increased Nr4a1-Blue expression when stimulated in vivo.

(A) Flow cytometry plots of Nr4a1-blue and Nr4a1-red expression in non-GCs cells were gated as $CD38^{+}Fas^{-}$. (B) Flow cytometry plots of Nr4a1-blue and Nr4a1-red expression in GC B cells were gated as $CD38^{-}Fas^{+}$. (C) Nr4a1- $blue^{+}$ expression as percentage of non-GC B cells. (D) Nr4a1- $blue^{+}$ expression as percentage of GC B cells. (E) Frequency of GC B cells as percentage of total B cells. Data statistical tests were performed as mean ± SEM Two-way ANOVA test mixed-effects analysis with Šídák's multiple comparisons test (**, $p < 0.01$; ****, $p < 0.0001$; ns, not significant). Data from one experiment. Each symbol represents one mouse.

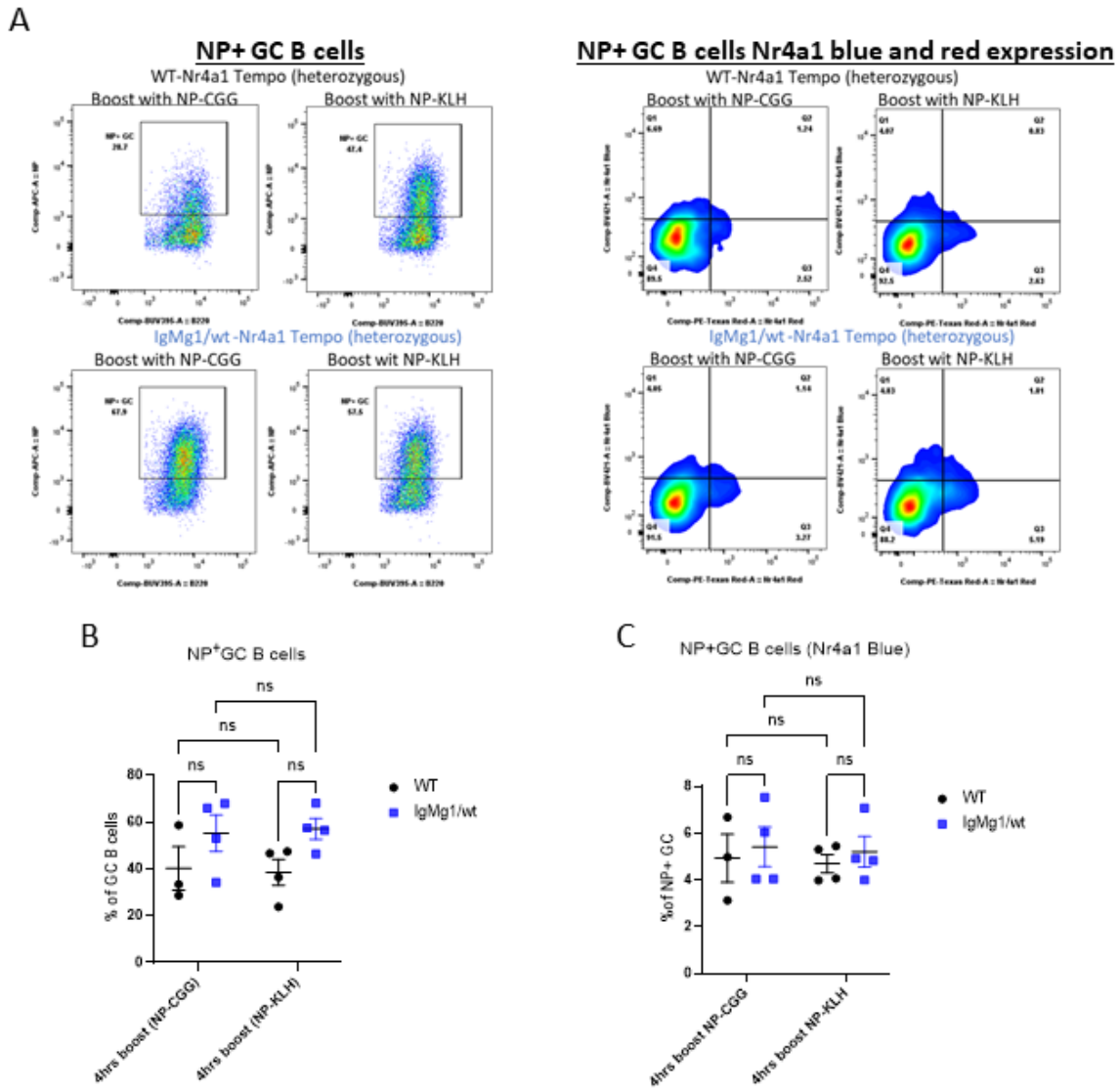

Figure 4.35 NP-specific GC B cells toward be significant in heterozygous IgMg1 mice. But did not show any strong expression of Nr4a1 gene after re-challenged with soluble antigen.

(A) Flow cytometry plots of NP-specific GC B cells gated as NP-APC^{+} and NP^{+} GC B cells Nr4a1 blue and red expression. (B) Frequency of NP-specific B cells as percentage of GC B cells. (C) Frequency of NP^{+} -GC B cells Nr4a1 blue as percentage of NP^{+} GC. Data statistical tests were performed as mean ± SEM Two-way ANOVA test mixed-effects analysis with Šídák's multiple comparisons test (*, $p < 0.05$; **, $p < 0.01$; ***, $p < 0.001$; ****, $p < 0.0001$; ns, not significant). Data from one experiment. Each symbol represents one mouse.

4.4. Discussion

B cell-Tfh cell interactions play a fundamental role in promoting BCR affinity maturation and can sense increased strength of BCR – antigen interaction (Victora et al., 2010). B cells with high affinity BCR capture antigens more efficiently than low affinity BCR, and receive help preferentially from Tfh cells. B cells with low affinity BCRs will not access antigen, not efficiently be rescued by Tfh cells, and therefore will undergo the default pathway of GC B cells, which is to be removed by apoptosis (Meyer-Hermann et al., 2006, Allen et al., 2007b, Zhang et al., 2013).

The experiments presented in this chapter aimed to investigate how altering BCR affinity or reducing activation-induced cytidine deaminase (AID) activity affects B cell-Tfh cell interactions. To detect TCR activity, the mouse models used in these experiments expressed a reporter driven by the regulatory elements of the Nr4a3 gene, allowing for novel tracking of Tfh cell activation.

Upon re-challenge with soluble antigen, the frequency of Tfh cells increased in IgMg1 mice. However, in IgG1M mice, which have IgG1 as their only B cell receptor (BCR), the frequency of Tfh cells was reduced after boosting with soluble antigen, although before boost cells numbers in IgMg1, IgG1M, and WT mice when were similar (Figure 4.2 C). Although Tfh cell percentage increased in IgMg1 mice but not in WT mice, Nr4a3-blue+ expression, indicating recent Tfh activation, was not increased than in WT mice. On the other hand, despite a reduction of Tfh numbers in IgG1M mice, if anything stronger Nr4a3-blue+ expression was observed in IgG1M Tfh cells (Figure 4.3 B). The frequency of long-activated T cells, identified as blue-red+ cells at day 5, was clearly increased in IgMg1 mice compared to WT and IgG1M mice. Over time, by day 8 post-immunisation, these long-activated B cell populations were

highly increased in all genotypes compared to day 5, and reactivation led to a loss of these cells (Figure 4.3 D).

The increased frequency of Tfh cells and NP-specific GC B cells in IgMg1 mice after boosting with soluble antigen was unexpected given the reduction in total GC size at day 5 and day 8 compared to WT mice (Figure 4.4 A, and B). One possible explanation is that IgMg1 B cells might have higher average affinity in GCs, enabling them to capture more antigen and present more peptide to Tfh cells. Another, that the cytoplasmic chain of IgG1 improving antigen-presentation. In contrast, IgG1M mice showed reduced Tfh cell numbers but increased Nr4a3 blue^{+} MFI after boosting with soluble antigen. Despite decreased GC size at day 5, by day 8 IgG1M mice formed GCs comparable in size to WT mice. However, the frequency of NP-specific GC B cells was impaired in IgG1M mice after soluble antigen boost (Figure 4.4 A and B). This suggests IgG1M mice are able to effectively present antigen despite fewer NP-specific GC B cells. The mismatch between Tfh cell proportion, Nr4a3 expression, and GC size requires further investigation to understand the dynamics between these populations in IgMg1 and IgG1M mice. Better understand the interactions between Tfh cells and GC B cells, situ imaging can be used to visualize their spatial relationships within GC. Additionally, BCR sequencing can be performed to analyse the diversity and affinity of B cell receptors, present insights into the quality of the antibody response. Key genes to examine include IGHV, which reveals the diversity and mutation patterns of BCRs, and IGHD, which contributes to the generation of varied antigen-specific receptors.

It is thought that T cell help results in more positively selected B cells and increased plasma cell output from germinal centres (Nakagawa and Calado, 2021). In our study, we showed an increased frequency of plasma cells in IgMg1 mice, but PCs were impaired in IgG1M mice. This

impairment in IgG1M mice could be due to the absence of IgM, which helps form immune complexes on follicular dendritic cells (Zhang et al., 2013). The increased T cell help in IgMg1 mice likely promotes more positively selected B cells and plasma cell output, while the lack of IgM in IgG1M mice reduces immune complex formation and subsequently impairs plasma cell differentiation.

Tfh cell frequency was determined after expanding the time of T cell re-stimulation. Again, the Tfh cells were clearly reduced in IgG1M mice after stimulation with soluble antigen, but IgMg1 mice remained at similar levels to WT mice. WT mice maintained Nr4a3 blue^{+} expression after stimulation with soluble antigen for 18 hours. However, both the TCR timer blue^{+}red^{+} population and the red MFI within blue^{+}red^{+} persistent Tfh cells increased (Figure 4.8 B and H), suggesting B and T cells interacted for 18 hours despite the clear reduction in germinal centre size at this time point (Figure 4.10 B). While the duration of T-B cell interaction was increased, there was no clear observation of GC B cell selection in the dark zone among mice with altered BCRs, even though NP-specific GC B cell frequencies did not change before or after re-challenge with soluble antigen (Figures 4.11 C and 4.12 B).

It is unclear why IgMg1 mice showed a significant increase in class-switched IgG1^{+} and clearly increased IgG1^{+} NP-binding cells during the primary response compared to WT mice (Figure 4.13 C ,4.15 B). A possible explanation could be that, as B cells in IgMg1 mice are anergic, they have a reduced BCR density. This might require increased affinity to access and present sufficient antigen to receive Tfh help. In contrast, IgG1M mice only contained NP-specific cells with low affinity (Figure 4.15 B). Plasma cell numbers were elevated during the primary response in IgMg1 mice and antigen-specific PCs were clearly enhanced, but in IgG1M mice they remained at similar levels to WT mice (Figure 4.16 A and B). After antigen challenge, both

NP-specific and total plasma cells dramatically decreased in IgMg1 and IgG1M mice, while WT mice showed high variability (Figures 4.16 A and B). These data suggest IgMg1 mice can mount an efficient response to T-dependent antigens by presenting more antigen to Tfh cells, but this was not altered during chronic antigen stimulation. IgG1M mice showed increased TCR timer blue despite reduced Tfh cell frequencies, indicating an impaired immune response to T-dependent antigens by reducing NP-specific GC B cells and plasma cells output.

Central memory T (TcM) cell populations increased in frequency after receiving soluble antigen in both the DrLN and spleen. It has been reported that Tfh cells can downregulate expression of markers like CXCR5, Bcl6, and PD1 and transition into memory T cells (Barr and Gray, 2012). We identified TcMs by their expression of $CD62L^+$ and $CD44^+$. Using the Tocky mouse model, timer blue expression increased after stimulation, however these timer $blue^+$ populations were more abundant in both IgMg1 and IgG1M mice and showed strong Nr4a3 $blue^+$ expression (Figure 4.18 B). IgMg1 and IgG1M DrLNs also exhibited increased timer red^+ cells after acute 4-hour stimulation, indicating these cells were quickly activated and maintained triggered TCR signalling, unlike Tfh cells (Figure 4.18 C). However, these features did not significantly change in any genotype with prolonged antigen exposure in local DrLNs (Figures 4.20 B, C, D).

Since TcMs can circulate between SLOs, we examined the spleen as an example. The frequency of timer $blue^+$ TcMs was reduced in IgMg1 mice after boosting with soluble antigen (Figure 4.21 B) but still showed activated TCR $blue^+$ and red^+ expression after 18 hours, similar to WT mice (Figure 4.22 C). Surprisingly, IgG1M mice had reduced timer $blue^+$ and red^+ cells, with only strong newly activated timer $blue^+$ cells. This suggests IgG1 B cells may only internalize antigen in early stages upon encounter, losing contact with chronic antigen

exposure (Figure 4.22 C). These data suggest that repeat immunisations with antigen for short or long durations allows reactivation of T cells to differentiate into TcM populations in DrLNs, which can also be detected in distant SLOs like the spleen.

In an experiment to investigate the role of B-T cells interaction in the absence of affinity maturation and class-switched B cells by crossing AIDcre/cre to Nr4a3-Tocky mice could help to give clue how strong of these cells communicate in GC. Our result represented that more Tfh cells were detected in AIDcre/cre at day 5 but not elevated by day 8 compared to the AIDcre/wt control (Figure 4.26 A and 4.28 C). Additionally, immunisation with soluble antigen 4 hours before mice were culled at the timepoint of harvesting the DrLN (i.e day5 and day8) resulted in timer intensity in newly activated and arrested Tfh cells being unchanged in both genotypes (Figure 4.26 B, C, D, and Figure4.28 D, E, and F). Interestingly, at day 5 GC B cells and NP-binding cells were higher frequency in AIDcre/cre mice but remained similar by day 8 (Figure 4.27 A, B and 4.29 B, C). These data suggest that a lack of AID activity did not impact the interaction between B cells and Tfh cells, as indicated by similar timer intensity. Despite more antigen binding at day 8 in AIDcre/cre and it could be that B cells that lack AID were caused by genotoxicity and AID-mediated effects on cell viability (Sherman et al., 2010).

The Nr4a3-Tocky mouse was used to analyse TCR signalling strength in Tfh cells and investigate antigen presentation to Tfh cells in different mouse models with altered BCR signalling. Although previous studies reported that Nr4a3 is induced by BCR signalling following stimulation (Tan et al., 2020), Nr4a3 was not upregulated in B cells in our Nr4a3-Tocky mouse model. Therefore, we used an alternative novel mouse strain expressing a timer protein und the control of the regulatory elements of the Nr4a1 gene, allowing analysis of both TCR and BCR signalling (Elliot et al., 2022). Due to time constraints for this project, the

Nur77 (Nr4a1)-Tempo mice were crossed with IgMg1 heterozygous mice carrying one IgMg1 allele. During a T cell-dependent immune response soluble antigen was injected into the foot. While this resulted in induction of Nr4a1-timer protein, there was no difference in Tfh cell frequency between IgMg1 and WT mice at day 5 post-immunization (Figure 4.31 B). Additionally, Tfh cells did exhibit similar substantial and Nr4a1 reporter activity in both genotypes post-immunisation (Figure 4.32 B). Moreover, Nr4a1-Tempo mice displayed stronger Nr4a1-mediated fluorescence indicating accumulation of more antigenic peptides and enhanced TCR signalling compared to Nr4a3 reporter mice. This suggests Nr4a1 is more sensitive and has lower background than Nr4a3 (Bending et al., 2018, Jennings et al., 2020). TcM populations were also examined in this model. While TcM frequency was unchanged between IgMg1 and wildtype mice, wildtype mice exhibited increased Nr4a1 reporter activity in antigen-experienced TcM following re-challenge with soluble NP-KLH (Figures 4.33 B and 4.33 C).

The Nur77 (Nr4a1) gene has previously been studied using the Nur77-eGFP transgenic reporter mouse model. These studies show GFP expression is dependent on antigen stimulation and B cell receptor (BCR) signalling. Specifically, naive Nur77-GFP B cells upregulate GFP following BCR engagement (Mueller et al., 2015). Additionally, light zone germinal centre B cells exhibit active Nr4a1 reporter activity upon receiving stimuli (Tan et al., 2020). In our studies, we examined the role of Nr4a1 in B cell responses to acute antigen-mediated BCR stimulation. However, neither GC B cells nor NP-specific GC B cells displayed substantial Nr4a1 timer blue reporter activity, despite the increased NP-specific GC B cells in IgMg1 mice compared to WT (Figure 4.34 D) (Figure 4.35 B and C). For future studies, it would be informative to assess Nr4a1 expression following low dose antigen stimulation and determine how antigen dose impacts B cell responses during T cell-dependent immune

responses, which could increase competition of B cells to access limited antigen and receive T cell help. Additionally, assess whether Nur77 is upregulated in B cells within this mouse model following exposure to the T-independent immunogen NP-Ficoll. It could also be valuable to analyse how modified BCR signalling affects interactions with other cells, such as FDCs or other stromal cells that play a crucial role in the germinal center. Further, these experiments should be repeated in Nr4a1-Timer homozygous mice, which were not available at the time when these experiments were done.

Additionally, analysis of fluorescent timer reporters in tissue sections was difficult given potential fading during processing (Bending et al., 2018). Intravital microscopy could be utilized to detect TCR reporter genes in Tocky and Tempo mouse models and examine Tfh cells localization. Thus, transferring labelled NP^+ B cells from an QM eYFP mice mouse (Srinivas et al., 2001) into Tocky or Tempo mice prior to immunisation would allow tracking of GC formation by green fluorescence. Subsequent re-stimulation with soluble antigen could trigger Nr4a genes to assess timer blue and red localisation and B and T cell interactions.

Chapter 5. General discussion

Since the identification of antibody-mediated adaptive immunity, extensive research has been directed to understanding the mechanisms behind of the GC response. Understanding these processes has the potential to significantly advance the development of vaccines against harmful microorganisms, leading to more robust humoral immune responses. Vaccination triggers the rapid production of high-affinity antibodies, which protect the body by marking microorganisms for destruction (opsonization) and blocking toxins and viruses from entering cells (neutralization). These responses arise from the proliferation of B lymphocytes, which differentiate into antibody-secreting cells. The process is enhanced by immunoglobulin (Ig) hypermutation, generating receptors with varied affinities.

Many studies have been done using flow cytometry, genomics, and intravital microscopy technologies to reveal the complex cellular dynamics and molecular mechanisms regulating GC responses. In the GC, Tfh cells regulate the process of affinity maturation and the generation of memory B cells and long-lived plasma cells by generating selective pressure and essential helper signals. Tfh helper signals play a vital part in developing strong GC responses that effectively mount humoral immunity against infections.

In this thesis, firstly, we characterised GCs and Tfh cells and evaluate their regulation by antibodies. We used three mouse models - IgMi, AIDko, and IgG1M - to study how antibody and class-switching impact GC regulation. IgMi mice lack secreted antibody with only IgM BCRs. AIDko mice cannot somatically hypermutate or class switch their antibodies due to absence of the AID enzyme. IgG1M mice express IgG1 as their singular BCR and antibody. Comparing these strains reveals requirements for GC initiation, hypermutation, and class switching. Secondly, we utilized Nr4a3-Tocky and Nr4a1-Tempo mouse models to assess how

T cell receptor (TCR) signals regulate Tfh cells in the altering BCR mouse models IgMg1 and IgG1M mice. We also generated AIDko-Tocky mice to analyse Tfh cell TCR signalling in the absence of SHM and CSR. Together, these complementary approaches provide insight into antibody and TCR-mediated regulation of Tfh cells and GC responses.

A previous study demonstrated that while B cells developed normally, IgMi mice are unable to secrete antibodies because genetic deletion of the secretory element of the immunoglobulin heavy chain constant region, though cytokine secretion remains intact (Sahputra et al., 2018). Moreover, examination of mesenteric lymph nodes showed increased GC B cells and Tfh cells following parasitic infection in IgMi mice. Natural antibodies, particularly IgM, are thought to play a crucial role in linking the innate and adaptive immune systems(Baumgarth et al., 2000). Building upon these findings, we evaluated whether the absence of secreted antibodies in IgMi mice or provision of exogenous low affinity antibodies bound to antigen to form immune complex (IC) impacts GC and Tfh cell responses. We found that compared to WT controls, IgMi mice exhibited larger GC size and NP-specific GC responses (Figure 3.4 B). These phenomena are consistent with those observed in the AIDko experiment (Chapter 3.3.2) and are also similar to findings from a previous study involving the AID-/-µS-/- double mutant mouse (Lino et al., 2013). Furthermore, the ratio of GC dark zone (DZ) to light zone (LZ) B cells was elevated in IgMi mice, indicative of altered selection dynamics (Figures 3.5 A and B). This was accompanied by increased Tfh cells (Figure 3.6) parallel with the GC expansion. Tfh cell – GC B cell interaction are important mutually for the maintenance of GC B as well as Tfh cells (Qi et al., 2008). Thus, the accumulation of GC B cells in IgMi mice likely sustains the increase in Tfh cells. Given prior evidence from our lab a few years ago that higher affinity antibodies secreted by PC generated from GC B cells can negatively regulate ongoing GC reactions (Zhang et al., 2013), we conclude that the lack of

antibody feedback regulation in IgMi mice permits uncontrolled GC B cell proliferation and differentiation. Collectively, our data suggest that as IgMi mice do not produce IgM or any antibodies they did not regulate GC through antibody feedback mechanism. Thus, higher-affinity antibodies secreted by B cells typically limit B cell access to antigens within the GC (Zhang et al., 2013). However, in IgMi mice, the absence of secreted antibodies enhances B cell access to antigens on follicular dendritic cells, leading to an increased GC population. This is because GC B cells must internalize and process antigens via the BCR before presenting them on MHC class II for recognition by helper T cells (Borrero and Clarke, 2002).

Affinity maturation and immunoglobulin G (IgG) feedback regulation are important processes regulating GC responses and the development of long-lived plasma and memory B cells (Muramatsu et al., 2000, Ehrenstein et al., 1998). However, the particular roles of activation-induced cytidine deaminase (AID) and IgG feedback in GC reactions remain incompletely understood. To investigate this, we utilized two genetically modified mouse models - AIDko and IgG1 membrane-bound (IgG1M) mice. We hypothesised that abrogating affinity maturation through deletion of AID or altering IgG signalling would disturb normal GC B cell selection and GC organisation.

Following immunisation, AIDko mice formed GCs with increased proportions and numbers of NP-specific GC B cells compared to WT controls (Figure 3.9 B and C). This accumulation occurred despite an absence of affinity maturation. Flow cytometric analysis showed an imbalance in light and dark zone compartments in AIDko GCs, with reduced dark zone to light zone cell ratios and increased $CD86^{hi}$ centrocytes in the light zone (Figure 3.10 A). It is possible that loss of AID activity on B cells gene leads to increased genetic toxicity of GC B cells, and absence of IgG1 signals FcγRIIB can impair apoptosis of GC B cells (Boulianne et al., 2013). The

cell transfer experiments indicate that it is likely that detrimental mutations impacting on BCR affinity are absent in AIDko, and that leads to better proliferation of AIDko GC B cells. The changes may also reflect reduced apoptosis due to reduced IgG1 feedback signalling in the absence of AID.

By comparison, it has also been shown that IgG+ GC B cells have a selective advantage within GCs (Sundling et al., 2021). But, IgG1M mice generated normal total GC B cell numbers but reduced NP-specific GC B cells after immunisation compared to controls (Figure 3.9 B and C). IgG1M GCs also exhibited a defect in dark zone to light zone organization not seen in other groups, implying abnormal B cell selection mechanisms. IgG1M mice further displayed substantially impaired NP-specific antibody production and affinity maturation over time (Figure 3. 12 C). The basis for these defects remains unclear but may involve a lack of secreted IgM and subsequent impacts on GC regulation. Secreted IgM is crucial for immune complex formation and GC regulation, supporting antigen trapping on FDCs (Boes et al., 2000, Zhang et al., 2013). Studies using the sIgM-/- mouse model show impaired T-dependent antibody responses, indicating soluble IgM is essential for GC development and IgG antibody production, as demonstrated by sIgM-/- mice (Baumgarth et al., 2000, Ehrenstein et al., 1998). However, in the cell transfer experiments described here, the transferred cell population was able to produce IgM and IgG antibody. Despite the presence of these antibodies, AIDko B cells were still having a selective advantage.

Affinity maturation and antibody feedback signals are critical for GC B cell selection, how these processes shape responses in established GCs were previously investigated in our lab by histology. In the current study only Flow cytometry was used, so mouse models to study the impact of soluble antibodies, we introduced exogenous antibodies and examined impacts

on GC dynamics in WT, activation-induced cytidine deaminase knockout (AIDko), and non-secreted IgM (IgMi) mice. We hypothesised antibody providing would reduce GC sizes and antigen-specific GC B cells by raising affinity thresholds, with varying effects across genotypes due to differences in selection stringencies.

High affinity anti-NP IgM^a administration slightly decreased GC size in WT mice (Figure 3.14 B), and slightly increased NP-specific plasma cell output, implying GC competition remains intact through affinity-based selection. However, AIDko and IgMi mice showed no differences in GC or antigen-specific B cell proportions with antibody treatment. While AIDko GCs exhibit arrested affinity maturation, IgMi GCs display continued somatic hypermutation without secreted IgM feedback regulation. The lack of impact suggests these GCs may utilize free antigen to be selected, rather than signals from follicular dendritic cells. This can be investigated by examining tissue sections of GCs using immunohistochemistry to visualize the distribution of antigens and FDCs.

Introducing intermediate affinity antibodies in established GCs moderately reduced GC size and antigen-binding cells in AIDko and IgMi mice but not WT controls (Figure3.20 B). Concurrently, WT mice generated more plasma cells, potentially counterbalancing the exogenous antibodies through GC output. Ongoing GCs response in AIDko and IgMi mice appear sensitive to antibody competition, which was different in early experiment when high avidity antibody was injected. Differences in experimental timing may explain this inconsistency.

We were not able to measure antibody affinity by ELISA in these different mouse models. Since AID knockout mice cannot undergo hypermutation, IgM antibodies from these mice could not be detected in ELISA assays testing presence of high affinity antibody binding using

NP_2-BSA coated plate. However, these antibodies only can detect for low-affinity binding (i.e., NP14-BSA). Additionally, because IgMi mice do not produce antibodies, serum from these mice does not show any high or low-affinity antibody in ELISA.

Notably, both experiments displayed decreased in the percentage of Tfh cells (Figure 3.23 B) after antibody administration. This likely impairs antigen presentation to T cells, disrupting their supportive role in B cell selection. The lower light zone B cell percentages remain unclear but may reflect insufficient antigen acquisition. In summary, our findings suggest that the administration of intermediate low-avidity antibodies has a dampening effect on Tfh cell populations, particularly in AIDko mice, and consequently impacts the critical B cell–T cell interactions within the GC.

To better understand the effects of injected anti-NP IgM^a with different avidity antibodies, further studies could examine histology of the spleen tissues by quantifying GC size and staining for markers such as IRF4 to quantify plasma cells and Bcl6 to quantify Tfh cells. Additionally, qPCR could be utilized to evaluate changes in gene expression following antibody treatment. These approaches would provide further insights into the immuno-histology and molecular impacts on GC B cell selection and differentiation.

GC B cells undergo affinity-based selection, where B cells expressing higher affinity B cell receptors (BCRs) outcompete lower affinity clones. It remains unclear how affinity maturation through activation-induced cytidine deaminase (AID) controls this competitive process. We utilized an adoptive transfer QM Cg1cre mTmG cells approach with AIDcre/wt and AIDcre/cre hosts to examine impacts on donor GC B cell dynamics. We hypothesized donor cells would be increasingly selected in AIDko hosts over time due to sufficient affinity maturation.

Transferred FP^+ B cells showed significantly lower frequencies in AIDko compared to AIDwt hosts (Figure 3.25 B). Over the same period, host AIDko GC responses clearly increased (Figure 3.25 C). This implies competing AIDwt B cells experiencing greater selection pressures in the AIDko environment, leading to preferential persistence of endogenously generated low affinity clones.

Assessing antigen-specific B cells, donor populations declined quickly in AIDcre/cre hosts. Host GC cells were unaffected across groups (Figure 4.25 C). Donor cells are able to express the AID enzyme and affinity mature. On the other hand, in the AIDko host mice, NP-specific GC B cells clearly increased, taking most space of the GCs. This observation might be caused by genotoxicity, negative effects on BCR affinity, or AID-mediated effects on cell viability (Sherman et al., 2010). AIDcre/cre mice do not secrete IgG, which is important for inhibiting BCR signalling by binding to the FcγRIIB1 inhibitory receptor (Getahun and Cambier, 2015). IgG class-switched from donor cells could explain the reduction in AIDcre/cre donor GC size, but GCs in the host mice remained clearly enlarged in AIDcre/cre compared to the AIDcre/wt control (Figures 3.25 B and 3.25 C). in summary, absent AID activity delays DNA damage, preserving GC B cell antigen reactivity. This competitive advantage may be enhanced by delayed antigen clearance. Prolonged antigen exposure can disrupt normal tolerance induction, enabling production of self-reactive antibodies in AID-deficient mice and humans, may precipitate autoimmune reactions (Kuraoka et al., 2011, Meyers et al., 2011). The findings from this experiment did not provide sufficient observations. More experiments should be done. One suggestion as I described in the result chapter, would be to adoptively transferring B1-8^{lo} cells into AID knockout (AIDko) mice and using B1-8^{hi} cells transferred into AID wildtype (AIDwt) mice as a control. The prediction would be that transferring B1-8^{hi} cells into the competitive environment of AIDwt mice will allow them to predominate in GCs and

outcompete endogenous polyclonal B cells. In contrast, transferring B1-8^{lo} cells into AIDko recipient mice could reveal whether these low affinity antigen-specific B cells can compete efficiently and undergo GC selection in a host. Thus, this approach may allow us to test if the relative affinity of the B cell receptor determines its ability to dominate the GC reaction, or if other factors are at play.

To study the impacts of altered B cell receptor affinity and signalling, or reduced AID activity, on B cell -T follicular helper cell interactions, we used mouse strains expressing Nr4a3 or Nr4a1 driven reporter genes to track T follicular helper activation through T cell receptor signalling.

Memory B cells can access and transport antigen from the subcapsular sinus to the germinal center within 20 mins (Zhang et al., 2022) We therefore estimated that an interval of 4 hr between antigen boost and analysis of tissues would allow sufficient time for these B cells to present the antigen to Tfh cells in the GC and induce Nr4a1/Nr4a3 expression dependent signals.

BCRs on GC B cells should repeatedly interact with antigens to assess specificity and binding competitiveness, particularly against antibodies in IC on FDC networks. The affinity of these BCR-antigen interactions is critical, as it impacts the amount of antigen B cells can take up, thereby affecting their positive selection by Tfh cells (Zhang et al., 2013, Victora et al., 2010). However, previous research showed that injecting soluble antigens during the peak of the germinal center response induces apoptosis in GC B cells without disrupting B-T cell interactions (Pulendran et al., 1995). Our findings here show that this injection boosts B cell antigen presentation and Tfh cell activation by increasing Timer Blue+ Nr4a3. The increase in

apoptosis observed by Han et al. (1995) may be due to an insufficient number of T cells to interact with all antigen-presenting B cells.

After a soluble antigen boost at 5 days post-immunisation, Tfh cell percentages remained steady in wildtype mice, increased significantly in IgMg1 mice, and decreased in IgG1M GCs. The observed increase in the percentage of Tfh cells in the IgMg1 group after boosting with soluble antigen at day 5 may be attributed to the early time point, as day 5 is relatively short. A similar pattern was observed on day 8, with more Tfh cells in IgMg1 GCs but fewer Tfh cells in IgG1M GCs versus WT (Figure 4.2 C). The Tfh cell loss after antigen boost was more pronounced on day 8 than day 5 across genotypes. While statistical power is weak due to low animal numbers available, the consistent Tfh cell changes at days 5 and 8 suggest reproducible effects. To gain further insight into the dynamics of Tfh cells and Nr4a3 blue^{+} cells, additional experiments are likely necessary to explain the mechanisms by which changes in BCR and co-stimulation signalling influence IgMg1, IgG1M GC B cell selection during the GC response. Specifically, these populations should be assessed at later time points, such as days 14 and 21.

The GC reaction in dependent on the ability of Tfh to interact with GC B cells (de Vinuesa et al., 2000). On the other hand, GC B cells play an important role for supporting Tfh cell differentiation by capture antigen and reactivated Tfh cells leading to TCR signal strength of Nr4a3. Nr4a3 showed to be highly expressed in the Tfh cells after mice received soluble antigen, which Nr4a3-blue+ were seen higher at day5 than the expression at day8 (Figure 4.3 B), which indicate that B cells in younger GCs induce stronger TCR signalling strength and/or show enhanced antigen presentation compared to mature GCs. There was a slight increase in the proportion of Nr4a3-blue+ expressing Tfh cells in IgG1M mice compared to WT and IgMg1

mice at day 5, becoming a significant increase by day 8. However, no difference was observed between IgMg1 and WT mice (Figure 4.3 B). Additionally, the Nr4a3-blue+ Tfh cells MFI were increased in newly activated Tfh cells in IgMg1, IgG1M versus WT mice after antigen boost (Figure4.3 F), indicating that the altered BCR of IgMg1 and IgG1M mice is more efficient at capturing and presenting antigen to Tfh cells inducing stronger TCR signalling compared to WT mice. However, it remained unclear whether this also links to the strength of BCR signalling, something that needs to be further investigated.

Despite having smaller GC sizes after an antigen boost, IgMg1 mice had an unexpected increase in Tfh cells and NP-specific GC B cells (Figure 4.4 A and B). A potential explanation is that IgMg1 B cells may have higher average affinity, enabling better antigen capture and presentation to Tfh cells (Figure 4.4 A and B). In contrast, boosted IgG1M mice had fewer Tfh cells and antigen-specific B cells yet comparable GCs and increased Nr4a3 expression, suggesting effective antigen presentation. Further analysis is required to understand the complex dynamics between T follicular helper (Tfh) cells, Nr4a3 expression, germinal center (GC) size, and antigen-specific B cells in IgMg1 and IgG1M mice. As the Tfh phenotype is transient and changes over time within a GC reaction (Baumjohann et al., 2013, Song and Craft, 2019) . Evaluating multiple timepoints and varying antigen re-stimulation doses could provide additional insights. Additionally, it remains undetermined whether enhanced Tfh activation by anergic GC B cells is a general feature or specific to the chimeric B cell receptor expressed in the IgMg1 model.

In an experiment to investigate the role of B-T cells interaction in the absence of affinity maturation and class-switching use of Nr4a3-Tocky mice crossed to an AIDcre/cre background could help to give insight how strong of these cells communicate in GC. Our result showed

that more Tfh cells tended to be present in AIDcre/cre GCs at day 5, but not by day 8 (Figure 4.26 A and 4.28 C). Expression levels of Nr4a3 remained unchanged in both genotypes (Figure 4.26 B, C, D, and Figure4.28 D, E, and F). These data suggest that lack of AID activity did not impact the B-Tfh cells interactions. An explanation may be that B cells lack AID are driven by enhanced B cell survival due to lack of AID activity, rather than by altered Tfh cell activation.

Nr4a3 expression was not detectable in B cells in the Nr4a3-Tocky mouse model, despite evidence that Nr4a3 can be induced by BCR signalling (Tan et al., 2020). Nr4a1-reporter strans have been reported that allow examination of both BCR signalling and at higher sensitive TCR signalling readouts (Moran et al., 2011, Zikherman et al., 2012, Elliot et al., 2022)

In this thesis we for the first time try to test the Nr4a1-reporter mouse model for GC B and T celle, to test whether better antigen capture affects the signalling of BCR and TCR stimulation downstream of antigen recognition. Newly activated (blue+red-) and persistently activated (blue+red+) Tfh cells increased in mice given a booster immunisation of soluble antigen. However, frequencies of recently activated Nr4a1-blue+ Tfh cells were similar between antigen-boosted IgMg1 and WT mice. Upregulation of Nr4a1 blue and red in GC B cells after antigen stimulation could not be reliably detected by flow cytometry, even in NP-specific GC B cells that were increased in IgMg1 versus WT mice. Despite IgMg1 mice trending to more NP+ GC B cells following immunisation, no distinguishable difference was observed in Nr4a1 expression compared to WT, unlike the signal seen in Tfh cells. Therefore, there were no detectable Nr4a1 reporter expression changes in GC B cells between IgMg1 and WT mice after booster immunisation. In this experiment we used reporter mice heterozygous for the IgMg1 BCR and for the Nr4a1 reporter. Repeating the experiment using reporter homozygous mice

should make the experiment more sensitive and should improve detection of Nr4a1 signalling in B cells.

Compared to Nr4a3 reporter mice, even the heterozygous Nr4a1-Tempo mice displayed stronger Nr4a1-mediated fluorescence, indicating stronger T cell receptor signalling and increased accumulation of antigenic peptides. The Nr4a1 system is therefore of higher sensitivity for detecting differences in antigen presentation (Bending et al., 2018, Jennings et al., 2020). As we used heterozygous reporter mice in this experiment, repeating the experiment by using homozygous Nr4a1, should make this much more sensitive, and should also improving detection of TCR signalling in T cells.

As mentioned in Chapter 4, applying alternative technique to test Nr4a gene expression may provide additional insights. Intravital microscopy could localization Tfh cells. Transferring NP+ B cells from a fluorescent QM eYFP donor into reporter mice prior to immunization enables both tracking of GC formation via green fluorescence and testing Nr4a timer genes after antigenic stimulation. This dual labelling would allow localized detection of TCR signalling dynamics and interactions between T and B cells within the germinal centre reaction.

Chapter 6. Limitations and Future Work:

Disruption in Experimental Testing: The investigation into the role of IgM in antibody feedback within the germinal center (GC) response was disrupted due to the limited availability of antibodies required for the experiments (Anti-IgM^a Fab82: low affinity, Anti-IgM^a 2.315: intermediate affinity, and Anti-IgM^a 1.197: high affinity). These antibodies are expected to facilitate the repetition of the experiments with optimized antibody administration timing. However, these studies require a large cohort of mice across three different genotypes, with varying administration plans and antibody affinities. This introduces significant challenges in terms of resource allocation and experimental possibility, particularly due to the substantial amounts of antibodies required (90 μg per mouse).

Limited Analytical Approaches: Our current analysis primarily depends on flow cytometry, which, while informative, offers a limited perspective on the cellular and structural dynamics within GCs. To gain a more comprehensive understanding of IgM's impact on the GC response, future studies should incorporate histological analysis. This would allow for a detailed examination of tissue architecture, cell distribution, and apoptosis rates. Additionally, incorporating gene expression analysis in GC cells via real-time RT-PCR for markers such as Bcl6, ICOS, and AID would provide deeper insights into the molecular mechanisms.

Measurement of IgG1 Affinities: The measurement of affinities for my newly generated monoclonal IgG1 antibodies using the T200 Biacore system was delayed due to COVID-19 disruptions. Producing sufficient quantities of these antibodies and conducting affinity measurements are crucial for future work. This will allow us to test whether IgG1 antibody feedback provides stronger negative signals for B cell selection than equivalent avidity IgM

during the GC reaction. This analysis will be conducted using a range of monoclonal IgG1 antibodies specific for NP.

Hypothesis Testing with Cell Transfer Models: The hypothesis testing involving the transfer of wild-type (wt) cells into AID knockout (AIDko) mice requires further improvement. Improving the experimental design, particularly through the repetition of experiments with careful consideration of antigen immunization timing and tissue collection protocols, is important. Additionally, future studies could benefit from adoptively transferring B1-8^{lo} cells into AIDko mice and B1-8^{hi} cells into AID wild-type (AIDwt) mice as controls. This approach would better test our prediction that B1-8^{hi} cells, when transferred into AIDwt mice, will predominate in GCs and outcompete endogenous polyclonal B cells. Conversely, transferring B1-8^{lo} cells into AIDko mice could reveal whether these low-affinity antigen-specific B cells can effectively compete and undergo GC selection in a competitive environment.

Statistical Power and Temporal Analysis in Nr4a3-Tocky and Nr4a1-Tempo Mice: Repetition of experiments using Nr4a3-Tocky and Nr4a1-Tempo mice is necessary to increase statistical power. Our current analysis was limited to early germinal center (GC) time points, focusing solely on the fluorescent timer. Future experiments should extend this analysis to later time points, such as day 14 or day 21, to better understand TCR signalling dynamics over time. It is important to note that the Nr4a1-Tempo mice used in this thesis were heterozygous for the Nr4a1-Tempo allele, and the limited availability of mice further constrained the study. Additionally, optimizing TCR signalling analysis through multiphoton microscopy could provide more detailed insights into the spatial and temporal aspects of B-Tfh cells within GC responses.

Chapter 7. References

ABRAMSON, J. & PECHT, I. 2007. Regulation of the mast cell response to the type 1 Fc epsilon receptor. *Immunol Rev,* 217**,** 231-54.

ALLEN, C. D., ANSEL, K. M., LOW, C., LESLEY, R., TAMAMURA, H., FUJII, N. & CYSTER, J. G. 2004. Germinal center dark and light zone organization is mediated by CXCR4 and CXCR5. *Nature immunology,* 5**,** 943-952.

ALLEN, C. D. & CYSTER, J. G. Follicular dendritic cell networks of primary follicles and germinal centers: phenotype and function. Seminars in immunology, 2008. Elsevier, 14-25.

ALLEN, C. D., OKADA, T. & CYSTER, J. G. 2007a. Germinal-center organization and cellular dynamics. *Immunity,* 27**,** 190-202.

ALLEN, C. D., OKADA, T., TANG, H. L. & CYSTER, J. G. 2007b. Imaging of germinal center selection events during affinity maturation. *Science,* 315**,** 528-31.

ALUGUPALLI, K. R., LEONG, J. M., WOODLAND, R. T., MURAMATSU, M., HONJO, T. & GERSTEIN, R. M. 2004. B1b lymphocytes confer T cell-independent long-lasting immunity. *Immunity,* 21**,** 379-90.

ANGELIN-DUCLOS, C., CATTORETTI, G., LIN, K. I. & CALAME, K. 2000. Commitment of B lymphocytes to a plasma cell fate is associated with Blimp-1 expression in vivo. *J Immunol,* 165**,** 5462-71.

ARNON, T. I., HORTON, R. M., GRIGOROVA, I. L. & CYSTER, J. G. 2013. Visualization of splenic marginal zone B-cell shuttling and follicular B-cell egress. *Nature,* 493**,** 684-688.

BANNARD, O., HORTON, R. M., ALLEN, C. D., AN, J., NAGASAWA, T. & CYSTER, J. G. 2013. Germinal center centroblasts transition to a centrocyte phenotype according to a timed program and depend on the dark zone for effective selection. *Immunity,* 39**,** 912-924.

BARNETT, L. G., SIMKINS, H., BARNETT, B. E., KORN, L. L., JOHNSON, A. L., WHERRY, E. J., WU, G. F. & LAUFER, T. M. 2014. B cell antigen presentation in the initiation of follicular helper T cell and germinal center differentiation. *The Journal of Immunology,* 192**,** 3607-3617.

BARR, T. & GRAY, D. 2012. T(FH) memory: more or less T(FH)? *Eur J Immunol,* 42**,** 1977-80.

BARRAL, P., ECKL-DORNA, J., HARWOOD, N. E., DE SANTO, C., SALIO, M., ILLARIONOV, P., BESRA, G. S., CERUNDOLO, V. & BATISTA, F. D. 2008. B cell receptor-mediated uptake of CD1d-restricted antigen augments antibody responses by recruiting invariant NKT cell help. *Proceedings of the National Academy of Sciences of the United States of America,* 105**,** 8345-8350.

BARRINGTON, R. A., POZDNYAKOVA, O., ZAFARI, M. R., BENJAMIN, C. D. & CARROLL, M. C. 2002. B lymphocyte memory: role of stromal cell complement and FcgammaRIIB receptors. *J Exp Med,* 196**,** 1189-99.

BATISTA, F. D. & HARWOOD, N. E. 2009. The who, how and where of antigen presentation to B cells. *Nat Rev Immunol,* 9**,** 15-27.

BATISTA, F. D. & NEUBERGER, M. S. 2000. B cells extract and present immobilized antigen: implications for affinity discrimination. *EMBO J,* 19**,** 513-20.

BAUMGARTH, N. 2011. The double life of a B-1 cell: self-reactivity selects for protective effector functions. *Nat Rev Immunol,* 11**,** 34-46.

BAUMGARTH, N., HERMAN, O. C., JAGER, G. C., BROWN, L., HERZENBERG, L. A. & HERZENBERG, L. A. 1999. Innate and acquired humoral immunities to influenza virus

are mediated by distinct arms of the immune system. *Proc Natl Acad Sci U S A,* 96**,** 2250-5.
BAUMGARTH, N., HERMAN, O. C., JAGER, G. C., BROWN, L. E., HERZENBERG, L. A. & CHEN, J. 2000. B-1 and B-2 cell-derived immunoglobulin M antibodies are nonredundant components of the protective response to influenza virus infection. *J Exp Med,* 192**,** 271-80.
BAUMJOHANN, D., PREITE, S., REBOLDI, A., RONCHI, F., ANSEL, K. M., LANZAVECCHIA, A. & SALLUSTO, F. 2013. Persistent antigen and germinal center B cells sustain T follicular helper cell responses and phenotype. *Immunity,* 38**,** 596-605.
BENDING, D., PRIETO MARTIN, P., PADURARU, A., DUCKER, C., MARZAGANOV, E., LAVIRON, M., KITANO, S., MIYACHI, H., CROMPTON, T. & ONO, M. 2018. A timer for analyzing temporally dynamic changes in transcription during differentiation in vivo. *J Cell Biol,* 217**,** 2931-2950.
BERLAND, R. & WORTIS, H. H. 2002. Origins and functions of B-1 cells with notes on the role of CD5. *Annu Rev Immunol,* 20**,** 253-300.
BLUM, J. S., WEARSCH, P. A. & CRESSWELL, P. 2013. Pathways of antigen processing. *Annu Rev Immunol,* 31**,** 443-73.
BOES, M., SCHMIDT, T., LINKEMANN, K., BEAUDETTE, B. C., MARSHAK-ROTHSTEIN, A. & CHEN, J. 2000. Accelerated development of IgG autoantibodies and autoimmune disease in the absence of secreted IgM. *Proc Natl Acad Sci U S A,* 97**,** 1184-9.
BORRERO, M. & CLARKE, S. H. 2002. Low-affinity anti-Smith antigen B cells are regulated by anergy as opposed to developmental arrest or differentiation to B-1. *J Immunol,* 168**,** 13-21.
BOSSALLER, L., BURGER, J., DRAEGER, R., GRIMBACHER, B., KNOTH, R., PLEBANI, A., DURANDY, A., BAUMANN, U., SCHLESIER, M., WELCHER, A. A., PETER, H. H. & WARNATZ, K. 2006. ICOS deficiency is associated with a severe reduction of CXCR5+CD4 germinal center Th cells. *J Immunol,* 177**,** 4927-32.
BOTHWELL, A. L., PASKIND, M., RETH, M., IMANISHI-KARI, T., RAJEWSKY, K. & BALTIMORE, D. 1981. Heavy chain variable region contribution to the NPb family of antibodies: somatic mutation evident in a gamma 2a variable region. *Cell,* 24**,** 625-37.
BOULIANNE, B., ROJAS, O. L., HADDAD, D., ZAHEEN, A., KAPELNIKOV, A., NGUYEN, T., LI, C., HAKEM, R., GOMMERMAN, J. L. & MARTIN, A. 2013. AID and caspase 8 shape the germinal center response through apoptosis. *J Immunol,* 191**,** 5840-7.
BRENNAN, P. J., BRIGL, M. & BRENNER, M. B. 2013. Invariant natural killer T cells: an innate activation scheme linked to diverse effector functions. *Nat Rev Immunol,* 13**,** 101-17.
BURRELL, B. E., DING, Y., NAKAYAMA, Y., PARK, K. S., XU, J., YIN, N. & BROMBERG, J. S. 2011. Tolerance and lymphoid organ structure and function. *Front Immunol,* 2**,** 64.
CALADO, D. P., SASAKI, Y., GODINHO, S. A., PELLERIN, A., KÖCHERT, K., SLECKMAN, B. P., DE ALBORÁN, I. M., JANZ, M., RODIG, S. & RAJEWSKY, K. 2012. The cell-cycle regulator c-Myc is essential for the formation and maintenance of germinal centers. *Nature immunology,* 13**,** 1092-1100.
CARRASCO, Y. R. & BATISTA, F. D. 2007. B cells acquire particulate antigen in a macrophage-rich area at the boundary between the follicle and the subcapsular sinus of the lymph node. *Immunity,* 27**,** 160-171.
CASAMAYOR-PALLEJA, M., KHAN, M. & MACLENNAN, I. C. 1995. A subset of CD4+ memory T cells contains preformed CD40 ligand that is rapidly but transiently expressed on

their surface after activation through the T cell receptor complex. *J Exp Med,* 181**,** 1293-301.
CASCALHO, M., MA, A., LEE, S., MASAT, L. & WABL, M. 1996a. A quasi-monoclonal mouse. *Science,* 272**,** 1649-52.
CASCALHO, M., MA, A., LEE, S., MASAT, L. & WABL, M. 1996b. A quasi-monoclonal mouse. *Science,* 272**,** 1649-52.
CASOLA, S., CATTORETTI, G., UYTTERSPROT, N., KORALOV, S. B., SEAGAL, J., HAO, Z., WAISMAN, A., EGERT, A., GHITZA, D. & RAJEWSKY, K. 2006. Tracking germinal center B cells expressing germ-line immunoglobulin gamma1 transcripts by conditional gene targeting. *Proc Natl Acad Sci U S A,* 103**,** 7396-401.
CESTA, M. F. 2006. Normal structure, function, and histology of the spleen. *Toxicol Pathol,* 34**,** 455-65.
CHAN, T. D., GATTO, D., WOOD, K., CAMIDGE, T., BASTEN, A. & BRINK, R. 2009. Antigen affinity controls rapid T-dependent antibody production by driving the expansion rather than the differentiation or extrafollicular migration of early plasmablasts. *The Journal of Immunology,* 183**,** 3139-3149.
CHAPLIN, D. D. 2010. Overview of the immune response. *J Allergy Clin Immunol,* 125**,** S3-23.
CHAUDHURI, J., TIAN, M., KHUONG, C., CHUA, K., PINAUD, E. & ALT, F. W. 2003. Transcription-targeted DNA deamination by the AID antibody diversification enzyme. *Nature,* 422**,** 726-30.
CHOI, Y. S. & BAUMGARTH, N. 2008. Dual role for B-1a cells in immunity to influenza virus infection. *J Exp Med,* 205**,** 3053-64.
CINAMON, G., ZACHARIAH, M. A., LAM, O. M., FOSS, F. W., JR. & CYSTER, J. G. 2008. Follicular shuttling of marginal zone B cells facilitates antigen transport. *Nat Immunol,* 9**,** 54-62.
COFFEY, F., ALABYEV, B. & MANSER, T. 2009. Initial clonal expansion of germinal center B cells takes place at the perimeter of follicles. *Immunity,* 30**,** 599-609.
COFFMAN, R. L., LEBMAN, D. A. & ROTHMAN, P. 1993. Mechanism and regulation of immunoglobulin isotype switching. *Adv Immunol,* 54**,** 229-70.
COLOMBO, M. J. & ALUGUPALLI, K. R. 2008. Complement factor H-binding protein, a putative virulence determinant of Borrelia hermsii, is an antigenic target for protective B1b lymphocytes. *J Immunol,* 180**,** 4858-64.
COMERFORD, I., HARATA-LEE, Y., BUNTING, M. D., GREGOR, C., KARA, E. E. & MCCOLL, S. R. 2013. A myriad of functions and complex regulation of the CCR7/CCL19/CCL21 chemokine axis in the adaptive immune system. *Cytokine & Growth Factor Reviews,* 24**,** 269-283.
CORLEY, R. B., MOREHOUSE, E. M. & FERGUSON, A. R. 2005. IgM accelerates affinity maturation. *Scand J Immunol,* 62 Suppl 1**,** 55-61.
CROTTY, S. 2011. Follicular helper CD4 T cells (TFH). *Annu Rev Immunol,* 29**,** 621-63.
CROTTY, S., KERSH, E. N., CANNONS, J., SCHWARTZBERG, P. L. & AHMED, R. 2003. SAP is required for generating long-term humoral immunity. *Nature,* 421**,** 282-7.
CUNNINGHAM, A. F., FLORES-LANGARICA, A., BOBAT, S., DOMINGUEZ MEDINA, C. C., COOK, C. N., ROSS, E. A., LOPEZ-MACIAS, C. & HENDERSON, I. R. 2014. B1b cells recognize protective antigens after natural infection and vaccination. *Front Immunol,* 5**,** 535.
CUNNINGHAM, A. F., GASPAL, F., SERRE, K., MOHR, E., HENDERSON, I. R., SCOTT-TUCKER, A., KENNY, S. M., KHAN, M., TOELLNER, K. M., LANE, P. J. & MACLENNAN, I. C. 2007.

Salmonella induces a switched antibody response without germinal centers that impedes the extracellular spread of infection. *J Immunol,* 178**,** 6200-7.
DE BONO, B., MADERA, M. & CHOTHIA, C. 2004. VH gene segments in the mouse and human genomes. *J Mol Biol,* 342**,** 131-43.
DE VINUESA, C. G., COOK, M. C., BALL, J., DREW, M., SUNNERS, Y., CASCALHO, M., WABL, M., KLAUS, G. G. & MACLENNAN, I. C. 2000. Germinal centers without T cells. *J Exp Med,* 191**,** 485-94.
DEENICK, E. K., CHAN, A., MA, C. S., GATTO, D., SCHWARTZBERG, P. L., BRINK, R. & TANGYE, S. G. 2010. Follicular helper T cell differentiation requires continuous antigen presentation that is independent of unique B cell signaling. *Immunity,* 33**,** 241-53.
DEN HAAN, J. M., MEBIUS, R. E. & KRAAL, G. 2012. Stromal cells of the mouse spleen. *Front Immunol,* 3**,** 201.
DI NOIA, J. M. & NEUBERGER, M. S. 2007. Molecular mechanisms of antibody somatic hypermutation. *Annu Rev Biochem,* 76**,** 1-22.
DICKERSON, S. K., MARKET, E., BESMER, E. & PAPAVASILIOU, F. N. 2003. AID mediates hypermutation by deaminating single stranded DNA. *J Exp Med,* 197**,** 1291-6.
DING, B. B., BI, E., CHEN, H., YU, J. J. & YE, B. H. 2013. IL-21 and CD40L synergistically promote plasma cell differentiation through upregulation of Blimp-1 in human B cells. *J Immunol,* 190**,** 1827-36.
DOGAN, I., BERTOCCI, B., VILMONT, V., DELBOS, F., MÉGRET, J., STORCK, S., REYNAUD, C.-A. & WEILL, J.-C. 2009. Multiple layers of B cell memory with different effector functions. *Nature immunology,* 10**,** 1292-1299.
DOMINGUEZ-SOLA, D., VICTORA, G. D., YING, C. Y., PHAN, R. T., SAITO, M., NUSSENZWEIG, M. C. & DALLA-FAVERA, R. 2012. The proto-oncogene MYC is required for selection in the germinal center and cyclic reentry. *Nature immunology,* 13**,** 1083-1091.
DUNN-WALTERS, D., TOWNSEND, C., SINCLAIR, E. & STEWART, A. 2018. Immunoglobulin gene analysis as a tool for investigating human immune responses. *Immunol Rev,* 284**,** 132-147.
EHRENSTEIN, M. R., O'KEEFE, T. L., DAVIES, S. L. & NEUBERGER, M. S. 1998. Targeted gene disruption reveals a role for natural secretory IgM in the maturation of the primary immune response. *Proc Natl Acad Sci U S A,* 95**,** 10089-93.
ELGUETA, R., BENSON, M. J., DE VRIES, V. C., WASIUK, A., GUO, Y. & NOELLE, R. J. 2009. Molecular mechanism and function of CD40/CD40L engagement in the immune system. *Immunol Rev,* 229**,** 152-72.
ELLIOT, T. A. E., JENNINGS, E. K., LECKY, D. A. J., ROUVRAY, S., MACKIE, G. M., SCARFE, L., SHERIFF, L., ONO, M., MASLOWSKI, K. M. & BENDING, D. 2022. Nur77-Tempo mice reveal T cell steady state antigen recognition. *Discov Immunol,* 1**,** kyac009.
ELLIOT, T. A. E., JENNINGS, E. K., LECKY, D. A. J., THAWAIT, N., FLORES-LANGARICA, A., COPLAND, A., MASLOWSKI, K. M., WRAITH, D. C. & BENDING, D. 2021. Antigen and checkpoint receptor engagement recalibrates T cell receptor signal strength. *Immunity,* 54**,** 2481-2496 e6.
ELOMAA, O., KANGAS, M., SAHLBERG, C., TUUKKANEN, J., SORMUNEN, R., LIAKKA, A., THESLEFF, I., KRAAL, G. & TRYGGVASON, K. 1995. Cloning of a novel bacteria-binding receptor structurally related to scavenger receptors and expressed in a subset of macrophages. *Cell,* 80**,** 603-609.
FEENEY, A. J. 1990. Lack of N regions in fetal and neonatal mouse immunoglobulin V-D-J junctional sequences. *J Exp Med,* 172**,** 1377-90.

FORSTER, R., MATTIS, A. E., KREMMER, E., WOLF, E., BREM, G. & LIPP, M. 1996. A putative chemokine receptor, BLR1, directs B cell migration to defined lymphoid organs and specific anatomic compartments of the spleen. *Cell,* 87**,** 1037-47.

FUKAO, S., HANIUDA, K., NOJIMA, T., TAKAI, T. & KITAMURA, D. 2014. gp49B-mediated negative regulation of antibody production by memory and marginal zone B cells. *J Immunol,* 193**,** 635-44.

GARSIDE, P., INGULLI, E., MERICA, R. R., JOHNSON, J. G., NOELLE, R. J. & JENKINS, M. K. 1998. Visualization of specific B and T lymphocyte interactions in the lymph node. *Science,* 281**,** 96-99.

GETAHUN, A. & CAMBIER, J. C. 2015. Of ITIMs, ITAMs, and ITAMis: revisiting immunoglobulin Fc receptor signaling. *Immunol Rev,* 268**,** 66-73.

GIGOUX, M., SHANG, J., PAK, Y., XU, M., CHOE, J., MAK, T. W. & SUH, W. K. 2009. Inducible costimulator promotes helper T-cell differentiation through phosphoinositide 3-kinase. *Proc Natl Acad Sci U S A,* 106**,** 20371-6.

GOLUB, R., TAN, J., WATANABE, T. & BRENDOLAN, A. 2018. Origin and Immunological Functions of Spleen Stromal Cells. *Trends Immunol,* 39**,** 503-514.

GRAKOUI, A., BROMLEY, S. K., SUMEN, C., DAVIS, M. M., SHAW, A. S., ALLEN, P. M. & DUSTIN, M. L. 1999. The immunological synapse: a molecular machine controlling T cell activation. *Science,* 285**,** 221-7.

GRAY, D., KUMARARATNE, D. S., LORTAN, J., KHAN, M. & MACLENNAN, I. C. 1984. Relation of intra-splenic migration of marginal zone B cells to antigen localization on follicular dendritic cells. *Immunology,* 52**,** 659-69.

GREEN, J. A., SUZUKI, K., CHO, B., WILLISON, L. D., PALMER, D., ALLEN, C. D., SCHMIDT, T. H., XU, Y., PROIA, R. L. & COUGHLIN, S. R. 2011. The sphingosine 1-phosphate receptor S1P2 maintains the homeostasis of germinal center B cells and promotes niche confinement. *Nature immunology,* 12**,** 672-680.

GUO, B., SU, T. T. & RAWLINGS, D. J. 2004. Protein kinase C family functions in B-cell activation. *Curr Opin Immunol,* 16**,** 367-73.

HAAS, K. M., POE, J. C., STEEBER, D. A. & TEDDER, T. F. 2005. B-1a and B-1b cells exhibit distinct developmental requirements and have unique functional roles in innate and adaptive immunity to S. pneumoniae. *Immunity,* 23**,** 7-18.

HANIUDA, K., NOJIMA, T., OHYAMA, K. & KITAMURA, D. 2011. Tolerance induction of IgG+ memory B cells by T cell-independent type II antigens. *J Immunol,* 186**,** 5620-8.

HARDY, R. R. & HAYAKAWA, K. 1994. Cd5 B-Cells, a Fetal B-Cell Lineage. *Advances in Immunology, Vol 55,* 55**,** 297-339.

HARDY, R. R. & HAYAKAWA, K. 2001a. B cell development pathways. *Annual Review of Immunology,* 19**,** 595-621.

HARDY, R. R. & HAYAKAWA, K. 2001b. B cell development pathways. *Annu Rev Immunol,* 19**,** 595-621.

HASE, K., TAKAHASHI, D., EBISAWA, M., KAWANO, S., ITOH, K. & OHNO, H. 2008. Activation-induced cytidine deaminase deficiency causes organ-specific autoimmune disease. *PloS one,* 3**,** e3033.

HODGKIN, P. D., LEE, J.-H. & LYONS, A. B. 1996. B cell differentiation and isotype switching is related to division cycle number. *The Journal of experimental medicine,* 184**,** 277-281.

HOEPEL, W., ALLAHVERDIYEVA, S., HARBIYE, H., DE TAEYE, S. W., VAN DER HAM, A. J., DE BOER, L., ZAAT, S. A., VAN WEEGHEL, M., BAETEN, D. L. & HOUTKOOPER, R. H. 2020.

IgG subclasses shape cytokine responses by human myeloid immune cells through differential metabolic reprogramming. *The Journal of Immunology,* 205**,** 3400-3407.
HOGAN, P. G., LEWIS, R. S. & RAO, A. 2010. Molecular basis of calcium signaling in lymphocytes: STIM and ORAI. *Annu Rev Immunol,* 28**,** 491-533.
HONJO, T., KINOSHITA, K. & MURAMATSU, M. 2002. Molecular mechanism of class switch recombination: linkage with somatic hypermutation. *Annual review of immunology,* 20**,** 165-196.
HORIKAWA, K., MARTIN, S. W., POGUE, S. L., SILVER, K., PENG, K., TAKATSU, K. & GOODNOW, C. C. 2007. Enhancement and suppression of signaling by the conserved tail of IgG memory-type B cell antigen receptors. *J Exp Med,* 204**,** 759-69.
IZADI, A., HAILU, A., GODZWON, M., WRIGHTON, S., OLOFSSON, B., SCHMIDT, T., SÖDERLUND-STRAND, A., ELDER, E., APPELBERG, S. & VALSJÖ, M. 2023. Subclass-switched anti-spike IgG3 oligoclonal cocktails strongly enhance Fc-mediated opsonization. *Proceedings of the National Academy of Sciences,* 120**,** e2217590120.
JANEWAY, C. A., JR. & MEDZHITOV, R. 2002. Innate immune recognition. *Annu Rev Immunol,* 20**,** 197-216.
JARJOUR, M., JORQUERA, A., MONDOR, I., WIENERT, S., NARANG, P., COLES, M. C., KLAUSCHEN, F. & BAJÉNOFF, M. 2014. Fate mapping reveals origin and dynamics of lymph node follicular dendritic cells. *Journal of Experimental Medicine,* 211**,** 1109-1122.
JENNINGS, E., ELLIOT, T. A. E., THAWAIT, N., KANABAR, S., YAM-PUC, J. C., ONO, M., TOELLNER, K. M., WRAITH, D. C., ANDERSON, G. & BENDING, D. 2020. Nr4a1 and Nr4a3 Reporter Mice Are Differentially Sensitive to T Cell Receptor Signal Strength and Duration. *Cell Rep,* 33**,** 108328.
JOHNSON, S. A., PLEIMAN, C. M., PAO, L., SCHNERINGER, J., HIPPEN, K. & CAMBIER, J. C. 1995. Phosphorylated immunoreceptor signaling motifs (ITAMs) exhibit unique abilities to bind and activate Lyn and Syk tyrosine kinases. *J Immunol,* 155**,** 4596-603.
JOHNSTON, R. J., POHOLEK, A. C., DITORO, D., YUSUF, I., ETO, D., BARNETT, B., DENT, A. L., CRAFT, J. & CROTTY, S. 2009. Bcl6 and Blimp-1 are reciprocal and antagonistic regulators of T follicular helper cell differentiation. *Science,* 325**,** 1006-10.
KABAK, S., SKAGGS, B. J., GOLD, M. R., AFFOLTER, M., WEST, K. L., FOSTER, M. S., SIEMASKO, K., CHAN, A. C., AEBERSOLD, R. & CLARK, M. R. 2002. The direct recruitment of BLNK to immunoglobulin alpha couples the B-cell antigen receptor to distal signaling pathways. *Mol Cell Biol,* 22**,** 2524-35.
KARASUYAMA, H., ROLINK, A. & MELCHERS, F. 1993. A complex of glycoproteins is associated with VpreB/lambda 5 surrogate light chain on the surface of mu heavy chain-negative early precursor B cell lines. *J Exp Med,* 178**,** 469-78.
KARASUYAMA, H., ROLINK, A. & MELCHERS, F. 1996. Surrogate light chain in B cell development. *Adv Immunol,* 63**,** 1-41.
KATAKAI, T. 2012. Marginal reticular cells: a stromal subset directly descended from the lymphoid tissue organizer. *Frontiers in immunology,* 3**,** 200.
KATAKAI, T., SUTO, H., SUGAI, M., GONDA, H., TOGAWA, A., SUEMATSU, S., EBISUNO, Y., KATAGIRI, K., KINASHI, T. & SHIMIZU, A. 2008. Organizer-like reticular stromal cell layer common to adult secondary lymphoid organs. *The Journal of Immunology,* 181**,** 6189-6200.
KING, I. L., FORTIER, A., TIGHE, M., DIBBLE, J., WATTS, G. F., VEERAPEN, N., HABERMAN, A. M., BESRA, G. S., MOHRS, M., BRENNER, M. B. & LEADBETTER, E. A. 2011. Invariant

natural killer T cells direct B cell responses to cognate lipid antigen in an IL-21-dependent manner. *Nat Immunol,* 13**,** 44-50.

KNOP, L., DEISER, K., BANK, U., WITTE, A., MOHR, J., PHILIPSEN, L., FEHLING, H. J., MÜLLER, A. J., KALINKE, U. & SCHÜLER, T. 2020. IL‐7 derived from lymph node fibroblastic reticular cells is dispensable for naive T cell homeostasis but crucial for central memory T cell survival. *European Journal of Immunology,* 50**,** 846-857.

KRAAL, G., VAN DER LAAN, L. J., ELOMAA, O. & TRYGGVASON, K. 2000. The macrophage receptor MARCO. *Microbes and infection,* 2**,** 313-316.

KURAOKA, M., HOLL, T. M., LIAO, D., WOMBLE, M., CAIN, D. W., REYNOLDS, A. E. & KELSOE, G. 2011. Activation-induced cytidine deaminase mediates central tolerance in B cells. *Proc Natl Acad Sci U S A,* 108**,** 11560-5.

LALOR, P. A. & MORAHAN, G. 1990. The peritoneal Ly-1 (CD5) B cell repertoire is unique among murine B cell repertoires. *Eur J Immunol,* 20**,** 485-92.

LANG, G. A., DEVERA, T. S. & LANG, M. L. 2008. Requirement for CD1d expression by B cells to stimulate NKT cell-enhanced antibody production. *Blood,* 111**,** 2158-62.

LENTZ, V. M. & MANSER, T. 2001. Cutting edge: germinal centers can be induced in the absence of T cells. *J Immunol,* 167**,** 15-20.

LI, L., WU, J., ABDI, R., JEWELL, C. M. & BROMBERG, J. S. 2021. Lymph node fibroblastic reticular cells steer immune responses. *Trends Immunol,* 42**,** 723-734.

LIN, K. I., ANGELIN-DUCLOS, C., KUO, T. C. & CALAME, K. 2002. Blimp-1-dependent repression of Pax-5 is required for differentiation of B cells to immunoglobulin M-secreting plasma cells. *Mol Cell Biol,* 22**,** 4771-80.

LIN, Y., WONG, K. & CALAME, K. 1997. Repression of c-myc transcription by Blimp-1, an inducer of terminal B cell differentiation. *Science,* 276**,** 596-9.

LINO, A. C., MOHR, E. & DEMENGEOT, J. 2013. Naturally secreted immunoglobulins limit B1 and MZ B-cell numbers through a microbiota-independent mechanism. *Blood,* 122**,** 209-18.

LINTERMAN, M. A., BEATON, L., YU, D., RAMISCAL, R. R., SRIVASTAVA, M., HOGAN, J. J., VERMA, N. K., SMYTH, M. J., RIGBY, R. J. & VINUESA, C. G. 2010. IL-21 acts directly on B cells to regulate Bcl-6 expression and germinal center responses. *J Exp Med,* 207**,** 353-63.

LINTERMAN, M. A., DENTON, A. E., DIVEKAR, D. P., ZVETKOVA, I., KANE, L., FERREIRA, C., VELDHOEN, M., CLARE, S., DOUGAN, G., ESPELI, M. & SMITH, K. G. 2014. CD28 expression is required after T cell priming for helper T cell responses and protective immunity to infection. *Elife,* 3.

LUTHER, S. A., TANG, H. L., HYMAN, P. L., FARR, A. G. & CYSTER, J. G. 2000. Coexpression of the chemokines ELC and SLC by T zone stromal cells and deletion of the ELC gene in the plt/plt mouse. *Proceedings of the National Academy of Sciences,* 97**,** 12694-12699.

MA, C. S., SURYANI, S., AVERY, D. T., CHAN, A., NANAN, R., SANTNER-NANAN, B., DEENICK, E. K. & TANGYE, S. G. 2009. Early commitment of naive human CD4(+) T cells to the T follicular helper (T(FH)) cell lineage is induced by IL-12. *Immunol Cell Biol,* 87**,** 590-600.

MACLENNAN, I. C. 1994. Germinal centers. *Annual review of immunology,* 12**,** 117-139.

MACLENNAN, I. C., TOELLNER, K. M., CUNNINGHAM, A. F., SERRE, K., SZE, D. M., ZUNIGA, E., COOK, M. C. & VINUESA, C. G. 2003. Extrafollicular antibody responses. *Immunol Rev,* 194**,** 8-18.

MAHAJAN, S., CERVERA, A., MACLEOD, M., FILLATREAU, S., PERONA-WRIGHT, G., MEEK, S., SMITH, A., MACDONALD, A. & GRAY, D. 2007. The role of ICOS in the development of CD4 T cell help and the reactivation of memory T cells. *Eur J Immunol,* 37**,** 1796-808.

MAIZELS, N., LAU, J. C., BLIER, P. R. & BOTHWELL, A. 1988. The T-cell independent antigen, NP-ficoll, primes for a high affinity IgM anti-NP response. *Mol Immunol,* 25**,** 1277-82.

MANIS, J. P., TIAN, M. & ALT, F. W. 2002. Mechanism and control of class-switch recombination. *Trends in immunology,* 23**,** 31-39.

MARCIAL-JUAREZ, E., PEREZ-TOLEDO, M., NAYAR, S., PIPI, E., ALSHAYEA, A., PERSAUD, R., JOSSI, S. E., LAMERTON, R., BARONE, F., HENDERSON, I. R. & CUNNINGHAM, A. F. 2023. Salmonella infection induces the reorganization of follicular dendritic cell networks concomitant with the failure to generate germinal centers. *iScience,* 26**,** 106310.

MARSHALL, J. L., ZHANG, Y., PALLAN, L., HSU, M. C., KHAN, M., CUNNINGHAM, A. C., MACLENNAN, I. C. & TOELLNER, K. M. 2011. Early B blasts acquire a capacity for Ig class switch recombination that is lost as they become plasmablasts. *Eur J Immunol,* 41**,** 3506-3512.

MARTIN, F. & KEARNEY, J. F. 2002. Marginal-zone B cells. *Nat Rev Immunol,* 2**,** 323-35.

MARTIN, S. W. & GOODNOW, C. C. 2002. Burst-enhancing role of the IgG membrane tail as a molecular determinant of memory. *Nat Immunol,* 3**,** 182-8.

MEBIUS, R. E. & KRAAL, G. 2005. Structure and function of the spleen. *Nat Rev Immunol,* 5**,** 606-16.

MEBIUS, R. E., NOLTE, M. A. & KRAAL, G. 2004. Development and function of the splenic marginal zone. *Critical Reviews™ in Immunology,* 24.

MEYER-HERMANN, M. E., MAINI, P. K. & IBER, D. 2006. An analysis of B cell selection mechanisms in germinal centers. *Math Med Biol,* 23**,** 255-77.

MEYERS, G., NG, Y. S., BANNOCK, J. M., LAVOIE, A., WALTER, J. E., NOTARANGELO, L. D., KILIC, S. S., AKSU, G., DEBRE, M., RIEUX-LAUCAT, F., CONLEY, M. E., CUNNINGHAM-RUNDLES, C., DURANDY, A. & MEFFRE, E. 2011. Activation-induced cytidine deaminase (AID) is required for B-cell tolerance in humans. *Proc Natl Acad Sci U S A,* 108**,** 11554-9.

MINNICH, M., TAGOH, H., BONELT, P., AXELSSON, E., FISCHER, M., CEBOLLA, B., TARAKHOVSKY, A., NUTT, S. L., JARITZ, M. & BUSSLINGER, M. 2016. Multifunctional role of the transcription factor Blimp-1 in coordinating plasma cell differentiation. *Nat Immunol,* 17**,** 331-43.

MORAN, A. E., HOLZAPFEL, K. L., XING, Y., CUNNINGHAM, N. R., MALTZMAN, J. S., PUNT, J. & HOGQUIST, K. A. 2011. T cell receptor signal strength in Treg and iNKT cell development demonstrated by a novel fluorescent reporter mouse. *J Exp Med,* 208**,** 1279-89.

MORAN, I., NGUYEN, A., KHOO, W. H., BUTT, D., BOURNE, K., YOUNG, C., HERMES, J. R., BIRO, M., GRACIE, G., MA, C. S., MUNIER, C. M. L., LUCIANI, F., ZAUNDERS, J., PARKER, A., KELLEHER, A. D., TANGYE, S. G., CROUCHER, P. I., BRINK, R., READ, M. N. & PHAN, T. G. 2018. Memory B cells are reactivated in subcapsular proliferative foci of lymph nodes. *Nat Commun,* 9**,** 3372.

MUELLER, J., MATLOUBIAN, M. & ZIKHERMAN, J. 2015. Cutting edge: An in vivo reporter reveals active B cell receptor signaling in the germinal center. *J Immunol,* 194**,** 2993-7.

MURAMATSU, M., KINOSHITA, K., FAGARASAN, S., YAMADA, S., SHINKAI, Y. & HONJO, T. 2000. Class switch recombination and hypermutation require activation-induced cytidine deaminase (AID), a potential RNA editing enzyme. *Cell,* 102**,** 553-63.

MURPHY, K. P., MURPHY, K., MURPHY, K. P., TRAVERS, P., WALPORT, M. & JANEWAY, C. 2008. *Janeway's immunobiology*.

MUZUMDAR, M. D., TASIC, B., MIYAMICHI, K., LI, L. & LUO, L. 2007. A global double-fluorescent Cre reporter mouse. *Genesis,* 45**,** 593-605.

NAKAGAWA, R. & CALADO, D. P. 2021. Positive Selection in the Light Zone of Germinal Centers. *Front Immunol,* 12**,** 661678.

NEUBERGER, M. S. & RAJEWSKY, K. 1981. Activation of mouse complement by monoclonal mouse antibodies. *Eur J Immunol,* 11**,** 1012-6.

NIMMERJAHN, F. & RAVETCH, J. V. 2005. Divergent immunoglobulin g subclass activity through selective Fc receptor binding. *Science,* 310**,** 1510-2.

NISHIMURA, M., MURAKAMI, A., HARA, Y. & AZUMA, T. 2011. Characterization of memory B cells responsible for affinity maturation of anti- (4-hydroxy-3-nitrophenyl)acetyl (NP) antibodies. *Int Immunol,* 23**,** 271-85.

NURIEVA, R. I., CHUNG, Y., MARTINEZ, G. J., YANG, X. O., TANAKA, S., MATSKEVITCH, T. D., WANG, Y. H. & DONG, C. 2009. Bcl6 mediates the development of T follicular helper cells. *Science,* 325**,** 1001-5.

NUTT, S. L., HODGKIN, P. D., TARLINTON, D. M. & CORCORAN, L. M. 2015. The generation of antibody-secreting plasma cells. *Nat Rev Immunol,* 15**,** 160-71.

OBUKHANYCH, T. V. & NUSSENZWEIG, M. C. 2006. T-independent type II immune responses generate memory B cells. *The Journal of experimental medicine,* 203**,** 305-310.

OCHIAI, K., MAIENSCHEIN-CLINE, M., SIMONETTI, G., CHEN, J., ROSENTHAL, R., BRINK, R., CHONG, A. S., KLEIN, U., DINNER, A. R., SINGH, H. & SCIAMMAS, R. 2013. Transcriptional regulation of germinal center B and plasma cell fates by dynamical control of IRF4. *Immunity,* 38**,** 918-29.

OETTINGER, M. A., SCHATZ, D. G., GORKA, C. & BALTIMORE, D. 1990. RAG-1 and RAG-2, adjacent genes that synergistically activate V(D)J recombination. *Science,* 248**,** 1517-23.

OKADA, T., MILLER, M. J., PARKER, I., KRUMMEL, M. F., NEIGHBORS, M., HARTLEY, S. B., O'GARRA, A., CAHALAN, M. D. & CYSTER, J. G. 2005. Antigen-engaged B cells undergo chemotaxis toward the T zone and form motile conjugates with helper T cells. *PLoS biology,* 3**,** e150.

PAPE, K. A., TAYLOR, J. J., MAUL, R. W., GEARHART, P. J. & JENKINS, M. K. 2011. Different B cell populations mediate early and late memory during an endogenous immune response. *Science,* 331**,** 1203-1207.

PELANDA, R. & TORRES, R. M. 2012. Central B-cell tolerance: where selection begins. *Cold Spring Harb Perspect Biol,* 4**,** a007146.

PELED, J. U., KUANG, F. L., IGLESIAS-USSEL, M. D., ROA, S., KALIS, S. L., GOODMAN, M. F. & SCHARFF, M. D. 2008. The biochemistry of somatic hypermutation. *Annu Rev Immunol,* 26**,** 481-511.

PEPPER, M. & JENKINS, M. K. 2011. Origins of CD4(+) effector and central memory T cells. *Nat Immunol,* 12**,** 467-71.

PEREIRA, J. P., KELLY, L. M., XU, Y. & CYSTER, J. G. 2009. EBI2 mediates B cell segregation between the outer and centre follicle. *Nature,* 460**,** 1122-1126.

PETERSONE, L., WANG, C. J., EDNER, N. M., FABRI, A., NIKOU, S.-A., HINZE, C., ROSS, E. M., NTAVLI, E., ELFAKI, Y. & HEUTS, F. 2023. IL-21 shapes germinal center polarization via light zone B cell selection and cyclin D3 upregulation. *Journal of Experimental Medicine,* 220**,** e20221653.

PILLAI, S. & CARIAPPA, A. 2009a. The follicular versus marginal zone B lymphocyte cell fate decision. *Nat Rev Immunol,* 9**,** 767-77.

PILLAI, S. & CARIAPPA, A. 2009b. The follicular versus marginal zone B lymphocyte cell fate decision. *Nature Reviews Immunology,* 9**,** 767-777.

PULENDRAN, B., SMITH, K. G. C. & NOSSAL, G. J. V. 1995. Soluble-Antigen Can Impede Affinity Maturation and the Germinal Center Reaction but Enhance Extrafollicular Immunoglobulin Production. *Journal of Immunology,* 155**,** 1141-1150.

QI, H., CANNONS, J. L., KLAUSCHEN, F., SCHWARTZBERG, P. L. & GERMAIN, R. N. 2008. SAP-controlled T-B cell interactions underlie germinal centre formation. *Nature,* 455**,** 764-9.

QIN, D., WU, J., VORA, K. A., RAVETCH, J. V., SZAKAL, A. K., MANSER, T. & TEW, J. G. 2000. Fc gamma receptor IIB on follicular dendritic cells regulates the B cell recall response. *J Immunol,* 164**,** 6268-75.

RAMIRO, A. R., STAVROPOULOS, P., JANKOVIC, M. & NUSSENZWEIG, M. C. 2003. Transcription enhances AID-mediated cytidine deamination by exposing single-stranded DNA on the nontemplate strand. *Nat Immunol,* 4**,** 452-6.

RANKIN, A. L., MACLEOD, H., KEEGAN, S., ANDREYEVA, T., LOWE, L., BLOOM, L., COLLINS, M., NICKERSON-NUTTER, C., YOUNG, D. & GUAY, H. 2011. IL-21 receptor is critical for the development of memory B cell responses. *J Immunol,* 186**,** 667-74.

RAUCH, M., TUSSIWAND, R., BOSCO, N. & ROLINK, A. G. 2009. Crucial role for BAFF-BAFF-R signaling in the survival and maintenance of mature B cells. *PLoS One,* 4**,** e5456.

REVY, P., MUTO, T., LEVY, Y., GEISSMANN, F., PLEBANI, A., SANAL, O., CATALAN, N., FORVEILLE, M., DUFOURCQ-LABELOUSE, R., GENNERY, A., TEZCAN, I., ERSOY, F., KAYSERILI, H., UGAZIO, A. G., BROUSSE, N., MURAMATSU, M., NOTARANGELO, L. D., KINOSHITA, K., HONJO, T., FISCHER, A. & DURANDY, A. 2000. Activation-induced cytidine deaminase (AID) deficiency causes the autosomal recessive form of the Hyper-IgM syndrome (HIGM2). *Cell,* 102**,** 565-75.

ROCO, J. A., MESIN, L., BINDER, S. C., NEFZGER, C., GONZALEZ-FIGUEROA, P., CANETE, P. F., ELLYARD, J., SHEN, Q., ROBERT, P. A., CAPPELLO, J., VOHRA, H., ZHANG, Y., NOWOSAD, C. R., SCHIEPERS, A., CORCORAN, L. M., TOELLNER, K. M., POLO, J. M., MEYER-HERMANN, M., VICTORA, G. D. & VINUESA, C. G. 2019. Class-Switch Recombination Occurs Infrequently in Germinal Centers. *Immunity,* 51**,** 337-350 e7.

RODDA, L. B., LU, E., BENNETT, M. L., SOKOL, C. L., WANG, X., LUTHER, S. A., BARRES, B. A., LUSTER, A. D., YE, C. J. & CYSTER, J. G. 2018. Single-cell RNA sequencing of lymph node stromal cells reveals niche-associated heterogeneity. *Immunity,* 48**,** 1014-1028. e6.

ROOZENDAAL, R., MEBIUS, R. E. & KRAAL, G. 2008. The conduit system of the lymph node. *International Immunology,* 20**,** 1483-1487.

RUSH, J. S., LIU, M., ODEGARD, V. H., UNNIRAMAN, S. & SCHATZ, D. G. 2005. Expression of activation-induced cytidine deaminase is regulated by cell division, providing a mechanistic basis for division-linked class switch recombination. *Proceedings of the National Academy of Sciences,* 102**,** 13242-13247.

SAGE, A. P., TSIANTOULAS, D., BINDER, C. J. & MALLAT, Z. 2019. The role of B cells in atherosclerosis. *Nat Rev Cardiol,* 16**,** 180-196.

SAHPUTRA, R., YAM-PUC, J. C., WAISMAN, A., MULLER, W. & ELSE, K. J. 2018. Evaluating the IgMi mouse as a novel tool to study B-cell biology. *Eur J Immunol,* 48**,** 2068-2071.

SAITO, M., GAO, J., BASSO, K., KITAGAWA, Y., SMITH, P. M., BHAGAT, G., PERNIS, A., PASQUALUCCI, L. & DALLA-FAVERA, R. 2007. A signaling pathway mediating downregulation of BCL6 in germinal center B cells is blocked by BCL6 gene alterations in B cell lymphoma. *Cancer Cell,* 12**,** 280-92.

SALFELD, J. G. 2007. Isotype selection in antibody engineering. *Nat Biotechnol,* 25**,** 1369-72.

SCHWICKERT, T. A., VICTORA, G. D., FOOKSMAN, D. R., KAMPHORST, A. O., MUGNIER, M. R., GITLIN, A. D., DUSTIN, M. L. & NUSSENZWEIG, M. C. 2011. A dynamic T cell-limited checkpoint regulates affinity-dependent B cell entry into the germinal center. *J Exp Med,* 208**,** 1243-52.

SHARPE, A. H. & FREEMAN, G. J. 2002. The B7-CD28 superfamily. *Nat Rev Immunol,* 2**,** 116-26.

SHERMAN, M. H., KURAISHY, A. I., DESHPANDE, C., HONG, J. S., CACALANO, N. A., GATTI, R. A., MANIS, J. P., DAMORE, M. A., PELLEGRINI, M. & TEITELL, M. A. 2010. AID-induced genotoxic stress promotes B cell differentiation in the germinal center via ATM and LKB1 signaling. *Mol Cell,* 39**,** 873-85.

SHIMODA, M., LI, T., PIHKALA, J. P. & KONI, P. A. 2006. Role of MHC class II on memory B cells in post-germinal center B cell homeostasis and memory response. *J Immunol,* 176**,** 2122-33.

SHINKAI, Y., RATHBUN, G., LAM, K. P., OLTZ, E. M., STEWART, V., MENDELSOHN, M., CHARRON, J., DATTA, M., YOUNG, F., STALL, A. M. & ET AL. 1992. RAG-2-deficient mice lack mature lymphocytes owing to inability to initiate V(D)J rearrangement. *Cell,* 68**,** 855-67.

SHINNAKASU, R., INOUE, T., KOMETANI, K., MORIYAMA, S., ADACHI, Y., NAKAYAMA, M., TAKAHASHI, Y., FUKUYAMA, H., OKADA, T. & KUROSAKI, T. 2016. Regulated selection of germinal-center cells into the memory B cell compartment. *Nature immunology,* 17**,** 861-869.

SHULMAN, Z., GITLIN, A. D., TARG, S., JANKOVIC, M., PASQUAL, G., NUSSENZWEIG, M. C. & VICTORA, G. D. 2013. T follicular helper cell dynamics in germinal centers. *Science,* 341**,** 673-7.

SIMPSON, T. R., QUEZADA, S. A. & ALLISON, J. P. 2010. Regulation of CD4 T cell activation and effector function by inducible costimulator (ICOS). *Curr Opin Immunol,* 22**,** 326-32.

SONG, W. & CRAFT, J. 2019. T follicular helper cell heterogeneity: Time, space, and function. *Immunol Rev,* 288**,** 85-96.

SRINIVAS, S., WATANABE, T., LIN, C. S., WILLIAM, C. M., TANABE, Y., JESSELL, T. M. & COSTANTINI, F. 2001. Cre reporter strains produced by targeted insertion of EYFP and ECFP into the ROSA26 locus. *BMC Dev Biol,* 1**,** 4.

STONE, E. L., PEPPER, M., KATAYAMA, C. D., KERDILES, Y. M., LAI, C. Y., EMSLIE, E., LIN, Y. C., YANG, E., GOLDRATH, A. W., LI, M. O., CANTRELL, D. A. & HEDRICK, S. M. 2015. ICOS coreceptor signaling inactivates the transcription factor FOXO1 to promote Tfh cell differentiation. *Immunity,* 42**,** 239-251.

SU, T. T. & RAWLINGS, D. J. 2002. Transitional B lymphocyte subsets operate as distinct checkpoints in murine splenic B cell development. *J Immunol,* 168**,** 2101-10.

SUAN, D., KRÄUTLER, N. J., MAAG, J. L., BUTT, D., BOURNE, K., HERMES, J. R., AVERY, D. T., YOUNG, C., STATHAM, A. & ELLIOTT, M. 2017a. CCR6 defines memory B cell precursors in mouse and human germinal centers, revealing light-zone location and predominant low antigen affinity. *Immunity,* 47**,** 1142-1153. e4.

SUAN, D., SUNDLING, C. & BRINK, R. 2017b. Plasma cell and memory B cell differentiation from the germinal center. *Curr Opin Immunol,* 45**,** 97-102.

SUNDLING, C., LAU, A. W. Y., BOURNE, K., YOUNG, C., LAURIANTO, C., HERMES, J. R., MENZIES, R. J., BUTT, D., KRAUTLER, N. J., ZAHRA, D., SUAN, D. & BRINK, R. 2021. Positive selection of IgG(+) over IgM(+) B cells in the germinal center reaction. *Immunity,* 54**,** 988-1001 e5.

TAKATSUKA, S., YAMADA, H., HANIUDA, K., SARUWATARI, H., ICHIHASHI, M., RENAULD, J. C. & KITAMURA, D. 2018. IL-9 receptor signaling in memory B cells regulates humoral recall responses. *Nat Immunol,* 19**,** 1025-1034.

TAN, C., HIWA, R., MUELLER, J. L., VYKUNTA, V., HIBIYA, K., NOVISKI, M., HUIZAR, J., BROOKS, J. F., GARCIA, J., HEYN, C., LI, Z., MARSON, A. & ZIKHERMAN, J. 2020. NR4A nuclear receptors restrain B cell responses to antigen when second signals are absent or limiting. *Nat Immunol,* 21**,** 1267-1279.

TANGYE, S. G., LIU, Y.-J., AVERSA, G., PHILLIPS, J. H. & DE VRIES, J. E. 1998. Identification of functional human splenic memory B cells by expression of CD148 and CD27. *The Journal of experimental medicine,* 188**,** 1691-1703.

TARLINTON, D. M. 2008. Evolution in miniature: selection, survival and distribution of antigen reactive cells in the germinal centre. *Immunol Cell Biol,* 86**,** 133-8.

TODO, K., KOGA, O., NISHIKAWA, M. & HIKIDA, M. 2014. IgG1 cytoplasmic tail is essential for cell surface expression in Igbeta down-regulated cells. *Biochem Biophys Res Commun,* 445**,** 572-7.

TOELLNER, K. M. 2014. Cognate interactions: extrafollicular IL‐4 drives germinal‐center reactions, a new role for an old cytokine. *European Journal of Immunology,* 44**,** 1917-1920.

TOELLNER, K. M., GULBRANSON-JUDGE, A., TAYLOR, D. R., SZE, D. M. & MACLENNAN, I. C. 1996. Immunoglobulin switch transcript production in vivo related to the site and time of antigen-specific B cell activation. *J Exp Med,* 183**,** 2303-12.

TOELLNER, K. M., JENKINSON, W. E., TAYLOR, D. R., KHAN, M., SZE, D. M., SANSOM, D. M., VINUESA, C. G. & MACLENNAN, I. C. 2002. Low-level hypermutation in T cell-independent germinal centers compared with high mutation rates associated with T cell-dependent germinal centers. *J Exp Med,* 195**,** 383-9.

TOELLNER, K. M., LUTHER, S. A., SZE, D. M., CHOY, R. K., TAYLOR, D. R., MACLENNAN, I. C. & ACHA-ORBEA, H. 1998. T helper 1 (Th1) and Th2 characteristics start to develop during T cell priming and are associated with an immediate ability to induce immunoglobulin class switching. *J Exp Med,* 187**,** 1193-204.

VIANT, C., WEYMAR, G. H. J., ESCOLANO, A., CHEN, S., HARTWEGER, H., CIPOLLA, M., GAZUMYAN, A. & NUSSENZWEIG, M. C. 2020. Antibody Affinity Shapes the Choice between Memory and Germinal Center B Cell Fates. *Cell,* 183**,** 1298-1311 e11.

VICTORA, G. D. & NUSSENZWEIG, M. C. 2012. Germinal centers. *Annual review of immunology,* 30**,** 429-457.

VICTORA, G. D., SCHWICKERT, T. A., FOOKSMAN, D. R., KAMPHORST, A. O., MEYER-HERMANN, M., DUSTIN, M. L. & NUSSENZWEIG, M. C. 2010. Germinal center

dynamics revealed by multiphoton microscopy with a photoactivatable fluorescent reporter. *Cell,* 143**,** 592-605.
VIDARSSON, G., DEKKERS, G. & RISPENS, T. 2014. IgG subclasses and allotypes: from structure to effector functions. *Front Immunol,* 5**,** 520.
VIJAY, G. K. M. & SINGH, H. 2021. Cell fate dynamics and genomic programming of plasma cell precursors. *Immunological Reviews,* 303**,** 62-71.
WAISMAN, A., KRAUS, M., SEAGAL, J., GHOSH, S., MELAMED, D., SONG, J., SASAKI, Y., CLASSEN, S., LUTZ, C., BROMBACHER, F., NITSCHKE, L. & RAJEWSKY, K. 2007. IgG1 B cell receptor signaling is inhibited by CD22 and promotes the development of B cells whose survival is less dependent on Ig alpha/beta. *J Exp Med,* 204**,** 747-58.
WARD, J. 1999. Thymus, spleen, and lymph nodes. *Pathology of the Mouse, Reference and Atlas*.
WEISEL, F. J., ZUCCARINO-CATANIA, G. V., CHIKINA, M. & SHLOMCHIK, M. J. 2016. A Temporal Switch in the Germinal Center Determines Differential Output of Memory B and Plasma Cells. *Immunity,* 44**,** 116-130.
WOOF, J. M. & KERR, M. A. 2006. The function of immunoglobulin A in immunity. *J Pathol,* 208**,** 270-82.
YAM-PUC, J. C., ZHANG, L., ZHANG, Y. & TOELLNER, K.-M. 2018. Role of B-cell receptors for B-cell development and antigen-induced differentiation. *F1000Research,* 7.
YAO, X. R., FLASWINKEL, H., RETH, M. & SCOTT, D. W. 1995. Immunoreceptor tyrosine-based activation motif is required to signal pathways of receptor-mediated growth arrest and apoptosis in murine B lymphoma cells. *J Immunol,* 155**,** 652-61.
ZAHEEN, A., BOULIANNE, B., PARSA, J. Y., RAMACHANDRAN, S., GOMMERMAN, J. L. & MARTIN, A. 2009. AID constrains germinal center size by rendering B cells susceptible to apoptosis. *Blood,* 114**,** 547-54.
ZEHENTMEIER, S. & PEREIRA, J. P. 2019. Cell circuits and niches controlling B cell development. *Immunol Rev,* 289**,** 142-157.
ZHANG, Y., GARCIA-IBANEZ, L., ULBRICHT, C., LOK, L. S. C., PIKE, J. A., MUELLER-WINKLER, J., DENNISON, T. W., FERDINAND, J. R., BURNETT, C. J. M., YAM-PUC, J. C., ZHANG, L., ALFARO, R. M., TAKAHAMA, Y., OHIGASHI, I., BROWN, G., KUROSAKI, T., TYBULEWICZ, V. L. J., ROT, A., HAUSER, A. E., CLATWORTHY, M. R. & TOELLNER, K. M. 2022. Recycling of memory B cells between germinal center and lymph node subcapsular sinus supports affinity maturation to antigenic drift. *Nat Commun,* 13**,** 2460.
ZHANG, Y., MEYER-HERMANN, M., GEORGE, L. A., FIGGE, M. T., KHAN, M., GOODALL, M., YOUNG, S. P., REYNOLDS, A., FALCIANI, F., WAISMAN, A., NOTLEY, C. A., EHRENSTEIN, M. R., KOSCO-VILBOIS, M. & TOELLNER, K. M. 2013. Germinal center B cells govern their own fate via antibody feedback. *J Exp Med,* 210**,** 457-64.
ZHANG, Y., TECH, L., GEORGE, L. A., ACS, A., DURRETT, R. E., HESS, H., WALKER, L. S. K., TARLINTON, D. M., FLETCHER, A. L., HAUSER, A. E. & TOELLNER, K. M. 2018. Plasma cell output from germinal centers is regulated by signals from Tfh and stromal cells. *J Exp Med,* 215**,** 1227-1243.
ZIKHERMAN, J., PARAMESWARAN, R. & WEISS, A. 2012. Endogenous antigen tunes the responsiveness of naive B cells but not T cells. *Nature,* 489**,** 160-4.
ZOTOS, D., COQUET, J. M., ZHANG, Y., LIGHT, A., D'COSTA, K., KALLIES, A., CORCORAN, L. M., GODFREY, D. I., TOELLNER, K. M., SMYTH, M. J., NUTT, S. L. & TARLINTON, D. M.

2010. IL-21 regulates germinal center B cell differentiation and proliferation through a B cell-intrinsic mechanism. *J Exp Med,* 207**,** 365-78.

ZUCCARINO-CATANIA, G. V., SADANAND, S., WEISEL, F. J., TOMAYKO, M. M., MENG, H., KLEINSTEIN, S. H., GOOD-JACOBSON, K. L. & SHLOMCHIK, M. J. 2014. CD80 and PD-L2 define functionally distinct memory B cell subsets that are independent of antibody isotype. *Nature immunology,* 15**,** 631-637.